Theses & Dissertations   Graduate Studies

Fall 12-16-2016

Target Validation and Pharmacological Characterization of Novel NMDAR Modulators

Kiran Sapkota
University of Nebraska Medical Center

TARGET VALIDATION AND PHARMACOLOGICAL CHARACTERIZATION OF NOVEL NMDAR MODULATORS

by

Kiran Sapkota

A DISSERTATION

Presented to the Faculty of
the University of Nebraska Graduate College
in Partial Fulfillment of the Requirements
for the Degree of Doctor of Philosophy

Pharmacology and Experimental Neuroscience
Graduate Program

Under the Supervision of Professor Daniel T. Monaghan

University of Nebraska Medical Center
Omaha, Nebraska

December, 2016

Supervisory Committee:
Wallace B. Thoreson, Ph.D.   Huangui Xiong, M.D., Ph.D.
Shelley D. Smith, Ph.D.   Woo-Yang Kim, Ph.D.
Shashank Dravid, Ph.D.

Acknowledgments

First, I sincerely thank my advisor, Dr. Daniel T. Monaghan, for his continuous support, encouragement, and guidance. Thank you for believing in me and providing me an opportunity to work under your mentorship. I am very much thankful for your valuable time spent on me. During my graduate life under your supervision, I had the opportunity to learn about science as well as life. Your mentoring has changed my way of thinking about science, and definitely, your suggestions and instructions will remain valuable throughout my career in being a better scientist and, most importantly, a better person.

I would also like to thank my graduate advisory committee members: Dr. Wallace B. Thoreson, Dr. Huangui Xiong, Dr. Shelley D. Smith, Dr. Woo-Yang Kim and Dr. Shashank Dravid, for their suggestions, guidance, and critical comments throughout the years of my graduate school, which always directed me to focus on goal-oriented research.

I am also thankful to Dr. Keshore Bidasee and Dr. Myron Toews. You were always there to help when I had questions, whether it be about academic courses or about scientific research.

I am grateful to my laboratory members: Hasaan Alsaad, Zhihao Mao, and Dr. Kang Tang for helping me in different ways. The time spent with each of you will be a happy memory.

I appreciate the help from the administrative staff in the Department of Pharmacology and Experimental Neuroscience for their continuous support in various aspects during my graduate life, whether it be for arranging the room for a committee meeting or arranging a travel itinerary for scientific conferences. I am thankful to Dr. Howard fox and his laboratory staff for letting us use their NanoDrop and PCR machine.

Finally, I would like to thank my parents, my wife, and my family for believing in me. Without your continuous support and encouragement, this process would not have been possible.

TARGET VALIDATION AND PHARMACOLOGICAL CHARACTERIZATION OF NOVEL

NMDAR MODULATORS

Kiran Sapkota, Ph.D.

University of Nebraska, 2016

Supervisor: Daniel T. Monaghan, Ph.D.

Abstract

The N-methyl-D aspartate receptors (NMDARs) are ligand-gated ion channels, which play important roles in learning and memory. Excessive activity of NMDARs is implicated in damage due to stroke and neurodegenerative diseases, whereas hypoactivity of NMDARs contributes to schizophrenia. The initial goal of my dissertation is to evaluate the potential role of the GluN2D-containing NMDARs in neuropathological, behavioral and cognitive alterations associated with schizophrenia and characterize the pharmacology and mechanisms of action of NMDAR modulators which could potentially be used to modulate these receptors in schizophrenia.

A subanesthetic dose of the NMDAR antagonist ketamine elicits symptoms of schizophrenia. This property led to the well-supported theory of NMDARs-hypofunction in schizophrenia. We found that ketamine increases $[^{14}C]$-2-deoxy-glucose uptake in the medial prefrontal cortex and entorhinal cortex in wild type (WT) but not in GluN2D-knock out (KO) mice. Ketamine also increases locomotor activity and gamma-band oscillatory power in WT but not in GluN2D-KO mice. These results suggest a critical role of GluN2D-containing NMDARs in ketamine-induced schizophrenia-like symptoms in mice. Also, consistent with a role for GluN2D in schizophrenia is that the GluN2D-KO mice displayed impaired spatial memory acquisition and reduced parvalbumin (PV)-immunopositive staining compared to control mice.

To develop NMDAR modulator for treating schizophrenia and other neurological diseases, we characterized several different naphthalene and phenanthrene based compounds for their positive allosteric modulator (PAM), negative allosteric modulator (NAM) and competitive antagonistic activity at NMDARs. We discovered that UBP684 and UBP753 are general NMDAR PAMs, UBP792 is a GluN2C/GluN2D-preferring NAM and UBP791 is a GluN2C/GluN2D-preferring competitive antagonist.

Subsequent studies identified the mechanisms of action of the new compounds. The general PAMs UBP684/UBP753 increase agonist efficacy. They increase the channel open probability (P_{open}), and prolong the deactivation time upon glutamate removal. They bind to both the inactive and active states of the receptor and stabilize the glutamate-bound state of the GluN2 ligand-binding domain (LBD). The GluN2C/GluN2D-selective NAM UBP792 is a non-competitive antagonist and acts in a voltage-independent manner. Like the PAMs UBP684 and UBP753, UBP792 also acts by stabilizing the GluN2 LBD.

Table of Contents

List of Tables

List of Figures

List of Abbreviations

% E_{Max}	percent of maximal efficacy
% I_{Max}	percent of maximal inhibition
$[^{14}C]$-2DG	$[^{14}C]$-2-deoxy-glucose
AMPAR	(*S*)-α-amino-3-hydroxy-5-methyl-4-isoxazolepropanoic acid receptor
ANOVA	analysis of variance
ATD	amino terminal domain
BLA	basolateral/lateral amygdala
CNS	central nervous system
CNS	central nervous system
CPu	caudate putamen
CTD	c-terminal domain
DAAO	d-amino acid oxidase
dHC	dorsal hippocampus
DLPFC	dorsolateral prefrontal cortex
DMSO	dimethyl sulfoxide
DTT	dithiothreitol
EC_{50}	half-maximal effective concentration

ECoG	electrocorticography
EPSC	excitatory postsynaptic current
GABA	gamma-amino butyric acid
GAD	glutamic acid decarbocylase
GluN2D-KO	GluN2D knockout
HEPES	2-[4-(2-hydroxyethyl)piperazin-1-yl]ethanesulfonic acid
HEPES	4-(2-hydroxethyl)-1-piperazineethanesulfonic acid
HFO	high frequency oscillations
IC	inferior colliculus
IC_{50}	half-maximal inhibitory concentration
iGluRs	ionotropic glutamate receptors
KA	kainic acid
K_i	inhibition constant
K_{off}	dissociation reate constant
K_{on}	association rate constant
KO	knock out
LBD	ligand binding domain

LTP	long-term potentiation
MK-801	dizoclipine maleate
NAM	negative allosteric modulator
NMDAR	N-methyl-D-aspartate receptor
OFT	open field test
PAM	positive allosteric modulator
PAS	pregnanolone sulfate
PBS	phosphate buffer saline
PCP	phencyclidine
PFA	paraformaldehyde
PFC	medial prefrontal cortex
PPI	prepulse inhibition
PS	pregnenolone sulfate
PSD	post synaptic density
PV	parvalbumin
P_{open}	open probability
SAP	synapse associated protein

SNR	substantia nigra reticulata
SSC	somatosensory cortex
TEVC	two-electrode voltage clamp
TMD	transmembrane domain
UBP684	6-(4-methylpent-1-yl)-2-naphthoic acid
UBP753	(*RS*)-6-(5-Methylhexan-2-yl)-2-naphthoic acid
UBP791	1-(7-(2-carboxyethyl)phenanthrene-2-carbonyl)piperazine-2,3-dicarboxylic acid
UBP792	(*E*)-3-hydroxy-7-(2-nitrostyryl)-2-naphthoic acid
vHC	ventral hippocampus
WT	wild type

Chapter 1 Introduction

1   NMDARs, schizophrenia, and NMDAR modulators

1.1   N-methyl-D-aspartate receptors (NMDARs)

L-Glutamate is the primary excitatory neurotransmitter in the vertebrate central nervous system (Watkins, Evans 1981) and glutamatergic neurotransmission is mediated by two subtypes of receptors (i) ionotropic glutamate receptors (iGluRs; ligand-gated ion channels) that mediate the fast synaptic responses and (ii) metabotropic glutamate receptors (mGluRs; G-protein coupled receptors, GPCRs) that cause slow synaptic effect (Traynelis, Wollmuth et al. 2010, Conn, Pin 1997). The ligand-gated ionotropic glutamate receptors are further divided into 3 subtypes. They are named for agonists which selectively activate them (NMDA, AMPA and kainate) (Krogsgaard-Larsen, Honore et al. 1980, Watkins 1962, Curtis, Watkins 1963, Johnston, Kennedy et al. 1979, Traynelis, Wollmuth et al. 2010, Monaghan, Bridges et al. 1989, Watkins, Evans 1981, Dingledine, Borges et al. 1999). Pharmacological studies with antagonists confirmed the classification based on agonists (Biscoe, Evans et al. 1977, Davies, Watkins 1979, McLennan, Lodge 1979, Evans, Francis et al. 1978, Evans, Francis et al. 1979). The ionotropic glutamate receptors are also classified as NMDA and non-NMDA receptors (Monaghan, Bridges et al. 1989, Seeburg 1993, Young, Fagg 1990). Autoradiographic studies also show the anatomical distribution of different types of glutamate receptors (Monaghan, Holets et al. 1983, Monaghan, Cotman 1985, Monaghan, Cotman 1982).

1.1.1   Structure and pharmacology of NMDARs

When rat GluN1 receptors were first cloned and expressed in *Xenopus* oocytes, they exhibited pharmacological properties similar to neuronal NMDARs. Hence, these NMDARs were considered to be homomeric receptors similar to AMPA and kainate receptors (Moriyoshi, Masu et al. 1991). However, the current which was believed to be from homomeric GluN1 receptors is actually from heteromeric NMDARs formed by GluN1 and endogenously expressed GluN2 subunits in *Xenopous laevis* oocytes (Schmidt, Hollmann 2008, Schmidt, Hollmann 2009). Four

other subunits of NMDAR were later cloned and they formed functional NMDARs when co-expressed with GluN1 subunit in *Xenopus laevis* oocytes (Monyer, Sprengel 1992, Monyer, Burnashev et al. 1994, Meguro, Mori et al. 1992, Ikeda, Nagasawa et al. 1992, Ishii, Moriyoshi et al. 1993). For rat proteins, these subunits were originally named as NR2A-D and for mouse proteins, they were named as ε1-4. Now, these subunits are referred to as GluN2A-D (Collingridge, Olsen et al. 2009).

Most of the N-methyl-D-aspartate receptors (NMDARs) expressed in brain are hetero-tetrameric complexes (Karakas, Furukawa 2014, Laube, Kuhse et al. 1998, Ulbrich, Isacoff 2008, Schorge, Colquhoun 2003, Sobolevsky, Rosconi et al. 2009, Lee, Lü et al. 2014) composed of two glycine-binding obligatory GluN1 subunits (Johnson, Ascher 1987) and either two similar or different glutamate-binding GluN2 subunits or a combination of GluN2 and GluN3 subunits or two GluN3 subunits (Figure 1.1) (Hollmann 1999, Brothwell, Barber et al. 2008, Jones, Gibb 2005, Brickley, Misra et al. 2003, Perez-Otano, Schulteis et al. 2001, Ciabarra, Sullivan et al. 1995, Sucher, Akbarian et al. 1995, Cavara, Orth et al. 2009, Chatterton, Awobuluyi et al. 2002, Smothers, Woodward 2007, Smothers, Woodward 2009, Awobuluyi, Yang et al. 2007, Madry, Mesic et al. 2007). Upon activation, these receptors allow Ca^{2+}, Na^+ and K^+ through the receptor ion channel and show voltage-dependent block by magnesium (Mayer, Westbrook et al. 1984, Ascher, Nowak 1988). The GluN1 subunit is encoded by a single gene which has 22 exons. Exon 5, 21 and 22 can be alternatively spliced to yield 8 GluN1 splice variants (Sugihara, Moriyoshi et al. 1992, Hollmann, Boulter et al. 1993) whereas GluN2 subunits (GluN2A-D) are encoded by four separate genes (Monyer, Burnashev et al. 1994, Monyer, Sprengel 1992, Ishii, Moriyoshi et al. 1993, Ikeda, Nagasawa et al. 1992, Kutsuwada, Kashiwabuchi et al. 1992). The subtype of the GluN2 subunits (GluN2A-D) in the receptor complex determines the electrophysiological, biochemical and pharmacological properties of NMDARs (Monyer, Burnashev et al. 1994, Vicini, Wang et al. 1998, Ishii, Moriyoshi et al. 1993, Buller, Larson et al. 1994). NMDARs are

often thought of as being diheteromeric where two GluN1 receptors co-assemble with two same GluN2 subunits (e.g. GluN1-1a/GluN2B) (Dingledine, Borges et al. 1999). However, studies have shown that triheteromeric NMDARs (e.g. GluN1/GluN2A/GluN2B) also exist in the brain regions and that these receptors have different pharmacological properties compared to di-heteromeric NMDARs (Hansen, Ogden et al. 2014, Cheriyan, Balsara et al. 2016, Rauner, Kohr 2011, Tovar, McGinley et al. 2013, Hatton, Paoletti 2005, Brickley, Misra et al. 2003, Jones, Gibb 2005, Brothwell, Barber et al. 2008, Chazot, Stephenson 1997). The relative contribution of diheteromeric and triheteromeric NMDARs during synaptic transmission is still not clear. NMDARs are distinct from AMPA and kainate receptors in that (i) require simultaneous binding of two distinct agonists, glycine (or D-serine) and L-glutamate for channel activation, (ii) also require several simultaneous excitatory inputs to sufficiently depolarize and relieve Mg^{2+} blockade (Mayer, Westbrook et al. 1984, Nowak, Bregestovski et al. 1984) and hence NMDAR functions as a molecular coincidence detector (Bliss, Collingridge 1993, Paoletti, Bellone et al. 2013) (iii) they also have high Ca^{2+} permeability. Ca^{2+} acts as a NMDAR second messenger and activates a variety of Ca^{2+}-dependent signaling pathways that underlie synaptic plasticity under normal physiologic conditions (Lisman, Yasuda et al. 2012) and neuronal death under pathological conditions. NMDARs display remarkably slow activation and deactivation kinetics, which enable them to have distinct roles in coincidence detection in associative learning and to participate in oscillatory pattern generation. NMDAR activation is also voltage dependent, which provides an essential property for associative learning and oscillatory pattern generation.

A.
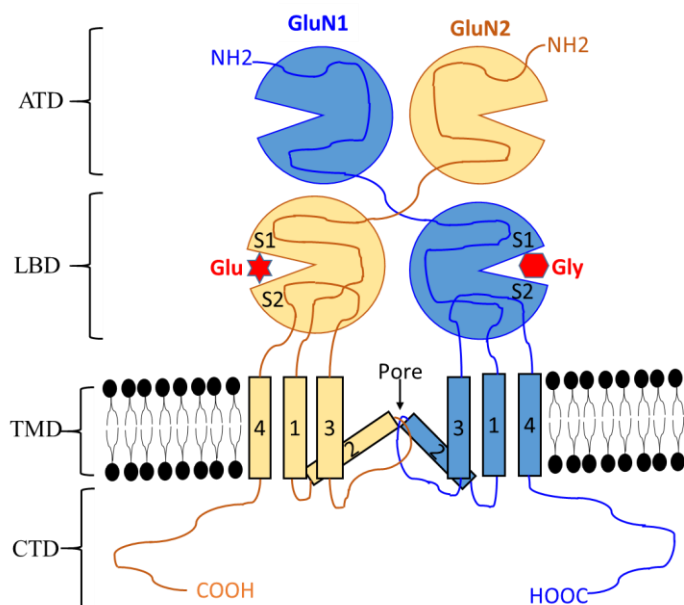
B.
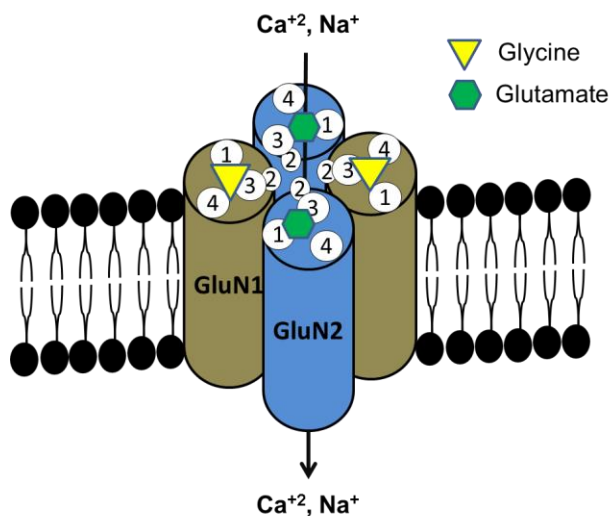
Figure 1.1 Schematic diagram of NMDAR structure

(**A**) Schematic representation of 4 modular domains: amino-terminal domain (ATD); ligand-binding domain (LBD), transmembrane domain (TMD) and C-terminal domain (CTD) of GluN1 and GluN2 subunits of NMDARs. (**B**) Schematic diagram of NMDARs subunit composition showing assembly of two glycine-binding GluN1 and two glutamate-binding GluN2 subunits forming a 'dimer of dimers' structure which is permeable to cations such as Ca^{2+}, Na^+ and K^+. Numbers 1-4 in each subunit represent the transmembrane domains (1, 3, and 4) and the re-entrant loop (2) lines the pore of the channel.

Each subunit of the NMDAR (or any ionotropic glutamate receptor) consists of four modular domains: (i) an extracellular amino-terminal domain (ATD), (ii) an extracellular ligand-binding domain (LBD), (iii) a pore-forming transmembrane domain (TMD) and (iv) a cytoplasmic C-terminal domain (CTD) as shown in the Figure 1.1. A crystal structure of GluN1/GluN2B with intact ATD, LBD and TMD shows that NMDARs are formed by dimers of heterodimers and that the ATD and LTD in NMDARs are more tightly packed than those of non-NMDARs (Karakas, Furukawa 2014). Previously reported high-resolution crystal structures of NMDARs with isolated ATDs and ABDs also have provided the information about the quaternary arrangements of subunits (Furukawa, Gouaux 2003, Furukawa, Singh et al. 2005, Karakas, Simorowski et al. 2009, Karakas, Simorowski et al. 2011, Farina, Blain et al. 2011). Although previous studies had suggested a possible arrangements of GluN1 and GluN2 subunits in 1-1-2-2- fashion (Schorge, Colquhoun 2003, Qiu, Hua et al. 2005, Papadakis, Hawkins et al. 2004), recent studies with cross-linked cysteine residues in NMDARs (Salussolia, Prodromou et al. 2011, Riou, Stroebel et al. 2012) as well as crystal structures, suggest that the GluN1 and GluN2 subunits in NMDARs are arranged in a 1-2-1-2 manner (Karakas, Furukawa 2014, Lee, Lü et al. 2014).

Both the ATD and LBD form bi-lobed clamshell structures and have sequence homology to bacterial periplasmic amino acid binding proteins. The extracellular ATD is the most diverse region with 20 - 35 % identical residues between functional classes of glutamate receptors (Hansen, Furukawa et al. 2010) and there is no sequence identity between NMDA and non-NMDARs. There is 35 - 55 % sequence identity among GluN2A-D NMDAR subunits and 15 % sequence identity between GluN1 and GluN2A-D subunits (Furukawa 2012). ATD in iGluRs harbors many putative sites for allosteric modulators (Hansen, Furukawa et al. 2010, Paoletti 2011, Gielen, Retchless et al. 2009).

The LBD is highly conserved among different subunits within different glutamate classes. Clampshell structure of the LBD is formed by S1 domain and S2 domain which form glycine binding site in GluN1 and glutamate binding site in GluN2 subunits. S1 segment is located on N-terminal side of M1 helix and forms the one half of the clamshell. The S2 segment is located between M3 and M4 helices and contributes to other half of the clamshell (Stern-Bach, Bettler et al. 1994). Each of the LBDs in iGluRs are connected to transmembrane helices by three short linkers (Sobolevsky, Rosconi et al. 2009) through which they control the gating of NMDAR channel pore (Kazi, Gan et al. 2013, Dai, Zhou 2013, Talukder, Wollmuth 2011). Glycine (Johnson, Ascher 1987, Kleckner, Dingledine 1988, Forsythe, Westbrook et al. 1988), and D-serine (Mothet, Parent et al. 2000, Martineau, Baux et al. 2006, Schell, Molliver et al. 1995, Yang, Ge et al. 2003) act as co-agonists of NMDARs. It is reported that glycine acts as a co-agonist at extra-synaptic NMDARs and D-serine at synaptic NMDARs (Papouin, Ladépêche et al. 2012). Other studies also provided evidence for glycine binding at GluN1 LBD (Hirai, Kirsch et al. 1996, Furukawa, Gouaux 2003, Kuryatov, Laube et al. 1994) and glutamate binding at GluN2 LBD of NMDARs (Furukawa, Singh et al. 2005, Laube, Hirai et al. 1997).

The TMD of NMDARs has 3 membrane passing segments (M1, M3 and M4) and one re-entrant pore loop (M2). The M2 loop of NMDARs has sequence and structural homolgy to the P-loop of potassium channels (Kuner, Seeburg et al. 2003, Wood, VanDongen et al. 1995). Variations in amino acid residues in the TMD are attributed to distinctive pore properties of NMDAR, AMPA receptors and KA receptors (Traynelis, Wollmuth et al. 2010). QRN site near the apex of the pore loop is important in controlling the permeability of cations through the channel. High Ca^{2+} permeability of NMDARs is attributed to DRPEER motif in GluN1 subunit, which serves as a binding site for Ca^{2+} and is located in the extracellular vestibule near C-terminal to the M3 helix (Watanabe, Beck et al. 2002). The M4 helix controls the assembly and trafficking of the receptors (Schorge, Colquhoun 2003, Kaniakova, Lichnerova et al. 2012).

Single amino acid residue (Ser632 in GluN2A and Leu657 in GluN2D) in the M3 region of

GluN2 subunits controls the NMDAR subtype-specificity of Ca^{2+} permeability, single-channel

conductance and Mg^{2+} block (Retchless, Gao et al. 2012). Also, the aspargine reside at the tip of

M2-loop, which lines the pore of the channel, is important for Ca^{2+} permeabilty and Mg^{2+} block

of NMDARs (Kuner, Wollmuth et al. 1996, Wollmuth, Kuner et al. 1998). TMD contains binding

sites for NMDAR channel blockers such as PCP, ketamine and MK-801. Amino acids residues at

or near Q/R/N site or along the permeation pathway are critical for block by these channel

blockers (Kashiwagi, Masuko et al. 2002, Mori, Masaki et al. 1992, Chen, Lipton 2005,

Limapichat, Yu et al. 2012, Chang, Kuo 2008, Sakurada, Masu et al. 1993).

The intracellular CTD is the most diverse region between different subunits of NMDARs

not only in the amino acid sequence but also in length. This region contains binding sites for

intracellular proteins involved in receptor trafficking, localization and signaling (Lau, Zukin

2007, Collingridge, Isaac et al. 2004). A motif (HLFY) in the CTD of GluN2 subunit

immediately after the M4 helix is important for the release of NMDARs from endoplasmic

reticulum (Hawkins, Prybylowski et al. 2004). The CTD also has multiple phosphorylation sites.

The CTD of GluN2A and GluN2B are targets for CaM Kinase II, tyrosine kinase, protein kinase

C and protein kinase A (Omkumar, Kiely et al. 1996, Wang, Salter 1994, Moon, Apperson et al.

1994, Tingley, Ehlers et al. 1997, Leonard, Hell 1997). In the GluN1 CTD, PKC phosphorylates

S890 and S896 residues and PKA phosphorylates S897 residues (Tingley, Ehlers et al. 1997,

Sánchez-Pérez, Felipo 2005). Similarly, in GluN2A CTD, PKC phosphorylates at S1291, S1312

and S1416 (Gardoni, Bellone et al. 2001, Jones, Leonard 2005) and PKA phosphorylates at S900

and S929 (Krupp, Vissel et al. 2002). In GluN2B CTD, PKC phosphorylates at S1303 and S1323

(Omkumar, Kiely et al. 1996, Liao, Wagner et al. 2001) and CaM kinase II at S1303 residue

(Omkumar, Kiely et al. 1996). Other novel phosphorylation sites on GluN2A- and GluN2B-

containing hippocampal NMDARs have also been identified using mass spectrometry (Ghafari,

Höger et al. 2012). The CTD of GluN1has has also been shown to reduce mean open time and channel open probability (P_{open}) through Ca^{2+} dependent calmodulin binding (Ehlers, Zhang et al. 1996) . It is believed that the NTD modulates agonist potency, deactivation time, P_{open} and mean open/shut time (Yuan, Hansen et al. 2009, Gielen, Retchless et al. 2009). However, the CTD can also regulate the gating properties of NMDARs. GluN2 CTD deletion increases the glutamate deactivation time and reduces the peak P_{open} of synaptic NMDARs and NMDARs expressed in HEK cells (Mohrmann, Köhr et al. 2002, Rossi, Sola et al. 2002, Punnakkal, Jendritza et al. 2012).

1.1.2   Developmental expression of NMDARs in brain

The developmental expression pattern of different NMDAR subunits changes during postnatal life altering the properties of NMDARs. In general, in rodents there is greater expression of GluN2B, 2D and 3A in early life compared to the expression of GluN2A, 2C and 3B, which peak later in life (Laurie, Bartke et al. 1997, Wenzel, Fritschy et al. 1997). There is a regional variation in gene expression of these subunits as well (Goebel, Poosch 1999, Monyer, Burnashev et al. 1994). The GluN2D protein expression is high in embryonic days, reaches its peak level at P7 and reduces in adulthood. In contrast, GluN2C is absent in embryonic brain, starts increasing after P6, peaks at P20 and remains at steady levels afterwards (Laurie, Bartke et al. 1997). GluN2A receptors are predominantly expressed in cortex, hippocampus and cerebellum and GluN2B are highly distributed in forebrain areas. GluN2C-containing receptors are mainly expressed in cerebellum and GluN2D subunits are expressed in midbrain and thalamus (Monyer, Sprengel 1992).

1.2   Schizophrenia

NMDARs are involved in a variety of neurological and neuropsychiatric disorders. In particular, NMDAR involvement in schizophrenia suggests that it may be possible to treat schizophrenia with NMDAR modulating agents. The goal of Chapter 2, is to determine if GluN2D subunits contribute to schizophrenia related neuronal activation and behaviors induced by NMDAR antagonists. Thus, a brief overview of the relevant pathophysiology of schizophrenia is presented here. Such findings would suggest that GluN2D potentiators may be useful for treating schizophrenia.

Schizophrenia is a chronic psychiatric disorder, which affects nearly 1 % of the population worldwide. It is a complex trait that results from both genetic and environmental etiological factors (Sullivan, Kendler et al. 2003). People with schizophrenia show three categories of symptoms: 1) positive- hallucinations, delusions and thought disorder 2) negative- anhedonia, deficit in social interaction, depression and 3) profound cognitive deficits in attention, learning and memory (Robert Freedman 2003). For decades, schizophrenia research was mainly focused on the dopamine hypothesis, which postulates that schizophrenia symptoms arise from excessive dopaminergic neurotransmission mainly in the striatum and a deficit in dopaminergic transmission in frontal brain areas such as prefrontal cortex (PFC) (Davis, Kahn et al. 1991). However, studies have shown that blocking of dopamine receptors has been able to improve only the positive symptoms of schizophrenia and not improve the negative and cognitive symptoms. Thus, current therapies are usually sufficient to allow schizophrenia patients to leave the hospital, but not sufficient for them to maintain jobs and social relationships. Amphetamine induces only positive symptoms of schizophrenia and (Davis, Chen et al. 2003) clozapine does enhance PFC activity by an unknown mechanism and this agent has some beneficial effects on negative and cognitive schizophrenia symptoms. Since antipsychotics typically are effective in treating positive symptoms only, dopamine alone cannot account for all of the neuropathological

symptoms of schizophrenia. Hence, involvement of another neurotransmitter in schizophrenia has been sought and growing body of evidence implicates NMDAR hypofunction in the pathophysiology of this disease.

1.2.1 *NMDAR hypofunction in schizophrenia*

The NMDAR hypofunction hypothesis of schizophrenia is mainly derived from the evidence of psycho-behavioral effects of NMDAR antagonists phencyclidine (PCP) and ketamine (Javitt, Zukin 1991, Tamminga 1999, Anis, Berry et al. 1983). These compounds were able to cause schizophrenia-like symptoms in healthy individuals and exacerbated the symptoms in people with schizophrenia (Krystal, Karper et al. 1994). A sub-anesthetic dose of ketamine in healthy subjects produces a broad range of symptoms, behaviors and cognitive deficits similar to that seen in schizophrenics (Krystal, Karper et al. 1994, Lahti, Koffel et al. 1995, Malhotra, Pinals et al. 1997). NMDAR channel blockers like ketamine- and PCP-induced psychotic disorders that more broadly mimic the diverse symptoms of schizophrenia-thought disorder, cognitive disorder and negative symptoms than that seen with amphetamine induced psychosis (Abel, Allin et al. 2003, Lahti, Weiler et al. 2001, Morgan, Mofeez et al. 2004). Antipsychotics like clozapine and haloperidol were effective in reducing the symptoms induced by ketamine (Malhotra, Pinals et al. 1997, Lahti, Weiler et al. 2001, Oranje, Gispen-de Wied et al. 2002). Schizophrenia-like behavioral symptoms are displayed by the NMDAR hypofunction mouse model of reduced GluN1 expression (Mohn, Gainetdinov et al. 1999) and haloperidol and clozapine were able to rescue the associated deficits in prepulse inhibition (Duncan, Moy et al. 2006). Human studies also support the theory of reduced NMDAR function in schizophrenia. The activity of D-amino acid oxidase (DAAO) is increased and the level of the endogenous ligand for NMDARs, D-serine, is decreased in the brain and blood of schizophrenics (Madeira, Freitas et al. 2008, Hashimoto, Fukushima et al. 2003). This finding is supported by the finding that increasing the

level of the co-agonist D-serine has shown beneficial, but limited, effects in several clinical trials (Tsai, Lin 2010).

NMDAR hypofunction in schizophrenia might be due to reduced expression and/or activity of NMDARs particularly in GABAergic inhibitory interneurons (Snyder, Gao 2013). Since, single interneurons form connections with several pyramidal neurons, NMDAR hypofunction of a single interneuron may disinhibit the firing of several cortical pyramidal neurons (Homayoun, Moghaddam 2007). This response accounts for the ability of NMDAR antagonists to increase the general excitatory levels within the PFC as seen in fMRI studies in humans or [^{14}C]-2-deoxyglucose in rodent studies.

While aberrations in dopamine activity cannot explain all of the symptoms of schizophrenia, hypoactivation of NMDAR can explain all of the symptoms as well as explain the role of dopamine as it is regulated by NMDAR activity (in particular by GluN2D). Hence, the NMDAR hypofunction hypothesis (Figure 1.2), which relies primarily on reduced NMDAR-mediated neurotransmission particularly due to reduced NMDAR activity in PV-positive GABAergic interneuron and its possible role on etiology and pathology of the disease, has drawn much interest in this field.
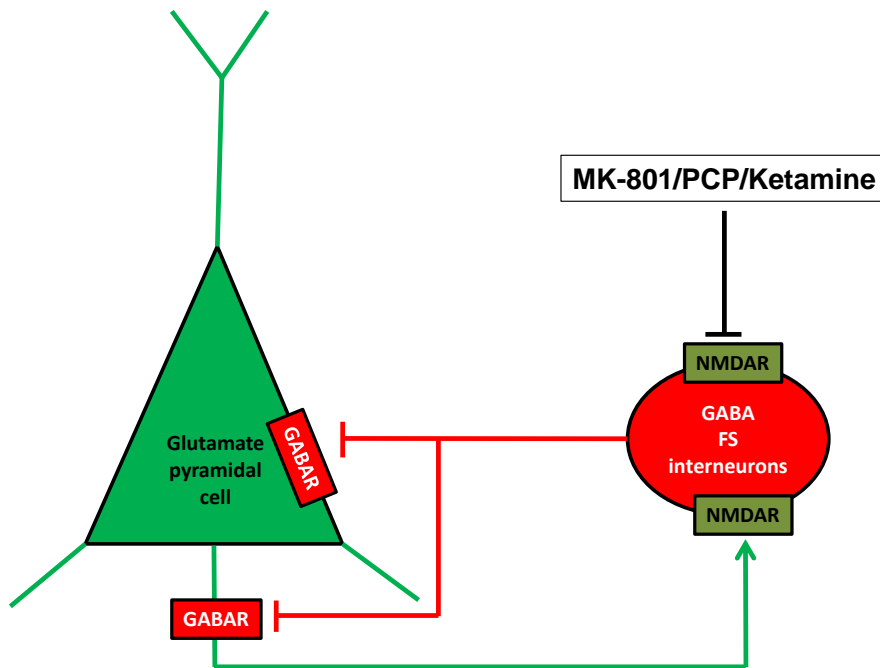
Figure 1.2 NMDAR hypofunction hypothesis of schizophrenia

During normal physiological condition, there is a balance between excitatory function of pyramidal cells and inhibitory function of GABAergic interneurons. However, during some pathological conditions such as schizophrenia, there is a reduction in inhibitory function by GABAergic interneurons which causes disinhibition of pyramidal cell's firing. Animal models of schizophrenia could be mimicked by blocking NMDARs in the GABAergic interneurons by open channel blockers like ketamine and MK-801, which also leads to a reduction in GABA release in the synapses thereby causing disinhibition of pyramidal cells.

1.2.2 *Genes associated with schizophrenia*

Gene association studies have identified several NMDAR-related risk genes that either directly or indirectly alter NMDAR function (e.g., DAAO - the D-serine metabolizing enzyme and ErbB4 - a protein that associates with PSD-95 and hence with NMDARs). Other schizophrenia-linked risk genes are GRIN2B; G72 (a gene encoding a protein that binds to DAAO), neuregulin-1 (modulates NMDAR activity), and dysbindin (which is concentrated in glutamatergic terminals) (Harrison, Weinberger 2004, Greenwood, Light et al. 2012, Harrison, Owen 2003, Allen, Bagade et al. 2008). In addition, GluN3A gene is increased in DLPFC in schizophrenia (Mueller, Meador-Woodruff 2004).

1.2.3   NMDARs in parvalbumin cells and schizophrenia

NMDARs in parvalbumin (PV)-containing GABAergic interneurons, are thought to be important in schizophrenia. PV-cells are fast spiking interneurons which express the calcium binding protein called PV and receive NMDAR-dependent excitatory input from pyramidal cells (Jones, Bühl 1993). Impairment in normal functioning of these fast spiking PV-cells is considered to underlie cognitive disturbance in psychiatric disorders (Uhlhaas, Haenschel et al. 2008, Roopun, Cunningham et al. 2008, Gonzalez-Burgos, Lewis 2008). PV-cells have neuronal network functions such as feedback and feed-forward inhibition, generation of gamma oscillations and transmission of information between cortical areas (Bartos, Vida et al. 2007). Synchronous neuronal activity of these cells produces gamma oscillations (30-80 Hz) (Sohal, Zhang et al. 2009, Cardin, Carlén et al. 2009), which are correlated with cognitive tasks like planning, learning, attention and memory (Uhlhaas, Singer 2010, Sohal, Zhang et al. 2009). Gamma oscillations are critical for the normal flow of neuronal activity within and between cortical regions, which is essential for cognitive processes (Fries 2009). NMDARs in PV-containing cells have been shown to be involved in potentiation or disruption of gamma rhythms. Selective deletion of NMDARs from PV-cells leads to deficit in gamma oscillation induction, and the development of schizophrenia-like phenotype (Carlen, Meletis et al. 2011, Korotkova, Fuchs et al. 2010, Belforte, Zsiros et al. 2009). Several possible mechanisms might be involved in the disruption of inhibitory function in schizophrenia, many of may converge to the PV-cells as a central player.

Various studies support the association between NMDAR function and PV-containing interneurons. Blocking of NMDAR activity reduces either the expression of PV or the number of PV-positive interneurons. Selective deletion of NMDARs from PV-containing cells leads to a deficit in gamma oscillation induction (Carlen, Meletis et al. 2011). A chronic administration of ketamine to rats reduces the number of PV-immunoreactive interneurons in the hippocampus of

rats, which is correlated with the strengthening of oscillations resulting from an acute administration of ketamine (Kittelberger, Hur et al. 2012). Reduced expression of PV and GAD67, an enzyme responsible for GABA synthesis in the brain, has been found in multiple studies involving postmortem brain from schizophrenics (Benes, Berretta 2001, Reynolds, Zhang et al. 2001, Lewis, Hashimoto et al. 2005, Hashimoto, Volk et al. 2003). Reduction of GAD67 occurs mainly in PV-positive interneurons (Beasley, Reynolds 1997, Hashimoto, Volk et al. 2003) and PV- positive interneuron loss occurs in mammillary bodies (Bernstein, Krause et al. 2007) and cortical layers III and IV (Beasley, Reynolds 1997). Similar changes occur with pharmacologically-induced NMDAR hypofunction. Ketamine also reduces the expression of PV and GAD67 in cultured neurons (Kinney, Davis et al. 2006). Likewise, a sub-chronic dose of PCP administration causes a deficit in the reversal of learning and a reduction in PV-positive interneurons in rat hippocampus (Abdul-Monim, Neill et al. 2007). Repeated administration of a sub-anesthetic dose of ketamine induces neuronal nitric oxide synthase and c-FOS gene expression in the hippocampus of rats (Keilhoff, Becker et al. 2004).

Treatment with NMDAR antagonists during early development or rearing in stressed environment also has an impact on PV-expression. Postnatal exposure to MK 801 reduces PV levels in the cingulate cortex (Turner, DeBenedetto et al. 2010). Rats treated with PCP in postnatal life (P7, 9 and 11) have reduced PV-positive cells in the mPFC as adults (Kaalund, Riise et al. 2013). Rearing rats in isolation also reduces the PV-expression in the adult hippocampus (Harte, Powell et al. 2007, Schiavone, Sorce et al. 2009) and rearing in an enriched environment increases the number of PV-positive cells in the basolateral amygdala and a reduction in anxiety-like behavior (Urakawa, Takamoto et al. 2013).

NMDAR activity is critical for maturation of PV cells during development. In mice, maturation of PV-interneurons begins at the end of 1st week of postnatal life (Lecea 1995, Doischer, Hosp et al. 2008). At P5, they start responding to glutamate and GABA transmission

and express PV by P7 (Lecea 1995, Sauer, Bartos 2010) and they mature into fast spiking inhibitory neurons in another three weeks (Okaty, Miller et al. 2009, Doischer, Hosp et al. 2008). Inhibitory networks play an important role in experience-dependent refinement of neuronal circuits, which starts at the end of 1st week and lasts through 4th week of postnatal life of rodents (Lema Tomé, Miller et al. 2008, Huang 2009). Hippocampal PV-interneurons, among all other interneuronal subtypes, receive the highest number of glutamatergic synapses from the thalamus (Gulyas, Megias et al. 1999). Expression of NMDARs in PV-cells is high in early postnatal life and undergoes profound functional changes during adolescence (Wang, Gao 2009). Studies also have shown that there is a switch in the subtype of GluN2 subunit expressed in PV-cells during development. This switch is also affected by treatment with NMDAR antagonists (Kinney, Davis et al. 2006, Zhang, Sun 2011). Taken together, the activity of NMDARs appears to be critical for the maturation process of PV-cells. Although there is no definite answer to why the level of PV in these cells goes down in schizophrenia, one possible explanation might be that PV expression is decreasing in response to a reduced excitatory drive from pyramidal cells after having a decreased calcium influx due to reduced NMDAR activity (Zhang, Behrens et al. 2008).

1.2.4   *Role of specific NMDAR subtypes in schizophrenia*

Different NMDAR subtypes have distinct anatomical and developmental patterns of expression and different physiological properties. Studies have measured the expression level of different subtypes of NMDARs in postmortem brain from schizophrenics. In thalamus from younger schizophrenics, there was an increase in GluN2B and a decrease in transcripts for the NMDARs associated proteins NF-L, PSD 95 and SAP 102 (Clinton, Meador-Woodruff 2004). The same researchers also reported that the thalamus from older schizophrenics have a reduced level of GluN1 and GluN2C and increased level of NF-L and SAP-102 transcripts (Clinton, Haroutunian et al. 2003). Although there was no difference in ligand binding to NMDA, AMPA and kainate receptors between post mortem hippocampal tissue of healthy people and schizophrenics, there

was lower GluN1 and higher GluN2B expression in schizophrenics (Gao, Sakai et al. 2000). GluN1 and GluN2A, but not GluN2B, expression was increased in the dorsolateral prefrontal cortex (DLPFC) and the occipital cortex of patients with schizophrenia (Dracheva, Marras et al. 2001). Reduced GluN1 mRNA in DLPFC and reduced GluN2C mRNA in frontal cortex schizophrenics was also reported (Weickert, Fung et al. 2013). Since GluN1 is critical for NMDAR activity, reduction in GluN1 subunits in the hippocampus of schizophrenia may suggest reduced NMDAR-mediated neurotransmission in the hippocampus and other brain regions, supporting the NMDAR hypofunction hypothesis of schizophrenia.

Various studies show how altering the levels of different NMDAR subunits can affect behavior and cognition in mice. GluN1 hypomorphic mice show social withdrawal, working memory and attention deficits, and basal metabolic reduction in the brain (Bickel, Lipp et al. 2007, Duncan, Miyamoto et al. 2002, Duncan, Moy et al. 2004, Halene, Ehrlichman et al. 2009). Transgenic mice with overexpressed GluN2B receptors in forebrain show enhanced performance in different learning and memory tests (Cao, Cui et al. 2007). In contrast, mice lacking GluN2C receptor subunits show deficits in associative and working memory suggesting its functional role in cognition, which is impaired in schizophrenia (Hillman, Gupta et al. 2011). It has been reported that postnatal ablation of GluN1 subunit selectively from cortical and hippocampal PV interneurons, results in schizophrenia-like symptoms after adolescence (Belforte, Zsiros et al. 2009). These mice show novelty-induced hyperlocomotion, a reduced preference for sweets (a model of anhedonia), a deficit in spatial working memory and impaired prepulse inhibition (PPI), reduced expression of PV and GAD67 in cortical neurons. However, they do not have such deficits if GluN1 is ablated at a post-adolescent age. Also, removing the GluN1 subunit from PV-cells impairs spatial working and spatial recognition memory (Korotkova, Fuchs et al. 2010). A targeted disruption of the GluN2A subunit in mice reduces NMDAR-mediated currents, reduces long-term potentiation (LTP) at the hippocampal CA1 synapses and moderately impairs spatial

learning (Sakimura, Kutsuwada et al. 1995). Mice lacking GluN2B in the forebrain have impaired

spatial and non-spatial memory (von Engelhardt, Doganci et al. 2008). NMDAR knockout (KO)

in the hippocampal CA1 region impairs reference memory (McHugh, Blum et al. 1996) whereas

deleting NMDAR in the hippocampal CA3 or DG region impairs working memory (McHugh,

Jones et al. 2007, Niewoehner, Single et al. 2007). PCP increases striatal dopamine release and

motor impairment in WT and GluN2A KO mice but not in GluN2D KO (Hagino, Kasai et al.

2010, Yamamoto, Kamegaya et al. 2013). Together, these studies provide genetic evidence of

NMDARs in behaviors that are impaired in schizophrenia. We can also observe in these studies

that different subunits of NMDAR are responsible for different aspects of behavioral and

cognitive impairments relevant to schizophrenia. This is the rationale for my Chapter 2 in which

we have tried to explore the role of GluN2D subunits in schizophrenia related behavioral,

neurological and cognitive impairments.

1.2.5   *Glutamatergic agents for schizophrenia treatment in future*

As discussed in previous sections, reduced NMDAR function is involved in pathophysiology of

schizophrenia. Other studies have implicated the reduced function of metabotropic glutamate

receptor in schizophrenia. Hence, drugs that enhance overall glutamatergic function could be

alternative or supplementary therapeutic agents for current antipsychotic treatments (Duncan,

Zorn et al. 1999, Goff, Coyle 2001). Use of allosteric modulators is a better option than the use of

agonists as therapeutics. Glutamate agonists would induce excitation of all glutamatergic

synapses, which would cause neuronal cell death by excitotoxicity and seizures. Studies have

shown beneficial effects after the treatment with agents that enhance NMDAR function. When

glycine, D-serine or D-cycloserine, which are NMDAR co-agonists, were administered as a

supplement to antipsychotic treatments in patients with schizophrenia, they were able to improve

negative and cognitive symptoms (Goff, Henderson et al. 1999, Goff, Tsai et al. 1999, Javitt,

Zylberman et al. 1994, Heresco-Levy, Javitt et al. 1999). As an alternative approach to increase

brain D-serine levels, it is possible to reduce the catabolism of D-serine by administration of the D-amino acid oxidase (DAAO) inhibitor AS057278. Interestingly, this agent normalizes PCP-induced behavioral deficits in mice. Combining a DAAO inhibitor with a low dose of D-serine shows superior activity than either agent alone in reducing NMDA antagonist MK-801 (dizocilpine)-induced deficit in prepulse inhibition (Hashimoto, Fujita et al. 2009, Adage, Trillat et al. 2008). Increasing the synaptic glycine level by use of a glycine reuptake inhibitor glycyldodecylamide inhibits PCP-induced hyper-locomotion more effectively than the direct use of glycine itself (Javitt, Sershen et al. 1997). Another approach to enhance glutamate receptor response would be to increase synaptic L-glutamate levels by using glutamate reuptake inhibitors, like EAAT3 antagonists. However, high levels of glutamate could be detrimental to normal functioning cells. NMDAR antagonist-induced behavioral effects such as hyper-locomotion and stereotypy (repetitive behavior) could also be due to the action of increased glutamate release, which may enhance the function of non-NMDARs like AMPA and kainate receptors. However, it has been found that blocking the activity of AMPA/kainate receptors by the antagonist LY-293558 can partially reverse ketamine-induced deficit in working memory (Moghaddam, Adams et al. 1997). Synaptic levels of L-glutamate can also be reduced by activation of presynaptic group II metabotropic glutamate autoreceptors (mGluR2/3). Activation of those receptors by LY-354740 reduces glutamate release and the behavioral activation induced by PCP in the rat (Moghaddam, Adams 1998).

1.3   Allosteric modulators of NMDARs

Under normal physiological conditions, NMDARs activate cellular signaling cascades important for growth, development, learning and memory. Under pathological conditions, it NMDARs can activate cellular signaling pathways that lead to excitotoxic neuronal cell death. Ca^{2+} entering through NMDARs activates Ca^{2+}/calmodulin-dependent protein kinase II (Giese, Fedorov et al. 1998, Lisman, Yasuda et al. 2012, Pettit, Perlman et al. 1994, Miller, Kennedy 1986), protein kinase A (Roberson, Sweatt 1996), protein kinase C (Malinow, Schulman et al. 1989, Malinow, Madison et al. 1988, Lovinger, Wong et al. 1987) and phosphoinositide-3-kinase (PI3K) (Kim, Lee et al. 2011, Man, Wang et al. 2003) which are important in causing long-term changes in synaptic strength during development as well as during the process of learning and memory. However, in pathological conditions such as in ischemia, there is increased release of glutamate (Benveniste, Drejer et al. 1984, Nilsson, Hillered et al. 1990, Qureshi, Ali et al. 2003, Kanthan, Shuaib et al. 1995) that causes hyperactivation of NMDARs leading to excitotoxicity and cell death (Choi 1988, Choi, Maulucci-Gedde et al. 1987, Choi 1992, Olney 1969, Rothman, Olney 1987). Early studies, showing that the blockade of NMDAR activity can protect against neurological damages in ischemia and brain injury, were (Faden, Demediuk et al. 1989, Ozyurt, Graham et al. 1988, Simon, Swan et al. 1984, Swan, Meldrum 1990, McIntosh, Vink et al. 1989). However, no related therapeutic agents have made to the clinic for these indications.

Until today, very little progress has been made in the development of NMDAR modulators. Still, most of the compounds, which had been shown to be effective in preclinical studies, are unable to translate into therapeutic benefit in humans. One of the reasons for this might be that the blockade of all NMDARs may cause undesired side effects such as psychotomimetic effects. Also, these antagonists non-selectively block all NMDARs throughout the brain both hyper-activated and normal functioning receptors in healthy brain areas. If we could block only the over-activated NMDARs that are responsible for pathology, without having

any effect at inactive receptors, or normal-functioning receptors, it should be possible to improve the therapeutic benefit to side effect ratio. Also, as discussed before, there is hypoactivation of NMDAR function in schizophrenia. Thus, selectively enhancing the activity of those NMDARs responsible should be beneficial. Hence, a drug that acts at allosteric sites and targets a specific NMDAR subunit should be beneficial for both of these scenarios and they should display fewer side effects compared to the side effects from the use of channel blockers or competitive antagonists. This type of drug would not only be an important agent in treating pathological conditions, but also would serve as a valuable tool for experimental purposes. Recent progress in NMDAR modulators has been reviewed (Monaghan, Irvine et al. 2012).

1.3.1 *Positive allosteric modulators (PAMs) of NMDARs*

Compounds that bind to an allosteric site and enhance NMDAR activity are called positive allosteric modulators (PAMs) of NMDARs. Since these types of modulators often have an increased therapeutic/toxicity ratio, interest in finding allosteric modulators is growing. Such NMDAR PAMs may be helpful in treating schizophrenia where there is evidence of hypofunction of these type of receptors (Olney, Newcomer et al. 1999).

Various NMDAR PAMs have been identified in the last few years. Different studies have been conducted to identify the structural features required for potentiating activity and to identify their binding sites. The pyrrolidone derivative PYD-106 is a GluN2C selective PAM, which binds at the ATD/LBD interface of GluN2C-containing NMDARs (Khatri, Burger et al. 2014). PYD-106 binds to the ATD and S1 domains of GluN2C receptors (Khatri, Burger et al. 2014). CIQ is another PAM that acts at GluN2C/GluN2D-containing NMDARs (EC_{50} of 2.7 μM at GluN2C and 2.8 μM at GluN2D) (Mullasseril, Hansen et al. 2010) and Thr592 in the M1 region of GluN2D and the linker region between LBD and NTD is critical for CIQ activity (Mullasseril, Hansen et al. 2010). The helical segment before M1 in GluN2D subtypes of NMDAR is also critical for the activity of CIQ (Ogden, Traynelis 2013). One structural modification of CIQ by replacing

chlorine with the bromine, makes it more GluN2C- ($EC_{50} = 90$ nM) than GluN2D- preferring ($EC_{50} = 220$ nM) (Santangelo Freel, Ogden et al. 2013). Similarly, GNE-6901 is a GluN2A-selective PAM which has an EC_{50} value of 330 nM (Hackos, Lupardus et al. 2016). However, it also displays significant potentiating activity at GluN2D receptors as well. X-ray crystallography shows that this compound binds at the GluN1/GluN2A dimer interface of the ligand binding domains (LBDs) (Hackos, Lupardus et al. 2016). Other GluN2A-selective PAMs, such as GNE-0723, with higher potency have also been identified ($EC_{50} = 210$ nM at GluN2A) (Volgraf, Sellers et al. 2016).

Polyamines such as spermine and neurosteroids such as pregnenolone sulfate (PS) are endogenous modulators of NMDAR. Spermine selectively potentiates GluN1/GluN2B receptors with an EC_{50} of more than 100 µM (Benveniste, Mayer 1993, Traynelis, Hartley et al. 1995). These compounds are thought to bind at the heterodimer interface of GluN1/GluN2B NTD and by binding to the negatively charged amino acid residues in lower lobe. By binding at this location, they appear to block the NTD clamshell closure thereby causing NMDAR current potentiation (Mony, Zhu et al. 2011). Mutation of aspartate residue 669 in the extracellular loop of heteromeric GluN1a reduces the potentiation by spermine and inhibition by protons and ifenprodil (Kashiwagi, Fukuchi et al. 1996).

Recently, our group has identified a diverse series of NMDAR PAMs with a unique pattern of subunit selectivity. Phenanthrene derivatives with a carboxylic acid group at the 3-position have NMDAR current-enhancing activity. The UBP512 selectively potentiates the GluN2A subtype of NMDARs but inhibits GluN2C and GluN2D-containing NMDARs. Similarly, UBP710 potentiates GluN2A and GluN2B subtypes of NMDARs whereas it inhibits GluN2C and GluN2D subtypes at higher doses. Naphthalene derivatives with a 2-position carboxyl group also display NMDAR PAM activity. UBP551 selectively potentiates GluN2D while inhibiting the other three subtypes of NMDARs (Costa, Irvine et al. 2010). This is the only

known compound so far with selective GluN2D PAM activity. The mechanisms of action and possible binding site for these compounds is a focus of our current studies. These compounds act in a non-competitive and voltage-independent manner. We also observed that the S2 and S1 segments of ligand binding domain were important for subunit-specific potentiating and inhibitory activity, respectively, and that the N-terminal domain is not required for either types of NMDAR activity (Costa, Irvine et al. 2010). These compounds also do not bind to the channel pore. Hence, a possible binding site for these compounds was predicted to be in LBD dimer interface.

In this current project, we have characterized another series of 2-naphthoic acid analogues as NMDAR PAMs and have identified compounds such as UBP684 and UBP753 with greater PAM activity (greater % of maximal efficacy; E_{Max}) at each of the four NMDAR subtypes. The mechanisms of allosteric modulation and enhancement of NMDAR function by these compounds are discussed in Chapter 4. Possible binding sites of NMDAR allosteric modulators with both PAM and NAM activity, as well as of competitive antagonists and channel blockers, are shown in Figure 1.3.
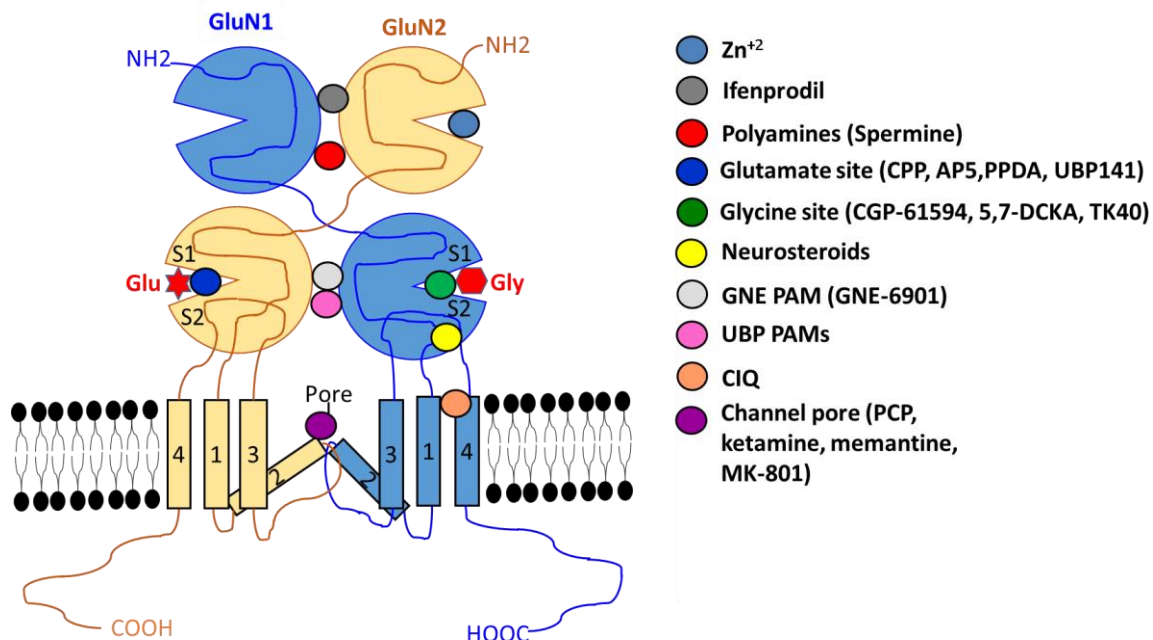
Figure 1.3 Potential binding sites of NMDAR allosteric modulators, competitive antagonists and channel blockers

Schematic diagram of GluN1/GluN2 dimer structure of NMDARs displaying known and predicted binding sites for different NMDAR PAMs, NAMs, competitive antagonists and channel pore blockers.

1.3.2   *Negative allosteric modulators (NAMs) of NMDARs*

Although optimal activity of NMDAR is crucial for maintaining normal brain function, hyperactivity of NMDAR function will lead to excitotoxicity. In such cases, drugs that inhibit activated NMDARs would be therapeutically beneficial. Inhibitory modulators that bind to sites other than orthosteric sites are called NMDAR negative allosteric modulators (NAMs). Since NAMs do not bind to agonist binding site, which is highly conserved among NMDAR subunits, it provides a high opportunity for getting subtype selectivity.

Compounds such as ifenprodil and ions such as protons and Zn^{2+} have long been known for their allosteric inhibitory activity at NMDARs (Williams 1993, Traynelis, Cull-Candy 1990, Traynelis, Hartley et al. 1995, Peters, Koh et al. 1987, Chen, Moshaver et al. 1997). Zn^{2+} inhibits

only GluN2A-containing receptors in nano-molar concentration and inhibits both GluN2A- and GluN2B-containing receptors in micromolar concentration (Paoletti, Perin-Dureau et al. 2000, Low, Zheng et al. 2000, Rachline, Perin-Dureau et al. 2005). Ifenprodil selectively inhibits the GluN2B-containing receptors.

Progress has been made in the last few years in the development of subunit selective and more potent NMDAR NAMs. A quinazolin derivative QNZ46 allosterically inhibits GluN2C/2D-containing NMDARs (Mosley, Acker et al. 2010) and is believed to bind to the amino acid residues located in ligand binding domain near the interface with TMD (Hansen, Traynelis 2011). TCN201 and TCN213 are GluN2A specific NAMs which are believed to bind at the heterodimer interface of both ligand binding domains (LBDs) of GluN1/GluN2A receptors (Bettini, Sava et al. 2010). TCN201 requires glycine for its activity but is a non-competitive NMDAR antagonist (Edman, McKay et al. 2012). Similarly, DQP-1105 is a GluN2C/2D selective non-competitive NAM (Acker, Yuan et al. 2011). The anti-inflammatory drug sulfasalazine (Noh, Gwag et al. 2006) and hydrophobic anion dipicrylamine (DPA) (Linsenbardt, Chisari et al. 2013) also have non-competitive antagonistic action at NMDARs.

Our group has recently identified other NAMs with unique subunit selectivity. We synthesized and characterized different coumarin and 2-naphthoic acid derivatives for their NAM activity. A coumarin carboxylic acid derivative UBP608 inhibits GluN2A-containing receptors with 23-times more selectivity compared with GluN2D-containing receptors (Costa, Irvine et al. 2010) and when substituted with methyl group at 4-position of naphthalene ring, it yielded a allosteric potentiator (UBP 714) (Irvine, Costa et al. 2012). We also have identified naphthalene derivatives such as UBP618 and UBP552 as general NMDAR NAMs with high potency (Costa, Irvine et al. 2012).

New novel NAMs with higher GluN2C- and GluN2D- selectivity over GluN2A- and GluN2B-containing NMDARs have been characterized which are described in the following chapters. We selected one prototype compound, UBP792, from the series and studied the mechanisms of its allosteric inhibition at recombinant NMDARs expressed in *Xenopus laevis* oocytes as discussed in Chapter 5.

1.3.3   Allosteric modulation of NMDARs by neurosteroids

Neuroactive steroids have long been recognized as allosteric modulators of ionotropic glutamate and GABA receptors. They can be synthesized endogenously in neural tissues and have sites of action within the nervous system as well (Gibbs, Russek et al. 2006, Korinek, Kapras et al. 2011). Endogenous neurosteroids such as pregnenolone sulfate (PS, 3β-hydroxypregn-5-en-20-one-sulfate) and pregnanolone sulfate (PAS, 3α-hydroxy-5β-pregnan 20-one sulfate;3α5βS) are important for maintaining the excitatory and inhibitory balance in central nervous system since they exhibit both PAM and NAM activity at different receptors inside CNS.

Considerable interest has been shown on neurosteroids research (mainly PS and PAS) focusing on their mechanisms of action and their *in vivo* effect after the discovery that PS potentiated the NMDAR current in spinal cord neuron from chick embryos (Wu, Gibbs et al. 1991). PS inhibits non-NMDA glutamate receptors (AMPA, kainate), GABA-A, glycine and nicotinic receptors. However, it was found to potentiate agonist-induced responses at neuronal NMDARs (Wu, Gibbs et al. 1991) as well as GluN2A- and GluN2B-containing recombinant NMDARs (Malayev, Gibbs et al. 2002, Horak, Vlcek et al. 2006). PS potentiates the glutamate response at GluN2A- and GluN2B-containing receptors by five to eight fold compared to GluN2C and 2D-containing receptors (Horak, Vlcek et al. 2006). The neurosteroid chemistry determines the type of their activity (Kostakis, Smith et al. 2013). The inhibitory neuro-steroid PAS, which inhibits all NMDAR subtypes, is 4-fold more potent at GluN2C- and GluN2D- than at GluN2A- and GluN2B-containing NMDARs (Malayev, Gibbs et al. 2002).

Potentiating activity of PS is dis-use dependent (Horak, Vlcek et al. 2004) (affinity is higher in absence of agonist) while the inhibitory activity of PAS is use dependent (pre-application does not increase subsequent agonist response) (Petrovic, Sedlacek et al. 2005). PS dissociates faster from its inhibitory binding site (Horak, Vlcek et al. 2004) than its potentiating site (Horak, Vlcek et al. 2006). The mechanism of potentiation by PS is by increasing the peak channel open probability (P_{open}) (Horak, Vlcek et al. 2004) and the activity is PKA dependent (Petrovic, Sedlacek et al. 2009). The mechanism of NMDARs inhibition by PAS is by increasing the mean time in closed state and promoting the desensitized conformations of active receptors (Kussius, Kaur et al. 2009).

Different studies have tried to identify the possible binding site of PS and PAS at NMDARs although the precise binding site location is unknown. The M3-M4 loop is important for both potentiating and inhibitory action of PS (Horak, Vlcek et al. 2006). Another group reported that the SMD1 region (J/K helices in S2 domain and the M4 domain) is critical for PS potentiating activity (Jang, Mierke et al. 2004). Replacing this region in GluN2B with the corresponding region from GluN2D changes the potentiating activity of PS to inhibitory. Since, PS actions are voltage-independent and thus do not appear to bind within the receptor's channel pore (Malayev, Gibbs et al. 2002, Park-Chung, Wu et al. 1997). Also, PS does not compete with spermine or arachidonic acid for potentiating activity (Park-Chung, Wu et al. 1997). The sites for NAM and PAM activity of neurosteroids are also different. Point mutation (D813A/D815A) of residues preceding M4 prevents PS potentiation but not PAS inhibition. A GluN2A-A651T point mutation in SYTANLA<u>A</u>F at M3/S2 linker region reduces PAS inhibition but not PS potentiation (Kostakis, Jang et al. 2011). These findings are consistent with previous findings from our laboratory that replacing S2 domain in GluN2A with the S2 domain from GluN2C eliminated UBP512 and UBP710 potentiation on GluN2A but did not change the UBP608 inhibition (Costa, Irvine et al. 2010). The site of action of inhibitory neurosteroid PAS is located at extracellular

vestibule of the receptor's channel pore which is accessible only when the receptor is activated (Vyklicky, Krausova et al. 2015).

Attempts have been made at synthesizing steroid analogues with greater potency than that of PS. Kudova *et al.* synthesized a steroidal analogues that was more potent ($IC_{50} = 90$ nM) than PS at NMDARs (Kudova, Chodounska et al. 2015). This compound crosses the blood brain barrier (Rambousek, Bubenikova-Valesova et al. 2011) and reverses the excitotoxicity-induced damage and cognitive deficits in an animal model of schizophrenia (Vales, Rambousek et al. 2012).

1.3.4   *Allosteric modulation of NMDARs by protons*

The pH in the brain is altered during pathological conditions such as ischemia or schizophrenia. Acidification occurs in ischemia (Nemoto, Frinak 1981, Matsumoto, Obrenovitch et al. 1990) and schizophrenia (Torrey, Barci et al. 2005, Prabakaran, Swatton et al. 2004, Lipska, Deep-Soboslay et al. 2006, Halim, Lipska et al. 2008). Since the change in pH affects the activity of NMDARs as well as the activity of drugs at those receptors, we sought to find out the effect of different extracellular pH on the activity of UBP PAMs and NAMs, which are described in Chapters 4 and 5 respectively.

Extracellular, but not the intracellular, protons inhibit NMDARs in a voltage-independent and non-competitive manner (Traynelis, Cull-Candy 1990, Tang, Dichter et al. 1990) and this might be an endogenous mechanism of protection from excitotoxic neuronal death during ischemia as well as in other pathological conditions such as seizures which are characterized by acidosis in extracellular environment. Proton inhibition depends upon the types of GluN1variants as well as GluN2 subtypes. The GluN1-1b subunit (presence of exon-5) which has 21 extra amino acid residues in N-terminal domain (Durand, Gregor et al. 1992) is less sensitive to the tonic proton inhibition because those extra residues shield or cover the proton sensor site thereby

decreasing the proton sensitivity and increasing the current follow through the receptor

(Traynelis, Hartley et al. 1995). Proton sensitivity is subunit dependent. The GluN2C subunit is

the least sensitive (IC_{50} = pH 6.2) while GluN2B and GluN2D subunits are the most sensitive to

protons inhibition (IC_{50} = pH 7.3) (Traynelis, Hartley et al. 1995). The linker region between M3

and S2 segment of glycine binding site on GluN1 and the linker region between M4 and S2

portion of glutamate binding site on GluN2 controls the pH sensitivity. A mutagenesis study

showed that a mutant mGluN1 (A649C)/GluN2A (A651C) receptor has 145-fold reduction in the

IC_{50} for protons compared to wild type receptors (Low, Lyuboslavsky et al. 2003).

Protons not only affect the NMDAR function but also affect the activity of NMDAR

modulators such as PS and spermine. Protons affect the PS activity in a subunit dependent

manner. The potentiating activity of PS at GluN2B-containing receptors is independent of pH and

independent of exon-5 (Jang, Mierke et al. 2004, Kostakis, Jang et al. 2011) while at GluN2A

receptors, it is pH dependent (Kostakis, Jang et al. 2011) and the PS potentiation is higher at

lower pH like that of spermine. The inhibitory effect of PS at GluN2D is pH dependent and

enhanced by exon-5 while at GluN2C, PS inhibition is pH independent (Kostakis, Jang et al.

2011). Similarly, the inhibitory activity of PAS is independent of both pH and exon-5. Besides

pH, Ca^{2+} also affects the potentiation by the PS at GluN2A receptors (Chopra, Monaghan et al.

2015).

There are multiple drug targets for both types of the NMDAR allosteric modulators.

There are very few available drugs like memantine which are effective in neurological disorders.

Hence, there is a need of NMDAR subunit specific modulators for different neurological

diseases. We are potentially interested in developing GluN2D-specific NMDAR potentiators for

treating schizophrenia or autism spectrum disorder. So, an initial goal of my dissertation research

is to evaluate the role of GluN2D-containing NMDARs in schizophrenia related neuronal

functions and to characterize a potent, subunit selective NMDAR PAM.

1.4   Competitive antagonists of NMDARs

Competitive antagonists are the compounds that compete with endogenous ligands for binding at orthosteric site. As discussed before, GluN1 has a binding site for glycine and GluN2 has a binding site for L-glutamate. Since, four different genes encode for the GluN2 family, and GluN2 subunits confer different pharmacological and physiological properties to NMDARs, there is great potential for pharmacological modulation and distinction among four different NMDAR subunits (Monyer, Burnashev et al. 1994, Monyer, Sprengel 1992, Ishii, Moriyoshi et al. 1993, Buller, Larson et al. 1994). Development of antagonists for blocking glutamate-induced neurotransmission started after the discovery that compounds like α,ε-diaminopimelic acid, D-α-aminodipate and HA-966 inhibit glutamate-induced responses in isolated spinal cord from frogs and rat and mammalian spinal neurons (Evans, Francis et al. 1978, Biscoe, Evans et al. 1977).

Many NMDAR antagonists competing at the glutamate binding site have been developed (Figure 1.4A). NMDAR antagonist activity was observed for compound (*RS*)-α-AA, which was obtained by adding one extra carbon in the glutamate structure (Hall, McLennan et al. 1977). Replacement of ω carboxy group of (*R*)-α-AA with a phosphonate group gave compound D-AP5 (Evans, Francis et al. 1982) (Figure 1.4A). More potent antagonists such as CGS19755 and CPP were derived by incorporating the piperidine and piperazine rings to D-AP5 and D-AP7 respectively (Harris, Ganong et al. 1986, Davies, Evans et al. 1986). However, these glutamate site antagonists show weak subunit selectivity and the pattern of antagonism by such antagonists as CPP, D-AP5 and CGS-19755 was in the following order: GluN2A > GluN2B > GluN2C > GluN2D (Feng, Morley et al. 2005, Feng, Tse et al. 2004). However, NVP-AAM077, quinoxaline-2,3-dione derivative, displayed unusual selectivity for antagonism at GluN2A-containing receptors (Auberson, Allgeier et al. 2002). It was 100-fold more selective for human GluN2A- than GluN2B-containing NMDARs. However, in rodents, it is only 7-10 fold selective for GluN2A over GluN2B-containing receptors (Feng, Morley et al. 2005). Another compound,

PBPD, displayed higher affinity for GluN2B- and GluN2D-containing NMDARs (Buller, Monaghan 1997) and the antagonist PPDA, a derivative of PBPD, showed higher affinities for GluN2C and GluN2D and lowest affinity for GluN2A subunit-containing NMDARs (Feng, Tse et al. 2004, Morley, Tse et al. 2005). UBP141 and UBP145, derived from the structural modification of PPDA, although less potent than PPDA, displayed higher selectivity for GluN2D- and GluN2C- than for GluN2B- and GluN2A-containing NMDARs (Morley, Tse et al. 2005, Costa, Feng et al. 2009). There affinities were in the following order: GluN2D> GluN2C >GluN2B> GluN2A. Currently UBP141 and UBP145 are the most selective GluN2C/2D antagonists and they are widely used in research. However, they display only weak selectivity. In an attempt to develop even more potent and selective competitive antagonists, we have developed another series of PPDA derivatives, which interact at the glutamate binding site; these results are presented in Chapter 3.

Other competitive antagonists of NMDAR interact at the glycine binding site of the GluN1 subunit (Figure 1.4B). The first identified glycine site competitive antagonist was kynurenic acid (Watson, Hood et al. 1988). Modification of the kynurenic acid structure led to other potent competitive antagonists such as 5,7-DCKA (Leeson, Baker et al. 1991). The subunit selective photoaffinity label glycine site antagonist [^{3}H]CGP 61594 was also developed. This antagonist (CGP 61594) shows higher affinity for inhibition at GluN2B than at GluN2A-containing NMDARs (Benke, Honer et al. 1999, Honer, Benke et al. 1998). TK-40 is another glycine site antagonist with K_b values of 21- 63 nM at GluN1 glycine binding site of the four subtypes (GluN2A-D) of NMDARs (Kvist, Steffensen et al. 2013). It is >100 fold selective for GluN1/GluN2 receptors compared to GluN3A and GluN3B receptors.

A.

D-AP5

D-AP7

CPP

(R)-CPPene

CGS 19755

NVP-AAM007

(-) PPDA (UBP150)

UBP141

UBP145

B.

CGP-61594

5,7-DCKA

TK40
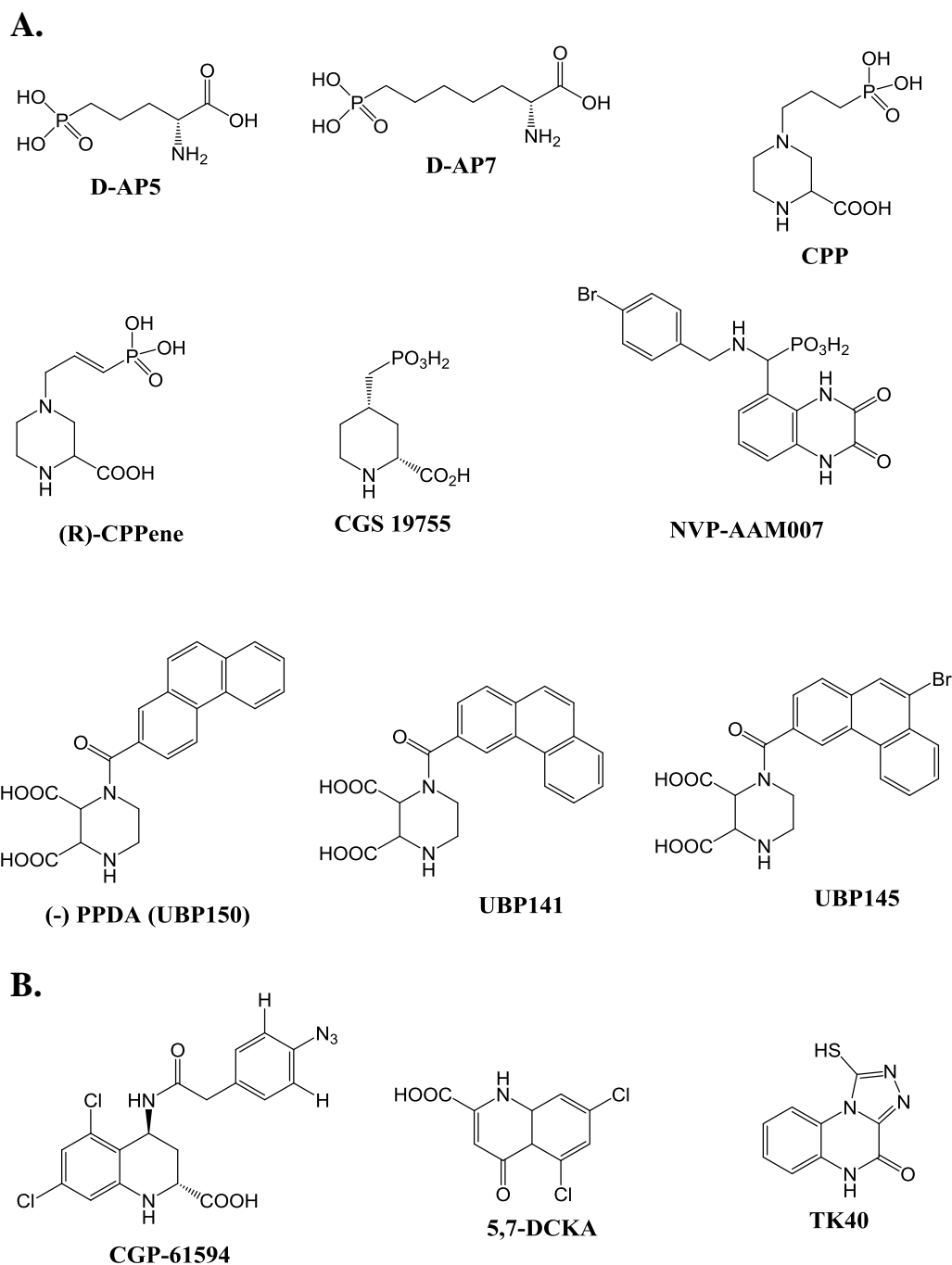
Figure 1.4 Chemical structures of known NMDAR competitive antagonists

(**A**) NMDAR antagonists interacting with the L-glutamate binding site on GluN2 subunit. (**B**) NMDAR antagonists interacting with glycine binding site on the GluN1 subunit.

Chapter 2 Evaluation of GluN2D as a potential target for treating schizophrenia

This chapter includes the following published manuscript (Sapkota, Mao et al. 2016):

Sapkota, K; Mao, Z; Synowicki, P; Lieber, D; Liu, M; Ikezu, T; Gautam, V; Monaghan, D. GluN2D N-methyl-D-aspartate subunit contribution to the stimulation of brain activity and gamma oscillations by ketamine: implications for schizophrenia. *Journal of Pharmacology and Experimental Therapeutics.*2016; 356:702-712.

2 GluN2D NMDAR subunit contribution to the stimulation of brain activity and gamma oscillations by ketamine; implications for schizophrenia

Kiran Sapkota, MS, Zhihao Mao, Paul Synowicki, Dillon Lieber, Meng Liu, Tsuneya Ikezu,

M.D., Ph.D., Vivek Gautam, Ph.D., and Daniel T. Monaghan, Ph.D.

Department of Pharmacology and Experimental Neuroscience, University of Nebraska Medical

Center (K.S., Z.M., P.S., D.L., M.L., D.T.M.); Department of Pharmacology and Experimental

Therapeutics and Neurology, Boston University School of Medicine (T.I.); and Department of

Neurology, Massachusetts General Hospital, Harvard Medical School (V.G.)

2.1 Abstract

The dissociative anesthetic ketamine elicits symptoms of schizophrenia at subanesthetic doses by blocking N-methyl-D-aspartate receptors (NMDARs). This property led to a variety of studies resulting in the now well-supported theory that hypofunction of NMDARs is responsible for many of the symptoms of schizophrenia. However, the roles played by specific NMDAR subunits in different symptom components are unknown. To evaluate the potential contribution of GluN2D NMDAR subunits to antagonist-induced cortical activation and schizophrenia symptoms, we determined the ability of ketamine to alter regional brain activity and gamma frequency band neuronal oscillations in wildtype (WT) and GluN2D-knockout (GluN2D-KO) mice. In WT mice, ketamine (30 mg/kg, i.p.) significantly increased [^{14}C]-2-deoxy-glucose ([^{14}C]-2DG) uptake in the medial prefrontal cortex (mPFC), entorhinal cortex (ERC) and other brain regions, and decreased activity in somatosensory cortex (SSC) and inferior colliculus (IC). In GluN2D-KO mice, however, ketamine did not significantly increase [^{14}C]-2DG uptake in any brain region examined, yet still decreased [^{14}C]-2DG uptake in SSC and IC. Ketamine also increased locomotor activity in WT mice but not in GluN2D-KO mice. In electrocorticographic analysis, ketamine induced a 111 ± 16 % increase in cortical gamma-band oscillatory power in WT mice, but only a 15 ± 12 % increase in GluN2D-KO mice. Consistent with GluN2D involvement in schizophrenia-related neurological changes, GluN2D-KO mice displayed impaired spatial memory acquisition and reduced parvalbumin (PV)-immunopositive staining compared to control mice. These results suggest a critical role of GluN2D-containing NMDARs in neuronal oscillations and ketamine's psychotomimetic, dissociative effects and hence suggests a critical role for GluN2D subunits in cognition and perception.

2.2   Introduction

The discovery that the N-methyl-D-aspartate receptor (NMDAR) antagonists ketamine and phencyclidine (Anis, Berry et al. 1983) can mimic the symptoms of schizophrenia prompted genetic, biochemical and pharmacological studies resulting in the NMDAR-hypofunction theory of schizophrenia (Coyle, Tsai et al. 2003, Lisman, Coyle et al. 2008, Kantrowitz, Javitt 2010). Pharmacological blockade of NMDAR in healthy humans elicits a spectrum of schizophrenia symptoms and NMDAR blockade in laboratory animals and provides a model for schizophrenia (Kantrowitz, Javitt 2010). Further support for the NMDAR hypofunction hypothesis comes from the identification of many schizophrenia candidate genes that impair NMDAR function (Sun, Jia et al. 2010, Balu, Coyle 2011, Greenwood, Light et al. 2012) and observations that decreasing NMDAR levels in mice through genetic manipulations leads to schizophrenia-associated symptoms (hyperlocomotor activity, impaired learning, reduced social interactions, and altered neuronal oscillations) (Mohn, Gainetdinov et al. 1999, Halene, Ehrlichman et al. 2009).

Precisely how NMDAR blockade induces schizophrenia symptoms is unclear, but many studies support the proposal that blockade of NMDARs in GABAergic interneurons containing parvalbumin (PV) is responsible for the psychotomimetic actions of NMDAR antagonists (Gonzalez-Burgos, Lewis 2008, Lisman, Coyle et al. 2008, Kantrowitz, Javitt 2010). Since PV-interneurons provide negative feedback to pyramidal neurons, inhibition of NMDAR in PV-cells causes an excitation of pyramidal neurons by disinhibition and thus alters the excitatory/inhibitory balance in cortical circuits (Li, Clark et al. 2002, Homayoun, Moghaddam 2007, Nakazawa, Zsiros et al. 2012). PV cell modulation also generates the gamma frequency band neuronal network oscillations that are important for cortical processing, working memory and perceptual integration (Sohal, Zhang et al. 2009, Yizhar, Fenno et al. 2011, Korotkova, Fuchs et al. 2010). Thus, acute administration of ketamine or PCP enhances excitatory activity in cortico-limbic structures and increases basal levels of gamma oscillations (Duncan, Miyamoto et

al. 2000, Duncan, Miyamoto et al. 1999, Homayoun, Moghaddam 2007, Nakazawa, Zsiros et al. 2012, Hunt, Kasicki 2013, Kocsis, Brown et al. 2013). Accordingly, selective reduction of the common GluN1 NMDAR subunit in PV-cells, increases basal gamma oscillations, decreases NMDAR antagonist-induced gamma oscillations, and promotes schizophrenia-associated behavioral symptoms (Belforte, Zsiros et al. 2009, Korotkova, Fuchs et al. 2010, Billingslea, Tatard-Leitman et al. 2014, Carlen, Meletis et al. 2011). These effects could also be mediated by PV-containing interneurons in the thalamic reticular nucleus (Frassoni, Bentivoglio et al. 1991, Llinás, Urbano et al. 2005). In schizophrenia, NMDAR-hypofunction may thus disturb excitatory/inhibitory balance thereby altering neuronal oscillations and disrupting cognitive function (Lisman, Coyle et al. 2008, Kantrowitz, Javitt 2010, Uhlhaas, Singer 2013).

The roles played by NMDARs with different subunit combinations in cortical processing and schizophrenia-related symptoms are unknown. Such information is necessary for resolving individual pathophysiological components of schizophrenia and for defining appropriate therapeutics. NMDARs are tetrameric complexes composed of two GluN1 subunits and two subunits from among the GluN2A-D and GluN3A-B subunits (Ikeda, Nagasawa et al. 1992, Ishii, Moriyoshi et al. 1993, Mishina, Mori et al. 1993, Monyer, Burnashev et al. 1994, Traynelis, Wollmuth et al. 2010). Pharmacological studies *in vivo* have indicated a predominant role for GluN2A subunits in NMDAR antagonist-induced neuronal oscillations (Kocsis 2012). However, *in vitro* experiments suggest a greater role for GluN2B subunits (McNally, McCarley et al. 2011) and the role of GluN2C and GluN2D subunits is unclear. We hypothesized that GluN2D-containing NMDARs may contribute to ketamine-induced schizophrenia symptoms since GluN2D NMDAR subunits are localized in PV-containing GABAergic interneurons in cortex, reticular nucleus of thalamus, and hippocampus (Monyer, Burnashev et al. 1994, Standaert, Bernhard Landwehrmeyer et al. 1996, Yamasaki, Okada et al. 2014, Engelhardt, Bocklisch et al. 2015) and because ketamine has higher affinity for GluN2D-containing NMDARs than for

NMDARs containing the more widely-expressed GluN2A and GluN2B subunits (Watanabe, Inoue et al. 1992, Watanabe, Inoue et al. 1993b, Dravid, Erreger et al. 2007, Kotermanski, Johnson 2009). GluN2D involvement in schizophrenia could potentially also be mediated by altering neuronal-oligodendrocyte signaling (Fields 2008, Micu, Plemel et al. 2016). Thus, in the present study, we sought to determine if ketamine-induced cortical activation and gamma oscillations are reduced in GluN2D-KO mice.

The ketamine-induced increase in neuronal activity and gamma oscillations was determined by [^{14}C]-2DG uptake (reflecting neuronal activation) and by electrocorticography (ECoG) in WT and GluN2D-KO mice. In addition, if GluN2D subunits do contribute to schizophrenia symptoms, then drug-free GluN2D-KO mice may have behavioral defects and reduced PV expression as seen in schizophrenia patients (Lisman, Coyle et al. 2008) and in rodents after chronic NMDAR blockade (Abekawa, Ito et al. 2007, Behrens, Ali et al. 2007, Benneyworth, Roseman et al. 2011). Consequently, we also evaluated spatial learning and PV expression levels in untreated WT and GluN2D-KO mice. These findings demonstrate that GluN2D-containing NMDARs are necessary for full neuronal activation induced by ketamine and that GluN2D-hypofunction potentially contributes to schizophrenia symptoms.

2.3   Materials and methods

2.3.1   *Drugs*

All chemicals were purchased from Sigma Aldrich Co. USA, unless otherwise specified.

Ketamine was purchased from Hospira, Inc., Lake Forest, IL and [^{14}C]-2-deoxy glucose ([^{14}C]-2DG) was purchased from PerkinElmer, Boston, MA, USA.

2.3.2   *Animals*

GluN2D-KO mice (Ikeda, Araki et al. 1995) that had been backcrossed onto a C57BL/6 background to 99.9 % homogeneity (Hizue, Pang et al. 2005) were used for these studies. The background strain was confirmed to be congenic with C57BL/6 (Charles River Laboratories genetic testing service). Mouse genotype was confirmed by PCR followed by sequencing of the reaction product and by Western blotting. Male C57BL/6 WT and GluN2D-KO mice 10-12 weeks of age were used for behavioral and 2-DG uptake studies; 10-15 week-old male mice were used for ECoG studies. Mice were handled in accordance with University of Nebraska Medical Center's Institutional Animal Care and Use Committee (IACUC) guidelines. In accordance with these guidelines, efforts were made to minimize animal suffering and the number of animals used.

2.3.3   *qRT-PCR for mRNA quantification*

WT and GluN2D-KO mice were sacrificed after 2 h of treatment with 30 mg/kg of ketamine or saline. Brains were isolated and 3 regions (two hemispheres, midbrain and cerebellum) were separated and stored at - 80 °C. Total RNA was isolated using Trizol reagent using the standard RNA isolation procedure and samples (1 µg/ml) were stored at -80 °C. Reverse transcription was carried out for 1 µg of RNA with reagents from applied bio-system. Reverse transcription reaction was carried out for cDNA preparation by running thermal cycler for 10 min at 25 °C, 40 min at 48 °C, 5 min at 95 °C followed by cooling at 4 °C. qPCR quantification of the cDNA carried out by using Taqman reagents and the reaction was carried out in StepOnePlus™ Real-Time PCR system (ThermoFisher scientific, USA). Relative gene expression was calculated by

LIVAK method [fold change = $2^{(-\Delta\Delta CT)}$] (Livak, Schmittgen 2001) and data are expressed as fold change compared to WT control.

2.3.4 2-Deoxy glucose uptake assay

Regional brain activity was determined by measuring [^{14}C]-2DG uptake (Kennedy, Des Rosiers et al. 1975) (Kennedy et al., 1975); as previously described (Kennedy, Des Rosiers et al. 1975, Duncan, Miyamoto et al. 1999) with minimal modifications. Animals were injected with ketamine (30 mg/kg, i.p.) or saline and then injected after 2 minutes with [^{14}C]-2DG (0.16 μCi/g). After another 15 minutes (i.e. 17 minutes after ketamine/saline injection), the mice were decapitated under isofluorane anesthesthesia. Brains were isolated, rapidly frozen, and stored at -80 °C. Horizontal brain sections (20 μm) were thaw-mounted onto glass slides, and processed for autoradiography along with ^{14}C-standards (ARC146, American Radiolabelled Chemicals) using KODAK BioMax MR film (Carestream Health Inc., New York, USA). Films were developed after 1-2 weeks of exposure and analyzed by quantitative image analysis (MCID^{TM} system, St. Catharines, Canada). Six to 8 brain sections were used for determining density for each brain region studied in each brain. Brain region absolute values were normalized by average radioactivity concentration of the whole corresponding section (Duncan, Miyamoto et al. 1999).

2.3.5 Electrocorticography (ECoG)

Wildtype and GluN2D-KO mice were surgically-implanted with tripolar electrodes (MS333/2, Plastics One, Roanoke, VA, USA) under xylazine/ketamine/acepromazine anesthesia as required by IACUC regulations. Two holes were made in the skull 3 mm posterior to bregma at 1 mm and 2.5 mm lateral. Two electrodes were placed in the medial hole onto the dura surface near the retrosplenial cortex and the third electrode was placed in the lateral hole for ground. The electrodes were secured to the skull as described elsewhere (Jeffrey, Lang et al. 2013). After 7 days of recovery, ECoG recordings were made with a DP-311 differential amplifier (Warner Instruments) with high pass/low pass filters set at 0.1 and 300 Hz and digitized/recorded

(Digidata 1400, pClamp 10, Molecular Devices). Following 30 minutes of baseline recordings, animals were injected i.p. with ketamine or saline and recorded for the period between 5 and 30 minutes post-injection. Ketamine administration (i.p.) in mice has an approximately 5 minute lag time and a peak ketamine response up to 30-45 minutes post-injection (Phillips, Cotel et al. 2012). In our initial studies, we found the peak response to be maintained through 20 minutes with a minor decrement by 30 minutes, so care was taken to match the recording periods between WT and GluN2D-KO mice. Power spectrum analysis was performed with Clampfit (Molecular Devices) using a Hamming window with 50 % overlap. In preliminary experiments, we found that the subanesthetic dose of 30 mg/kg i.p. gave a more robust augmentation of neuronal oscillations than 5 mg/kg. Ketamine is typically used in the 5 - 50 mg/kg range in electroencephalography experiments (Hunt, Kasicki 2013).

2.3.6 Open field test (OFT)

The floor of a plexiglass rectangular arena (40 x 30 cm) with 40 cm high walls was divided into twelve squares using black tape. Animals were treated with ketamine (30 mg/kg; i. p.) or saline and their behavior was video recorded for 15 minutes. The arena was cleaned and rinsed with 70 % ethanol between each animal. Video files were coded for blinded analysis of open-field line crosses (defined as both rear paws crossing over a line marked on the floor) and the number of entries into the 2 central squares. The number of rearings and wall-climbing attempts were also counted.

2.3.7 Parvalbumin immunohistochemistry

Anesthetized mice were transcardially-perfused with phosphate buffer saline (PBS, pH 7.4) followed by 4 % paraformaldehyde (PFA)/PBS. Brains were removed and post-fixed in 4 % PFA for 24 hours at 4 °C and then cryoprotected with 30 % sucrose for another 24 hours. Brains were snap frozen and kept at -80 °C until sectioned. Immunohistochemistry was carried out in every 5th coronal cryostat sections (40 µm) using the free-floating method. Sections were treated with 4 %

PFA for 15 minutes, rinsed (PBS) and treated with 3 % H_2O_2 for 30 minutes. After blocking with

10 % bovine serum (BS) with 0.3 % triton X-100, sections were incubated with primary antibody

(rabbit anti-PV, 1:10,000, Swant, Switzerland) for 48 hours at 4 ºC. Sections were washed and

incubated with biotinylated secondary antibody (Goat anti-rabbit, 1:200, Vectors Lab,

Burlingame, CA, USA). After washing, sections were treated with ABC solution (Vectors Lab),

developed with 3,3'-diaminobenzidine, and coverslipped. Images were obtained by laser-scanning

microscopy and PV-positive cells were counted using NIH ImageJ software.

2.3.8   *Spatial memory in the Morris water maze*

Mice were given a 2-minute free swim test the day before the start of training. Then for 3

sequential days, mice were given 4 trials separated by 15 minutes on each day with a submerged

platform located in the same position for all trials. In the training trials, mice were allowed up to 1

minute to find the platform and guided to the platform if they had not already found the platform.

Mice then were allowed to stay on the platform for 15 seconds. Mice were placed in a different

start location at the beginning of each trial with visual cues on the walls of the testing chamber.

On day 4, the mice were tested with the platform removed (probe test). For each trial, we

determined the time required to reach the platform. For each probe test, the percent time spent in

the correct quadrant outside of the starting quadrant and the number of platform-site crossovers

were determined.

2.3.9   *Statistical analysis*

Prism 6 (GraphPad Software Inc., San Diego, CA, USA) was used for statistical analysis. For

most experiments, data were analyzed by two-way analysis of variance (ANOVA) with Sidak's

multiple comparison test to determine the difference among groups or student t-test as described

elsewhere. Difference was considered to be significant if $p < 0.05$.

2.4   Results

2.4.1   *Effect of ketamine on c-fos gene expression*

C-fos is an early expressed gene and is regarded as a marker of neuronal activity. In order to see the effect of ketamine on neuronal activity in different anatomical regions, we measured c-fos mRNA by RT-qPCR. The mRNA expression was measured in 3 different areas of the brain (i) two cerebral hemispheres and hippocampi (ii) thalamus, hypothalamus and brain stem and (iii) cerebellum. In WT mouse, ketamine treatment significantly enhanced ($p = 0.04$, two-way ANOVA) the c-fos mRNA expression in cortex/hippocampus (1.96 ± 0.5; $n = 6$) as compared to saline treated control mice (1.13 ± 0.3; $n = 5$) (Figure 2.1). We did not observe any effect of ketamine treatment on c-fos expression in cortex/hippocampus of GluN2D-KO mice (1.39 ± 0.1; $n = 4$ for saline treated mice and 1.44 ± 0.3; $n = 5$ for ketamine treated mice). Similarly, there was no significant change in c-fos mRNA expression in midbrain and cerebellum also. However, although not significant, there was a reduced level of c-fos in cerebellum of GluN2D KO mice and ketamine did not alter its level. Using this method, it is difficult to see the subtle change in c-fos expression in a particular region of the brain since multiple brain regions were combined together. Hence, in order to visualize the anatomical change in the specific brain region after ketamine administration, we performed an autoradiographic ^{14}C-2-deoxy glucose assay.
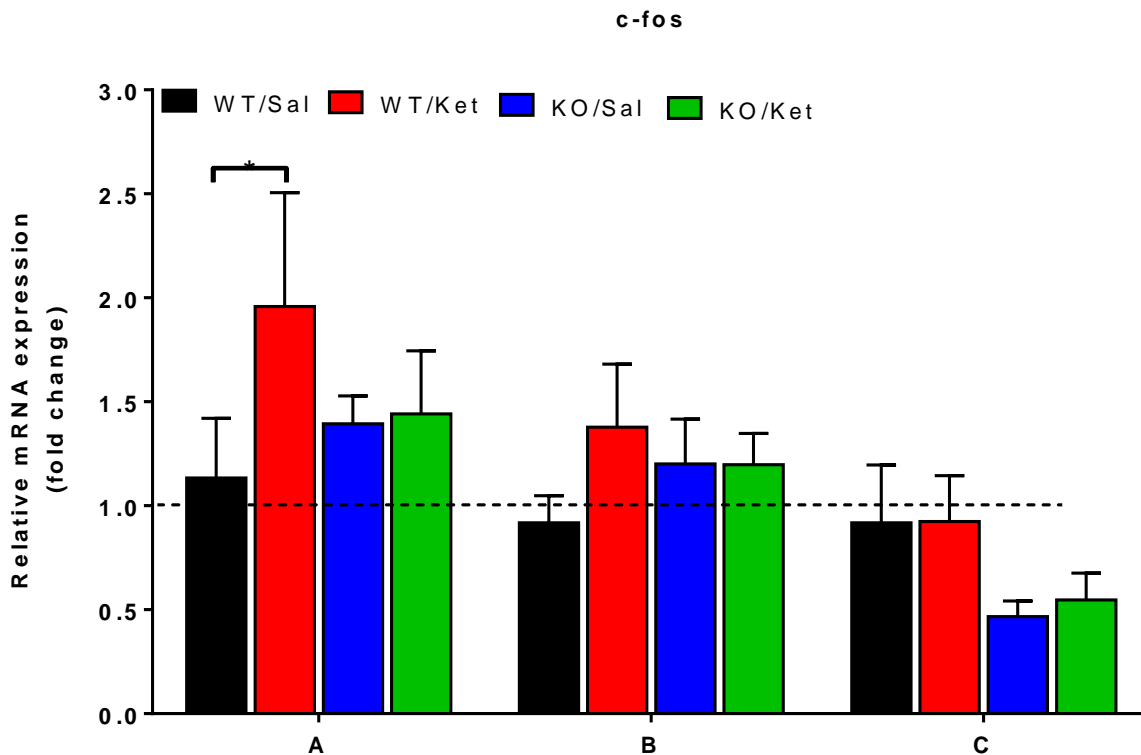
c-fos

Figure 2.1 Effect of ketamine on c-fos expression in different brain regions of WT and GluN2D-KO mice

The alteration in c-fos gene expression by ketamine after 2 h was measured by RT-qPCR in the following brain regions (A) cortex/hippocampus, (B) thalamus/hypothalamus (c) cerebellum. Tissue from four groups of mice [WT/saline (n = 5), WT/ketamine (n = 6), GluN2D-KO/saline (n = 4) and GluN2D-KO/ketamine (n = 5)] were analysed for mRNA expression. The change in mRNA level is expressed as fold change compared to WT/saline group as a control (mean ± S.E.M). *p < 0.05

2.4.2   Effect of ketamine on regional brain activity as demonstrated by 2-DG uptake

Ketamine-induced regional changes in neuronal activation were measured by [^{14}C]-2-DG uptake quantitative autoradiography. Consistent with previous reports (Duncan, Miyamoto et al. 1999, Miyamoto, Leipzig et al. 2000), ketamine (30 mg/kg) increased relative [^{14}C]-2-DG uptake (Figure 2.2) in several brain regions and reduced uptake in others. [^{14}C]-2-DG uptake was quantified in 11 brain regions and density differences were evaluated for statistical significance (Figure 2.3). Two-way ANOVA between regions and animal groups indicated an interaction effect [$F_{(30, 314)} = 6.00$, $p < 0.0001$], a region effect [$F_{(10, 314)} = 33.6$, $p < 0.0001$] and an

animal group effect [F (3, 314) = 13.9, $p < 0.0001$]. In WT mice, ketamine increased relative

[^{14}C]-2-DG uptake in medial prefrontal cortex (mPFC, 37 %, $p < 0.0001$), entorhinal cortex (34

%, $p = 0.0006$), presubiculum (39 %, $p < 0.0001$, and caudate putamen (21 %, $p = 0.018$), and

decreased relative uptake in inferior colliculus (26 %, p < 0.0001) and somatosensory cortex (23

%, p = 0.0008) (Figure 2.3). Also, as others have reported (Duncan et al., 1999), the whole

section, absolute levels of [^{14}C]-2-DG uptake did not significantly change with ketamine

(WT/saline: 0.57 ± 0.06 nCi/mg tissue, n = 8, WT/ketamine: 0.52 ± 0.09, n = 9, $p = 0.74$;

KO/saline: 0.40 ± 0.04 nCi/mg, n = 7; KO/ketamine 0.33 ± 0.04, n = 9, $p = 0.74$). The

distribution of [^{14}C]-2-DG uptake in GluN2D-KO mice following saline injection was similar to

that seen in saline-treated WT mice (Figure 2.2) and was not statistically different between

genotypes in any brain region (Figure 2.3). In contrast to WT mice, administration of ketamine

did not cause a relative increase in [^{14}C]-2-DG uptake in any of the regions examined. Ketamine,

however, decreased [^{14}C]-2-DG uptake in somatosensory cortex (15 %, $p = 0.0005$), inferior

colliculus (21 %, $p < 0.0001$), and thalamus (13 %, $p = 0.0043$).
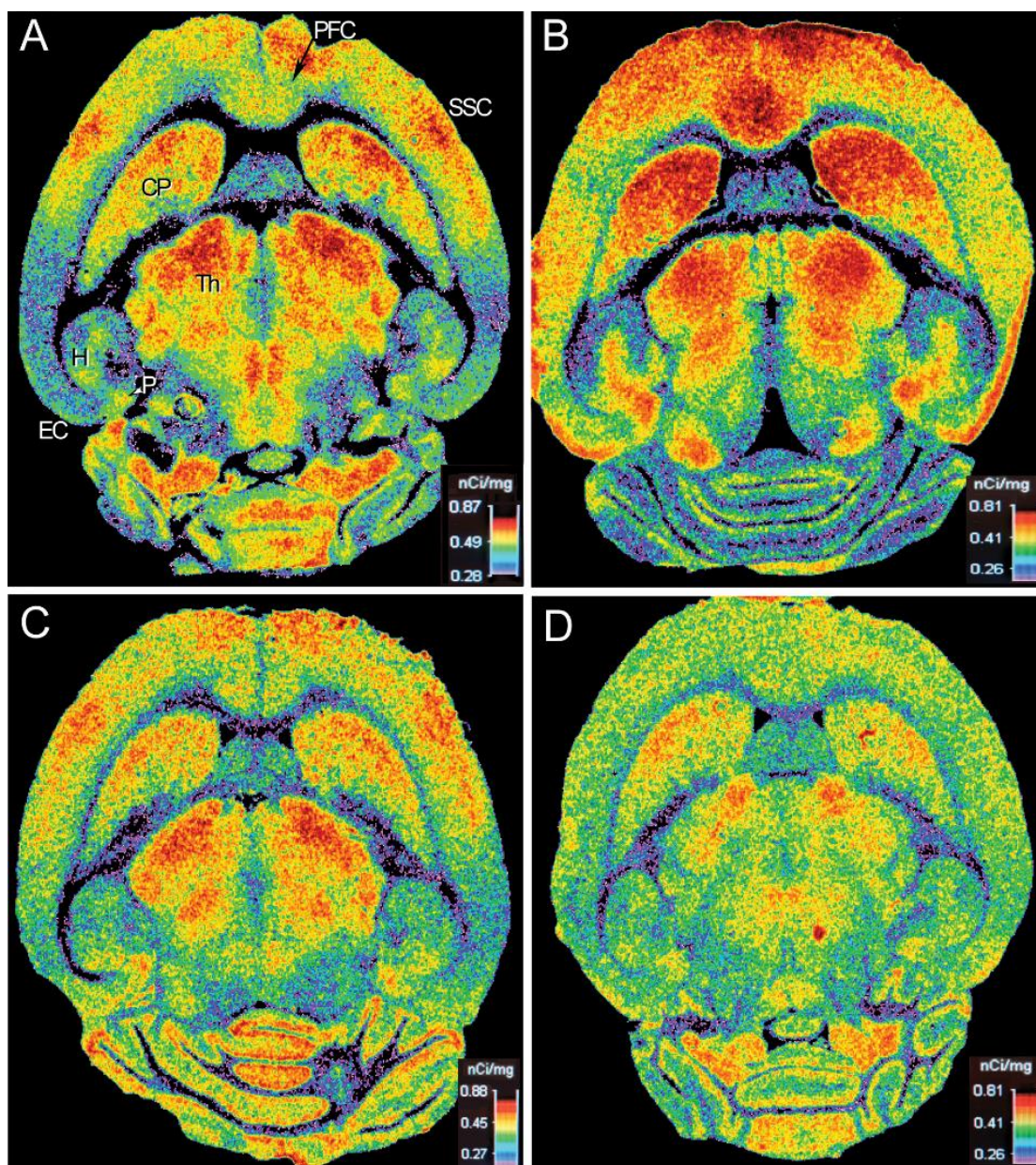
Figure 2.2 The effect of ketamine on [^{14}C]-2-DG uptake in WT mice and GluN2D-KO mice

Representative autoradiographic images showing the effect of administering saline (left panels) and ketamine (right panels; 30 mg/kg, i.p.) on [^{14}C]-2-DG uptake in horizontal sections of WT (top panels) and GluN2D-KO (bottom panels) mice. Red to blue color spectrum indicates high to low activity, respectively, as shown in the calibration bars. Abbreviations: CP/CPu, caudate putamen; EC/Ent Ctx, entorhinal cortex; H/HC, hippocampus; P/Presub, presubiculum; PFC medial prefrontal cortex; Rspl Ctx, retrosplenial cortex; SSC/Sens. Ctx., somatosensory cortex; and Th, thalamus.
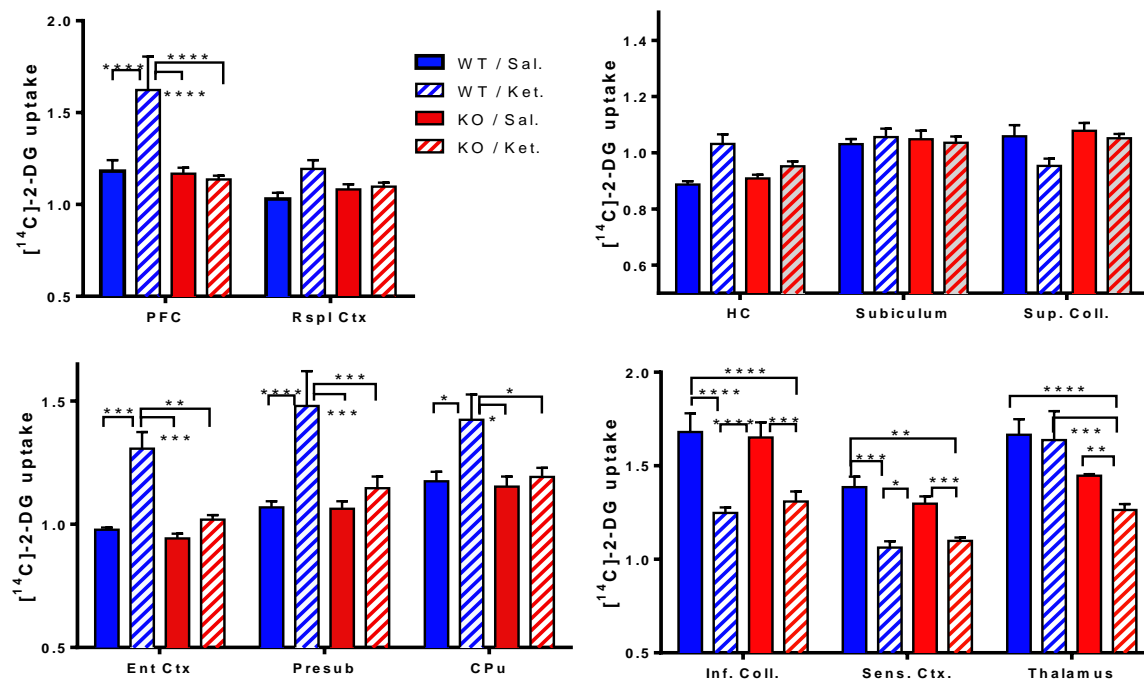
Figure 2.3 The effect of ketamine on [^{14}C]-2-DG uptake in WT mice and GluN2D-KO mice

[^{14}C]-2-DG uptake expressed as mean relative radioactivity concentration ± S.E.M, in WT and GluN2D-KO mice after saline (Sal.) or ketamine (Ket) injections, n = 7 - 9 per group. Statistical significance is indicated by * ($p < 0.05$), ** ($p < 0.01$), *** ($p < 0.001$), and **** ($p < 0.0001$). Abbreviations: CP/CPu, caudate putamen; EC/Ent Ctx, entorhinal cortex; H/HC, hippocampus; P/Presub, presubiculum; PFC medial prefrontal cortex; Rspl Ctx, retrosplenial cortex; SSC/Sens. Ctx., somatosensory cortex; and Th, thalamus.

2.4.3   *Ketamine modulation of neuronal oscillations*

ECoG recordings of awake, stationary WT mice ($n = 8$) displayed a typical awake ECoG trace

(Figure 2.4A). Power spectrum analysis revealed that ketamine administration increased gamma

frequency power (30 - 140 Hz) (Figure 2.4B,D) over baseline while ketamine in GluN2D-KO

mice ($n = 9$), elicited a relatively small increase in power in the gamma range (and increased

power between 140-170 Hz). As shown in Figure 2.4D, the two genotypes appeared different

between 60 Hz and 140 Hz, largely corresponding to high-frequency gamma oscillations as

defined by Colgin and colleagues (65-140 Hz) (Colgin, Denninger et al. 2009). Ketamine

increased high-gamma power more in WT mice (110.7 ± 16.4 %, Figure 2E) than in GluN2D-KO

mice (15.0 ± 11.6 %, $p = 0.0002$, two-tailed t-test). In GluN2D-KO mice, ketamine treatment was

associated with a peak of variable magnitude near 155 Hz while in ketamine-treated WT mice

there was a peak near 135 Hz (Figure 2.4D), also of variable magnitude but of consistent peak

frequency.
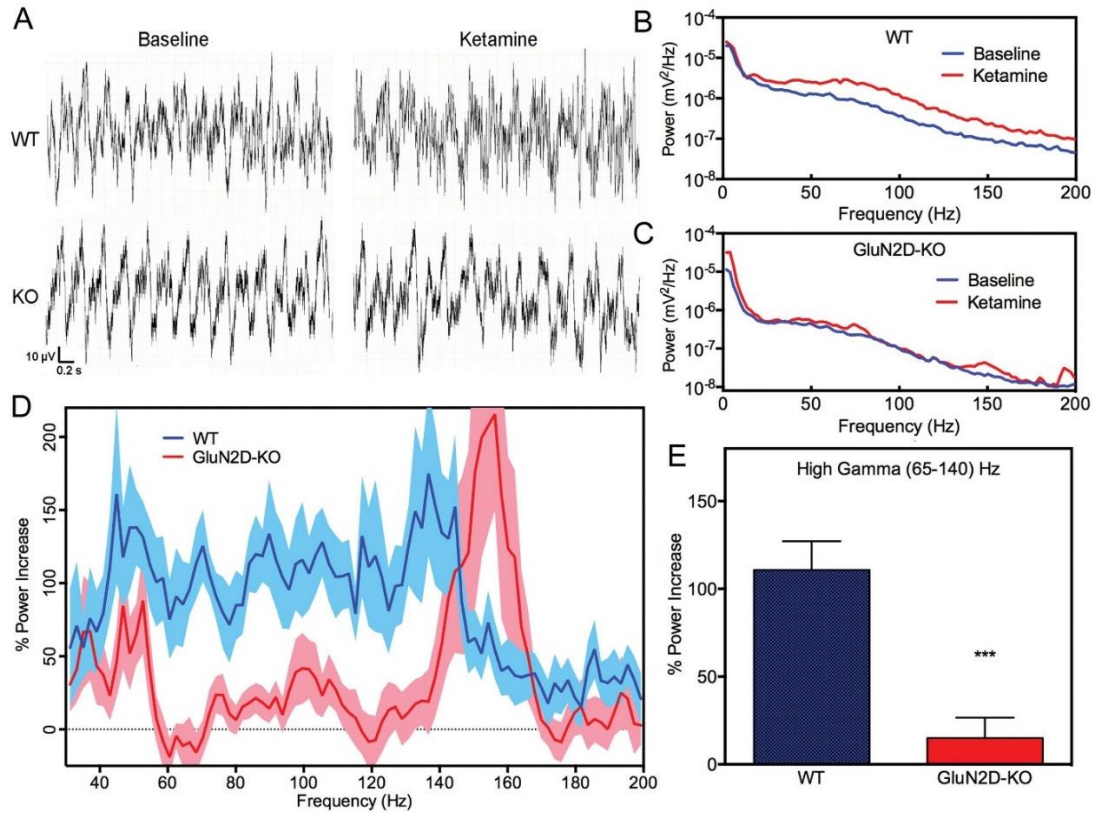
Figure 2.4 The effect of ketamine on neuronal oscillations

(**A**) Electrocorticographic recordings in WT and GluN2D-KO mice before and after administration of ketamine. Representative power spectrum analysis of WT (**B**) and GluN2D-KO mice (**C**) ECoG responses over 2 to 200 Hz before (baseline) or after ketamine injection. (**D**) The average percent power increase induced by ketamine-injection as a function of frequency in WT (blue line) and GluN2D-KO mice (red line), S.E.M is shown by light blue/red shading. The dotted line represents 0 % increase, no drug-induced change in power. Results shown represent the mean value ± SEM of WT and GluN2D-KO animals (*n* = 8 and 9, respectively). (**E**) Average ketamine-induced power increases in the upper gamma frequency band for WT and GluN2D-KO mice. *** ($p = 0.0002$).

2.4.4 Ketamine-induced motor activity

As measured in the open field test (OFT), ketamine (30 mg/kg, i.p.) increased locomotor activity in WT mice during the 15 minutes following injection (Figure 2.5A,B). In the WT mice, the average number of squares crossed after ketamine treatment was significantly greater (528.0 ± 62.3, $n = 8$) than after saline treatment (264.0 ± 43.4, n = 7, $p = 0.0005$). Ketamine did not significantly induce hyper-locomotion in GluN2D-KO mice (squares crossed in the saline condition: 171.4 ± 20.0, n = 7; ketamine: 222.7 ± 31.6, n = 10, $p = 0.64$). The two genotypes were different in the ketamine condition ($p < 0.0001$) but not in the saline condition ($p = 0.31$). In the open field test, avoidance of the central, open space can reflect anxiety levels in mice. The number of times that WT mice entered the central squares was nearly doubled in ketamine-treated mice than in the saline treated group (Figure 2.5C). Two-way ANOVA indicated significant effects of genotype ($p < 0.0001$) and treatment ($p = 0.0005$) and multiple comparisons testing (Sidak's) indicated a difference between saline and ketamine in the WT ($p = 0.0006$) but not in the GluN2D-KO mice ($p = 0.35$). Thus, ketamine failed to significantly increase entries into the central squares by GluN2D-KO mice in parallel with effects on locomotor activity. In contrast to the blunting effect that eliminating GluN2D had on ketamine-induced hyper-locomotion, ketamine fully reduced rearings and climbing attempts in both WT and GluN2D-KO mice (Figure 2.5).However, in the saline controls, GluN2D-KO mice had a significantly lower level of rearings and climbing attempts than WT mice ($p < 0.0001$, $p = 0.019$, respectively, Sidak's multicomparison test). The stereotypical behavior of walking in circles (rotations) was induced by ketamine administration in both genotypes (Figure 2.5F), but was significantly greater ($p = 0.0008$, Sidak's multicomparison test) in WT (56.4 ± 12.8, $n = 9$) than in GluN2D-KO mice (14.4 ± 3.0, $n = 10$).
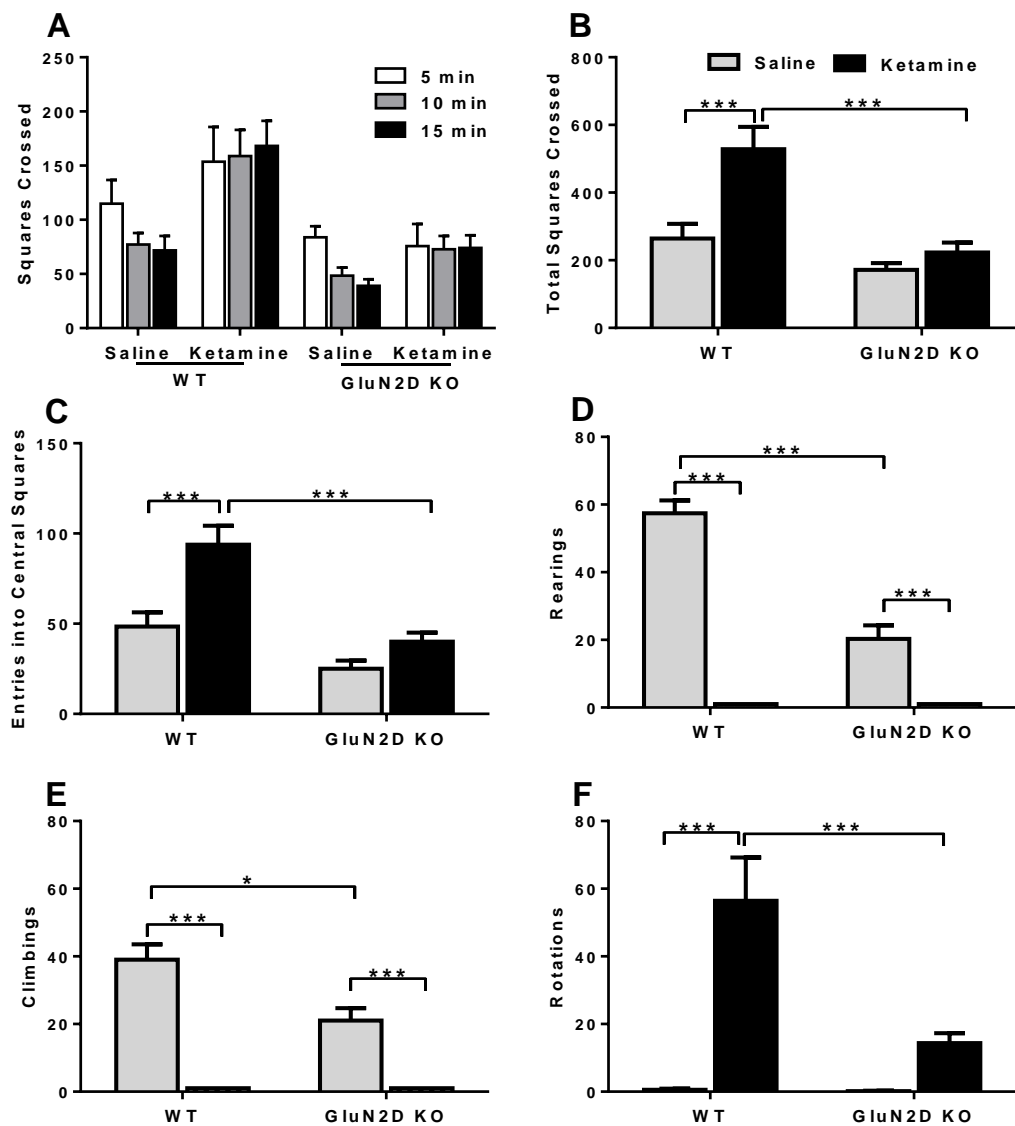
Figure 2.5 Reduced ketamine-induced locomotor behavior in the GluN2D-KO mouse

WT and GluN2D-KO mice (n = 7-10 per group) were treated with saline or ketamine and their motor behavior was monitored for 15 minutes by the open-field test. Locomotor behavior was measured by the average number of grid lines crossed in each of the 5-minute periods (**A**) or for the total period (**B**). Also measured were the number of entries into the open, central squares of the arena (**C**), rearings (**D**), wall-climbing attempts (**E**) and walking in circles, rotations (**F**). Results are represented as mean number ± S.E.M * $p < 0.05$; *** $p < 0.001$.

2.4.5   *Parvalbumin immunohistochemistry*

The inability of the psychotomimetic agent ketamine to increase activation of the prefrontal cortex and increase basal gamma oscillations in GluN2D-KO mice suggests that GluN2D-containing NMDARs contribute to psychotomimetic activity. If GluN2D subunit activity contributes to the defects seen with NMDAR hypofunction, which is associated with a decreased expression of parvalbumin (PV) in schizophrenia brain and in animal models following chronic NMDAR blockade (Abekawa, Ito et al. 2007), then the expression of PV may be reduced in the GluN2D-KO mouse. Two-way ANOVA of PV cell staining indicated an interaction effect [$F(5,36) = 2.865$, $p = 0.028$], a genotype effect [$F(1,36) = 19.5$, $p < 0.0001$], and a region effect [$F(5,36) = 124.1$, $p < 0.0001$] with multi-comparison testing indicating a significantly lower density of PV-positive cells in the GluN2D-KO substantia nigra ($p = 0.0038$) and in the basolateral/lateral amygdala ($p = 0.0051$) compared to WT mice (Figure 2.6). PV expression levels were also lower in mPFC and hippocampus in the GluN2D-KO, but these decreases were not statistically significant.
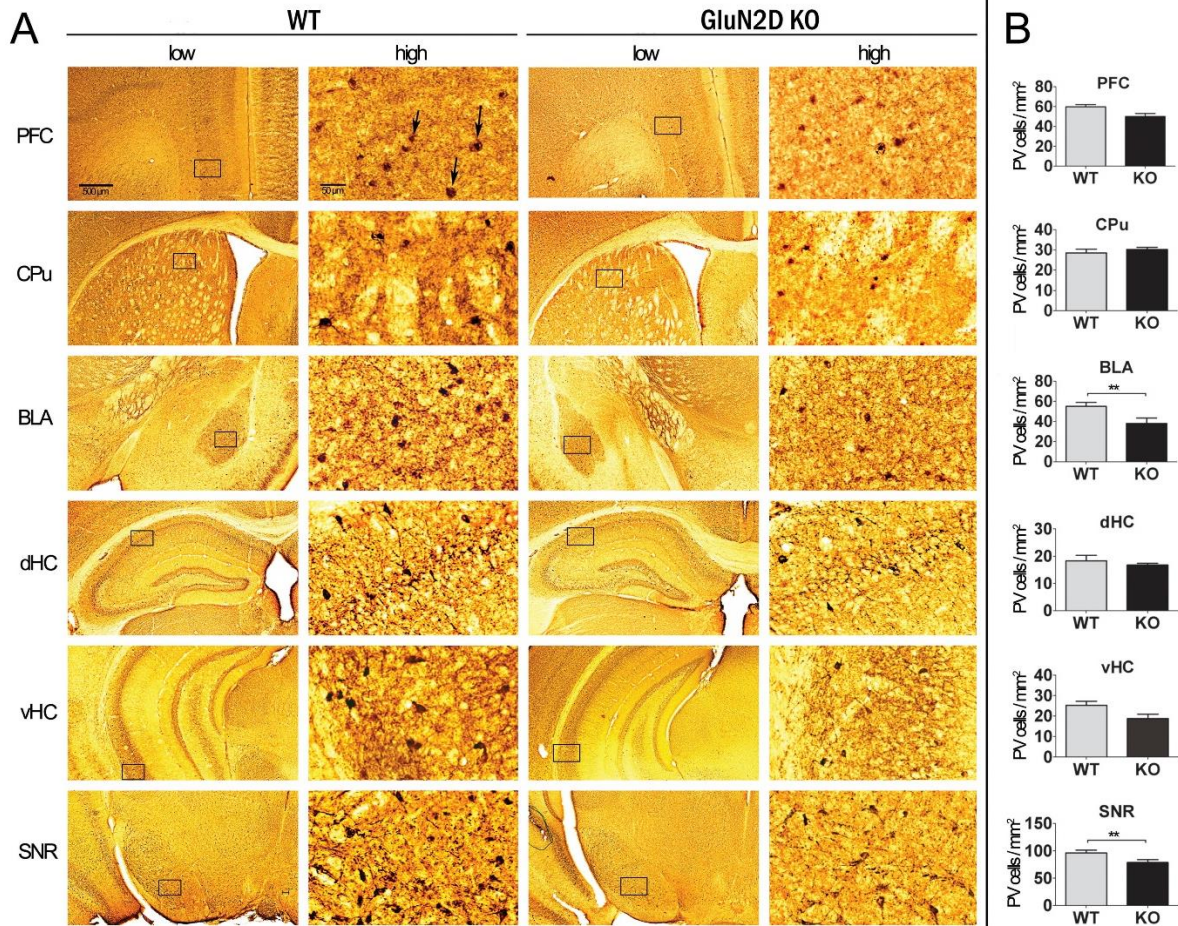
Figure 2.6 Parvalbumin immunoreactivity in different brain regions of WT and GluN2D-KO mice

(**A**) Photomicrographs are from representative coronal sections from WT (1st and 2nd columns) and GluN2D-KO mice (3rd and 4th column) stained by PV-immunohistochemistry at low magnification (1st and 3rd columns). Images from the boxes in the low-magnification photographs are shown at higher magnification in the adjacent column (2nd and 4th columns). Each row represents the brain region indicated on the left. Scale bars = 500 μm (1st photo) or 50 μm (2nd photo) as indicated, arrows in 2nd photograph indicate representative PV-positive cells. (**B**) Histograms show the mean density of PV-positive cells for each region ± S.E.M, ** $p < 0.01$, adjusted for multiple comparisons, $n = 4$ per group. Abbreviations: BLA, basolateral/lateral amygdala; CPu, caudate putamen; dHC, dorsal hippocampus; PFC, medial prefrontal cortex; SNR, substantia nigra reticulata; and vHC, ventral hippocampus.

2.4.6 *Evaluation of disruption in spatial memory and sensory-motor gating*

If elimination of GluN2D subunits reproduces some aspects of schizophrenia-related NMDAR hypofunction, then GluN2D-KO mice may have defects in spatial memory acquisition, a function disturbed in schizophrenia and related to cortical neuronal oscillations. During spatial learning task acquisition, WT mice appeared to show greater improvement from trial to trial than did GluN2D-KO mice (Figure 2.7A). Two-way ANOVA analysis indicated a significant effect of trial [$F(11,216) = 6.85$, $p < 0.0001$] and genotype [$F(11,216) = 7.95$, $p = 0.0053$] on the observed variation, with no significant interaction [$F(11,216) = 0.68$, $p = 0.76$] and no significant difference for any of the 12 individual training trials. However, following the 12th training trial, removal of the platform and measurement of the percent time spent in the correct quadrant of the time spent outside of the starting quadrant, revealed significantly better performance (more time in the correct quadrant) by the WT mice than the GluN2D-KO mice (Figure 2.7B, WT: 56.0 ± 6.0 %, $n = 10$, KO: 34.6 ± 3.5 %, $n = 10$, $p = 0.0063$, two-tailed t test). Similarly, WT mice crossed the former position of the removed platform a greater number of times than did the KO mice (Figure 2.7C, WT: 4.1 ± 0.7, n = 10, KO: 1.5 ± 0.5, n = 10, $p = 0.010$, two-tailed t test). Average swimming speed was not different between WT and KO mice. Thus, GluN2D-KO mice have impaired learning of the spatial memory task compared to WT mice.
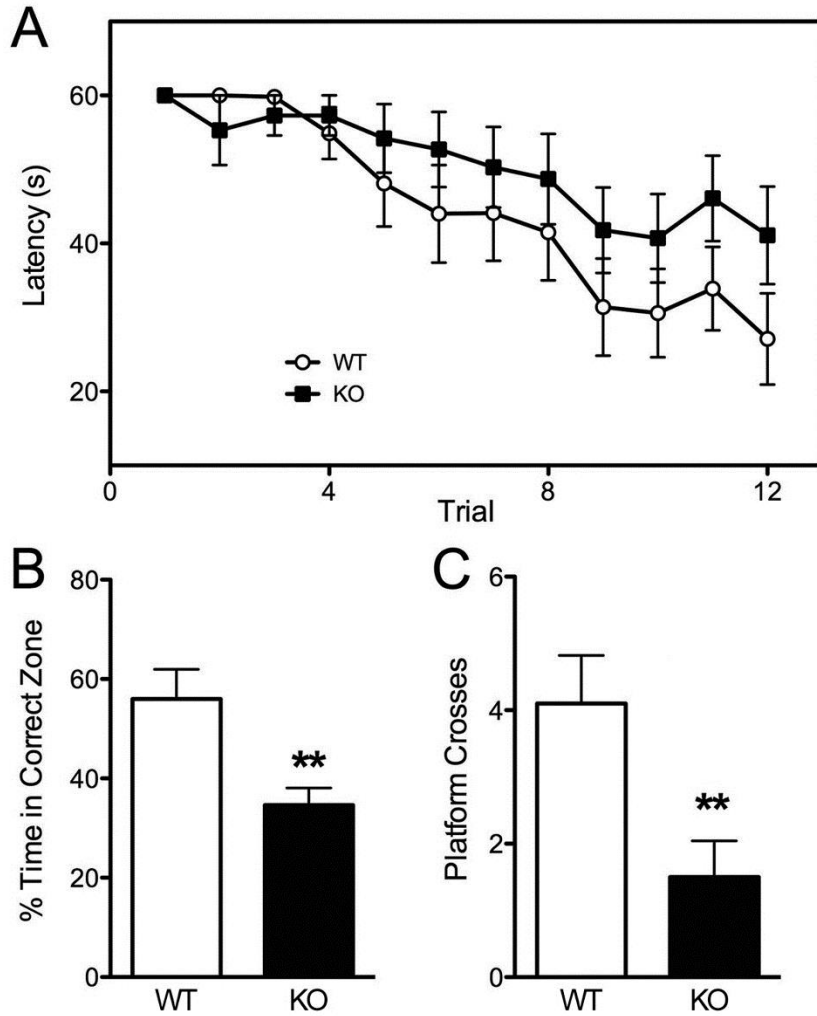
Figure 2.7 Spatial memory acquisition and prepulse inhibition in WT and GluN2D-KO mice

Spatial memory was tested in the Morris Water Maze with the time necessary to first reach the submerged platform (Latency) measured for each successive trial (4 per day, 3 successive days) shown in (**A**). On the fourth day, the submerged platform was removed and in the subsequent test trial, the % time spent in the correct quadrant outside of the starting quadrant was measured (**B**) as was the number of times the mouse passed over the prior location of the removed platform (**C**). Both test measures of task acquisition were statistically significant between WT and GluN2D-KO (n = 10 for each group, * $p < 0.05$; two-tailed t-test).

2.5   Discussion

Evidence from a variety of genetic, biochemical, and pharmacological studies support the concept that NMDAR hypofunction contributes to many of the diverse symptoms of schizophrenia (Coyle 2006, Lisman, Coyle et al. 2008, Kantrowitz, Javitt 2010). However, the relationships between specific NMDAR subtypes and schizophrenia symptom components are not well understood. Psychotomimetic agents, such as ketamine and PCP, produce many of the symptoms of schizophrenia by modulating the neuronal systems known to underlie schizophrenia, for reviews see (Lahti, Koffel et al. 1995, Javitt 2007, Lodge, Mercier 2015). Hence, resolving how these agents act on specific NMDAR subtypes to produce psychotomimetic symptoms should help define mechanisms of drug action as well as neurobiological mechanisms underlying schizophrenia.

In this study, we found that GluN2D-KO mice had a greatly reduced activation of brain activity in response to ketamine. Using $[^{14}C]$-2-DG uptake to reflect regional brain metabolic activity and the excitatory/inhibitory balance, we found that the characteristic increase in cortico-limbic activation seen in rodents (Duncan, Miyamoto et al. 1999) and humans (Vollenweider, Leenders et al. 1997) following ketamine administration, was not seen in GluN2D-KO mice. This finding is consistent with the very recent report that ketamine-induced nitric oxide synthase activation is dependent upon GluN2D subunits (Yamamoto, Nakayama et al. 2016). Since GluN2D subunits are found in PV-containing GABAergic interneurons of cortex, hippocampus, and thalamus (Standaert, Bernhard Landwehrmeyer et al. 1996, Yamasaki, Okada et al. 2014, Engelhardt, Bocklisch et al. 2015), these results support the hypothesis that ketamine causes cortico-limbic activation by disinhibiting PV interneurons. Interestingly, ketamine was still able to decrease 2-DG uptake in somatosensory cortex and inferior colliculus in GluN2D-KO mice as it does in WT mice (Figure 2.2, Figure 2.3). In contrast to these effects of GluN2D deletion, a global reduction in GluN1 subunits blunts both the NMDAR antagonist-induced increase in 2-DG

uptake in cortico-limbic regions as well as the antagonist-induced decrease in other brain regions (Duncan, Miyamoto et al. 2002). Thus, GluN2D subunits contribute to an important subset of ketamine's actions, excitatory disinhibition, but not to other effects of ketamine. The ketamine-induced reduction in 2-DG uptake in somatosensory cortex that persists in the GluN2D-KO potentially reflects ketamine blockade of GluN2C-containing receptors in thalamic reticular nucleus interneurons which would promote delta/theta oscillations and reduced activity in somatosensory cortex via the specific thalamo-cortical projections (Llinás, Urbano et al. 2005, Zhang, Llinas et al. 2009).

Our finding that GluN2D deletion reduces ketamine-induced gamma oscillations (Figure 2.4) suggests that GluN2D-containing NMDARs have an important role in modulating neuronal network oscillations. This has significant implications for schizophrenia. Neuronal oscillations in the gamma frequency band are thought to be integral to cognition and perception, and their impairment has been proposed to underlie the symptoms of schizophrenia (Gonzalez-Burgos, Lewis 2008, Uhlhaas, Singer 2013, Gonzalez-Burgos, Hashimoto et al. 2010). Since NMDARs in PV-cells are important for the modulation of gamma oscillations (Carlen, Meletis et al. 2011, Uhlhaas, Singer 2013), these results are also consistent with a key role of GluN2D subunits in cortical PV cell function. In addition, GluN2D subunits in the thalamus are likely to contribute to ketamine-induced dysrhythmias. Nucleus reuniens participates in circuits involved in schizophrenia-related symptoms (prefrontal cortex, hippocampus, and ventral tegmentum) (Lisman, Pi et al. 2010, Duan, Varela et al. 2015, Griffin 2015, Ito, Zhang et al. 2015) and is enriched in GluN2D subunits (Watanabe, Inoue et al. 1993a, Buller, Larson et al. 1994). Additionally, inhibition of NMDAR in the reticular nucleus, which contains GluN2D and GluN2C subunits (Watanabe, Inoue et al. 1993a, Yamasaki, Okada et al. 2014), generates telencephalic delta oscillations and potentially schizoprhenia-related symptoms (Zhang, Llinas et al. 2009). Thus, GluN2D subunit-containing NMDARs may have an essential role in the

pathophysiological expression of NMDAR hypofunction that underlies schizophrenia's cognitive symptoms. This suggestion is consistent with studies associating genetic variants of GluN2D subunits with schizophrenia risk (Makino, Shibata et al. 2005) and with reduced GluN2D expression in schizophrenia (Sodhi, Simmons et al. 2011) and in an animal model of schizophrenia (Bullock, Bolognani et al. 2009).

Ketamine also produced an increase in oscillations at frequencies corresponding to high frequency oscillations (HFO) as previously reported (Hunt, Kasicki 2013). In GluN2D mice, the ketamine-induced peak appeared at a higher frequency (~155 Hz) than in WT mice (~135 Hz). Interestingly, other groups have reported a similar finding in the methylazoxymethanol acetate neurodevelopmental model of schizophrenia. In both the nucleus accumbens (Goda, Olszewski et al. 2015) and motor cortex (Phillips, Cotel et al. 2012), ketamine elicited HFO with a higher peak frequency in the methylazoxymethanol-treated animals. The significance of this shift in peak frequency is unclear, but it may be noteworthy that the atypical antipsychotics (Olszewski, Piasecka et al. 2013) and glycine (Hunt, Olszewski et al. 2015) were found to reduce the peak frequency of NMDAR antagonist-induced HFOs.GluN2D subunits may also have key roles in other components of schizophrenia. Ikeda and colleagues (Hagino, Kasai et al. 2010) have shown that the enhanced release of dopamine and hyperlocomotor activity occurring after PCP administration is absent in GluN2D mice and thus GluN2D may be contributing to the positive symptoms of schizophrenia (Hagino, Kasai et al. 2010). These findings are supported by the reduction in ketamine-induced hyperlocomotor and rotation activity in GluN2D-KO mice (Figure 2.5) (Yamamoto, Nakayama et al. 2016). This action of PCP/ketamine may possibly be due to the presence of GluN2D subunits in the ventral tegmental area/substantia nigra, basal ganglia, and/or in the midline thalamic nuclei (Beaton, Stemsrud et al. 1992, Watanabe, Inoue et al. 1992, Buller, Larson et al. 1994, Monyer, Burnashev et al. 1994).

Other GluN2 NMDAR subunits also are likely to be involved in schizophrenia pathophysiology. Genetic studies show a strong association of schizophrenia with both GluN2A and GluN2B subunit genes (Allen, Bagade et al. 2008, Greenwood, Light et al. 2012). GluN2A subunits have also been implicated by pharmacological studies of gamma oscillation modulation *in vivo* (McNally, McCarley et al. 2011, Kocsis 2012) and PV-down-regulation (Kinney, Davis et al. 2006). However, GluN2B-selective antagonists were found to better augment kainate-induced gamma oscillations than a GluN2A-preferring antagonist (McNally, McCarley et al. 2011). GluN2C involvement in schizophrenia is suggested by the finding that GluN2C transcript levels are significantly reduced in schizophrenia patients (Weickert, Fung et al. 2013) and the presence of working memory and fear acquisition defects in GluN2C-KO mice (Hillman, Gupta et al. 2011). A potential role of GluN2C subunits in schizophrenia is also suggested by GluN2C expression in the reticular nucleus of the thalamus which modulates hippocampal delta oscillations and thus may explain delta oscillatory changes seen in schizophrenia patients (Zhang, Buonanno et al. 2012).

Schizophrenia and chronic blockade of NMDARs during development (Wang, McInnis et al. 2001) are associated with an altered excitatory/inhibitory balance, reduced PV expression and disturbed gamma oscillation modulation (Lisman, Coyle et al. 2008, Kantrowitz, Javitt 2010, Uhlhaas, Singer 2013). If GluN2D-containing NMDARs contribute to the excitatory/inhibitory balance during development then one might expect similar defects in the adult GluN2D-KO mouse as seen in schizophrenia or following chronic NMDAR blockade. Consistent with this possibility, untreated GluN2D-KO mice are associated with a reduced expression of PV in the substantia nigra reticulata and amygdala (Figure 2.6) and a reduced performance in a spatial memory task (Figure 2.7). The impact of PV levels in interneurons of the basolateral amygdala and substantia nigra on oscillations is not yet known. However, if the trend in reduced PV expression in other brain regions (Figure 4) is meaningful, these changes could potentially

contribute to facilitated gamma oscillations and behavioral deficits (Vreugdenhil, Jefferys et al. 2003, Wöhr, Orduz et al. 2015).

GluN2D-KO mice may thus model some, but not all components of schizophrenia. Reduction in prepulse-inhibition (PPI) is thought to be a sensitive measure in schizophrenia. However, GluN2D-KO mice, have a robust PPI response (Takeuchi, Kiyama et al. 2001), a result confirmed in our laboratory. Elimination of the PPI response appears to require actions at multiple NMDARs. Knocking-out or knocking-down individual GluN2 subunits does not reduce PPI (Takeuchi, Kiyama et al. 2001, Spooren, Mombereau et al. 2004), but combining pharmacological inhibition of GluN2B-containing receptors in the GluN2A KO mouse (Spooren, Mombereau et al. 2004), or knocking-down GluN1 subunits globally (Fradley, O'Meara et al. 2005), does reduce PPI. Reduction in PPI was also not seen following GluN1 ablation from PV-cells (Korotkova, Fuchs et al. 2010), thus the NMDAR-associated neural substrate for impaired PPI function appears distinct from the system modulating gamma oscillations through NMDARs on PV-cells. Our results are thus consistent with the report that low doses of ketamine increases, rather than decreases, PPI in humans (Abel, Allin et al. 2003).

In summary, the inability of the psychotomimetic agent ketamine to 1) increase metabolic activation in cortico-limbic regions, 2) increase basal gamma oscillations, 3) increase locomotor activity, and 4) increase stereotypical rotations in GluN2D-KO mice suggests that GluN2D-containing NMDARs contribute to the psychotomimetic activity of ketamine. We also find that GluN2D elimination through development results in a partial down-regulation of PV similar to that seen in schizophrenia and following chronic NMDAR blockade. Together, these results suggest that GluN2D subunits might contribute significantly to the neuronal networks thought to be pivotal in cognitive processing which are disrupted in schizophrenia. These findings suggest that pharmacological augmentation of signaling mediated by GluN2D-containing NMDARs may

be of therapeutic benefit in schizophrenia - a finding consistent with recent animal studies
(Suryavanshi, Ugale et al. 2014).

Acknowledgements

Chapter 3 Structure activity relationship of NMDAR modulators

3 Identification and structure activity relationships (SAR) of novel NMDAR: 1) positive allosteric modulators (PAMs) 2) negative allosteric modulators (NAMs) 3) competitive antagonists

3.1 Abstract

N-methyl-D aspartate receptors are ligand-gated ion channels which play important roles in learning and memory. Excessive activity of NMDARs is thought to be involved in neuronal loss in stroke and neurodegenerative diseases such as Alzheimer's disease and Parkinson's disease whereas hypoactivity of NMDARs contributes to schizophrenia. With the goal of developing new NMDAR-related therapeutic agents, we measured the effect of novel test compounds on agonist-induced NMDAR responses. We identified efficacious NMDAR positive allosteric modulators (PAMs), such as UBP684 and UBP753, which activated all NMDAR subtypes with similar affinity. We also identified NMDAR negative allosteric modulators (NAMs), such as UBP792, which inhibit GluN2D and GluN2C more than GluN2B and GluN2A receptors. Although the PAMs were still not very potent, NAMs such as UBP792, UBP783 and UBP789 displayed an IC_{50} in the range of 2-3 μM at GluN2D-containing receptors. We also characterized new PPDA and UBP141 derivatives as competitive antagonists of NMDARs. The most subtype-selective compound from the series was UBP791, which had a K_i value of 0.14 μM for GluN2D receptors which was >100 fold lower than for GluN2A and 19-fold lower than for GluN2B receptors. This now represents the most selective GluN2C/GluN2D competitive antagonist available.

3.2   Introduction

Glutamate receptors mediate the majority of excitatory neurotransmission in the central nervous system. NMDARs are a subtype of ionotropic glutamate receptors whose altered function appears to contribute to various neurological disorders. Hyperactivity of NMDAR may lead to disorders such as epilepsy and cell death in stroke and neurodegenerative disease. Their hypofunction may lead to neuropsychiatric disorders such as schizophrenia. Since NMDAR function is very important for normal functioning of the CNS, modulating their activity allosterically may be therapeutically useful. Since, allosteric drugs bind to different sites other than the orthosteric sites where transmitters bind, PAMs do not activate inactive NMDARs. They modulate the activity of only activated NMDARs. Hence, such compounds as PAMs do not activate all NMDARs in the brain and affect only the activity of activated receptors.

Our laboratory, in collaboration with Dr. David Jane's laboratory at the University of Bristol, is developing allosteric modulators for NMDARs. Some compounds decrease NMDAR activity and they are called negative allosteric modulators (NAMs) of NMDARs. Other compounds have the property to increase NMDAR activity and such compounds are called positive allosteric modulators (PAMs) of NMDARs. Since, different NMDAR subunits have differential contributions to different diseases, it may be beneficial to modulate the activity of specific NMDAR subtypes.

Previously, our laboratory has reported coumarin, phenanthrene, and naphthalene based compounds (Costa, Irvine et al. 2010, Irvine, Fang et al. 2015, Irvine, Costa et al. 2012, Costa, Irvine et al. 2012) with both PAM and NAM activity. For example, UBP512, was a GluN2A-selective phenanthrene derivative PAM. UBP512 weakly potentiates GluN2A-, moderately inhibits GluN2C- and GluN2D- and has no effect on GluN2B-containing NMDARs (Costa, Irvine et al. 2010). Replacement of the iodine in UBP512 with a cyclopropyl group gives the compound UBP710 with potentiating activity at GluN2A- and GluN2B-containing NMDARs and

inhibitory activity at GluN2C- and GluN2D- containing NMDARs. UBP646 is another phenanthrene derivative that potentiates all subtypes of NMDAR with slightly more preference for GluN2D-containing receptors. UBP551 is a naphthalene derivative that selectively potentiates GluN2D-containig NMDARs and inhibits the other three subtypes of NMDARs (Costa, Irvine et al. 2010). UBP552 is another naphthalene derivative that non-specifically inhibits all NMDAR subunits with IC_{50} of 3-7 μM at GluN2A-D-containing NMDARs. Replacement of the bromo group of UBP552 with a phenyl ring yields even more potent NAM UBP618 with IC_{50} values ranging from 1.8 to 2.4 μM at GluN2A-D receptors (Irvine, Costa et al. 2012). A structurally-related coumarin derivative, UBP608, also has NAM activity with relatively higher potency at GluN2A subunit-containing receptors and least potency at GluN2D-containing NMDARs (Irvine, Costa et al. 2012). A common structural feature of all these compounds is the position of the carboxylate group. These compounds displayed higher activity when the carboxylate group was at the 2-position on the naphthalene ring or the 3-position of the phenanthrene ring.

In our attempt to identify additional subunit-selective and potent compounds with PAM or NAM activity, as well as competitive antagonists, we have designed analogues of previously characterized naphthalene and phenanthrene derivatives. The main goals of this chapter are (i) to identify compounds with better subunit selectivity, (ii) to find compounds with greater potency and/or efficiency, (iii) to determine the structural requirements for subunit-selective PAM or NAM activity, (v) to determine the structural requirements for improved subunit selectivity of competitive antagonists. These goals are achieved by testing the effect of these compounds on agonist-evoked NMDAR-mediated current using the two-electrode voltage clamp (TEVC) electrophysiological assay on rat recombinant GluN1-1a/GluN2A-D subtypes of NMDARs individually expressed on *Xenopus laevis* oocytes.

3.3   Materials and methods

Frogs were handled in accordance with University of Nebraska Medical Center's Institutional Animal Care and Use Committee (IACUC) guidelines. In accordance with these guidelines, efforts were made to minimize animal suffering and the number of frogs used.

3.3.1   Compounds

All chemical compounds were synthesized at the University of Bristol and structures were confirmed by [1]H- and ^{13}C-nuclear magnetic resonance (NMR) as well as mass spectroscopy (Burnell, Fang, Irvine, Jane, unpublished data). All compounds had elemental analyses where the determined percentage of C, H and N were less than 0.4 % different from theoretical values. Details of synthesis will be provided elsewhere. All stock solutions were prepared in DMSO, unless otherwise indicated, to a stock concentration of 50, 25, or 10 mM. For some compounds such as UBP684, stock solution was prepared with 1 molar equivalent of NaOH. The working solution was prepared in recording buffer just before the experiment. Other chemicals were obtained from Sigma unless stated otherwise. Ketamine was purchased from Hospira, Inc., Lake Forest, IL.

3.3.2   cDNA preparation

cDNA constructs encoding the rat NMDAR subunits was generously provided by Dr. Shigetada Nakanishi, Kyoto, Japan (GluN1-1a), Dr. Peter Seeburg, Heidelburg, Germany (GluN2A, GluN2C, and GluN2D) and Drs. Dolan Pritchett and David Lynch, Philadelphia, USA (GluN2B). GluN1 and GluN2A constructs with two cysteines introduced at N499C and Q686C at GluN1 LBD (hereafter GluN1[c]) and at K487C and N687C in GluN2A LBD (hereafter GluN2A[c]) were kindly provided by Dr. Gabriela Popescu, University of Buffalo) (Kussius, Popescu 2010).

Plasmids containing NMDAR cDNA were extracted with the Qiagen plasmid mini kit following manufacturer's procedure. Concentration and purity of cDNA was determined by a

NanoDrop analyzer. cDNA was confirmed by restriction digestion and further purified by sequencing by the UNMC DNA sequencing core facility.

200 µL of bacterial stock was again grown in 200 mL of LB broth medium for propagation of cDNA. Bacteria were incubated in LB medium supplemented with 50 mg/mL ampicillin at 37 ºC for overnight under shaking condition (300 rpm/min). cDNA was extracted using a Qiagen plasmid maxi kit following the manufacturer's instructions. Some of the bacterial culture was cryopreserved at -80 ºC in 25 % glycerol in LB medium for future use.

3.3.3   cRNA synthesis

Linearization: Plasmid DNA was first linearized with a restriction enzyme that cuts at a single site at the 3' end of the cDNA insert right after the stop codon. 100 µL digest reaction was carried out at 37 ºC for 2-4 h until the digestion was complete which was monitored by gel electrophoresis. Gel electrophoresis was carried out by running 1 µL of DNA on 1 % agarose gel at 80 V for 45 min – 1 h and DNA bands were visualized by UV transillumination of ethidium bromide stained gel. For 10 µg of cDNA digestion, 3-5 µL of restriction enzyme, 10 µL of NEBbuffer specific to the restriction enzyme, 1 µL of 100X BSA if not supplemented in the buffer, and nuclease free water to bring the final volume to 100 µL was used.

Purification of linearized cDNA: After the completion of restriction digestion, 100 µL of nuclease free water was added and mixed with 200 µL of chloroform:phenol:isoamylalcohol (25:24:1) and centrifuged to separate the top aqueous layer. The aqueous layer was further extracted with an equal volume of chloroform and 1/10 volume of 3 M sodium acetate and 2.2 volume of 100 % ethanol were added. After chilling the aqueous layer at -20 ºC for more than 30 minutes, it was centrifuged in TOMY MTX-150 centrifuge at 15,000 rpm at 4 ºC for 15 minute. The pellet was washed with 75 % ethanol and air-dried. The pellet was then re-suspended in nuclease free water by gentle pipetting and the concentration was determined with the NanoDrop analyzer.

cRNA synthesis: cRNA was synthesized *in vitro* using mMESSAGE mMACHINE ultra kit

(Ambion, Austin, TX, USA) according to the manufacturer's manual. Reagents were thawed,

vortexed, centrifuged and placed in ice before use. The reaction was run with 1 µg of linear

cDNA and other reagents provided in the kit in total volume of 20 µL. After incubating the

reaction mixture for 2 h at 37 °C, 1 µL of TURBO DNase was added and incubated for additional

15 minutes at 37 °C. The polyA tailing reaction was also carried out with the reagents provided in

the same kit to increase the stability of cRNA. Using the LiCl precipitation solution, the reaction

mixture was chilled at -20 °C for more than 1 h and centrifuged at 15000 rpm at 4 °C for 15

minutes. The resulting RNA pellet was washed with chilled 70 % ethanol to remove the

unincorporated nucleotides. For RNA verification, gel electrophoresis was carried out in 1 %

agarose with 1 % bleach (Aranda, LaJoie et al. 2012). Restriction enzymes used for linearization

of the DNA and promoters used for the RNA synthesis of each of the subunits are given in Table

3.1.

Table 3.1 Restriction enzymes used for cDNA linearization and RNA promoters used for *in vitro* synthesis of cRNA

NMDAR Subunit	Plasmid	Restriction enzyme	RNA Promoter
GluN1-1a	pBS	Not I	T7
GluN2A	pCDM8	ECOR I	T7
GluN2B	pRK5	Sal I	SP6
GluN2C	pCDM8	Not I	T7
GluN2D	pCDM8	Not I	T7
GluN1[c]	pCDNA3	Not I	T7
GluN2A[c]	pCDNA3	Not I	T7

3.3.4   *Two-electrode voltage clamp (TEVC) assay*

Two-electrode voltage clamp (TEVC) electrophysiology was performed as described previously

(Costa, Irvine et al. 2010). Oocytes (stage V – VI) from mature female *Xenopus laevis* (Xenopus

One, Ann Arbor, MI, USA) were removed and incubated overnight with 0.25 mg/mL of

collagenase (type I, Sigma, USA) at 17 °C. Oocytes were washed first with the Ca^{2+} free OR-2

buffer [OR-2 (mM): NaCl (82.5), KCl (2.5), $MgCl_2$ (1.0), HEPES (5.0), pH:7.6)] and then with

the ND-96 medium [ND-96 (mM): NaCl (96.0), KCl (2.0), $CaCl_2$ (1.8), $MgCl_2$ (1.0), HEPES

(5.0); pH 7.6; supplemented with sodium pyruvate (2.5 mM) and gentamycin (50 µg/mL)].

GluN1-1a and GluN2 cRNAs were mixed in a molar ratio of 1:1-3 and microinjected (50 nl, 15-

30 ng total) into the cytoplasm (vegetal pole) of healthy appearing oocytes (no pigmentation on

vegetal pole, uniform color of the animal pole, no clear demarcation between animal and vegetal

pole) to obtain the currents of about 100-500 nA. If currents were high, cDNAs were diluted with

nuclease free water. Oocytes were incubated in ND-96 solution at 17 °C prior to

electrophysiological assay (1-7 days).

Electrophysiological responses were measured using the TEVC assay using a Warner

Instruments (Hamden, CT, U.S.A.) model OC-725B Oocyte Clamp amplifier and a Digidata 1440

data acquisition system with pClamp 10 software (Molecular Devices, Sunnyvale, CA, USA).

The recording buffer contained (mM): NaCl (116), KCl (2), $BaCl_2$ (0.3) and HEPES (5), EDTA

(0.005) or DTPA (0.01) with the pH was adjusted to 7.4. NMDAR-mediated current was recorded

by holding the membrane potential constant at − 60 mV. Steady-state NMDAR responses were

determined by bath application of 10 µM L-glutamate plus 10 µM glycine. Then the effects of

test compounds were determined by application of compounds in presence of agonists. In initial

screening studies, compounds were dissolved in recording buffer to a final concentration of 100

µM and applied by bath perfusion. Percent of potentiation or inhibition by the test compounds

was calculated for each oocyte by comparision to currents evoked by agonist alone. The activity

is presented as % potentiation (Y-axis value above zero) or % inhibition (Y-axis value below

zero) of agonist-evoked response. Concentration-response results were fit using GraphPad Prism

(ISI Software, San Diego, CA, U.S.A.).

Concentration-response curves were fit to a single site with variable slope and using non-

linear regression, EC_{50} value for PAM or IC_{50} value for NAM activity were calculated with Prism

(Prism 6, GraphPad Software Inc., San Diego, CA). Apparent K_i values of competitive antagonists were calculated by the equation $K_i = IC_{50}/(1+([\text{agonist}]/EC_{50})$ (Yung-Chi, Prusoff 1973) which corrects for agonist affinity. For agonist affinities, we averaged values from the literature (Costa, Feng et al. 2009). The L-glutamate K_d we used for the calulation of K_i were 2.92 µM for GluN2A, 1.93 µM for GluN2B, 1.11 µM for GluN2C, and 0.44 µM for GluN2D (Costa, Feng et al. 2009).

3.3.5   *Schild analysis*

UBP791 inhibition was evaluated by Schild plot (Arunlakshana, Schild 1959). Concentration-response curves for glutamate in absence and presence of increasing concentrations of UBP791 were obtained. The EC_{50} value of the agonist was determined from the glutamate concentration-response curve in the absence of UBP791. Also, the EC_{50} was determined from concentration-response curves in the presence of increasing concentrations of UBP71. The dose ratio (DR) for each concentration of UBP791was calculated by dividing the corresponding EC_{50}' by the agonist-alone EC_{50}. Then log (DR – 1) was plotted against the log [UBP791] and fitted by linear regression analysis, to obtain slope and pA_2 value (X-intercept). The slope is expected to = 1 for a competitive antagonist at equilibrium. Schild's equation is given by: log (DR – 1) = pA_2 + log [B], where DR is dose ratio, pA_2 is a negative log of antagonist (UBP791) concentration that produces a two-fold shift of the agonist EC_{50} and [B] is the concentration of antagonist.

3.3.6   *Statistical analysis*

Prism 6 (GraphPad Software Inc., San Diego, CA, USA) was used for statistical analysis. All values are expressed as mean ± S.E.M. Concentration-response relationships were fit to a single site with variable slope. EC_{50}, IC_{50}, percent of maximal efficacy (% E_{Max}) and percent of maximal inhibition (% I_{Max}) values were calculated using a nonlinear regression analysis using prism.

3.4 Results

3.4.1 *Effect of alkyl side-chain length at the 6-position of 2-naphthoic acid on NMDAR activity*

Various analogues of 2-naphthoic acid with varying length of alkyl chain at the C-6 position of the 2-naphthoic acid were characterized Figure 3.1. As the length of the side-chain increased, compound activity switched from NAM to PAM. Compounds with a shorter alkyl side-chain UBP762 and UBP763 were inhibitors. UBP762 with a 2-carbon side-chain inhibited the GluN2B receptor the most (51.0 ± 12.0 %, n = 3). It also inhibited the response at GluN2A (28.2 ± 4.0 %, n = 4), GluN2C (28.9 ± 17.8 %, n = 4), and GluN2D receptors (16.9 ± 8.1 %, n = 3). UBP765 which had 4-carbon alkyl chain showed potentiating activity at GluN2A receptors (26.7 ± 9.7 %, n = 10) and had almost no effects at the other subtypes: weak potentiation at GluN2B (6.3 ± 7.4 %, n = 11), inhibition at GluN2C (8.0 ± 4.4 %, n = 7), and GluN2D receptors (4.8 ± 2.5 %, n = 8)). When an isohexyl group was substituted at the 6-position ring, it yielded a pan-PAM compound, UBP684, which displayed a potentiating activity at each of the four NMDAR subtypes. UBP684 is an analogue of the previously characterized potentiator, UBP646, in which the unsubstituted ring C of the phenanthrene is removed. UBP684 potentiated GluN2A receptors by 71.0 ± 5.6 % (n = 17), GluN2B receptors by 71.0 ± 9.4 % (n = 11), GluN2C receptors by 92.0 ± 6.2 % (n = 22), and GluN2D receptors by 107 ± 15.6 % (n = 9) (Figure 3.1). UBP684 potentiated GluN2C- and GluN2D-containing receptors more than GluN2A- and GluN2B-containing receptors. Removal of the ring C from the phenanthrene nucleus of UBP647 (a previously characterized PAM) led to the 2-naphthoic acid analogue UBP676 which also potentiated GluN2A- and GluN2C-containing receptors to similar efficacy as the parent compound UBP647. However, UBP676 displayed lower efficacy at GluN2D-containing receptors and no activity at GluN2B-containing NMDARs (Figure 3.2). UBP692, which was obtained by replacing the isohexyl sidechain of UBP684 with *n*-butylcyclopentane, displayed reduced potentiating activity. However, it still showed a general PAM activity. UBP692 potentiated

agonist-induced response at GluN2A receptors by 42.0 ± 6 % (n = 4), GluN2B receptors by 47.0 ± 9.0 % (n = 4), GluN2C receptors by 71.0 ± 16.0 % (n = 4), and GluN2D receptors by 47.0 ± 16.0 % (n = 4) (Figure 3.4).

Although the maximal potentiation by UBP684 was higher, it was, 3-6-fold less potent than the 9-*n*-pentyl phenanthrene derivative UBP647 at GluN2A-D receptors with an EC_{50} of 28.0-37.2 µM (Table 3.2, Figure 3.2B). However, UBP684 had similar potency to that of UBP676 at GluN2A-containing receptors (Table 3.2, Figure 3.2).

A.

Compound	R
UBP762	
UBP763	
UBP765	
UBP676	
UBP684	
UBP692	
UBP736	

B.
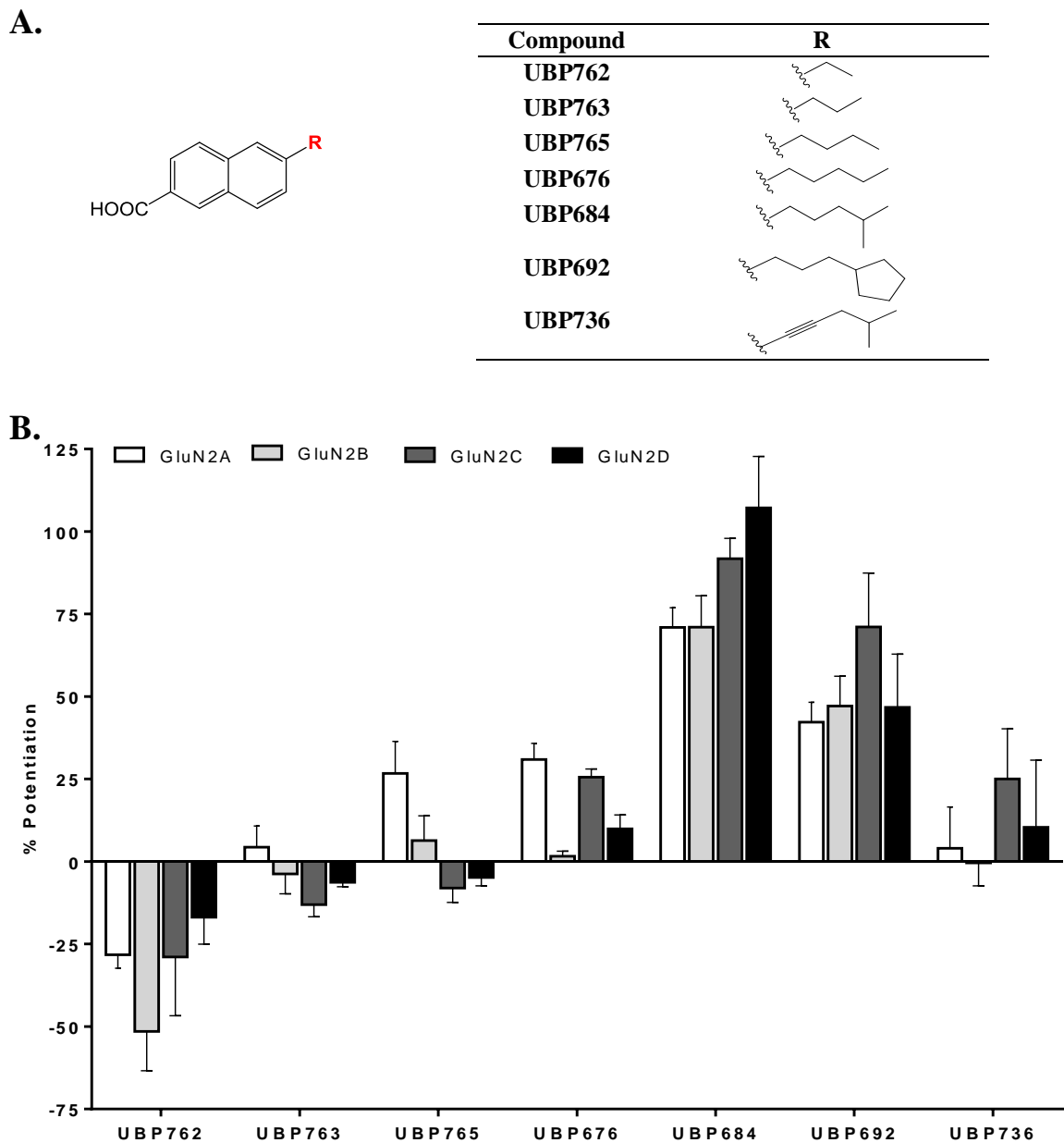
Figure 3.1 SAR studies to determine the effect of length of the alkyl side-chain at the 6-position of naphthalene ring on NMDAR activity

(**A**) Structures of tested UBP compounds with different length of alkyl side-chains. (**B**) NMDAR activity of UBP compounds (100 µM) was measured by TEVC assay at rat recombinant NMDARs (GluN1-1a/GluN2A-D) expressed in *Xenopus laevis* oocytes. The effect of compound on agonist (L-glutamate and glycine, 10 µM each)-induced NMDAR current was measured and expressed as % potentiation (mean ± S.E.M.) of agonist-induced response (positive value is % potentiation and negative is % inhibition; n>4).
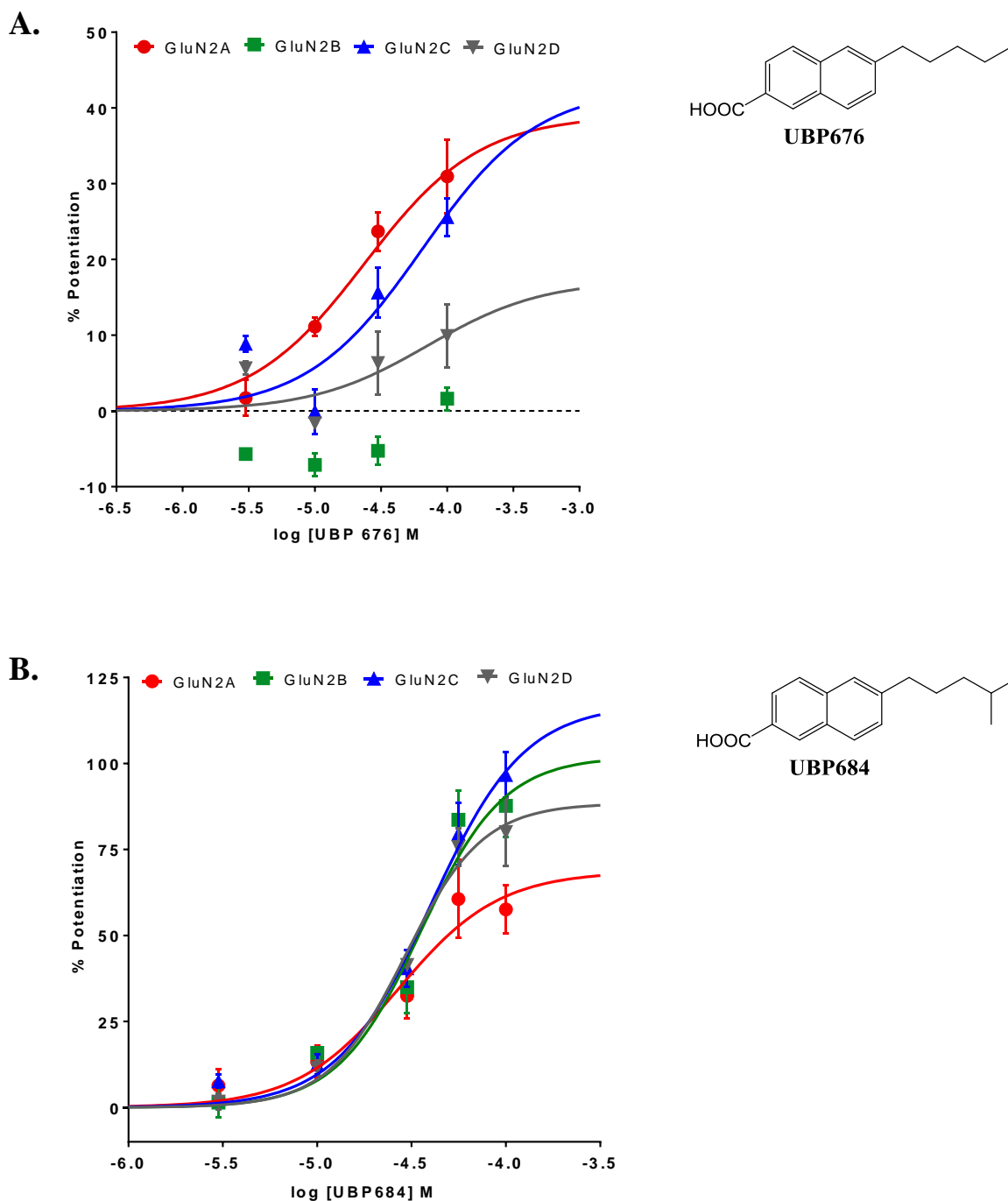
Figure 3.2 Concentration-response study of the potentiation of NMDAR responses by (A) UBP676 and (B) UBP684

Select PAMs were tested for activity at increasing concentrations to determine their affinity and maximal efficacy at different NMDAR subunits. Using the TEVC assay, the current produced by co-application of different concentrations of the compounds and the agonists (10 μM of L-glutamate and 10 μM of glycine) at rat recombinant NMDARs (GluN1-1a/GluN2A-D) expressed in *Xenopus laevis* oocytes was measured and expressed as % potentiation (mean ± S.E.M) above agonist-alone induced response (n > 4).

3.4.2 Effect of heteroatoms or methylene substitution of alkyl side-chain at 6-position of 2-naphthoic acid on NMDAR activity

Another series of compounds were developed by incorporation of different heteroatoms like nitrogen or oxygen or a methylene group into the isohexyl side-chain of UBP684. Replacing the second CH2 group in the isohexyl sidechain of UBP684 with an oxygen (UBP742) or sulfur (UBP741), making an ether or thioether, eliminated the potentiating activity of UBP684. Incorporating the amide (UBP740), or ester (UBP748) in the isohexyl side-chain of UBP684 made them moderate inhibitors. Although inserting an ether group (UBP742) or a ketone group (UBP751) eliminated the potentiating activity, incorporating an ester group into the isohexyl chain close to the naphthalene ring (UBP744) resulted in a *pan*-potentiator with activity similar to UBP684 at each of the NMDAR subtypes (Figure 3.3). Incorporation of a double bond into the isohexyl chain of UBP684 led to compound UBP752, which showed more potent activity than its parent compound UBP684. It potentiated all subtypes with more preference for GluN2B, GluN2C and GluN2D receptors (EC_{50} values ranged from 26 to 161 μM, Table 3.2,). UBP752 potentiation at GluN2A, GluN2B, GluN2C and GluN2D receptors was 63.0 ± 12.0 % (n = 16), 165.0 ± 29.0 % (n = 18), 249.0 ± 45.0 % (n = 19), 210.0 ± 49.0 % (n = 18) respectively (Figure 3.4B). From this study, it appears that polar substitution on the alkyl side-chain are tolerated as in UBP744, which could be beneficial in enhancing the hydrophilicity of these compounds. However, polar group substitution on the alkyl chain reduced the potentiating activity by most of the tested compounds. Methylene group addition at the 1-position of the alkyl chain reduced the affinity on GluN2A and GluN2B but increased the efficacy (UBP752).

A.

Compound	Formula	X	Z
UBP742	A	O	-
UBP741	A	S	-
UBP744	B	O	O
UBP740	B	NH	O
UBP748	C	-	-
UBP751	B	CH_2	O
UBP752	B	CH_2	CH_2

B.
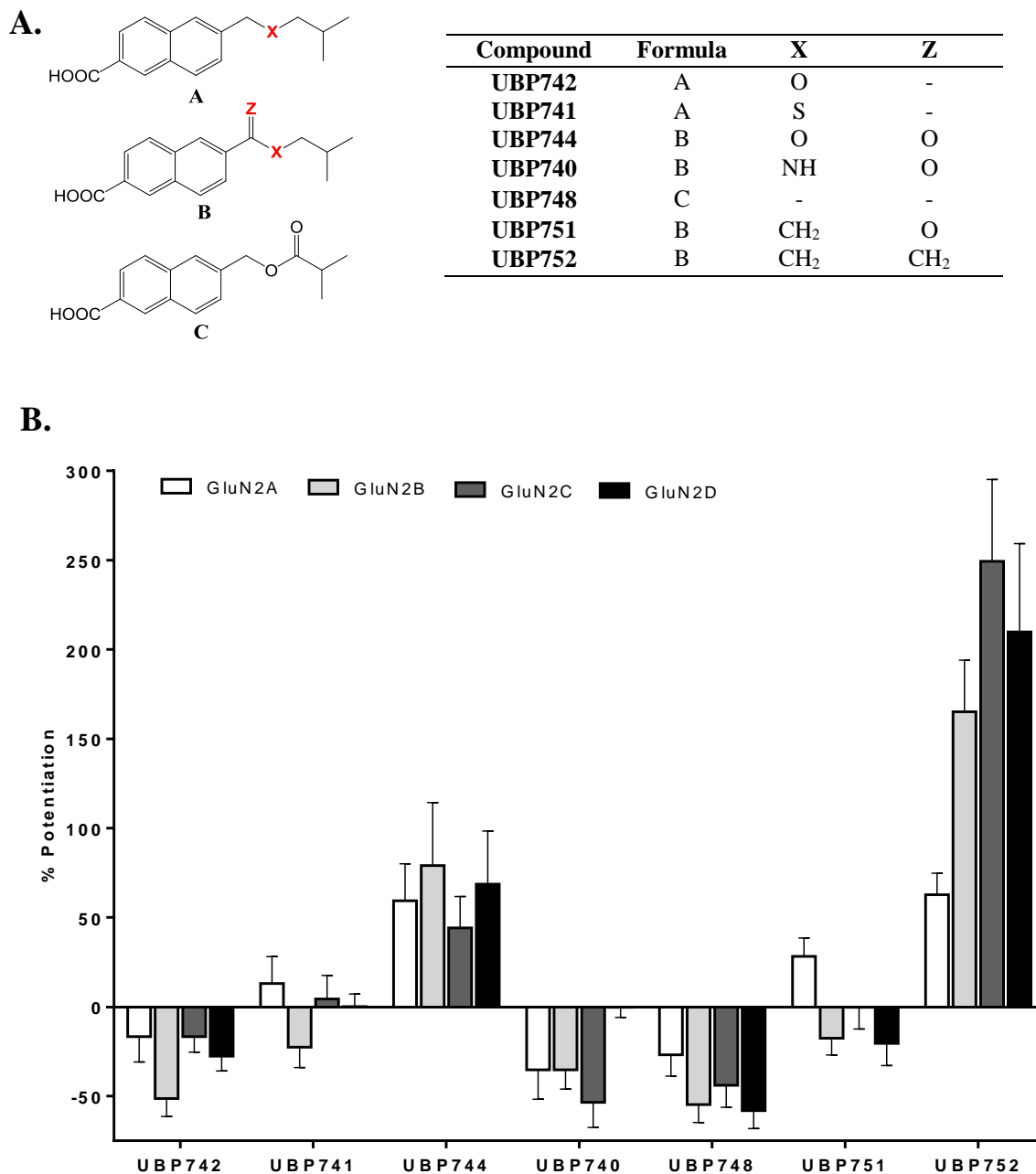
Figure 3.3 SAR studies to determine the effect of heteroatom or methylene substitution to the alkyl side-chain at 6-position of naphthalene ring on NMDAR activity

(**A**) Structures of UBP compounds with different heteroatom or methylene substitutions to the alkyl side-chain of UBP684. (**B**) NMDAR activity of UBP compounds (100 μM) was measured by TEVC assay at rat recombinant NMDARs (GluN1-1a/GluN2A-D) expressed in *Xenopus laevis* oocytes. The effect of compound on agonist-induced (L-glutamate and glycine, 10 μM each) NMDAR current was measured and expressed as % potentiation (mean ± S.E.M.) of agonist-induced response (positive value is % potentiation and negative value is % inhibition; n > 4).
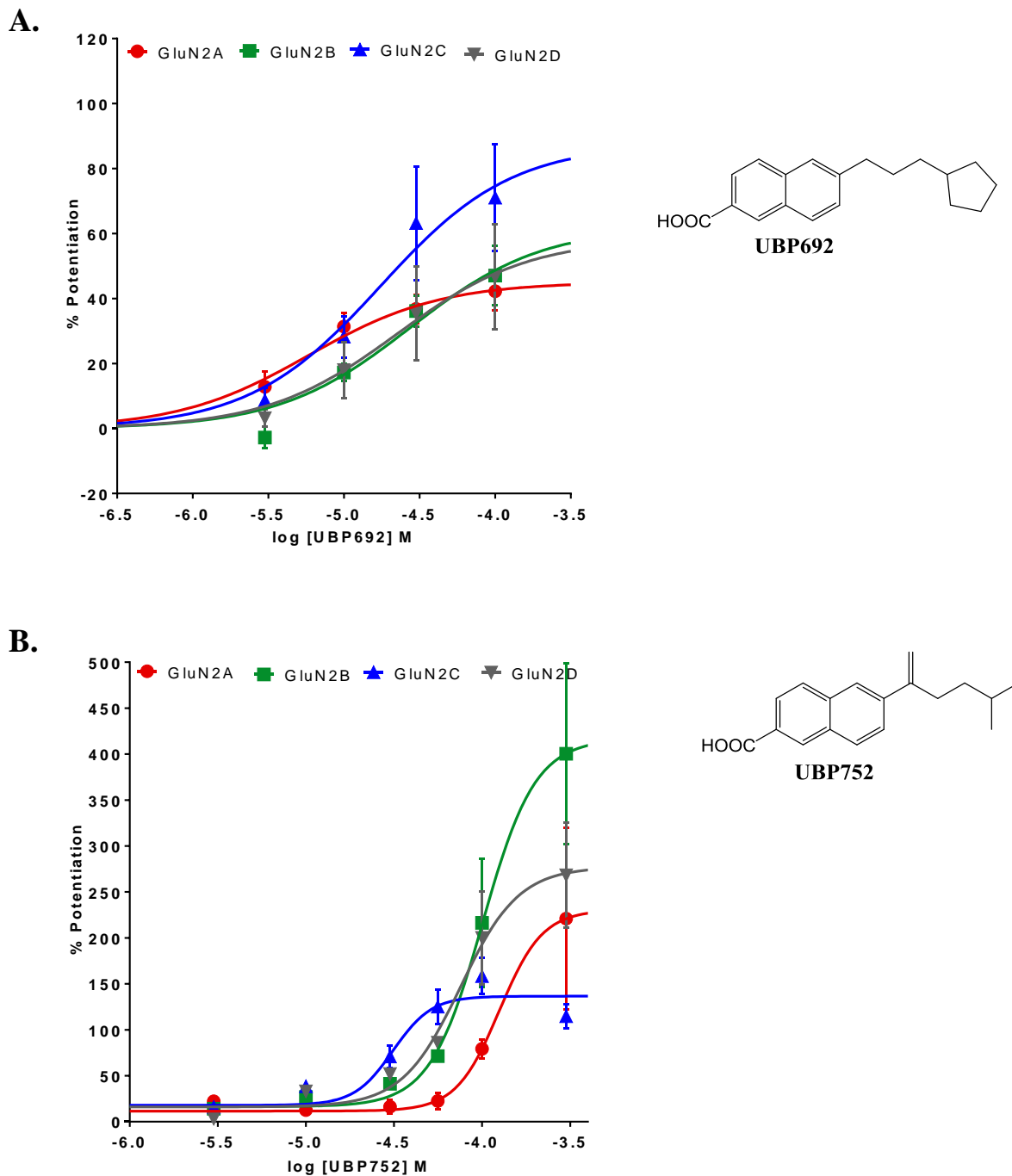
Figure 3.4 Concentration-response study on potentiation of NMDAR responses by (A) UBP692 and (B) UBP752

Select PAMs were tested for activity at increasing concentrations to determine their affinity and maximal efficacy at different NMDAR subunits. Using TEVC assay, the current produced by co-application of different concentrations of test compound and agonists (10 μM of L-glutamate and 10 μM of glycine) at rat recombinant NMDARs (GluN1-1a/GluN2A-D) expressed in *Xenopus laevis* oocytes was measured and expressed as % potentiation (mean ± S.E.M) above agonist-alone induced response (n > 4).

3.4.3   Effect of changing the position of carboxyl or hydroxyl groups on the naphthalene ring of UBP684 on NMDAR activity

Adding a hydroxyl group to the 3-position of the naphthalene ring of UBP684 yielded the compound UBP743 that displayed a general PAM activity increasing the response at each of the NMDAR subtypes. This compound showed greater activity at GluN2B-D receptors compared to that of UBP684. It potentiated GluN2A by 78.0 ± 30 % (n = 17), GluN2B by 208.7 ± 107.0 % (n = 15), GluN2C by 257.0 ± 92.0 % (n = 17), and GluN2D by 201.0 ± 112.6 % (n = 16) (Figure 3.5). When the position of carboxyl and hydroxyl group of UBP743 were swapped, it yielded compound UBP738 which displayed reduced potentiating activity at GluN2B, GluN2C and GluN2D subtypes compared to UBP684 and showed weak inhibitory activity on GluN2A receptors. Moving the carboxyl group from the 2-position to the 3-position of the naphthalene ring of UBP684 yielded the compound UBP749 which showed dramatically reduced potentiating activity at GluN2A, GluN2B and GluN2C receptors compared to UBP684 and weak inhibitory activity at the GluN2D receptor. These results show that carboxyl group at 2-position of naphthalene ring is very important for the potentiating activity of UBP684 analogues.

A. .
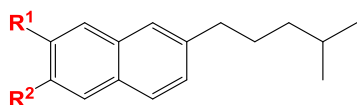
Compound	R^1	R^2
UBP743	OH	COOH
UBP738	COOH	OH
UBP749	COOH	H

B.
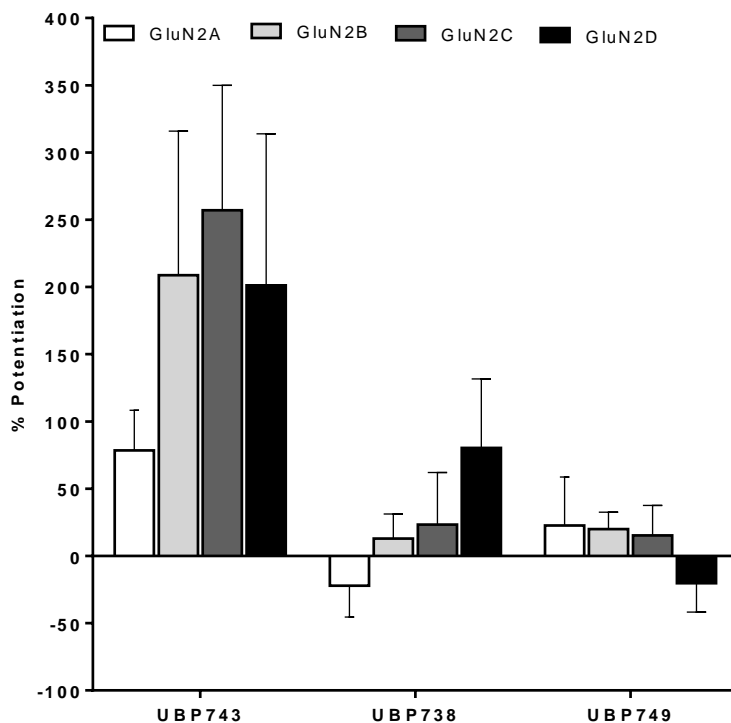
Figure 3.5 SAR studies to determine the effect of changing the position of carboxyl and hydroxyl group substitution at naphthalene ring on NMDAR activity

(**A**) Structures of tested UBP compounds with carboxylic and hydroxyl group substitution at the 2- and 3-positions on the naphthalene ring of UBP684. (**B**) NMDAR activity of UBP compounds (100 µM) was measured by TEVC assay at rat recombinant NMDARs (GluN1-1a/GluN2A-D) expressed in *Xenopus laevis* oocytes. The effect of compounds on agonist-induced (L-glutamate and glycine, 10 µM each) NMDAR current was measured and expressed as % potentiation (mean ± S.E.M.) of agonist-induced response (positive value is % potentiation and negative value is % inhibition; n>4).

3.4.4   Effect of nitro, amino and halogen substitution at the 1- and 7-position of the naphthalene ring of UBP684 on NMDAR activity

Another series of UBP684 analogues were synthesized by substitution at the 1- and 7-positions of the naphthalene ring of UBP684 with nitro, amino, hydroxyl group or halogen atoms (Figure 3.6). The compound retained potentiating activity when a hydroxyl group was substituted at the 1-position (UBP767). UBP767 had similar activity on GluN2B and GluN2C as that of UBP684. However, it exhibited reduced potentiating activity at GluN2A (9.7 ± 13.7 %, n = 3) and GluN2D (20.0 ± 26.7 %, n = 3) receptors. Substitution at the 7-position of the naphthalene ring with a halogen atom reduced or eliminated the potentiating activity of parent compound UBP684. Iodine substitution at 7-position of the naphthalene ring (UBP770) was toleratede but the potentiation was reduced. Substitution with bromine (UBP771) or chlorine (UBP772) at the 7-position of the naphthalene ring completely eliminated the potentiating activity of the parent compound UBP684. They exhibited a weak inhibitory activity at NMDARs. Substitution at the 1-position of the naphthalene ring of UBP684 with a *nitro* group yielded UBP759, which displayed a strong inhibitory effect on NMDAR activity instead of exhibiting the potentiating effect of its parent compound (Figure 3.6). At 100 μM, UBP759 inhibited GluN2A receptors by 27.3 ± 10.3 % (n = 11), GluN2B receptors by 74.3 ± 5.2 %, (n = 9), GluN2C receptors by 86.0 ± 2.6 %, (n = 10) and GluN2D receptors by 85.4 ± 2.6 % (n = 10). Substitution at the 7-position of the naphthalene ring of UBP684 with an *amino* group yielded UBP768, which also converted the potentiator parent compound into an inhibitor. UBP768 at 100 μM inhibited GluN2A receptors by 29.4 ± 4.0 % (n = 8), GluN2B receptors by 53.4 ± 3.7 %, (n = 9), GluN2C receptors by 76.5 ± 2.3 %, (n = 9) and GluN2D receptors by 90.7 ± 2.0 % (n = 8). UBP774 was designed by combining the structural features thought to be important for potentiating activity by compounds UBP684 and GNE compounds. However, this hybrid compound did not display any potentiation at any of the subunits of NMDARs at tested concentration.

Concentration-response studies were also performed to investigate the subunit selectivity, affinity and maximal efficacy at each of the NMDAR subtypes. UBP759 and UBP768 showed more inhibitory preference for GluN2D- and least preference for GluN2A-containing NMDARs (Figure 3.7). Neither of the NAMs showed complete inhibition of the NMDAR responses at the maximum tested concentration. However, UBP768 was 8-fold more potent at inhibiting the GluN2D- than GluN2A-containing receptors. The IC_{50} for inhibition of NMDAR responses by UBP768 was 66 µM at GluN2A- and 8 µM at GluN2D-containing receptors (Table 3.4). The IC_{50} for inhibition by UBP759 at GluN2A-, GluN2B-, GluN2C-, and GluN2D-containing receptors was > 100, 30.9 ± 5.3, 19.9 ± 2.7 and 17.4 ± 2.7 µM respectively. This tells us that substitution at the 3- and 7-position of the naphthalene ring of UBP684 with an electronegative group is not tolerated for potentiating activity. However, this information might be helpful in designing the GluN2D-selective NAMs.

A.

Compound	Formula	R^1	R^2
UBP759	A	NO$_2$	H
UBP769	A	H	NO$_2$
UBP767	A	OH	H
UBP768	A	H	NH$_2$
UBP770	A	H	I
UBP771	A	H	Br
UBP772	A	H	Cl
UBP773	A	H	(NHC(O)Ph)
UBP774	B	-	-

B.
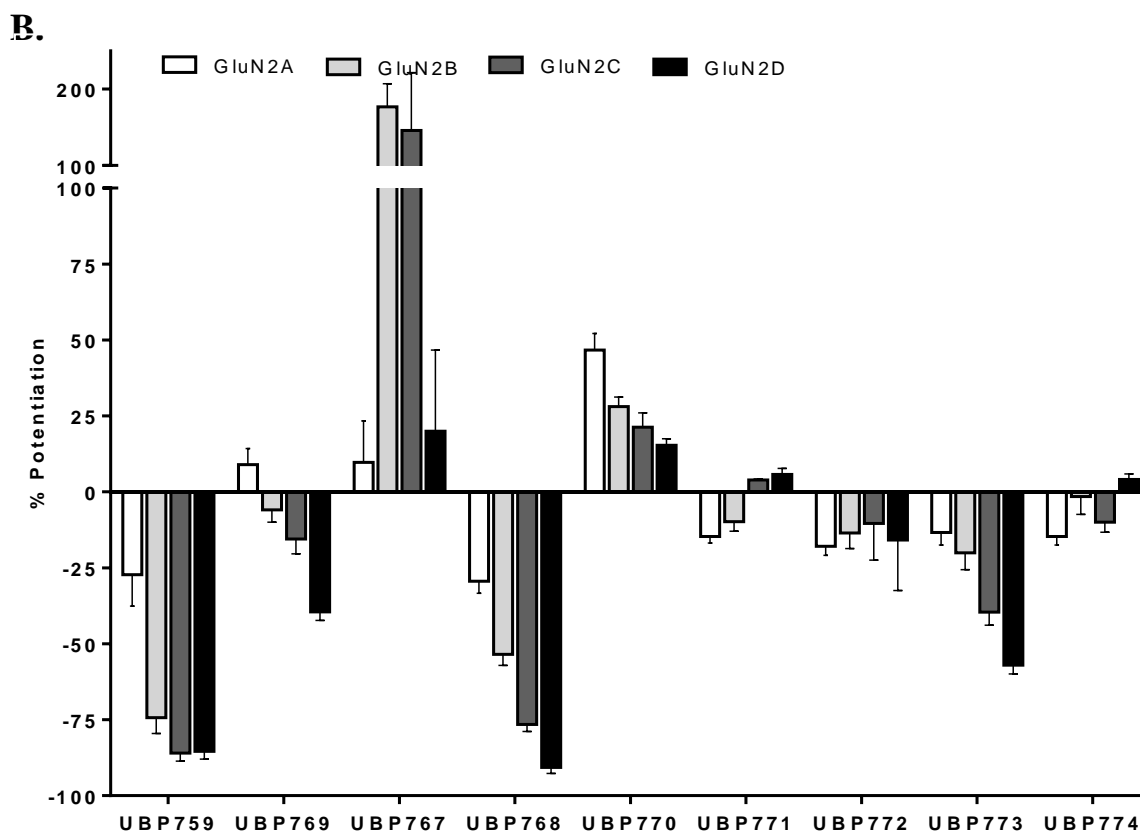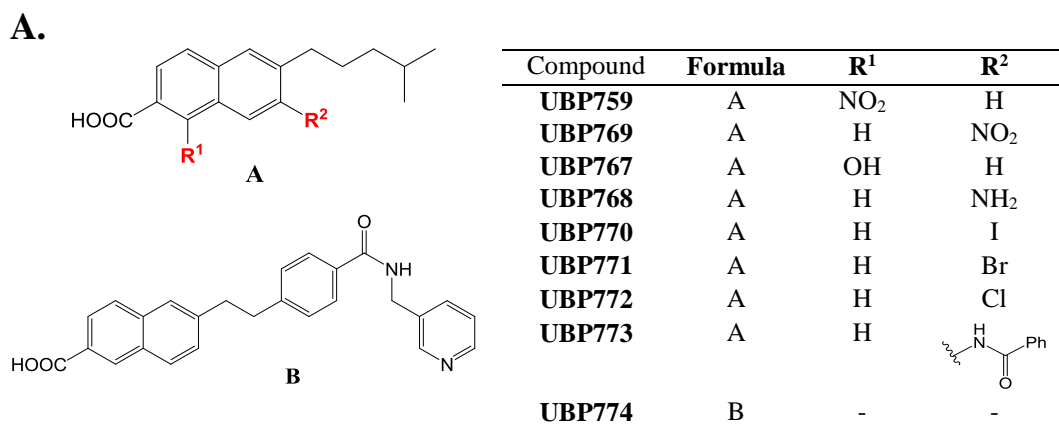
Figure 3.6 SAR studies to determine the effect of nitro, amino and halogen substitution at the 1- and 7-position of the naphthalene ring on NMDAR activity

(**A**) Structures of tested UBP compounds with nitro, amino and halogen substitution on the naphthalene ring of UBP684. (**B**) NMDAR activity of UBP compounds (100 µM) was measured by TEVC assay at rat recombinant NMDARs (GluN1-1a/GluN2A-D) expressed in *Xenopus laevis* oocytes. The effect of compound on agonist-induced (L-glutamate and glycine,10 µM each) NMDAR current was measured and expressed as % potentiation (mean ± S.E.M.) of agonist-induced response (positive value is % potentiation and negative value is % inhibition; n>4).
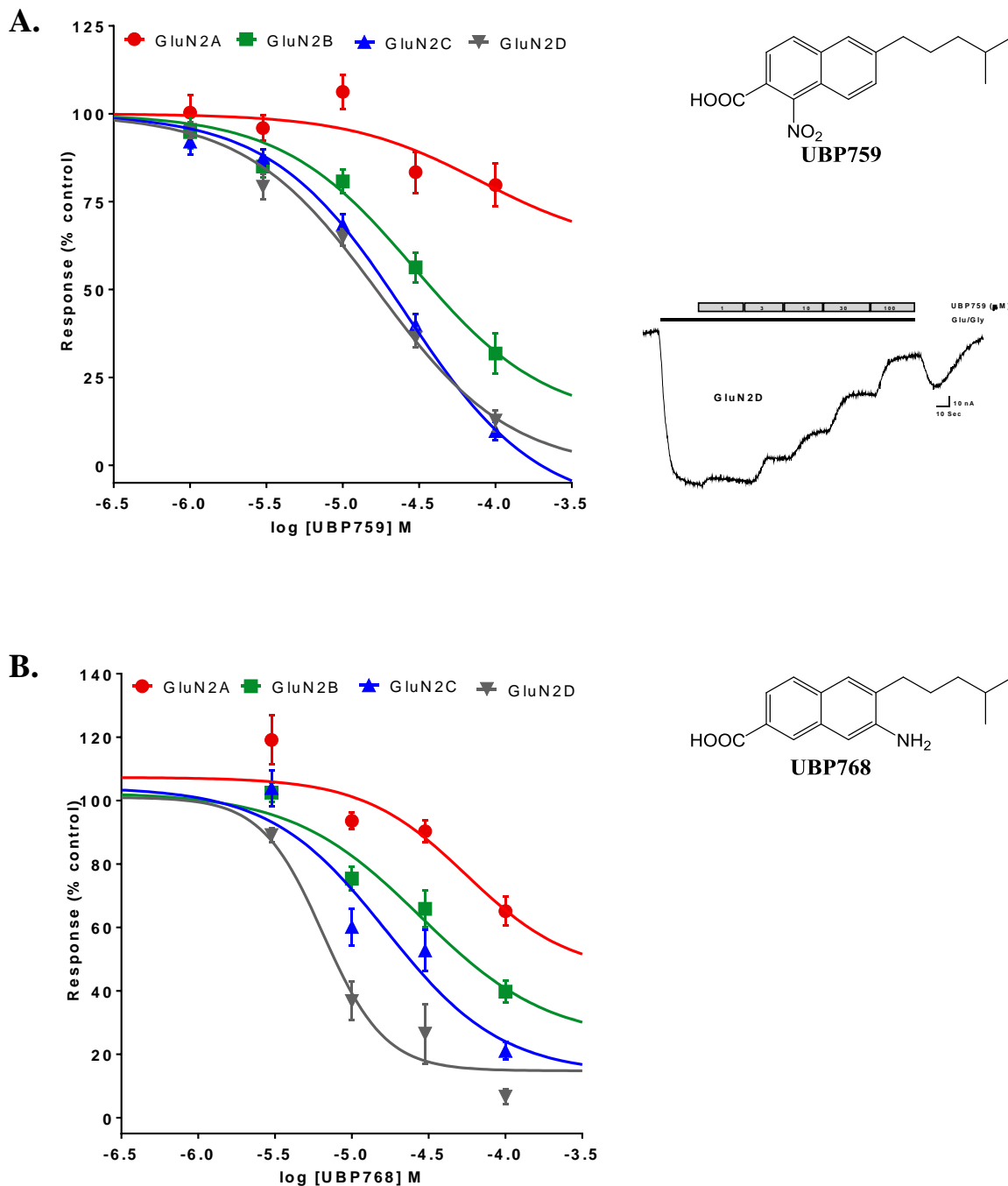
Figure 3.7 Concentration-response study on inhibition of NMDAR current by (A) UBP759 and (B) UBP768

Select NAMs were tested for activity at increasing concentrations to determine their affinity and maximal inhibition at NMDARs (GluN1-1a/GluN2A-D) expressed in *Xenopus laevis* oocytes. Using TEVC assay, the inhibition of agonist-evoked (10 µM of L-glutamate and 10 µM of glycine) current by co-application of different concentrations of compounds and agonist was measured and expressed as % NMDAR response (mean ± S.E.M) considering agonist-alone induced response as 100 % (n > 4).

3.4.5 Effect of substitution at the 6-position on the alkyl/alkene side-chain of 2-naphthoic acid of UBP684

Addition of a double bond to the 1-position of the isohexyl side-chain of UBP684 gave the compound UBP727 which displayed comparable activity to that of parent compound and UBP744, which had an ester group close to the naphthalene ring. UBP727, at 100 μM, potentiated GluN2A receptors by 35.0 ± 11.3 % (n = 4), GluN2B receptors by 52.0 ± 9.3 %, (n = 5), GluN2C receptors by164.2 ± 41.3 %, (n = 5), and GluN2D receptors by 120.0 ± 39.2 % (n = 5) (Figure 3.8). When the end methyl group of the isohexyl chain of UBP727 was replaced with carboxyl group, it yielded compound UBP729 that led to elimination of the potentiating activity. When a CH_2COOH group replaced the methyl group at the R^1 position of side-chain of UBP727 to yield UBP756, it also eliminated the potentiating activity. UBP756 showed moderate inhibitory activity on GluN2A-, GluN2B- and GluN2D-containing NMDARs and no activity on GluN2C receptors. Substitution at R^1 position (Figure 3.8, Formula B) of the isohexyl side-chain of UBP684 with a methyl group gave UBP753 which potentiated all GluN2 subtypes with a similar potency (EC_{50} values ranged from 25.0 to 39.4 μM across all NMDAR subtypes (Table 3.2) to that of UBP684 and showed even higher maximal potentiation compared to UBP684 (Figure 3.8). UBP753 at 100 μM potentiated GluN2A receptors by 181.0 ± 41.9 % (n = 17), GluN2B receptors by 124.7 ± 25.3 %, (n = 20), GluN2C receptors by 237.1 ± 54.8 %, (n = 21) and GluN2D receptors by 217.5 ± 36.8 % (n = 19) (Figure 3.8). Adding a carboxylic acid at the R^2 position of the isohexyl side-chain of UBP684 (Figure 3.8, Formula B) gave UBP757 which showed a weak potentiating activity at GluN2C-, no activity at GluN2A- and weak inhibitory activity at GluN2B- and GluN2D-containing NMDARs. However, the substitution with a CH_2SH group at the R^3 position of n-pentyl side-chain of structure B (UBP766, Figure 3.8) was tolerated for potentiating activity. UBP766 exhibited comparable potentiating activity as that of UBP684 as shown in Figure 3.8. UBP766, at 100 μM, potentiated GluN2A receptors by 81.5 ± 15.1 % (n = 5), GluN2B receptors by 73.4 ± 10.3 %, (n = 4), GluN2C receptors by 42.0 ± 2.8 %, (n = 3) and

GluN2D receptors by 43.1 ± 9.5 % (n = 4). When ring A of the UBP684 naphthalene ring was replaced with cyclohexane, it gave compound UBP764 which at 100 µM showed a moderate potentiating activity at GluN2A (60.6 ± 8.8 %, n = 4) and a weak potentiating activity at GluN2B (5.2 ± 7.3 %, n = 4), GluN2C (12.0 ± 2.8 %, n = 4) and GluN2D-contining receptors (16.4 ± 6.1 %, n = 4) (Figure 3.8).

Concentration-response studies were performed for UBP753 and UBP764 (Figure 3.9). UBP753 potentiated all subtypes with almost equal affinity (EC_{50} values was ranged from ~ 30-40 µM across all subtypes, Figure 3.9, Table 3.2). Although UBP764 was not efficacious, concentration-response study shows that it potentiates GluN2A receptors more than GluN2B receptors and does not potentiate GluN2C- and GluN2D-containing receptors. (Figure 3.9).

The results from this series of compounds shows that the addition of a double bond or substitution with a methyl group at 1-position of isohexyl side-chain is tolerated for potentiating activity. However, substitution with a carboxyl group in the isohexyl side-chain of UBP684 is not tolerated for potentiating activity. Substitution with a carboxyl group on the isohexyl chain either eliminates the potentiating activity or converts the compound from a potentiator to an inhibitor.

A.

Compound	Formula	R¹	R²	R³
UBP727	A	CH_3	-	-
UBP729	A	COOH	-	-
UBP756	A	CH_2COOH	-	-
UBP753	B	CH_3	H	CH_3
UBP757	B	H	COOH	CH_3
UBP766	B	H	H	CH_2SH
UBP764	C	-	-	-

B.
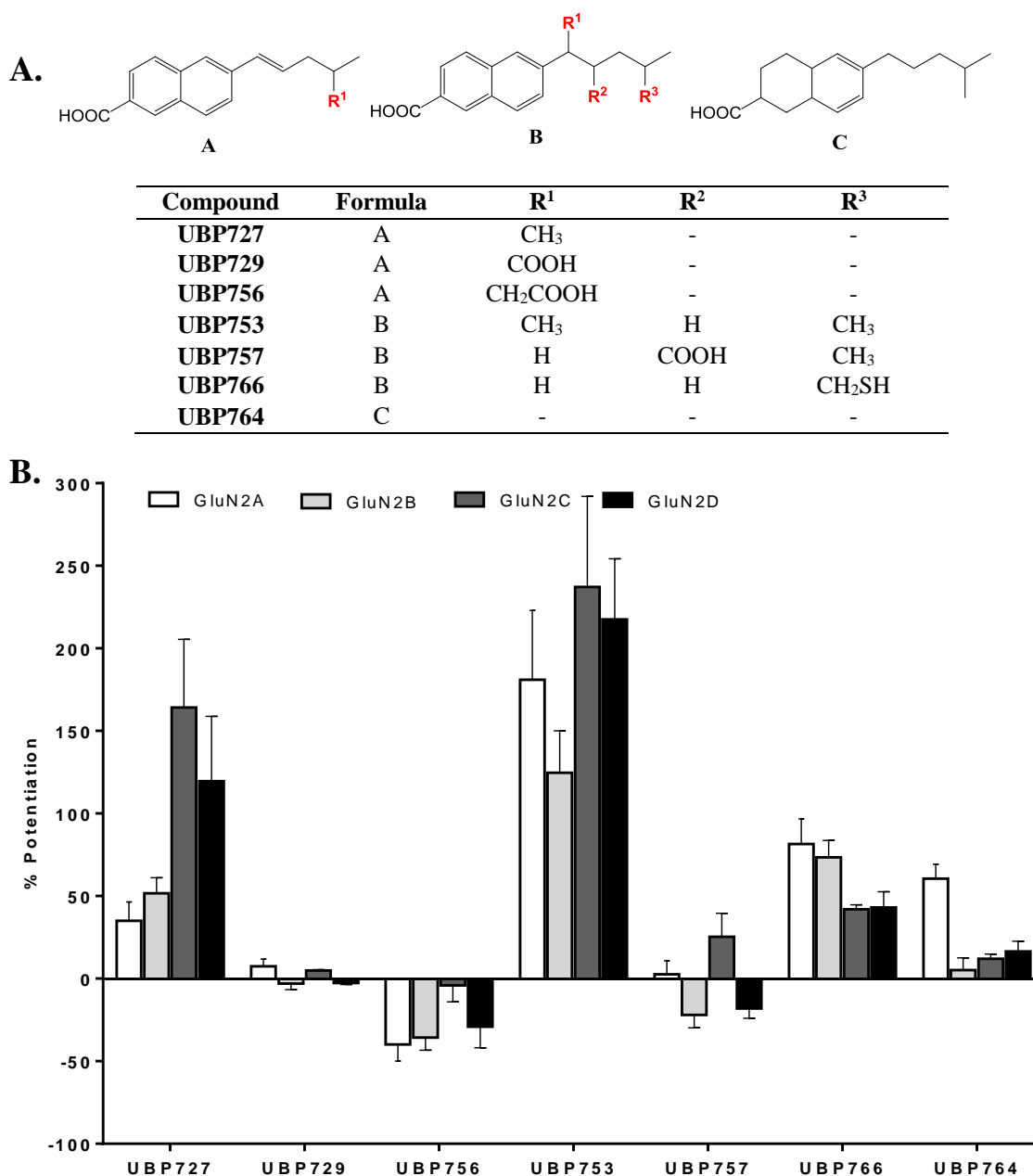
Figure 3.8 SAR studies to determine the effect of substitution of the alkyl and alkene side-chain at the 6-position of the naphthalene ring on NMDAR activity

(**A**) Structures of test UBP compounds with different substitutions on the alkyl and alkene side-chain at C-6 position of the naphthalene ring. (**B**) NMDAR activity of UBP compounds (100 µM) was measured by TEVC assay at rat recombinant NMDARs (GluN1-1a/GluN2A-D) expressed in *Xenopus laevis* oocytes. The effect of compound on agonist-induced (L-glutamate and glycine, 10 µM each) NMDAR current was measured and expressed as % potentiation (mean ± S.E.M.) of agonist-induced response (positive value is % potentiation and negative value is % inhibition; n > 4).

A.

B.
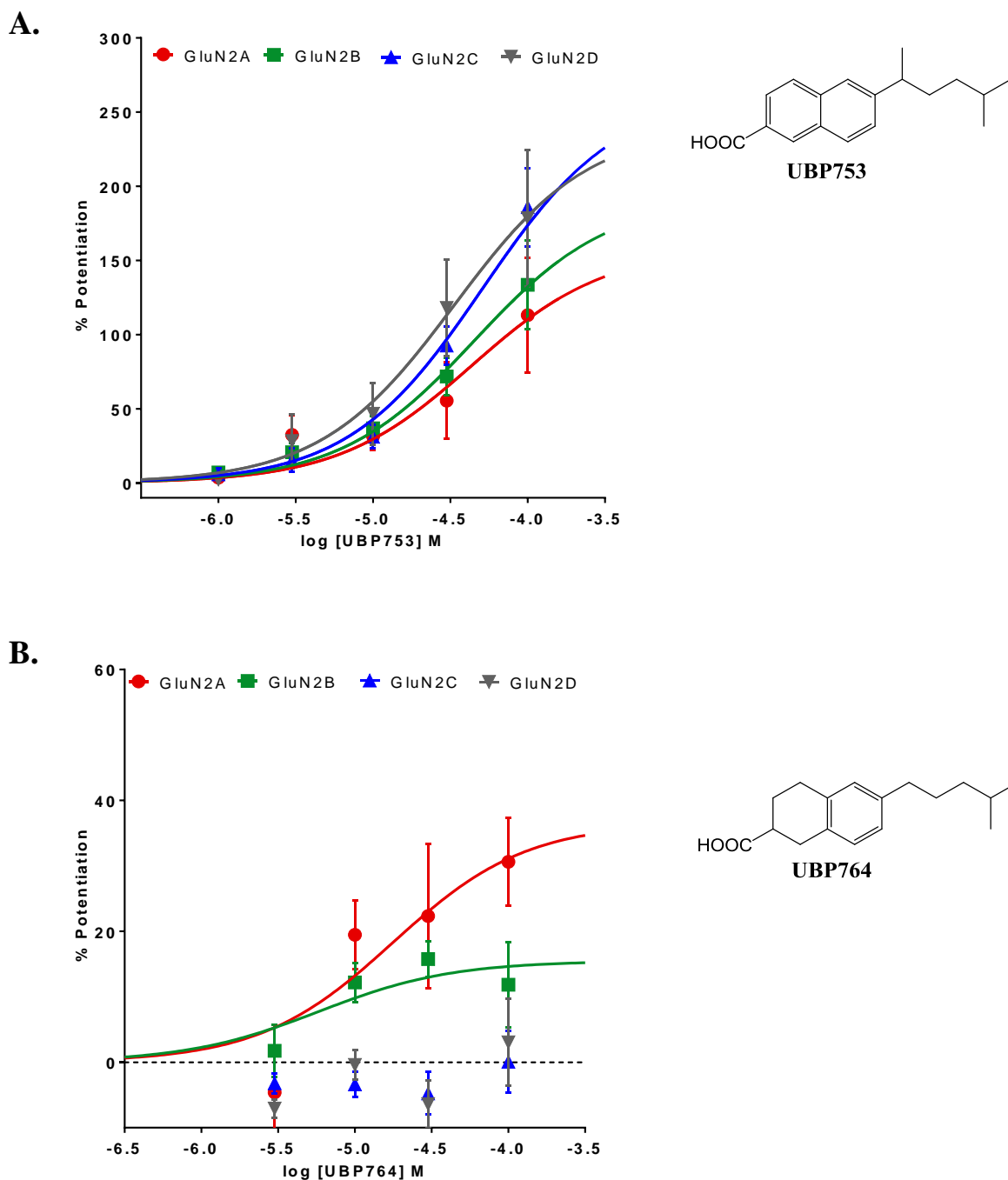
Figure 3.9 Concentration-response study of the potentiation of NMDAR responses by (A) UBP753 and (B) UBP764

Select PAMs were tested for activity at increasing concentrations to determine their affinity and maximal efficacy at different NMDAR subunits. Using TEVC assay, the current produced by co-application of different concentrations of the compound and the agonists (10 μM of L-glutamate and 10 μM of glycine) at rat recombinant NMDARs (GluN1-1a/GluN2A-D) expressed in *Xenopus laevis* oocytes was measured and expressed as % potentiation (mean ± S.E.M) above agonist-alone induced response (n > 4).

3.4.6   Effect of replacement of naphthalene ring of UBP684 with heterocyclic ring on modulation of NMDAR activity

Derivatives of UBP684 with different heterocyclic structures were also tested for their NMDAR activity (Figure 3.10). When ring A of UBP684 was replaced with pyridine, it gave compound UBP750 which at 100 µM exhibited a moderate inhibitory activity at GluN2B- (20.3 ± 12.3 %, n = 8), GluN2C (40.0 ± 10.1 %, n = 11), and GluN2D-containing receptors (46.4 ± 8.8 %, n = 9), and displayed no activity at GluN2A receptors (1.0 ± 8.0 %, n = 8). When naphthalene ring B of UBP684 was replaced with imidazole, oxazole or thiazole, it yielded compounds UBP734, UBP754 and UBP755 respectively. Although UBP734 retained weak potentiating activity, compounds UBP754 and UBP755 were inhibitors with moderate activity (Figure 3.10). When naphthalene ring A was replaced with pyridine-2-one, it gave UBP747 which moderately inhibited GluN2B, GluN2C and GluN2D receptors and did not have any activity at GluN2A-containing NMDARs. Similarly, when ring B of naphthalene of UBP684 was replaced with pyrrole-2,5-dione, it gave compound UBP745. UBP745 displayed no NMDAR modulatory activity at GluN2A receptors (2.8 ± 9.2 %, n = 9), weak inhibitory activity at GluN2C (18.3 ± 5.2 %, n = 8) and GluN2D receptors (10.3 ± 7.7 %, n = 5), and moderate inhibitory activity at GluN2B receptors (48.8 ± 8.8 %, n = 11). Hence, insertion of electronegative heteroatoms in the naphthalene ring, or replacement with different heterocyclic ring, was not tolerated for the potentiating activity.

A.
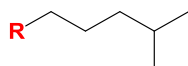
Compound	R
UBP750	
UBP747	
UBP734	
UBP754	
UBP755	
UBP745	

B.
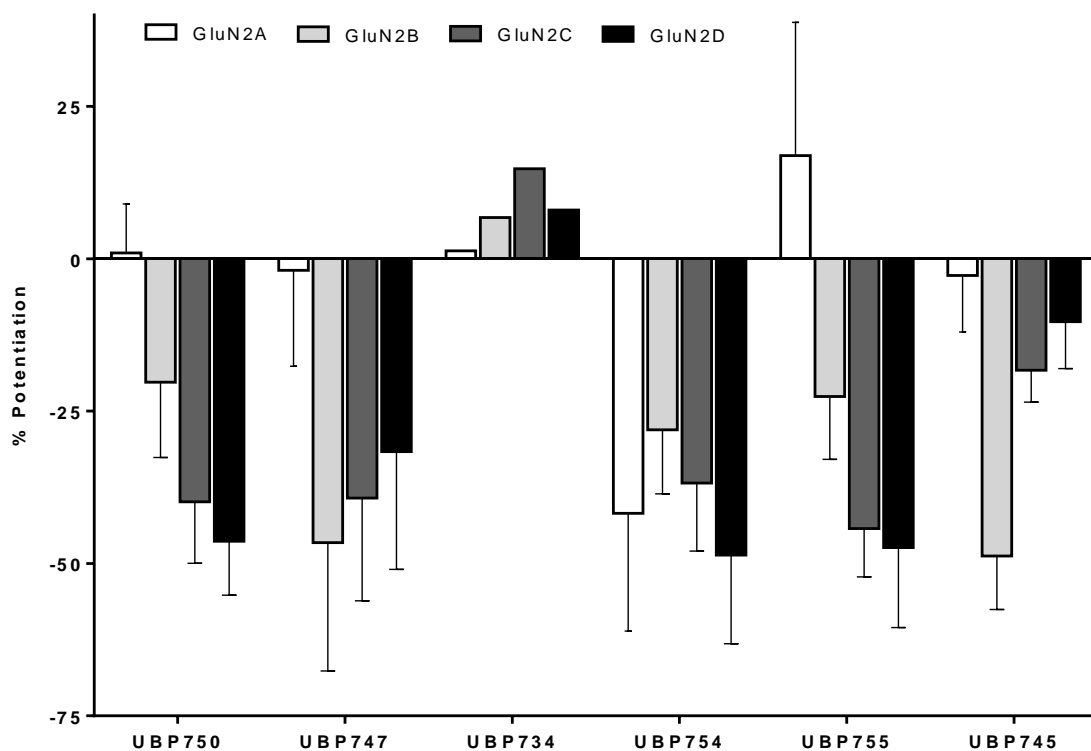
Figure 3.10 Heterocyclic analogues of UBP684

(**A**) Structures of test compounds with different modifications at ring A and ring B of the naphthalene ring of UBP684. (**B**) NMDAR activity of UBP compounds (100 μM) was measured by TEVC assay at rat recombinant NMDARs (GluN1-1a/GluN2A-D) expressed in *Xenopus laevis* oocytes. The effect of the compounds on agonist-induced (L-glutamate and glycine, 10 μM each) NMDAR current was measured and expressed as % potentiation (mean ± S.E.M.) of agonist-induced response (positive value is % potentiation and negative value is % inhibition; n > 4). (Note: UBP734 was screened by Georgia Culley, Ph.D.).

3.4.7   *Phenanthrene analogues of UBP684*

Different analogues of UBP684 were also synthesized by adding a ring C to the

naphthalene ring. When an aromatic ring was added to the naphthalene ring of UBP684, it

yielded UBP646 which potentiated all four subtypes of NMDARs as parent compound UBP684.

Other 9-substituted 3-carboxyphenanthrenes were also characterized. UBP646 at 100 μM

potentiated GluN2A, GluN2B, GluN2C and GluN2D receptors by 131 ±10 %, 134 ± 8 %, 122 ±

8 %, and 124 ± 4 % respectively. When the isohexyl side-chain at 9-position of UBP646 was

replaced with *n*-butyl, *n*-pentyl, it gave UBP709 and UBP647 (Figure 3.11). Both of these

compounds showed potentiating activity at each of the four NMDAR subtypes. However,

potentiation by UBP709 at GluN2A and GluN2B was higher than that at GluN2C and GluN2D

receptors. UBP709 at 100 μM potentiated GluN2A, GluN2B, GluN2C and GluN2D receptors by

58.3 ± 8.3 % (n = 6), 47.9 ± 11.0 % (n = 5), 8.3 ± 1.8 % (n = 4), and 12.3 ± 1.7 % (n = 4)

respectively. Potentiation by UBP647 was 25.1 ± 5.7 % (n = 4), 34.8 ± 4.1 % (n = 3), 35.0 ± 7.6

% (n = 4), and 42.8 ± 10.3 % (n = 4) at GluN2A, GluN2B, GluN2C and GluN2D receptors

respectively. Interestingly, UBP798, which was obtained by 9-substitution with

difluorocyclopropyl group, displayed PAM activity at GluN2A- and GluN2B receptors whereas a

NAM activity at GluN2C- and GluN2D-containing NMDARs (Figure 3.11). Substitution at the 7-

position of the 3-phenanthroic acid led to a reduction in PAM activity as shown by UBP785.

Concentration-response study of UBP709 showed that it potentiates the 10 μM agonist-

induced NMDAR response at GluN2A and GluN2B receptors more than at GluN2C- and

GluN2D-containing receptors (Figure 3.12). Although not highly potent, the selectivity of

UBP709 was better than UBP647 (Table 3.2). Unlike UBP709, UBP647 potentiated GluN2B-D

subunits with almost equal selectivity and potentiated GluN2A receptors with least preference

(Figure 3.12). It is important for the drug to be active at high agonist concentration because there

is a release of high concentrations of L-glutamate during neurotransmission. When we performed

the concentration-response study of UBP709 in high agonist concentration, the potentiating activity at GluN2A receptors was not affected but it was reduced at GluN2B-containing receptors. The potentiation at GluN2D-containing receptors was increased at higher agonist concentration compared to the potentiation obtained at lower agonist concentration (Figure 3.13). When we studied UBP709 concentration-response with different concentrations of both of the agonists at GluN2B-containing NMDARs, we found that the potentiation was especially reduced when we used a higher concentration of L-glutamate (Figure 3.13).
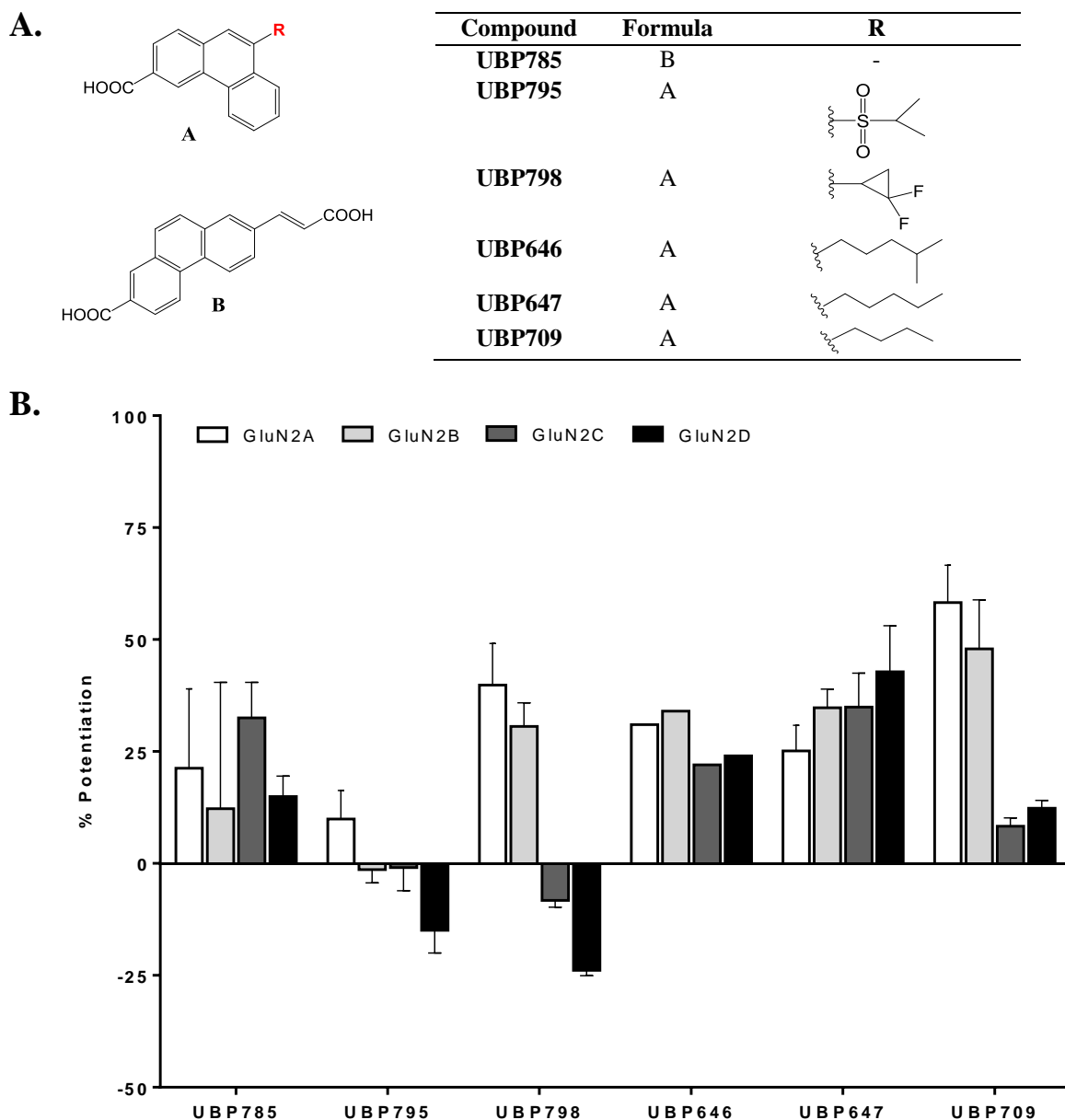
Figure 3.11 SAR studies of phenanthrene 3-carboxylic acid analogues with position-9 substitution on the phenanthrene ring on NMDAR activity

(**A**) Structural analogues of phenanthrene 3-carboxylic acid with position-9 substitution on the phenanthrene ring. (**B**) NMDAR activity of UBP compounds (100 μM) was measured by TEVC assay at rat recombinant NMDARs (GluN1-1a/GluN2A-D) expressed in *Xenopus laevis* oocytes. The effect of compound on agonist-induced (L-glutamate and glycine, 10 μM each) NMDAR current was measured and expressed as % potentiation (mean ± S.E.M.) of agonist-induced response (positive value is % potentiation and negative value is % inhibition; n>4). (Note: UBP646 was screened by Blaise Costa, Ph.D.).

A.

UBP647

B.
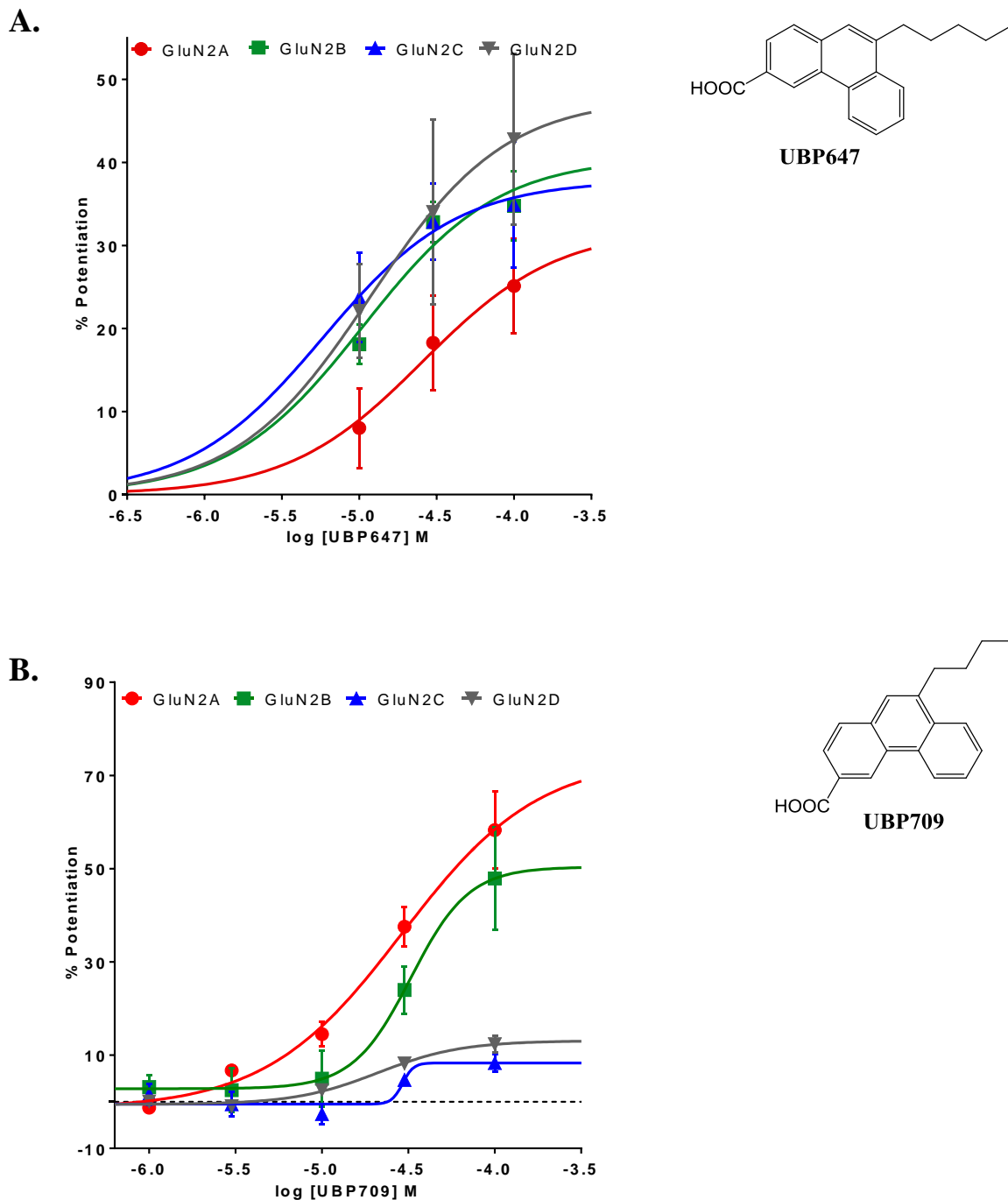
UBP709

Figure 3.12 Concentration-response study of the potentiation of NMDAR responses by (A) UBP647 and (B) UBP709

Select PAMs were tested for activity at increasing concentrations to determine their affinity and maximal efficacy at different NMDAR subtypes. Using the TEVC assay, the current produced by co-application of increasing concentrations of test compounds and agonists (10 μM L-glutamate and 10 μM glycine) at rat recombinant NMDARs (GluN1-1a/GluN2A-D) expressed in *Xenopus laevis* oocytes was measured and expressed as % potentiation above responses induced by agonist-alone (mean ± S.E.M; n > 4).

A.

B.
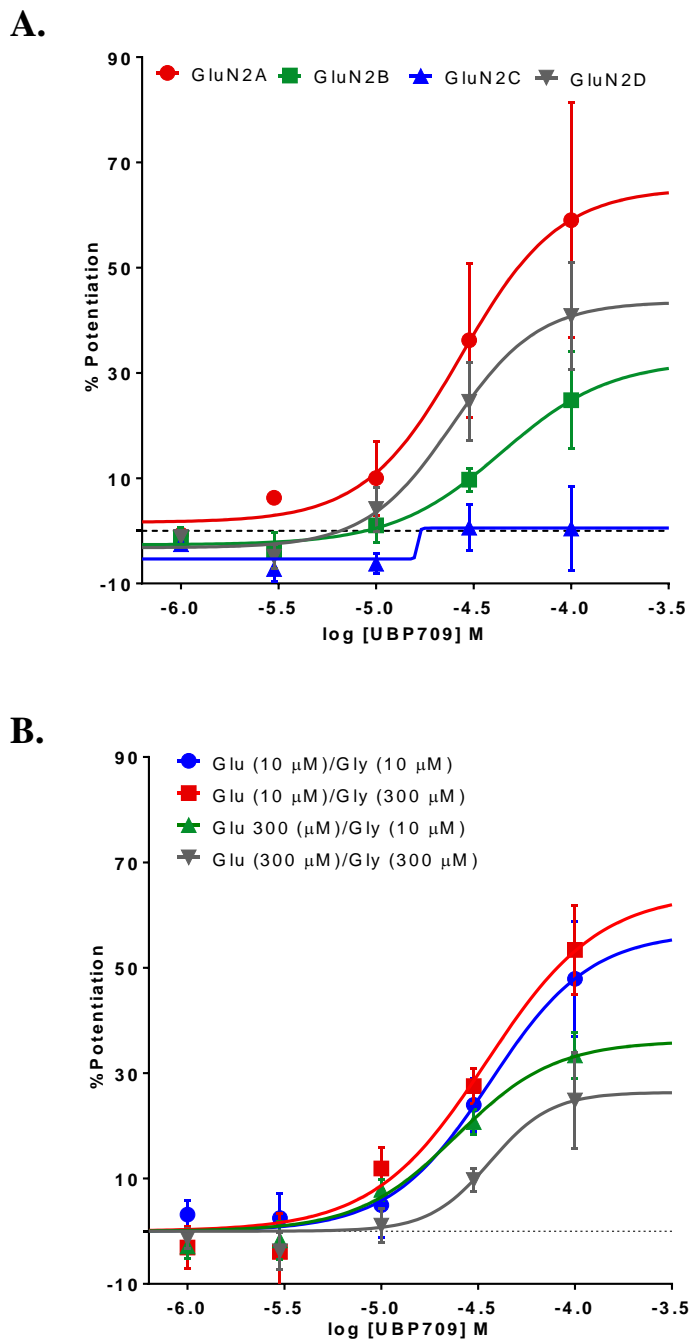
Figure 3.13 UBP709 potentiation of NMDAR currents evoked by different concentrations of agonists

(**A**) UBP709 was tested for activity at increasing concentrations to determine its affinity and maximal efficacy at rat recombinant NMDARs (GluN1-1a/GluN2A-D) expressed in *Xenopus laevis*. Using the TEVC assay, the current induced by co-application of different concentrations of the compound and the agonists (300 μM L-glutamate and 300 μM glycine) was measured and expressed as % potentiation (mean ± S.E.M) above agonist-alone induced response (n > 4). (**B**) Effect of increasing concentrations of UBP709 at GluN1-1a/GluN2B-containing NMDARs on agonist-induced (10 μM L-glutamate and 10 μM glycine) current was also measured (n > 4).

Table 3.2 EC$_{50}$ (µM, n ≥ 4) values for potentiation of GluN1/GluN2 NMDAR subtypes[a]

Compounds	GluN2A	GluN2B	GluN2C	GluN2D
UBP647	8.2 ± 4.3	9.4 ± 0.1	5.8 ± 5.1	11.8 ± 5.9
	(34.5 ± 10.7)	(34.6 ± 3.9)	(35.0 ± 5.6)	(44.9 ± 10.0)
UBP676	26.7 ± 5.6	ND	113 ± 66	61 ± 33
	(39.0 ± 5.9)		(42.7 ± 16.1)	(17.3 ± 16.2)
UBP684	28.0 ± 4.6	34.6 ± 3	37.2 ± 2.8	28.9 ± 4.1
	(68.6 ± 16.2)	(102.0 ± 17.8)	(117.2 ± 22.3)	(88.4 ± 9.6)
UBP684[b]	10.3 ± 4.8	24.8 ± 2.8	33.8 ± 9.7	55.8 ± 4.1
	(50.3 ± 14.1)	(61.5 ± 4.2)	(108.2 ± 37.9)	(119.3 ± 37.9)
UBP692	7.5 ± 2.8	27.0 ± 6.3	22.4 ± 3.6	34.7 ± 10.3
	(38.4 ± 4.7)	(61.9 ± 10.9)	(105.3 ± 26.1)	(65.6 ± 18.4)
UBP752	114.4 ± 7.2	116.4 ± 19.8	26.1 ± 4.5	72.3 ± 15.5
	(230.4 ± 84.6)	(416.6 ± 70.9)	(136.6 ± 11.6)	(277.2 ± 36.8)
UBP753	39.4 ± 27.5	25.0 ± 11.6	36.2 ± 5.7	30.6 ± 7.5
	(277.2 ± 36.8)	(192.3 ± 46.6)	(262.6 ± 33.9)	(240.3 ± 63.6)
UBP709	34.9 ± 5.2	29.5 ± 3.5	30.2 ± 3.4	24.3 ± 1.9
	(73.9 ± 26.7)	(50.4 ± 14.6)	(1.0 ± 2.2)	(13.1 ± 1.5)
UBP709[b]	45.5 ± 29.1	32.6 ± 1.8	ND	41.6 ± 21.2
	(65.1 ± 28.0)	(32.4 ± 36.3)		(43.5 ± 10.2)

[a]EC$_{50}$ values (mean ± S.E.M.) for the potentiation of GluN1/GluN2 NMDAR responses. Values in parentheses are the maximal potentiation values expressed as a percentage (± S.E.M.) above the agonist-alone response (L-glutamate, 10 µM and glycine, 10 µM). ND = not determined

[b]Higher concentration of agonists was used (L-glutamate, 300 µM and glycine, 300 µM).

3.4.8 *Effect of styryl group substitution at the 7-position of 2-naphthoic acid on NMDAR activity*

Substitution at 7-position of 2-naphthoic acid with a styryl group led to compounds such as UBP718 (Figure 3.14), which displayed strong inhibitory activity at each of the four NMDAR subtypes. UBP718 (100 μM) inhibited GluN2A, GluN2B, GluN2C and GluN2D receptors by 67.3 ± 3.8 % (n = 6), 92.7 ± 1.6 % (n = 5), 78.3 ± 0.7 % (n = 4) and 89.0 ± 3.3 % (n = 6) respectively. When the 3-position hydroxyl group of UBP718 was replaced with a carboxyl group, it gave UBP758, which displayed a moderate inhibitory activity at each of the NMDAR subtypes and the NAM activity was highly reduced especially at GluN2B-containing NMDARs. When a carboxyl group was substituted at the *ortho-*, *meta-* and *para-*positions of the styryl ring, it led to compounds UBP793, UBP794 and UBP723 all of which exhibited weak inhibitory activities at all GluN2 subtypes of NMDAR compared to its parent compound UBP718 (Figure 3.14). Replacement of naphthalene ring A of UBP718 with pyran-2-one led to UBP788, which showed a weak potentiating activity on GluN2C and GluN2D receptors and almost no effect on GluN2A- and GluN2B-containing receptors. This shows that naphthalene ring is critical for inhibitory activity of styryl analogues.

We also performed a concentration-response study for UBP718 which inhibited GluN2B and GluN2D receptors with higher potency than GluN2A and GluN2C receptors (Figure 3.15). Its IC_{50} for inhibition was 18 μM for GluN2A, 8 μM for GluN2B and GluN2D and 14 μM for GluN2C and maximal inhibition was > 83 % at each of the four NMDAR subtypes (Table 3.3).

A.

Compound	Formula	R¹	R²	R³
UBP718	A	H	H-	H-
UBP758	B	-	-	-
UBP793	A	COOH	H	H
UBP794	A	H	COOH	H
UBP723	A	H	H	COOH
UBP788	C	-	-	-

B.

Figure 3.14 SAR studies to determine the effect of styryl group substitution at the 7-position of 2-naphthoic acid on NMDAR activity

(**A**) Structures of test UBP compounds with styryl group substitution at C-7 of 2-naphthoic acid. (**B**) NMDAR activity of UBP compounds (100 µM) was measured by TEVC at rat recombinant NMDARs (GluN1-1a/GluN2A-D) expressed in *Xenopus laevis* oocytes. The effect of compound on agonist-induced (L-glutamate and glycine,10 µM each) NMDAR current was measured and expressed as % potentiation (mean ± S.E.M.) of agonist-induced response (positive value is % potentiation and negative value is % inhibition; n > 4). (Note: UBP723 was screened by Georgia Culley, Ph.D.)
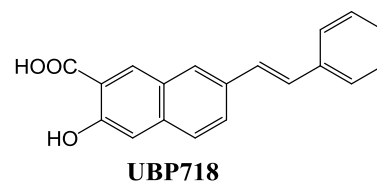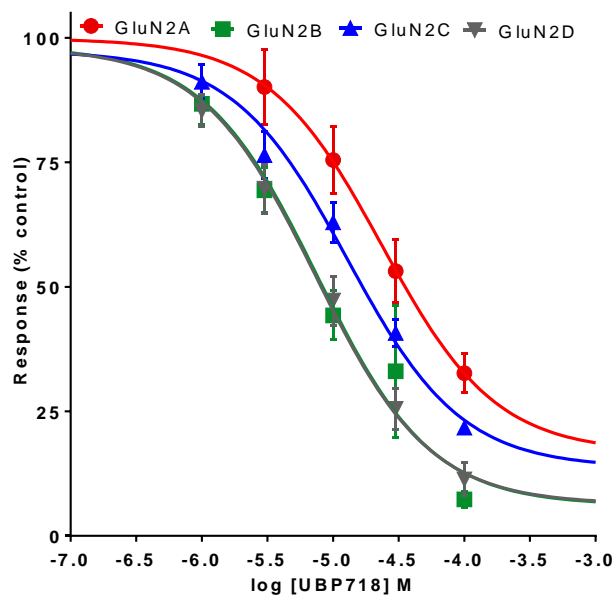
Figure 3.15 Concentration-response for inhibition of NMDAR responses by UBP718

UBP718 was tested for activity at increasing concentrations to determine its affinity and maximal inhibition at NMDARs (GluN1-1a/GluN2A-D) expressed in *Xenopus laevis* oocytes. Using the TEVC assay, the inhibition of agonist-evoked (10 µM of L-glutamate and 10 µM of glycine) current by co-application of increasing concentrations of test compound and the 10 µM agonists was measured. Data are expressed as % of control NMDAR response (mean ± S.E.M; n > 4).

*3.4.9   Effect of nitro and methoxy group substitution on the aromatic ring of the 7-
           position styryl group of 3-hydroxy 2-naphthoic acid on NMDAR activity*

Since, the compounds with 7-styryl substitution exhibited strong NMDAR inhibitory activity,

other analogues were developed by nitro and methoxy group substitution at *ortho-*, *para-* and

*meta-*position of the styryl aromatic ring in UBP718 (Figure 3.16). Nitro group substitution at the

*ortho-*position of the styryl ring of UBP718 led to compound UBP792 which, at 100 μM, strongly

inhibited GluN2C (65.0 ± 3.2 %, n = 12) and GluN2D receptors (73.1 ± 3.4 %, n = 14),

moderately inhibited GluN2B receptors (43.9 ± 7.8 %, n = 11) and weakly inhibited GluN2A

receptors (19.5 ± 4.7 %, n = 25) (Figure 3.16). Nitro group substitution at the *meta-* and *para-*

positions of the styryl aromatic ring of UBP718 yielded compounds UBP783 and UBP789 which

also inhibited all NMDAR subtypes at 100 μM (Figure 3.16).

    The subunit selectivity for UBP792 inhibition was in the following order: GluN2D >

GluN2C > GluN2B > GluN2A (Figure 3.17). It inhibited GluN2D- and GluN2C-containing

receptors with an IC_{50} value of 3 and 8 μM respectively and inhibited 80 % of the agonist-

induced NMDAR current (Table 3.3). UBP783 inhibited GluN2B, GluN2C, and GluN2D with

equal efficacy (Figure 3.17). Methoxy substitution at the *ortho-*position of the styryl ring of

UBP718 yielded compound UBP780 which showed weak inhibitory activity. However, when the

methoxy group was substituted at the *meta-*position, it (UBP782) retained the inhibitory activity

of UBP718 and inhibited GluN2B-D subtypes with equal preference and GluN2A receptors with

least preference (Figure 3.18). From this series of compounds, it shows that *o-*nitro is important

for subunit selectivity and *o-*methoxy substitution reduces the inhibitory activity. All of these

derivatives showed strong inhibitory preference for GluN2D subunits compared to other subunits

of NMDARs.

A.

Compound	R^1	R^2	R^3
UBP792	NO_2	H	H
UBP783	H	NO_2	H
UBP789	H	H	NO_2
UBP780	OMe	H	H
UBP782	H	OMe	H
UBP781	H	H	OMe

B.
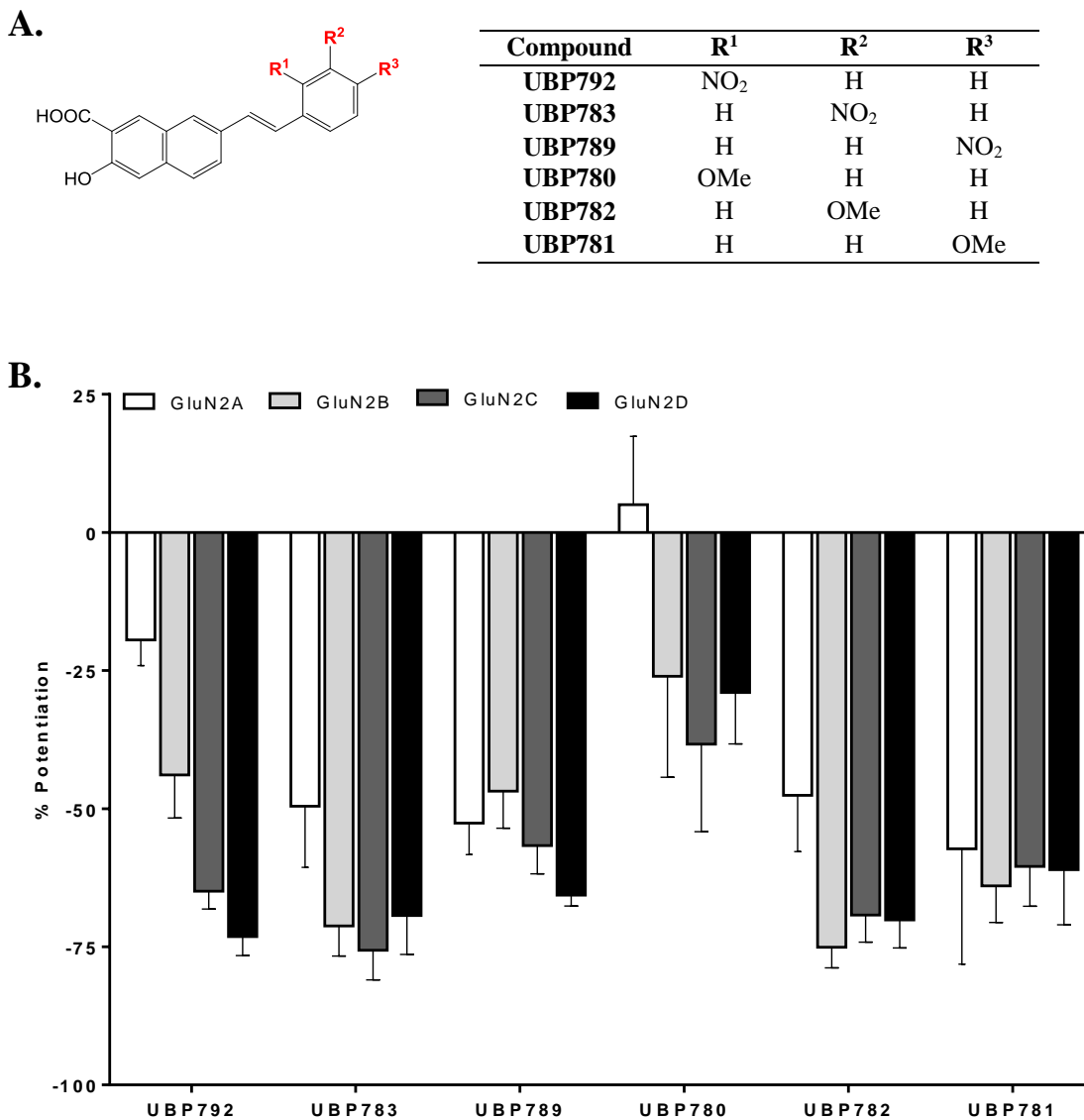
Figure 3.16 SAR studies to determine the effect of nitro and methoxy group substitution on the aromatic ring of the 7-position styryl group of 3-hydroxy 2-naphthoic acid on NMDAR activity

(**A**) Structures of test UBP compounds with *ortho*-, *meta*-, *para*-substitution of nitro and methoxy groups on the styryl ring. (**B**) NMDAR activity of UBP compounds (100 μM) was measured by TEVC assay at rat recombinant NMDARs (GluN1-1a/GluN2A-D) expressed in *Xenopus laevis* oocytes. The effect of test compounds on agonist-induced (L-glutamate and glycine, 10 μM each) NMDAR current was measured and expressed as % potentiation (mean ± S.E.M.) above control (agonist-alone) response (positive value is % potentiation and negative value is % inhibition; n > 4).

A.

B.
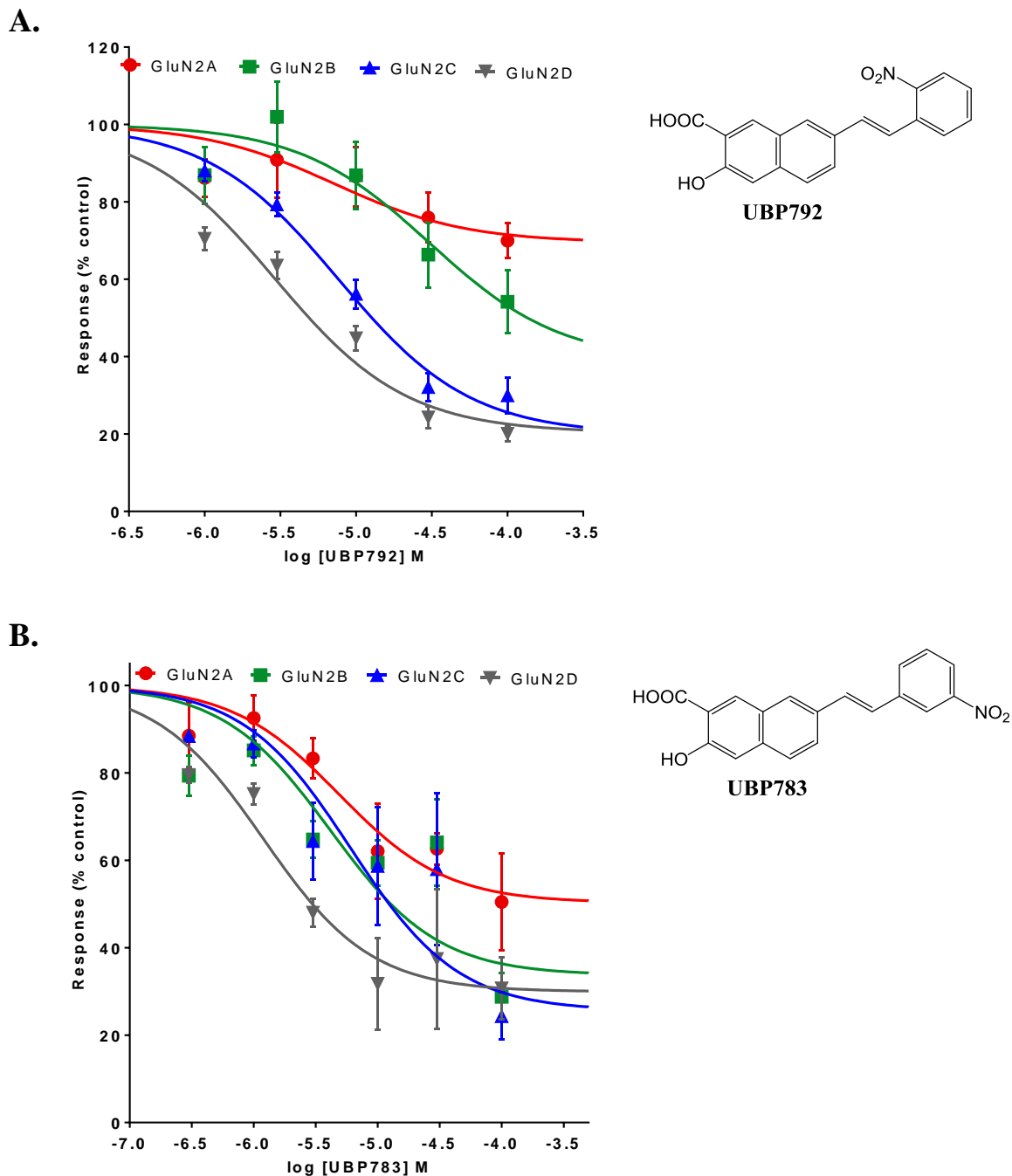
Figure 3.17 Concentration-response study of the inhibition of NMDAR responses by (A) UBP792 and (B) UBP783

Select NAMs were tested for their affinity and maximal inhibition at NMDARs (GluN1-1a/GluN2A-D) expressed in *Xenopus laevis* oocytes. Using the TEVC assay, the inhibition of agonist-evoked (10 μM of L-glutamate and 10 μM of glycine) current by co-application of increasing concentrations of the test compounds and the 10 μM agonists was measured and expressed as % of control NMDAR responses (mean ± S.E.M; n > 4).

A.

B.
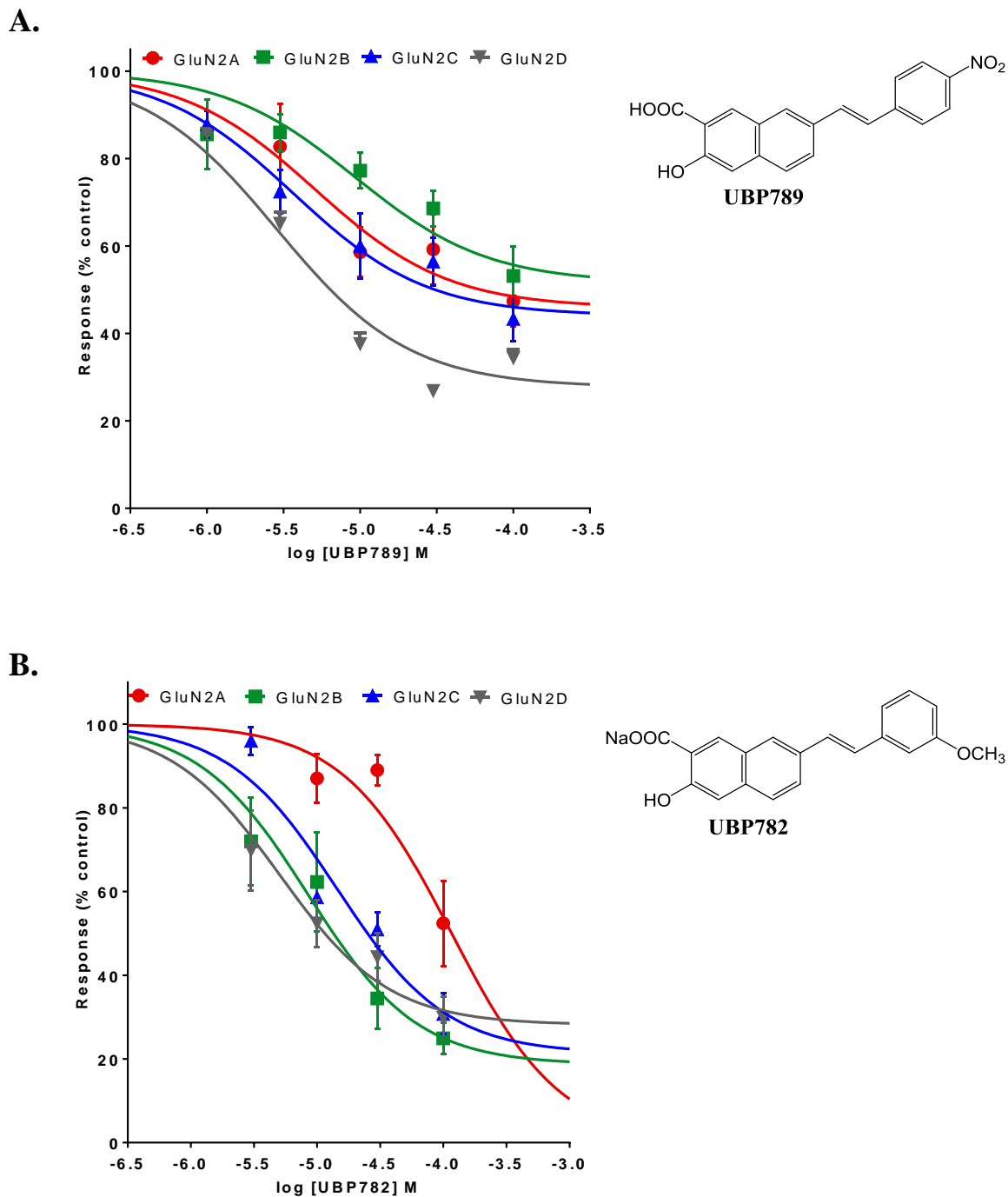
Figure 3.18 Concentration-response study of the inhibition of NMDAR responses by (A) UBP789 and (B) UBP782

Select NAMs were tested for their affinity and maximal inhibition at NMDARs (GluN1-1a/GluN2A-D) expressed in *Xenopus laevis* oocytes. Using the TEVC assay, the inhibition of agonist-evoked (10 µM of L-glutamate and 10 µM of glycine) current by co-application of increasing concentrations of the test compounds and the 10 µM of agonists was measured and expressed as % of control NMDAR responses (mean ± S.E.M; n > 4).

Table 3.3 IC$_{50}$ (µM, n ≥ 4) values of NAMs for inhibition of GluN1/GluN2 NMDAR subtypes[a]

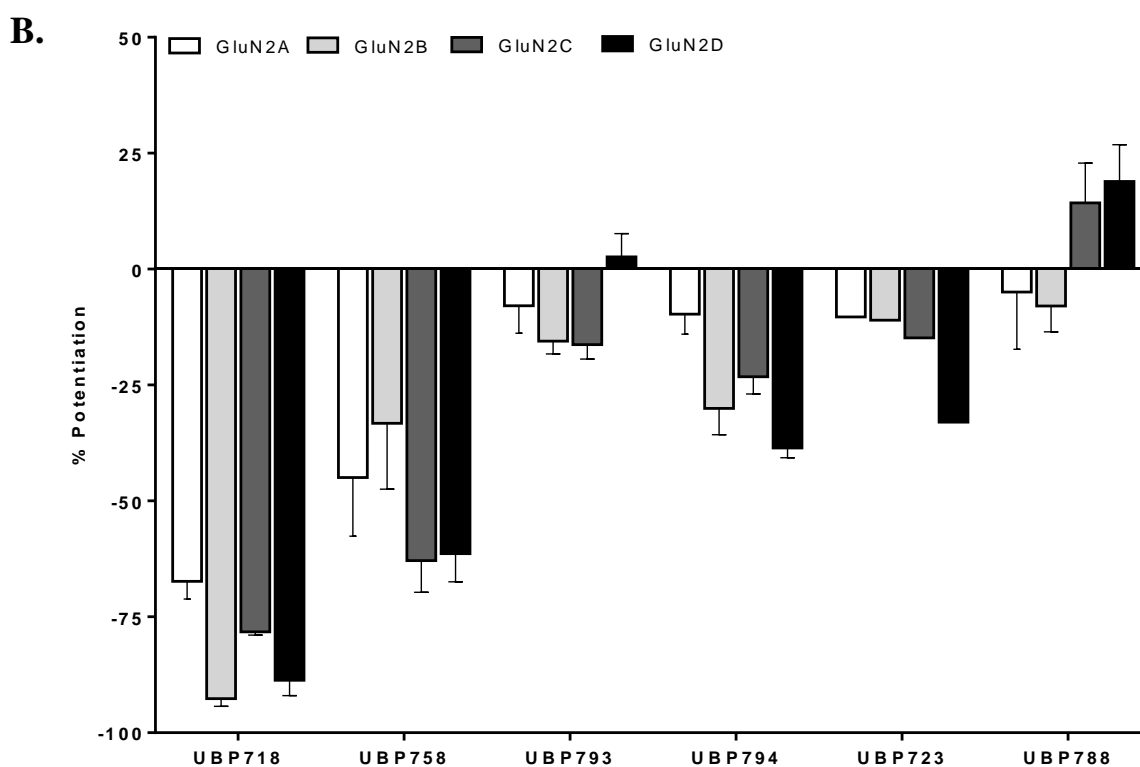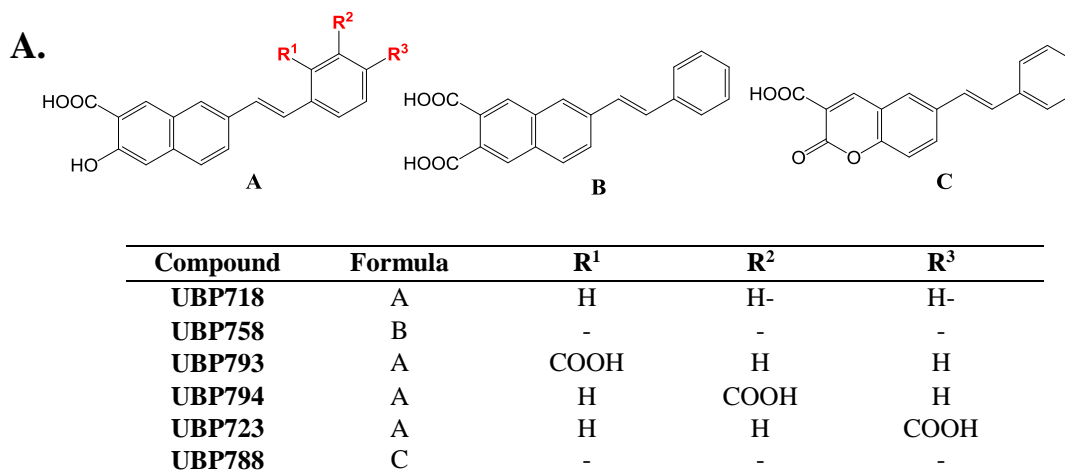| Compounds	GluN2A	GluN2B	GluN2C	GluN2D
UBP759	> 100	30.9 ± 5.3	19.9 ± 2.7	17.4 ± 2.7
	(38.3 ± 30.0)	(87.6 ± 8.8)	(112.0 ± 5.5)	(101.2 ± 4.2)
UBP768	65.9 ± 15.6	(32.7 ± 7.4)	20.7 ± 6.2	8.2 ± 1.4
	(43.2 ± 7.1)	(72.4 ± 9.8)	(89.1 ± 8.0)	(91.1 ± 7.2)
UBP718	17.8 ± 4.6	7.5 ± 2.0	13.8 ± 3.3	8.6 ± 1.9
	(83.2 ± 11.4)	(93.9 ± 7.3)	(86.3 ± 4.7)	(93.6 ± 4.2)
UBP782	ND	11.0 ± 4.2	14.6 ± 2.2	5.4 ± 2.2
		(81.2 ± 5.7)	(78.7 ± 5.8)	(71.6 ± 4.8)
UBP792	6.0 ± 4.1	32.2 ± 16.0	8.2 ± 1.2	2.9 ± 0.4
	(30.5 ± 6.3)	(61.3 ± 18.1)	(80.1 ± 4.1)	(79.7 ± 2.8)
UBP789	5.8 ± 1.1	11.1 ± 2.9	6.5 ± 2.8	2.9 ± 0.3
	(54.1 ± 5.5)	(48.4± 6.0)	(55.9 ± 3.9)	72.3 ± 2.1)
UBP783	9.7 ± 3.8	9.2 ± 5.3	7.9 ± 4.2	1.4 ± 0.4
	(49.7 ± 6.8)	(66.3 ± 5.2)	(74.4 ± 6.9)	(70.0 ± 4.6)

[a]IC$_{50}$ values (mean ± S.E.M.) for the inhibition of GluN1/GluN2 NMDAR responses. Values in parentheses are the maximal percentage inhibition values (± S.E.M.) of agonist-induced response (L-glutamate, 10 µM and glycine, 10 µM). ND = not determined.

3.4.10   SAR studies of PPDA and UBP141 derivatives

In an effort to develop improved subunit-selective competitive antagonists of NMDARs, a new

series of compounds were made based on previously published compounds (Morley, Tse et al.

2005, Costa, Feng et al. 2009) (2R*, 3S*)-1-(Phenanthrenyl-2-carbonyl)piperazine-2,3-

dicarboxylic acid (PPDA) and (2R*,3S*)-1-(Phenanthrenyl-3-carbonyl)piperazine-2,3-

dicarboxylic acid (UBP141) (Figure 3.19). UBP791 was a structural analogue of PPDA in which

propionic acid was substituted at the 7-position of the phenanthrene moiety. Both of these

compounds were more selective at GluN2C- and GluN2D- than at GluN2A- and GluN2B-

containing NMDARs than any known competitive antagonist (Figure 3.20). Inhibitory activity of

UBP791 at 100 μM was 59.1 ± 1.5 % (n = 5) at GluN2A-, 92.3 ± 1.7 % (n = 4) at GluN2B-, 99.7

± 0.1 % (n = 4) at GluN2C-, and 99.0 ± 0.8 % (n = 4) at GluN2D-containing NMDARs. Different

UBP141 analogues were also prepared by substitution of different groups at the 9-position of the

phenanthrene ring. Both ethyl (UBP784) and cyclopropyl group (UBP786) substitution led to

strong inhibition of GluN2C- and GluN2D-containing receptors while moderately inhibiting

GluN2A- and GluN2B-containing receptors (Figure 3.19). Although propionic acid substitution at

the 7-position of PPDA (UBP791) gave strong inhibition as well as GluN2C/GluN2D selectivity,

the propionic acid substitution at the 9-position of the phenanthrene ring of UBP 141, which

yielded compound UBP790, greatly reduced the inhibitory activity at each of the four NMDAR

subtypes. When the 9-position of the phenanthrene ring of UBP141 was substituted with –

$SCH(CH_3)_2$, it yielded compound UBP796 which showed moderate inhibitory activity at GluN2A

(41.0 ± 2.9 %, n = 7) and GluN2B (57.2 ± 1.7 %, n = 7) and strong inhibitory activity at GluN2C

(67.8 ± 1.5 %, n = 8) and GluN2D receptors (81.5 ± 1.8 %, n = 7) (Figure 3.19). Interestingly, the

9-position substitution with $-SO_2CH(CH_3)_2$ led to compound UBP797 which displayed

significantly reduced inhibitory activity at GluN2B- (5.8 ± 7.2 %, n = 7), GluN2C- (15.2 ± 3.5 %,

n = 4) and GluN2D-containing receptors (26.9 ± 3.0 %, n = 4). However, it exhibited strong

inhibition at GluN2A receptors (75.2 ± 3.6 %, n = 9). UBP799 (9-position of UBP141 substituted

with difluorocyclopropyl), strongly inhibited all NMDAR subtypes. UBP799 inhibited GluN2A receptors by 84.4 ± 3.2 % (n = 4), GluN2B receptors by 64.2 ± 2.7 % (n = 4), GluN2C receptors by 92.7 ± 0.1 % (n = 3), and GluN2D receptors by 92.2 ± 1.7 % (n = 4).

We performed a concentration-response study of UBP791 (Figure 3.20); the calculated K_i values for inhibition at GluN2A-, GluN2B- GluN2C- and GluN2D-containing NMDARs were 19 μM, 2.7 μM, 0.1 μM, and 1.14 μM respectively (Table 3.5). UBP786, UBP799 and UBP796 also inhibit GluN2C- and GluN2D- more than GluN2A- and GluN2B-containing receptors (Figure 3.21, Figure 3.22). Interestingly, higher concentrations of UBP797 showed strong inhibition at GluN2A receptors while displaying a weak inhibition at other subtypes (Figure 3.22). This was the only compound in this series displaying GluN2A subtype selectivity. Most of the other compounds in the series exhibited GluN2C- and GluN2D-subtype selectivity.

A.

Compound	Formula	R
UBP784	A	
UBP786	A	
UBP799	A	
UBP790	A	
UBP791	B	-
UBP796	A	
UBP797	A	

B.
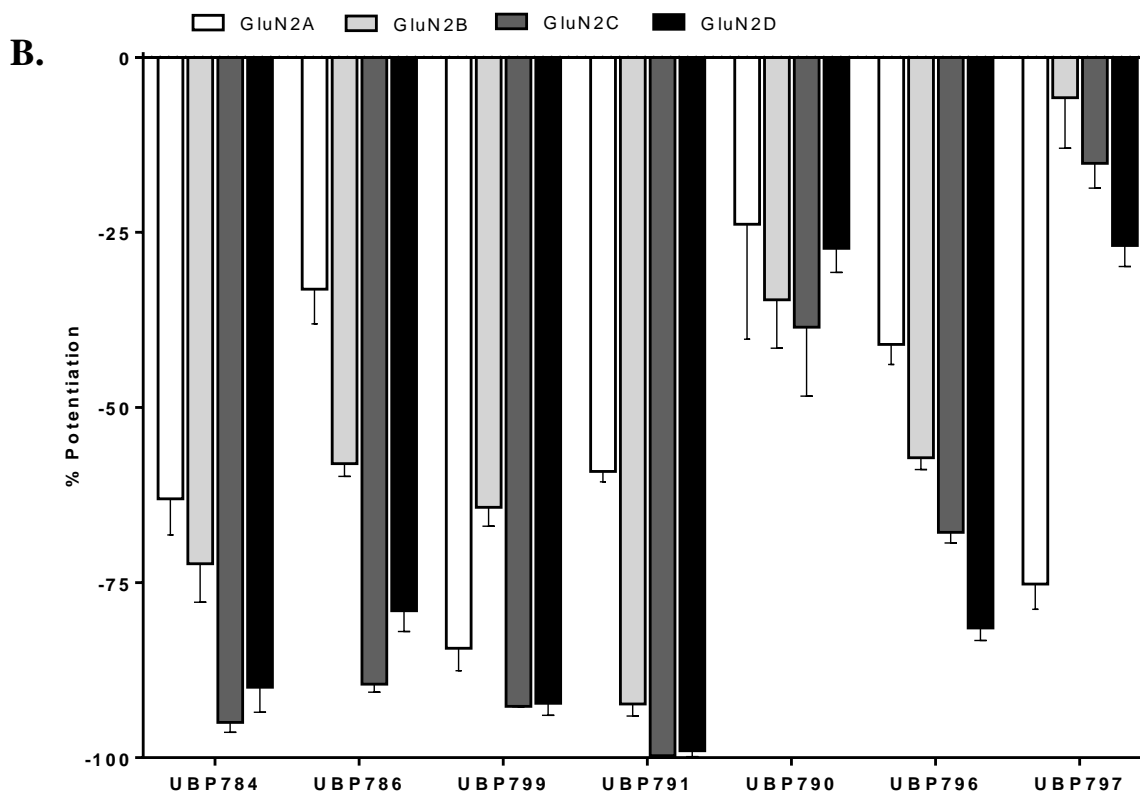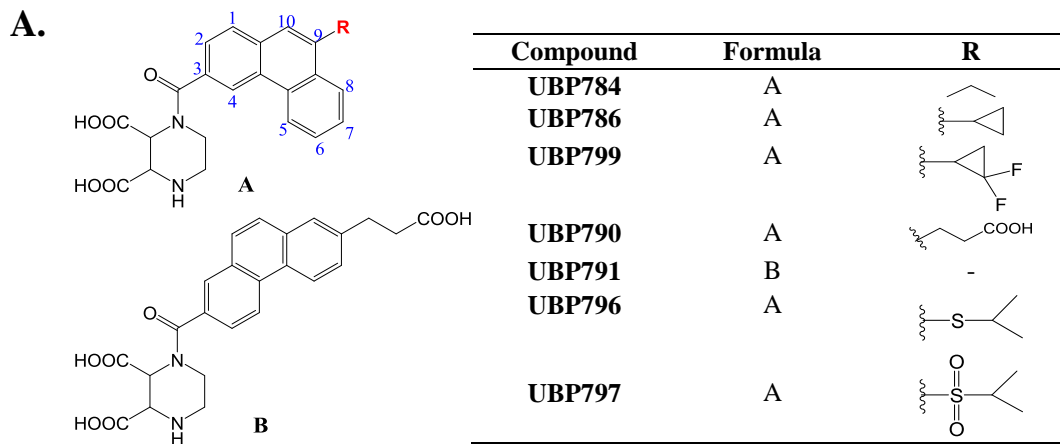
Figure 3.19 SAR studies of (2R*, 3S*)-1-(Phenanthrenyl-2-carbonyl)piperazine-2,3-dicarboxylic acid (PPDA) and (2R*,3S*)-1-(Phenanthrenyl-3-carbonyl)piperazine-2,3-dicarboxylic acid (UBP141) analogues at NMDARs

(**A**) Structural analogues of UBP141 and 145 synthesized by substitution with different groups at the C-9 position of the phenanthrene ring. (**B**) NMDAR activity of UBP compounds (100 μM) was measured by TEVC assay at rat recombinant NMDARs (GluN1-1a/GluN2A-D) expressed in *Xenopus laevis* oocytes. The effect of compound on agonist (L-glutamate and glycine, 10 μM each)-induced NMDAR current was measured and expressed as % potentiation (mean ± S.E.M.) of agonist-induced response (positive value is % potentiation and negative value is % inhibition; n>4).

A.

B.
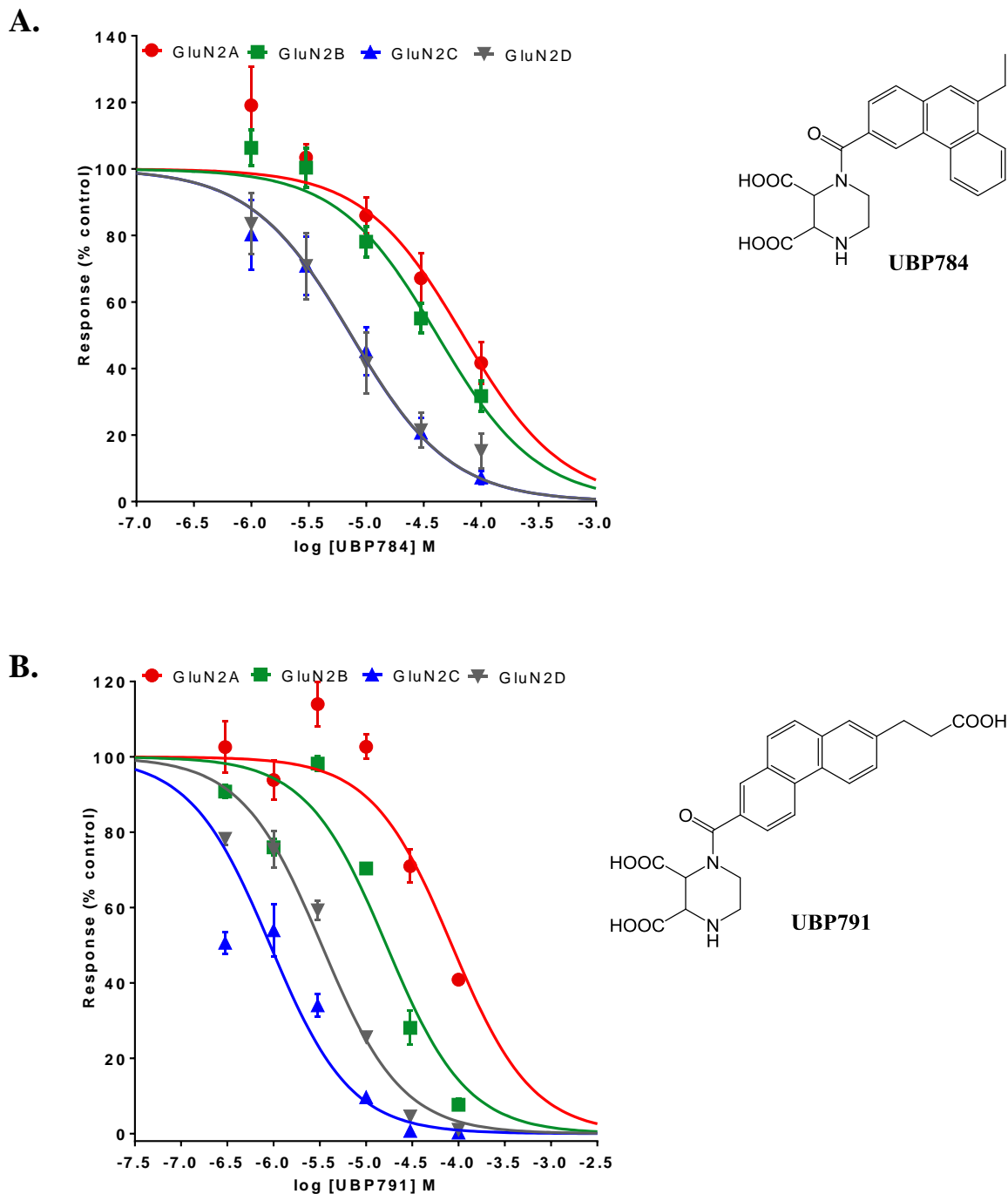
Figure 3.20 Concentration-response study of the inhibition of NMDAR responses by (A) UBP784 and (B) UBP791

Select NMDAR antagonists were tested for their affinity and maximal inhibition at NMDARs (GluN1-1a/GluN2A-D) expressed in *Xenopus laevis* oocytes. Using the TEVC assay, the inhibition of agonist-evoked (10 μM of L-glutamate and 10 μM of glycine) current by co-application of increasing concentrations of the test compounds and the 10 μM of agonists was measured and expressed as % of control NMDAR responses (mean ± S.E.M; n > 4).
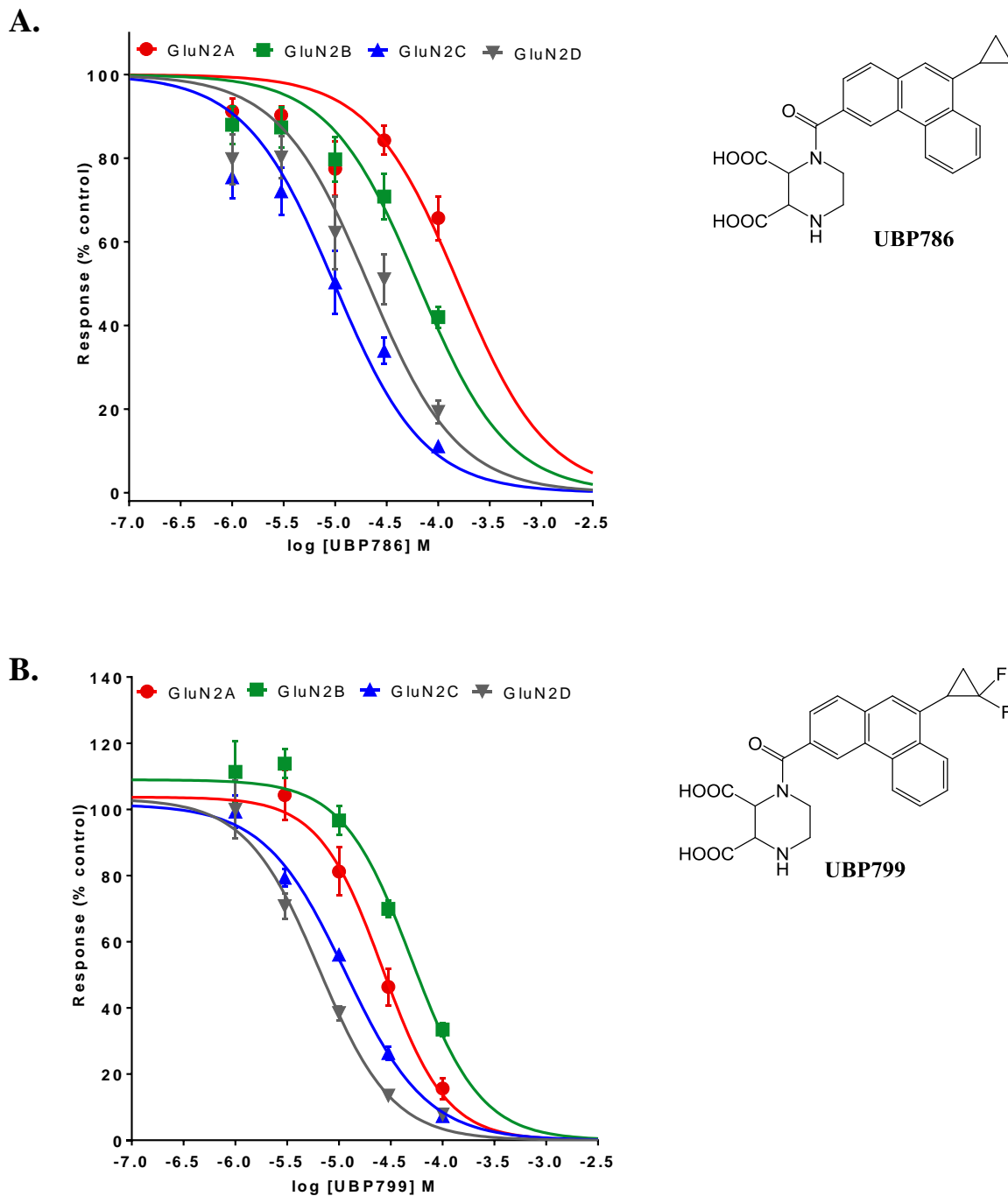
Figure 3.21 Concentration-response study of the inhibition of NMDAR responses by (A) UBP786 and (B) UBP799

Select NMDAR antagonists were tested for their affinity and maximal inhibition at NMDARs (GluN1-1a/GluN2A-D) expressed in *Xenopus laevis* oocytes. Using the TEVC assay, the inhibition of agonist-evoked (10 μM of L-glutamate and 10 μM of glycine) current by co-application of increasing concentrations of the test compounds and the 10 μM of agonists was measured and expressed as % of control NMDAR responses (mean ± S.E.M; n > 4).

A.

B.
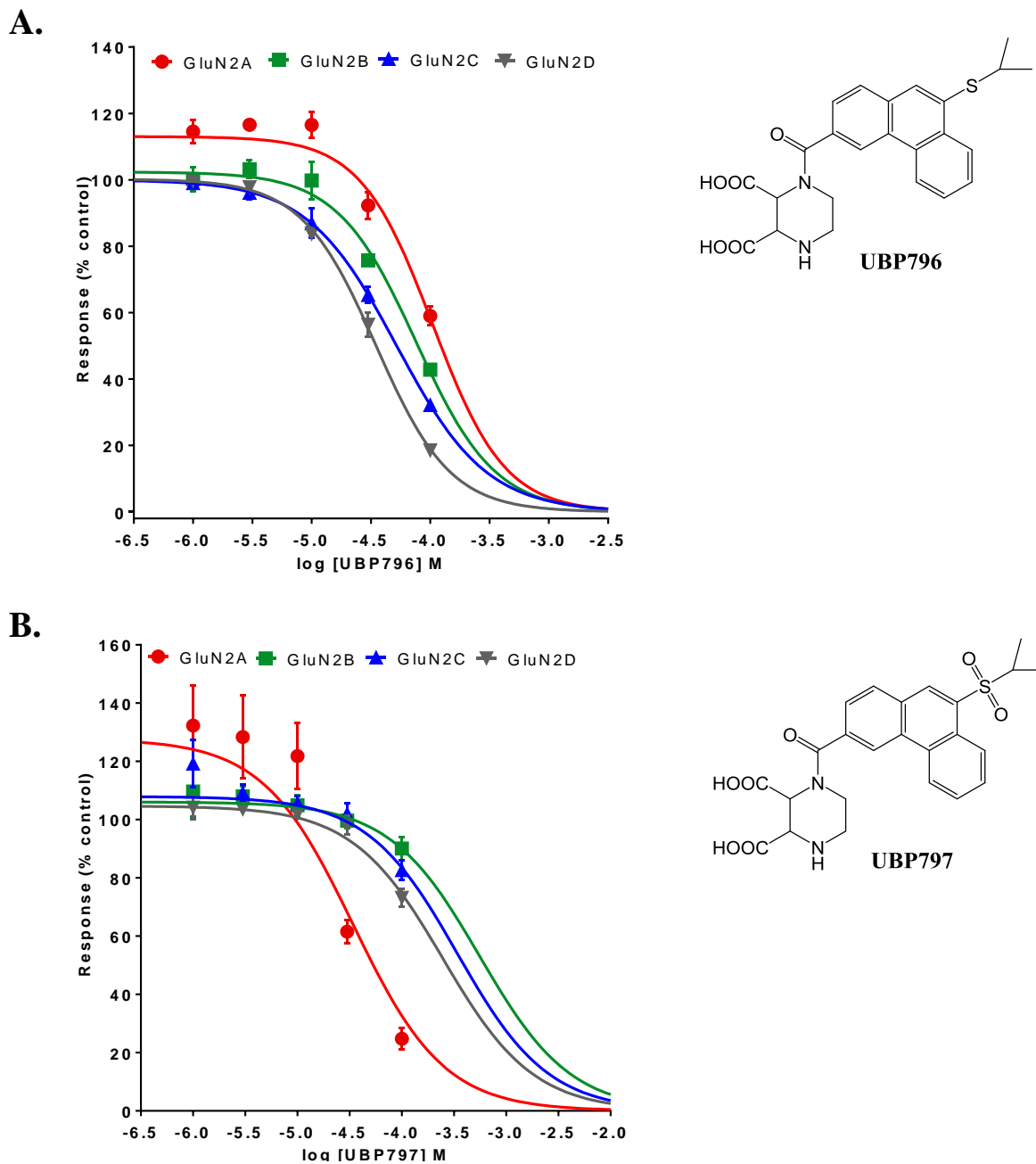
Figure 3.22 Concentration-response study of the inhibition of NMDAR responses by (A) UBP796 and (B) UBP797

Select NMDAR antagonists were tested for their affinity and maximal inhibition at NMDARs (GluN1-1a/GluN2A-D) expressed in *Xenopus laevis* oocytes. Using the TEVC assay, the inhibition of agonist-evoked (10 µM of L-glutamate and 10 µM of glycine) current by co-application of increasing concentrations of the test compounds and the 10 µM of agonists was measured and expressed as % of control NMDAR responses (mean ± S.E.M; n > 4).

3.4.11 *Effect of substitution at the 6-position of the naphthalene ring of 1-(2-naphthoyl) piperazine-2,3-dicarboxylic acid on NMDAR activity*

A series of UBP141 analogues with the unsubstituted aromatic ring of phenanthrene (ring C) removed, were also characterized (Figure 3.23). Different acid or ester groups were substituted at the 6-position of the naphthalene ring. Ethyl acrylate substitution gave compound UBP633 which inhibited all NMDARs with similar efficacy. UBP633 at 100 μM inhibited GluN2A receptors by 88.4 ± 0.5 % (n = 4), GluN2B receptors by 97.1 ± 0.6 % (n = 4), GluN2C receptors by 80.4 ± 2.9 % (n = 4), and GluN2D receptors by 96.9 ± 0.8 % (n = 5) (Figure 3.23). However, the acrylic acid substitution led to UBP634 which inhibited GluN2A (83.4 ± 5.5 %, n = 4), GluN2C (91.0 ± 2.8 %, n = 4) and GluN2D (83.1 ± 3.5 %, n = 4) with equal efficacy whereas it showed reduced inhibition at GluN2B-containing NMDARs (32.8 ± 9.3 %, n = 4). Propionic acid substitution gave UBP635 which displayed reduction in inhibition at GluN2B (34.7 ± 2.6 %, n = 5) and GluN2D (51.4 ± 6.6 %, n = 5) receptors and enhanced inhibition at GluN2A (80.0 ± 0.6 %, n = 5) and GluN2C receptors (76.7 ± 3.3 %, n = 5). When substitution was made at the 6-position of naphthalene ring with pentanoic acid (UBP639), it inhibited all NMDARs with slightly more activity at GluN2C and GluN2D receptors compared to GluN2A- and GluN2B-containing receptors. Methyl pent-4-enoate (ester) substitution or pent-4-enoic acid (acid) at 6-position of the naphthalene ring gave compounds UBP637 and UBP638 respectively. Both UBP637 and UBP638 showed strong inhibitory activity at each subtypes of NMDARs (Figure 3.23)

A.

Compound	R
UBP633	
UBP634	
UBP635	
UBP639	
UBP637	
UBP638	

B.
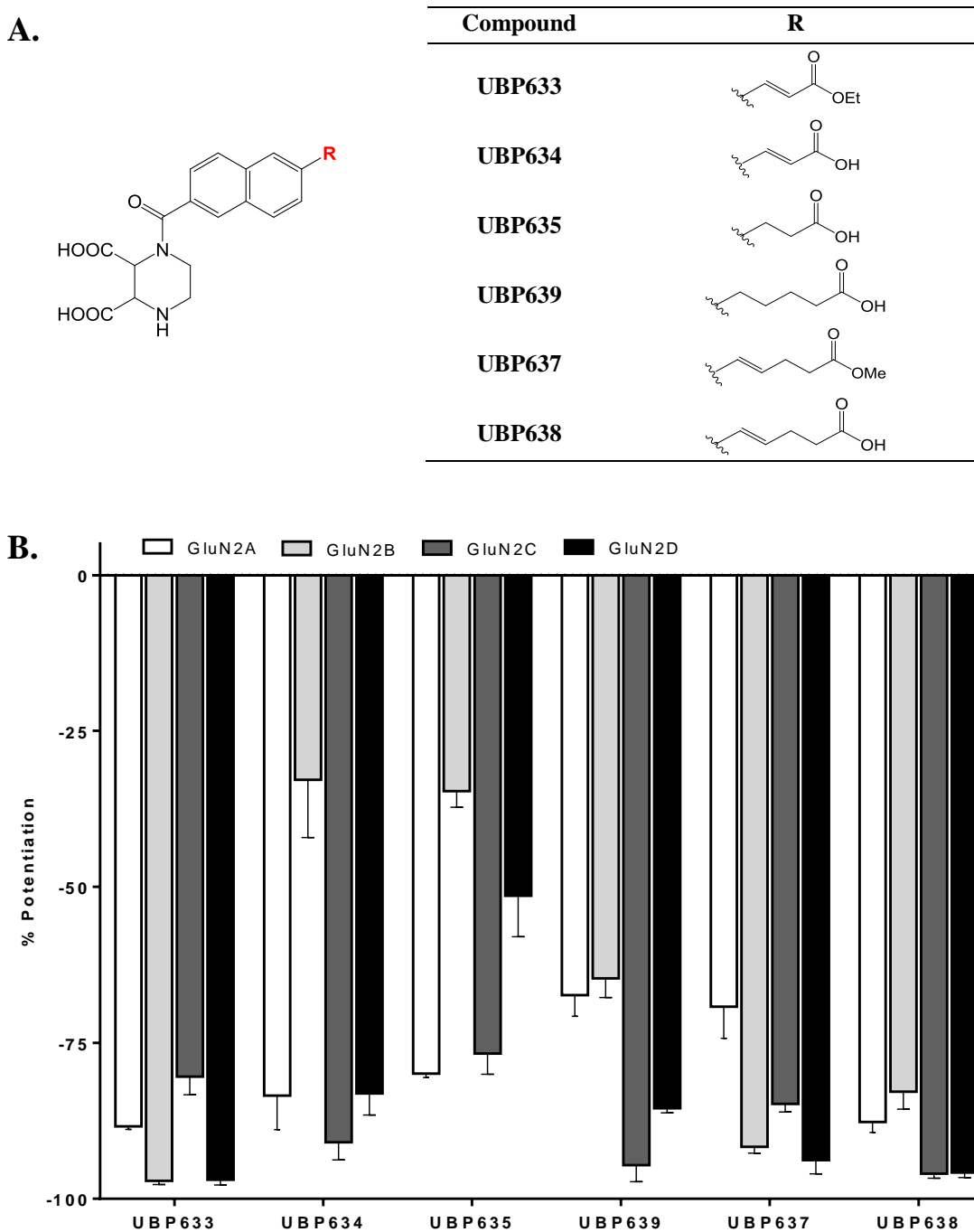
Figure 3.23 Effect of substitution at the 6-position of the naphthalene ring of 1-(2-naphthoyl) piperazine-2,3-dicarboxylic acid on NMDAR activity

(A) Structural analogues of 1-(2-naphthoyl) piperazine-2,3-dicarboxylic acid with 6-position substitution on the naphthalene ring. (B) NMDAR activity of UBP compounds (100 µM) was measured by TEVC assay at rat recombinant NMDARs (GluN1-1a/GluN2A-D) expressed in *Xenopus laevis* oocytes. The effect of compound on agonist-induced (L-glutamate and glycine, 10 µM each) NMDAR current was measured and expressed as % potentiation (mean ± S.E.M.) of agonist-induced response (positive value is % potentiation and negative value is % inhibition; n>4).

We further studied the concentration-response for the inhibition by these compounds at GluN2A-D receptors. UBP633 had ethyl acrylate (ester substitution) at the 6-position of the naphthalene ring and it showed greatest potency for inhibition at GluN2B-containing receptors and least inhibition at GluN2C-containing receptors (Figure 3.24). The K_i value for inhibition at GluN2A, GluN2B, GluN2C and GluN2D receptors were 3.7, 0.8, 3.5, and 0.6 μM respectively (Table 3.5). The hydrolysis of the ester group of UBP633 gave compound UBP634, which displayed the selectivity in opposite order than that of UBP633. UBP634 displayed more inhibitory activity at GluN2A-, GluN2C-, GluN2D- and least at GluN2B-containing receptors (Figure 3.24). We found a similar pattern of inhibitory activity with UBP635 which had propionic acid substitution at the 6-position of naphthalene. It inhibited GluN2A and GluN2C receptors more than GluN2B receptors (Figure 3.25). Compound (UBP639) with pentanoic acid substitution also showed least inhibition at GluN2A- and GluN2B- and more inhibition at GluN2C-containing receptors (Figure 3.25). The methyl pent-4-enoate (ester) substituted analogue UBP637 exhibited more inhibitory activity at GluN2B receptors and least inhibitory activity at GluN2A-containing receptors. Whereas when the ester group of UBP737 was hydrolyzed to pent-4-enoic acid analogues (UBP638), it led to a reduction in inhibitory activity at GluN2B receptors similar to the activity we observed with other carboxylic acid-substituted analogues (Figure 3.26). The K_i value for inhibition by UBP634 at GluN2D receptors was 16 fold-lower than that for inhibition at GluN2B receptors. Similarly, the K_i value for inhibition by UBP637 at GluN2D was 14-fold lower than that for inhibition at GluN2A.

A.
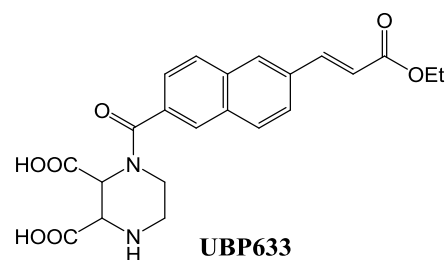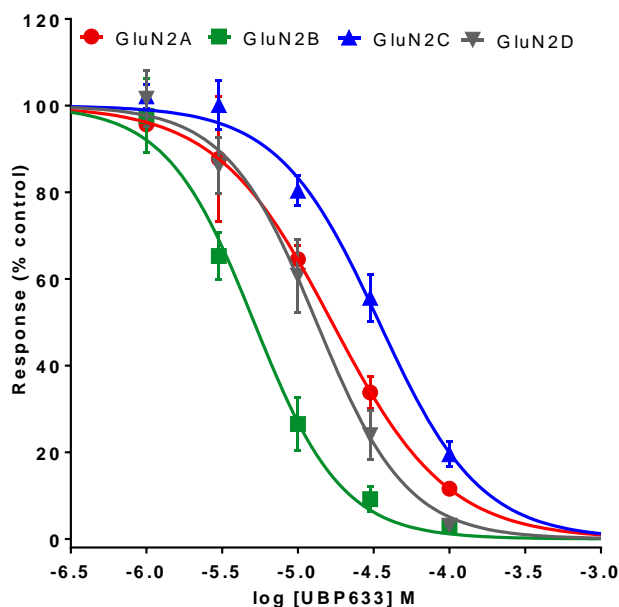
B.
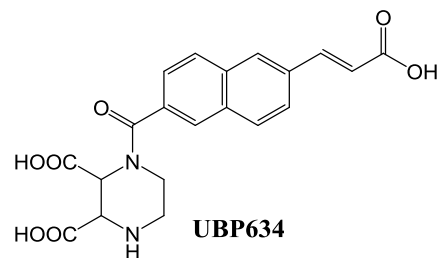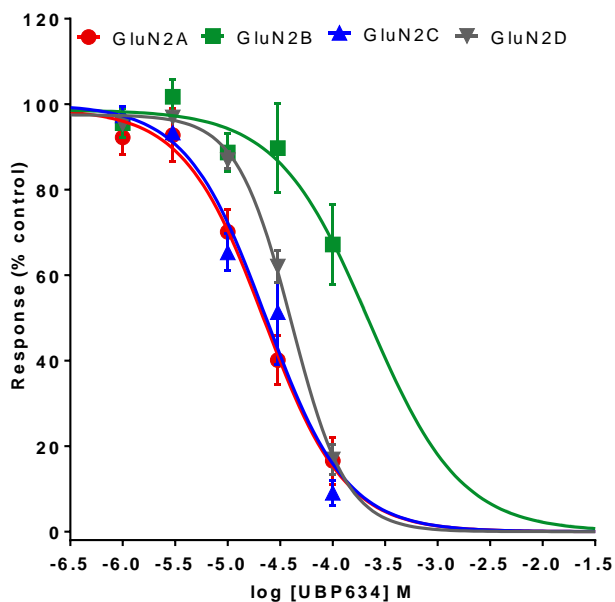
Figure 3.24 Concentration-response study of the inhibition of NMDAR responses by (A) UBP633 and (B) UBP634

Select NMDAR antagonists were tested for activity at various concentrations to determine the potency and efficacy at different NMDAR subtypes. NMDAR activity was measured by TEVC at recombinant NMDARs (GluN1a/GluN2A-D) expressed in *Xenopus laevis* oocytes. NMDAR-mediated current induced by increasing concentration of the test compounds co-applied with L-glutamate and glycine (10 µM each) was measured and expressed as % of control (agonist alone) NMDAR response (mean ± S.E.M; n > 4).
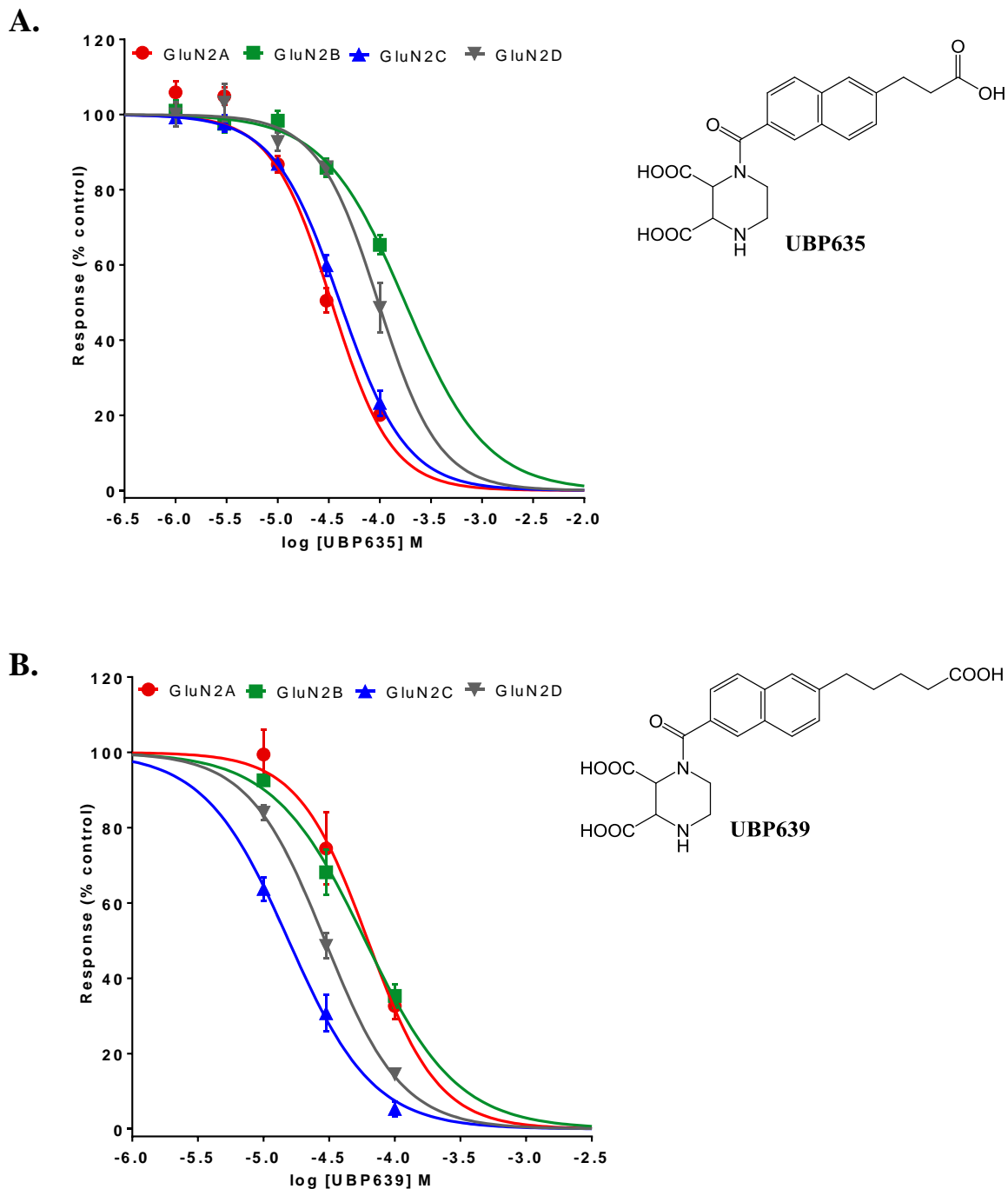
Figure 3.25 Concentration-response study of the inhibition of NMDAR responses by (A) UBP635 and (B) UBP639

Select NMDAR antagonists were tested for activity at various concentrations to determine the potency and efficacy at different NMDAR subtypes. NMDAR activity was measured by TEVC at recombinant NMDARs (GluN1a/GluN2A-D) expressed in *Xenopus laevis* oocytes. NMDAR-mediated current induced by increasing concentration of the test compounds co-applied with L-glutamate and glycine (10 µM each) was measured and expressed as % of control (agonist alone) NMDAR response (mean ± S.E.M; n > 4).

A.

B.
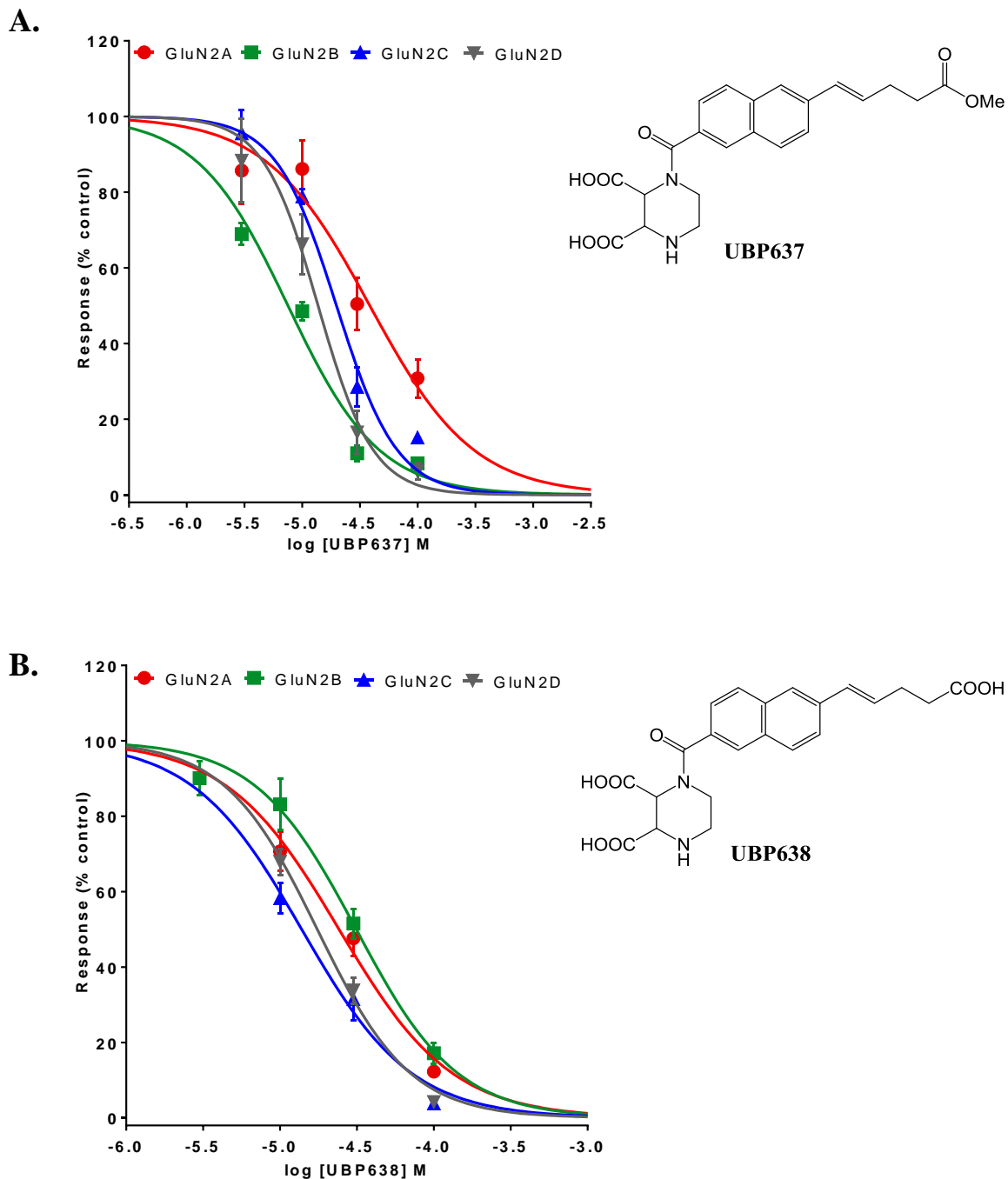
Figure 3.26 Concentration-response study of the inhibition of NMDAR responses by (A) UBP637 and (B) UBP638

Select NMDAR antagonists were tested for activity at various concentrations to determine the potency and efficacy at different NMDAR subtypes. NMDAR activity was measured by TEVC at recombinant NMDARs (GluN1a/GluN2A-D) expressed in *Xenopus laevis* oocytes. NMDAR-mediated current induced by increasing concentration of the test compounds co-applied with L-glutamate and glycine (10 µM each) was measured and expressed as % of control (agonist alone) NMDAR response (mean ± S.E.M; n > 4).

Table 3.4 Antagonist IC$_{50}$ (µM, n ≥ 4) values for inhibition of GluN1/GluN2 NMDAR subtypes[a]

Compounds	GluN2A	GluN2B	GluN2C	GluN2D
UBP633	16.3 ± 1.5	4.8 ± 0.8	35.6 ± 5.3	15.8 ± 2.2
UBP634	23.6 ± 5.3	137.3 ± 43.5	26.9 ± 7.2	39.7 ± 4.4
UBP635	33.4 ± 2.4	188.3 ± 25.1	42.7 ± 2.9	121.7 ± 17.4
UBP637	42.8 ± 9.1	7.9 ± 0.8	20.3 ± 1.9	15.6 ± 1.5
UBP638	25.9 ± 3.5	31.3 ± 4.3	15.3 ± 2.9	17.8 ± 1.9
UBP639	63.9 ± 10.2	61.3 ± 7.7	16.2 ± 1.6	29.5 ± 1.9
UBP784	49.3 ± 8.0	35.6 ± 3.2	8.7 ± 2.1	8.1 ± 2.2
UBP786	188.0 ± 39.4	68.0 ± 12.1	12.0 ± 2.8	24.1 ± 6.3
UBP791	85.4 ± 8.2	16.8 ± 1.2	1.0 ± 0.4	3.3 ± 0.3
UBP796	106.6± 5.8	75.3 ± 4.2	50.7 ± 1.7	35.3 ± 3.1
UBP797	48.9 ± 7.7	507.7 ± 300.4	376.6 ± 170.3	167.8 ± 27.7
UBP799	28.7± 5.0	59.7 ± 3.8	12.0 ± 1.0	6.8 ± 0.8

[a]IC$_{50}$ values (mean ± S.E.M.) for the inhibition of GluN1/GluN2 NMDAR responses evoked by agonist (L-glutamate, 10 µM and glycine, 10 µM).

Table 3.5 Antagonist K_i (µM, n ≥ 4) values of for inhibition of GluN1/GluN2 NMDAR subtypes[a]

Compounds	GluN2A	GluN2B	GluN2C	GluN2D
(R)-AP5	0.28 ± 0.02	0.46 ± 0.14	1.64 ± 0.14	3.71 ± 0.67
(R)-CPP	0.041 ± 0.003	0.27 ± 0.02	0.63 ± 0.05	1.99 ± 0.2
PPDA	0.55 ± 0.15	0.31 ± 0.02	0.096 ± 0.006	0.125 ± 0.035
UBP141	14.2 ± 1.1	19.3 ± 1.4	4.22 ± 0.52	2.78 ± 0.16
UBP145	11.5 ± 0.8	8.0 ± 0.35	2.8 ± 0.07	1.2 ± 0.06
UBP633	3.7 ± 0.3	0.8 ± 0.1	3.5 ± 0.5	0.6 ± 0.1
UBP634	5.3 ± 1.2	22.2 ± 7.0	2.7 ± 0.7	1.7 ± 0.2
UBP635	7.5 ± 0.5	30.5 ± 4.0	4.3 ± 0.3	5.1 ± 0.7
UBP637	9.7 ± 2.1	1.3 ± 0.1	2.0 ± 0.2	0.7 ± 0.1
UBP638	5.8 ± 0.8	5.1 ± 0.7	1.5 ± 0.3	0.7 ± 0.1
UBP639	14.4 ± 2.3	9.9 ± 1.2	1.6 ± 0.2	1.2 ± 0.1
UBP784	11.1 ± 1.8	5.8 ± 0.5	0.87 ± 0.2	0.34 ± 0.1
UBP786	42.4 ± 8.9	11.0 ± 2.0	1.2 ± 0.3	1.0 ± 0.3
UBP791	19.3 ± 1.9	2.7 ± 0.2	0.1 ± 0.04	0.14 ± 0.01
UBP796	24.1 ± 1.3	12.2 ± 0.7	5.1 ± 0.2	1.5 ± 0.1
UBP797	11.0 ± 1.7	82.1 ± 48.5	37.6 ± 17	7.1 ± 1.16
UBP799	6.5 ± 1.1	9.7 ± 0.6	1.3 ± 0.1	0.3 ± 0.03

[a]K_i values (mean ± S.E.M.) for the inhibition of GluN1/GluN2 NMDAR responses evoked by agonist (L-glutamate, 10 µM and glycine, 10 µM). Values for (R)-AP5, (R)-CPP, PPDA, UBP141 and UBP145 are previously reported (Morley, Tse et al. 2005, Costa, Feng et al. 2009) and are shown here for comparison.

Table 3.6. Potency relative to activity on GluN1/GluN2D (K_i GluN2/K_i GluN2D)

Compounds	GluN2A	GluN2B	GluN2C
(*R*)-AP5	0.075	0.123	0.44
(*R*)-CPP	0.02	0.14	0.32
PPDA	4.40	2.48	0.77
UBP141	5.1	6.9	1.5
UBP145	9.6	6.67	2.33
UBP633	6.2	1.3	5.8
UBP634	3.1	13.0	1.6
UBP635	1.5	6.0	0.8
UBP637	13.9	1.9	2.9
UBP638	8.3	7.3	2.1
UBP639	12	8.3	1.3
UBP784	32.6	17.1	2.6
UBP786	42.4	11.0	1.2
UBP791	137.9	19.3	0.7
UBP796	16.1	8.1	3.4
UBP797	1.5	11.6	5.3
UBP799	21.7	32.3	4.3

3.4.12   Mechanism of competitive inhibition of NMDARs by UBP791

To determine the mechanism of inhibition by UBP791, we performed L-glutamate and glycine

concentration-response analysis at GluN2D-containing receptors in different concentrations of the

antagonist UBP791. With increasing concentrations of UBP791, the glycine E_{Max} (maximal

response or efficacy) was changed but there was no significant change in the glycine EC_{50}.

However, with the increasing concentrations of UBP791, the E_{Max} response for L-glutamate was

similar but there was a reduction in L-glutamate EC_{50} values in the presence of higher

concentrations of the antagonist UBP791 (Figure 3.27, Table 3.7). These results are consistent

with UBP791 being a competitive glutamate antagonist. Schild plot analysis by linear fit of log

(Dose ratio - 1) *versus* log concentration of UBP791 gave a slope of 0.86 and pA2 of -7.1 (Figure

3.28) which corresponds to an affinity of 80 nM concentration. Which is close to the *Ki* value we

obtained from the dose- response study of UBP791 inhibition at GluN2D receptor.

Table 3.7 EC_{50} values of glutamate and glycine with/without different concentrations of UBP791[a]

	Glutamate		Glycine	
	µM	N	µM	N
Without UBP791 (EC_{50})	0.73 ± 0.04	5	0.31 ± 0.02	6
With UBP791 (1 µM; EC_{50}')	6.6 ± 0.4	5	0.68 ± 0.1	6
With UBP791 (3 µM; EC_{50}')	15.6 ± 0.8	6	0.8 ± 0.07	5
With UBP791 (10 µM EC_{50}')	36.9 ± 3.6	6	0.56 ± 0.06	5

[a]Data are presented as mean ± S.E.M.
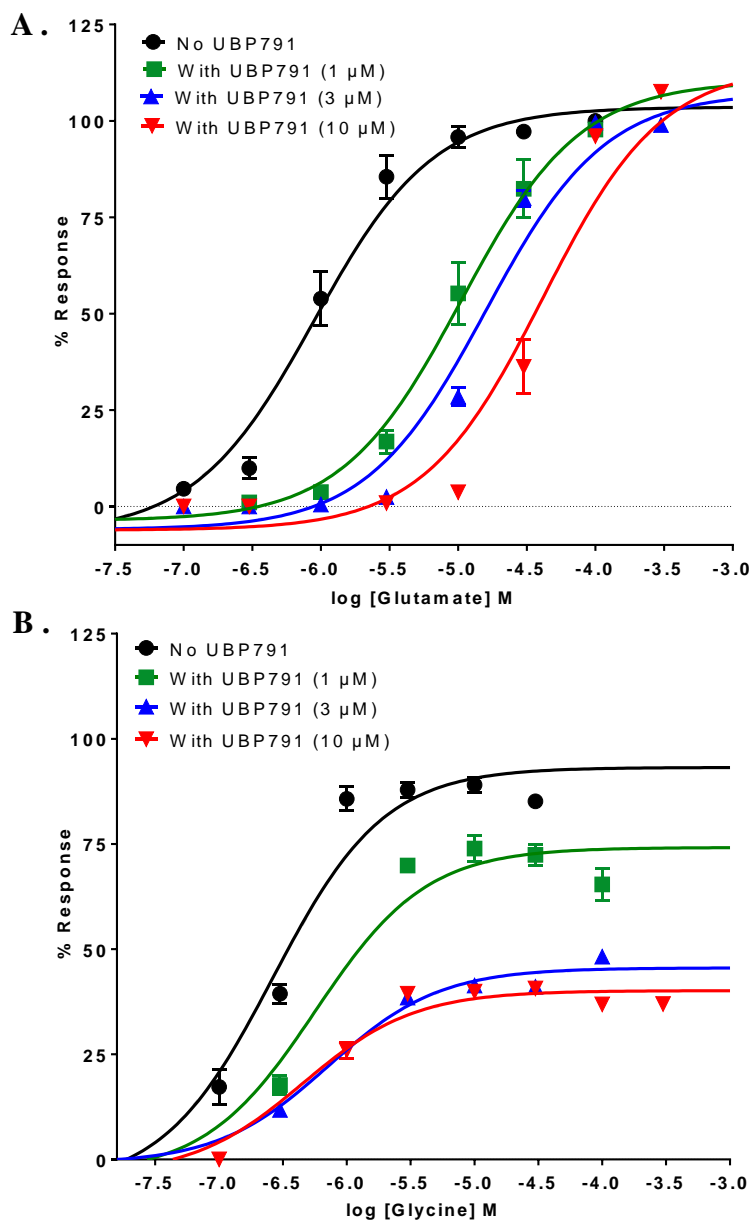
Figure 3.27 Effect of different concentrations of the antagonist UBP791 on L-glutamate and glycine potency at GluN2D-containing NMDARs

(**A**) Glutamate concentration-response curve at GluN1-1a/GluN2D receptors co-activated by glycine (10 μM) in absence or presence of different concentrations of UBP791. Data represent mean ± S.E.M from 5 − 6 oocytes. (**B**) Glycine concentration-response curve at GluN1-1a/GluN2D receptors co-activated by L-glutamate (10 μM) in absence or presence of different concentrations of UBP791. Data represent mean ± S.E.M from 5 − 6 oocytes.
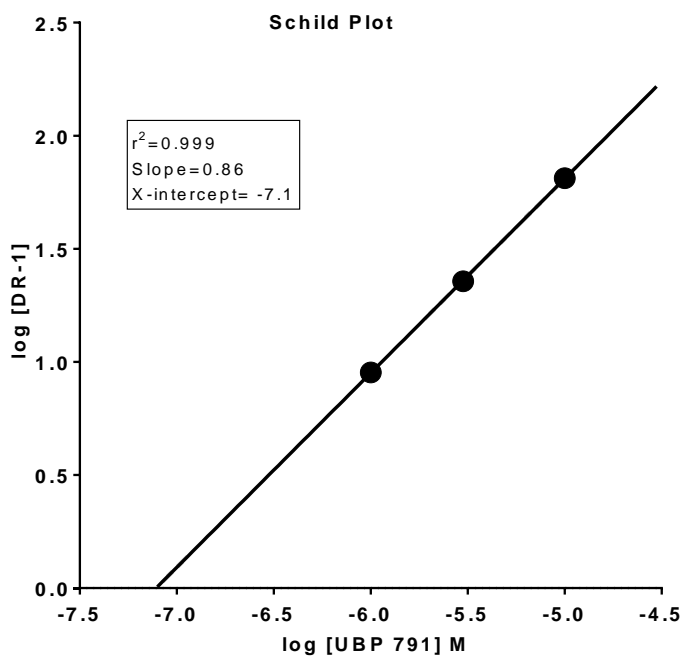
Figure 3.28 Schild plot analysis of UBP791 inhibition of glutamate response at GluN2D subtypes of NMDAR

The EC_{50} value of the agonist was determined from the glutamate concentration-response curve in the absence of and in the presence of increasing concentrations of UBP71. The dose ratio (DR) for each concentration of UBP791was calculated by dividing the corresponding EC_{50}' by the EC_{50} in the absence of UBP791. Then log [DR – 1] was plotted against the log [UBP791] M and fitted by linear regression, to obtain the slope and pA_2 value (X- intercept).

These results show that UBP791 competes with L-glutamate for binding and thus is likely to be binding at the L-glutamate binding site. However, since the slope of the Schild plot was not equal to one, it may be that the assumptions for ideal Schild analysis (Colquhoun 2007) are not valid for NMDARs. It is possible that the binding of antagonist to one glutamate binding site may alter the conformation of another glutamate binding site since the NMDAR has two glutamate binding sites. It is also possible that this compound can bind to an allosteric site as well as to the orthosteric glutamate binding site.

We also measured UBP791 inhibitory activity at GluN1 and GluN2A-containing NMDARs with a closed LBD cleft conformation using mutants with disulfide cross-linked LBD.

By co-expression of disulfide crosslinked GluN1^c (N499C and Q686C) with wildtype GluN2A or

of wildtype GluN1 with crosslinked GluN2A^c (K487C and N687C) in *Xenopus laevis* oocytes,

we evaluated the effect of constrained LBDs on the inhibitory activity of UBP791. The inhibition

by UBP791 (30 μM) at GluN1^c containing GluN2A receptors was similar to that of wild type

GluN2A receptors. As expected, UBP791 did not inhibit the NMDAR response at GluN2A^c

containing receptors and the response was significantly reduced (****$p<0.0001$, one-way

ANOVA followed by Tukey's multiple comparison test) compared to WT GluN2A receptors and

GluN1^c containing GluN2A receptors as shown in (Figure 3.29). The inhibition by UBP791 at

WT GluN2A, GluN1^c containing receptor and GluN2A^c containing receptor was 79.3 ± 11.2 % (n

= 13 oocytes), 76.5 ± 11.4 % (n = 14 oocytes), 11.1 ± 12.2 % (n = 18 oocytes) respectively. These

results suggest that the inhibition by UBP791 may require the opening of the GluN2 LBD. As we

know from the previous glutamate competition experiment, UBP791 likely binds at the L-

glutamate binding site and since LBD is locked in GluN2A^c containing NMDARs, it does not

allow the binding of UBP791 and hence is not able to cause any inhibition of the receptor's

response.
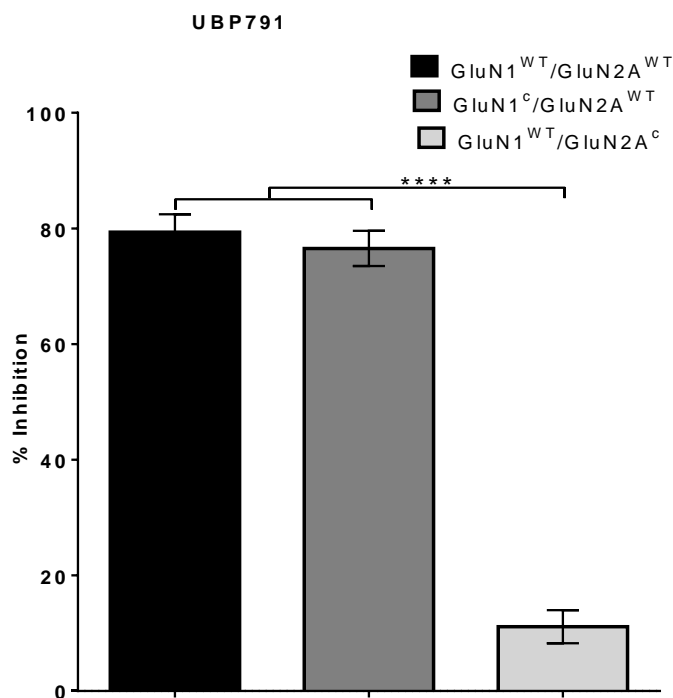
Figure 3.29 Effect of LBD cleft conformation on inhibitory activity of UBP791

Cross-linking the cleft of GluN1 LBD by introducing two cysteine point mutations (N499C and Q686C) mimics the glycine-bound conformation and cross-linking the cleft of GluN2A LBD by introducing two cysteine point mutations (K487C and N687C) leads to the L-glutamate-bound conformation. Both of these constructs were separately expressed with complimentary WT subunit in *Xenopus laevis* oocytes and the inhibitory activity of UBP791 (30 µM) was measured. A bar graph showing UBP791-mediated inhibition of agonists (10 µM L-glutamate and 10 µM glycine) evoked response from oocytes expressing WT (GluN1/GluN2A, n = 13 oocytes), GluN1 LBD-locked (GluN1^c/GluN2A, n = 14 oocytes) and GluN2A LBD-locked (GluN1/GluN2A^c, n = 18 oocytes) receptors. Data represent mean ± S.E.M. [**]p<0.01 (one-way ANOVA followed by Tukey's multiple comparison test).

3.5   Discussion

In this chapter, we screened multiple series of compounds, which displayed three types of activity at NMDARs. Some compounds exhibited PAM activity, some exhibited NAM and the others exhibited competitive antagonistic activity, which was confirmed by Schild plot analysis of L-glutamate concentration-response results.

To study the structure activity relationship (SAR) of 2-naphthoic acid derivatives for displaying PAM or NAM activity, various structural modifications were made and their activity was measured at GluN2A-D-containing NMDARs.

The SAR studies of the compounds displaying PAM activity revealed the following information: (i) a carboxylic group at the 2-position of the naphthalene ring is essential, (ii) a long alkyl chain at the 6-position of the naphthalene ring can be accommodated, (iii) a methyl substituent at the 1-position of the alkyl chain attached to the naphthalene ring can be accommodated, as can a phenyl or cyclopentyl group at the end of the chain, (iv) a hydroxyl group at the 3-position of the naphthalene ring can also be tolerated, and (v) a hydroxyl group at the 2-position of the naphthalene ring or ester group on the isohexyl chain is also tolerated which will help to reduce hydrophobicity of these PAMs and still retain the activity.

The SAR studies of the compounds displaying NAM activity revealed the following information: (i) addition of styryl group substituent to naphthalene ring at the 7-position increases activity, (ii) substitution with a hydroxyl group at the 3-position of the naphthalene ring in a styryl group-containing compounds enhances the activity while carboxylic group substitution reduces it, (iii) styryl group substitution at naphthalene ring is preferable but styryl group substitution on a coumarin ring is detrimental for NAM activity, (iv) nitro- and methoxy-substitution at the 7-position on the styryl ring is tolerated and nitro substitution at styryl aromatic ring makes them more GluN2D-selective.

The SAR studies of competitive antagonist derivatives revealed that the 9-position of the phenanthrene ring of UBP141 can accommodate different kinds of substituents and most of them display inhibitory preference for GluN2C- and GluN2D- over GluN2A- and GluN2B-containing NMDARs. Addition of piperazine-2,3-dicarboxylic acid (which mimics aspartate) was necessary in order to observe the competitive antagonism by phenanthrenyl-2-carbonyl compounds. Ring C from the phenanthrene ring of these phenanthrenyl-2-carbonyl analogues could be removed without a loss of NMDAR antagonism. Carboxylic acid substitution at position 6 of the naphthalene-2-carbonyl analogues yields compounds with the least inhibitory preference for GluN2B subunit whereas ester group substitution at the 6-position of naphthalene yields compounds with the highest preference for GluN2B receptors.

Competitive antagonists characterized in this project show more inhibitory activity at GluN2C- and GluN2D-containing receptors compared to GluN2A- and GluN2B-containing receptors. UBP791, which is a PPDA analogue (Morley, Tse et al. 2005), displayed greater selectivity toward GluN2C- and GluN2D-containing NMDARs compared to its parent compound. Similarly, other derivatives of previously characterized UBP141also demonstrated GluN2C/2D preference for their inhibitory activity. Removal of the unsubstituted ring C from the phenanthrene ring did not have any effect on inhibitory activity. Compounds such as UBP784, UBP791, UBP799, UBP633, UBP637, UBP638 showed high affinity for GluN2D receptors with nanomolar K_i values. Previous studies by our laboratory involving molecular modeling suggested that the phenanthrene ring of PPDA binds in the LBD cleft (S1/S2) along a groove in S2 at the base of 'H' helix (Kinarsky, Feng et al. 2005). This groove in GluN2D receptors has a non-conserved arginine residue (Arg737). The selectivity for GluN2D receptors by PPDA, UBP141 and their derivatives may be due in part to hydrophobic contact of the phenanthrene ring of these compounds with the hydrophobic side chain of Arg737.

It has been reported that a GluN2A NAM binds to the same site as do potentiators at the dimer interface of the LBDs of GluN1/GluN2A, with the major difference being that the conformation of Y535 on GluN1 is different in the two sites (Hackos, Lupardus et al. 2016). Thus, it is possible that some of the compounds in this study can bind in either of these two binding modes and that the combined effect of these two activities is being measured. However, it is also conceivable that the UBP-NAM and UBP-PAM sites are in different areas of the NMDAR complex. Indeed, one family of negative allosteric modulator is thought to bind at a site at the top of transmembrane regions 1 and 4 in a related family of ligand-gated ion channels known as AMPA receptors (Balannik, Menniti et al. 2005, Sobolevsky, Rosconi et al. 2009) and an equivalent binding site exists in NMDARs. Consistent with NAM and PAM binding sites that do not physical overlap, we also found that compound UBP512 non-competitively blocked the PAM activity of UBP684 (Chapter 4).

We also noticed that the PAMs displayed greater cell to cell variability in response magnitude than routinely seen with NAMs or competitive antagonists. It is possible that these PAMs are sensitive to a state-dependent variable such as that reported for neurosteroid potentiation being influenced by receptor phosphorylation state (Petrovic, Sedlacek et al. 2009).

Chapter 4 Functional properties and mechanisms of action of general NMDAR PAMs

4 Pharmacological and mechanistic characterization of NMDAR positive allosteric modulators (PAMs)

4.1 Abstract

N-methyl-D-aspartate receptors (NMDARs) are a subtype of receptors for L-glutamate, the primary excitatory neurotransmitter of the CNS. NMDAR activity is important for the induction of long-term potentiation (LTP) and long-term depression (LTD), two components of synaptic plasticity. Impairment in NMDARs function leads to various neuropathological consequences such as schizophrenia. In this study, we report the mechanism and pharmacology of two non-selective NMDAR positive allosteric modulators (PAMs), UBP684 and UBP753. They potentiate all subtypes of NMDARs with almost equal potency and efficacy. They enhance the efficacy of both of the NMDAR agonists L-glutamate and glycine. Their mode of NMDARs potentiation is independent of membrane potential. The mechanism of enhancement of the NMDAR-mediated response by these compounds is by increasing the channel open probability (P_{open}) and by prolonging the receptor deactivation time, especially slowing the deactivation time following glutamate removal. The binding sites for these potentiators are distinct from the binding sites of a class of structurally-related inhibitors that we have previously reported. These compounds can bind to both the agonist-bound and agonist-unbound conformations. These compounds stabilize the GluN2 LBD in the glutamate-bound state conformation. These compounds lose their potentiating activity at alkaline pH and the GluN1 C-terminal is necessary for their PAM activity. An allosteric interaction with the intracellular C-terminal is also suggested by the finding that PAM activity is potentiated by PKC activity. These PAMs may be valuable in enhancing NMDAR activity in schizophrenia where there is thought to be a reduction in NMDAR-mediated neurotransmission.

4.2   Introduction

The primary excitatory neurotransmitter in the vertebrate CNS, L-glutamate, activates three distinct families of ligand-gated ion channel receptors that are named for agonists by which they are selectively activated, N-methyl-D-aspartate (NMDA), AMPA (2-amino-3-hydroxy-5-methyl-4-isoxazole propionic acid) and kainate (Monaghan, Bridges et al. 1989, Dingledine, Borges et al. 1999, Traynelis, Wollmuth et al. 2010). While AMPA and kainate receptors underlie fast excitatory synaptic transmission in the CNS, NMDAR activation triggers multiple calcium-dependent intracellular responses that regulate distinct forms of synaptic plasticity such as long-term potentiation (LTP), long-term depression (LTD) and experience-dependent synaptogenesis (Collingridge, Isaac et al. 2004, Bliss, Collingridge 1993, Malenka, Bear 2004, Luscher, Malenka 2012, Matsuzaki, Honkura et al. 2004, Zhou, Homma et al. 2004). These and related NMDAR mechanisms play key roles in learning, memory, and cognition. However, excessive NMDAR activation is thought to be a common mechanism causing neuronal cell death in stroke, traumatic brain injury and various neurodegenerative diseases (Rothman, Olney 1987, Simon, Swan et al. 1984, Faden, Demediuk et al. 1989). NMDAR hypofunction is also associated with CNS dysfunction and may be responsible for the symptoms of schizophrenia (Olney, Newcomer et al. 1999, Coyle, Tsai et al. 2003, Coyle, Tsai 2004, Weickert, Fung et al. 2013). The findings regarding glutamate-induced cell death have led to the development of a large number of NMDAR inhibitors over the past 30 years to provide neuroprotection in stroke, seizures, and neurodegenerative disorders. More recently, agents that augment NMDAR activity have been identified and their potential application for treating neuropsychiatric and cognitive disorders is now being determined (Mullasseril, Hansen et al. 2010, Hackos, Lupardus et al. 2016, Costa, Irvine et al. 2010).

NMDAR complexes are composed of subunits from seven genes - GluN1, GluN2A-GluN2D, and GluN3A-GluN3B (Ishii, Moriyoshi et al. 1993, Moriyoshi, Masu et al. 1991).

These subunits assemble into hetero-tetrameric complexes in various combinations resulting in functionally-distinct NMDARs. The majority of NMDARs are thought to be composed of two GluN1 subunits and two GluN2 subunits and arranged in dimer of heterodimers (Karakas, Furukawa 2014, Lee, Lü et al. 2014). While the various GluN1 subunits are alternatively-spliced isoforms with largely similar pharmacological and physiological properties, the GluN2 subunits confer distinct physiological, biochemical, and pharmacological properties to the NMDAR complex (Monyer, Sprengel 1992, Monyer, Burnashev et al. 1994, Vicini, Wang et al. 1998, Buller, Larson et al. 1994, Mishina, Mori et al. 1993, Nakanishi 1992). These properties combined with the varied developmental profiles and anatomical distributions of GluN2 subunits (Watanabe, Inoue et al. 1993b, Monaghan, Holets et al. 1983, Sucher, Akbarian et al. 1995) imply that GluN2 subtype-selective agents should have distinct physiological and therapeutic properties. Indeed, many studies now suggest that different subtypes of NMDARs can have distinct, and even opposite, roles in neurobiological processes and in neurological disorders. Thus, the ability to differentially enhance the function of specific NMDAR subtypes while not affecting, or even inhibiting, other populations, may provide therapeutic advantages.

Neurosteroids such as PS have long been known for their NMDAR modulatory activity (Wu, Gibbs et al. 1991, Compagnone, Mellon 2000, Irwin, Maragakis et al. 1992). They can inhibit GABA-A, glycine, AMPA and kainate as well as GluN2C- and GluN2D-containing receptors (Park-Chung, Malayev et al. 1999). However, the neurosteroid pregnenolone sulfate potentiates GluN2A- and GluN2B-mediated NMDAR currents (Yaghoubi, Malayev et al. 1998, Malayev, Gibbs et al. 2002). Besides neurosteroids, other positive allosteric modulators of NMDARs have been recently identified (Mullasseril, Hansen et al. 2010, Hackos, Lupardus et al. 2016, Costa, Irvine et al. 2010). Their mechanism of action has been studied and their binding site predicted. Chemical structures of some of the known and novel PAMs is shown in Figure 4.1

In a recent study, we described a novel series of allosteric modulators that display both inhibitory activity (negative allosteric modulator, NAM) and enhancing activity (positive allosteric modulator, PAM) at NMDARs (Costa, Irvine et al. 2010, Costa, Irvine et al. 2012). These compounds also displayed distinct patterns of selectivity at NMDARs containing different GluN2 subunits. Thus, this class of agents offers the potential to develop agents with an optimal profile of therapeutic / adverse effects. These agents do not act at either glutamate or glycine binding sites nor at the N-terminal regulatory domain. They also do not appear to be NMDAR channel blockers. Initial experiments indicate that these agents may be binding in the dimer interface in a manner that may be homologous to the binding of the AMPA receptor allosteric modulators GYKI-52466 and cyclothiazide (Sun, Olson et al. 2002, Johansen, Chaudhary et al. 1995). This group of compounds should be valuable tools for identifying the physiological roles of distinct NMDAR subtypes and serve as lead compounds for a variety of therapeutic applications.

The precise effect that a PAM has on synaptic and extra-synaptic NMDAR currents depends upon various properties of the PAM's actions. The activity of NMDAR PAMs to influence the receptor response time-course and sensitivity can vary and function of agonist concentration. In turn, these properties can alter the synaptic NMDAR current's frequency-response and temporal integration properties, and also, differentially augment responses during synaptic agonist saturation or at low, tonic agonist concentrations. Thus, these properties influence the applicability of specific PAMs for the modulation of NMDAR activity in neurological or neuropsychiatric conditions. Recently we have identified UBP684 and UBP753 as non-selective, 2-naphthoic acid based NMDAR PAMs with relatively high efficacy in enhancing NMDAR-mediated currents. In this chapter, we sought a better understanding of the mechanisms by which UBP684 and UBP753 can enhance NMDAR currents.
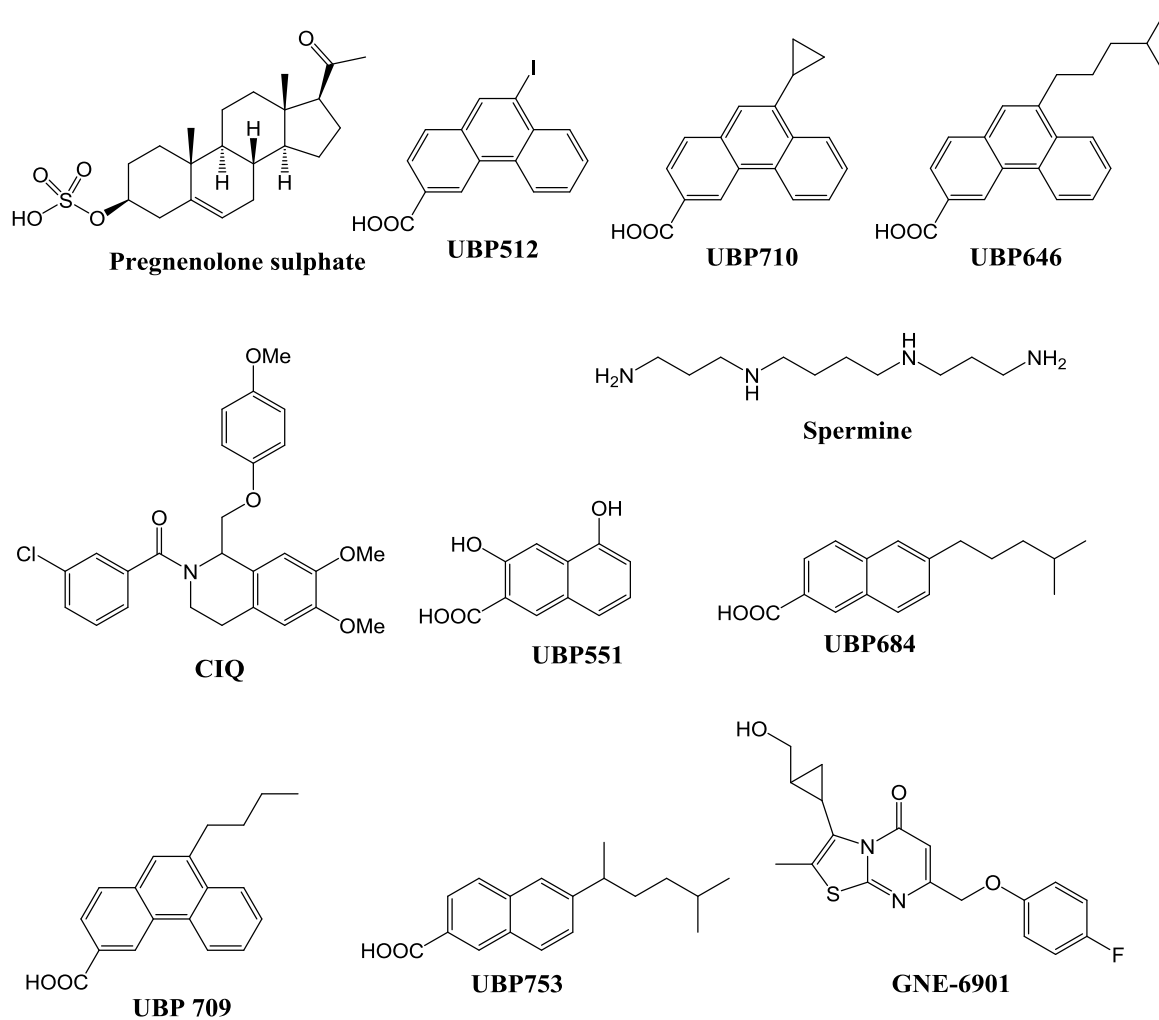
Figure 4.1 Structure of positive allosteric NMDAR modulators

4.3 Materials and methods

4.3.1 Compounds

UBP684, UBP753 and UBP792 were synthesized in Dr. David Jane's laboratory at University of

Bristol and verified as described previously (Chapter 3, section 3.2.1).

4.3.2 GluN subunit expression in Xenopus oocytes

cDNAs and cRNAs were prepared and expressed in *Xenopus* oocytes as described in the method

sections (3.2.2 and 3.2.3) of the previous Chapter 3.

4.3.3 Two-electrode voltage clamp (TEVC) assay

TEVC assays were performed as described before in Chapter 3 (section 3.2.4).

To study the effect of disulfide bond reduction on potentiation by UBP753 and UBP684,

oocytes were treated for 3 minutes with bath perfusion of 3 mM dithiothreitol (DTT) followed by

1-minute wash with recording buffer. Percent potentiation was calculated using the agonist-alone

response just before the co-application of UBP compounds and agonists.

4.3.4 Data analysis

For the calculation of association time constant (K_{ON}) of UBP753, we first calculated the

association time (τ_{ONSET}) of GluN2D-mediated current response by increasing concentrations of

UBP753 with a single fit exponential which is considered as the time required for association of

drug with the receptor. Linear regression analysis of the plotting of $1/\tau_{ONSET}$ versus UBP753

concentration gave K_{ON} (slope) and K_{off} (y-intercept) values which were used to calculate the K_D

($K_D = K_{OFF}/K_{ON}$).

4.3.5   Statistical analysis

Prism 6 (GraphPad Software Inc., San Diego, CA, USA) was used for statistical analysis. All values are expressed as mean ± SEM. Paired and unpaired t-test and one-way ANOVA were used to analyze the data. $p < 0.05$ was considered as statistically significant.

4.4   Results

4.4.1   UBP684 dose-response for the potentiation of GluN2A-D NMDARs

UBP684 enhanced the agonist-induced (10 μM L-glutamate and 10 μM glycine) current across

all subtypes of NMDARs (Figure 4.2). Maximal potentiation of GluN2A, GluN2B, GluN2C and

GluN2D receptors by UBP684 was 68.6 ± 16.2 %, 102.0 ± 17.85 %, 117.2 ± 22.3 5 % and 88.4 ±

9.6 % respectively. EC_{50} values at the four NMDAR subtypes ranged from 28 to 37.2 μM as

shown in the Table 4.1. When the concentration-response study of UBP684 was carried out using

high concentrations of agonists (300 μM of L-glutamate and 300 μM of glycine), its affinity for

GluN2A and GluN2B subtypes was slightly enhanced and the affinity for the GluN2D subtype

was slightly lowered. However, the maximal potentiation by UBP684 at GluN2B receptors was

lowered when agonists were used at 300 μM instead of at 10 μM (Table 4.1, Figure 4.2). There

was no significant change in maximal potentiation by UBP684 at GluN2A, GluN2C or GluN2D

in the high agonist concentration condition.

Table 4.1 EC$_{50}$ (μM, n ≥ 4) values for potentiation by UBP684 and UBP753 of GluN1/GluN2 NMDAR subtypes[a]

Compounds	Glu/Gly.	GluN2A	GluN2B	GluN2C	GluN2D
UBP684	10 μM each	28.0 ± 4.6	34.6 ± 3	37.2 ± 2.8	28.9 ± 4.1
		(68.6 ± 16.2)	(102.0 ± 17.8)[###]	(117.2 ± 22.3)	(88.4 ± 9.6
UBP684	300 μM each	10.3 ± 4.8[*]	24.8 ± 2.8*	33.8 ± 9.7	55.8 ± 4.1[**]
		(50.3 ± 14.1)	(61.5 ± 4.2)	(108.2 ± 37.9)	(119.3 ± 37.9)
UBP753	10 μM each	39.4 ± 27.5	25.0 ± 11.6	36.2± 5.7	30.6 ± 7.5
		(277.2 ± 36.8)	(192.3 ± 46.6)	(262.6 ± 33.9)	(240.3 ± 63.6)

[a]EC$_{50}$ values (mean ± S.E.M.) for the potentiation of GluN1/GluN2 NMDAR responses. Values in parenthesis represent the maximal potentiation (% E$_{Max}$) expressed as a percentage (± S.E.M.) above the agonist-alone response (10 μM L-glutamate and 10 μM glycine).

[*]p < 0.05 and [**]p < 0.01 (unpaired t-test) vs EC$_{50}$ value for UBP684 potentiation at 10 μM L-glutamate and 10 μM glycine.

[###]p < 0.001 (unpaired t-test) vs % E$_{Max}$ value for UBP684 potentiation at 10 μM L-glutamate and 10 μM glycine.

A.

B.
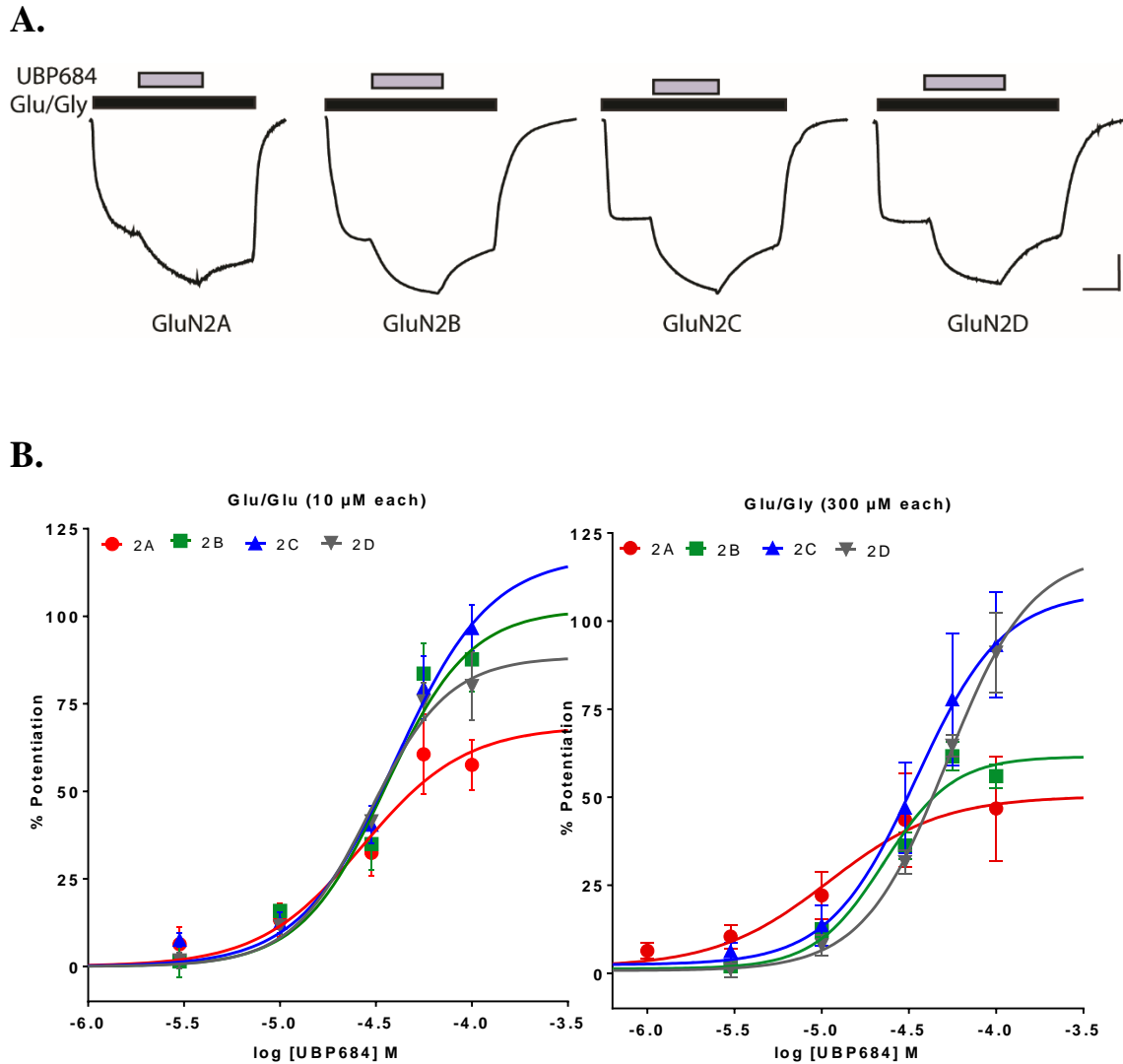
Figure 4.2 Concentration-response study of the potentiation of GluN2A-D NMDAR subtypes by UBP684

(A) Representative current traces showing UBP684 enhancement of current mediated by rat recombinant GluN1/GluN2A-D receptors expressed in *Xenopus laevis* oocytes as measured by TEVC. Current was first evoked by 10 µM L-glutamate and 10 µM glycine. After achieving a steady-state response, UBP684 (100 µM) was co-applied with the agonists. Scale bars: X-axis =21 s, 13 s, 13 s, and 20 s and y-axis = 75 nA, 125 nA, 110 nA and 120 nA for GluN2A, GluN2B, GluN2C, and GluN2D traces respectively. (B) UBP684 was tested for its activity at increasing concentrations to determine the potency and efficacy at different NMDAR subunits. NMDAR-mediated currents induced by co-application of different concentrations of UBP684 plus 10 µM L-glutamate and 10 µM glycine were measured and expressed as % potentiation over the agonist-alone response (n = 5-12 oocytes per subunit) (C) Potentiation of NMDAR-mediated current by increasing concentrations of UBP684 in presence of high agonist concentration (300 µM L-glutamate and 300 µM glycine) was also measured (n = 5 to 11 oocytes per subunit). Data represent mean ± S.E.M.

4.4.2 Effect of UBP684 on affinity and efficacy of agonists at GluN2B- and GluN2D-containing NMDARs

Agonist-response studies indicate that UBP684 enhances the response magnitude of both L-glutamate and glycine at GluN2B- and GluN2D-containing NMDARs. The reduction we observed in the potentiation by UBP684 when high agonist was used, at GluN2B could be because UBP684 may be potentiating, in part, by increasing the potency of the agonists at GluN2B receptors. UBP684 significantly ($p < 0.01$, unpaired t-test) enhanced the affinity of glycine (EC_{50} of 0.87 in absence of UBP684 vs 0.61 μM in presence of UBP684), but not of L-glutamate (EC_{50} of 2.01 in absence of UBP684 vs 2.08 μM in presence of UBP684) at GluN2B-containing NMDARs (Figure 4.3A,B; Table 4.2). UBP684 slightly decreased the affinity of L-glutamate and slightly enhanced the glycine affinity at GluN2D receptors (Figure 4.3C,D).
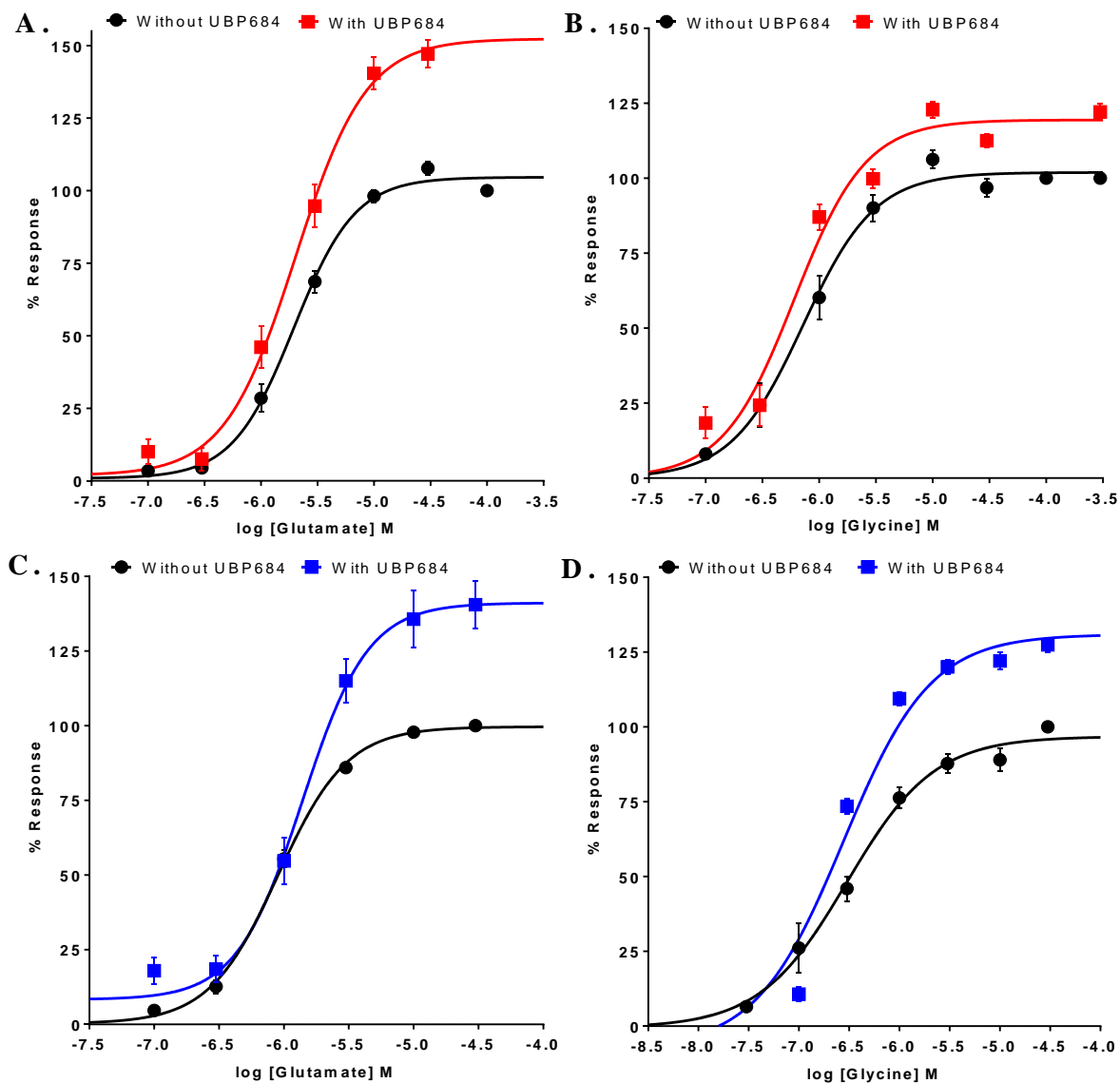
Figure 4.3 Effect of UBP684 on affinity and efficacy of NMDAR agonists

A concentration-response study of L-glutamate (**A**; **C**) and glycine (**B**, **D**) on GluN2B- (**A**, **B**) and GluN2D- (**C**, **D**) containing NMDARs was carried out by increasing the concentrations of a agonist in the absence (black) or presence (red, GluN2B; blue, GluN2D) of 50 μM of UBP684 to study the effect of UBP684 on affinity and efficacy of the NMDAR agonist for recombinant NMDARs expressed in *Xenopus laevis* oocytes. Concentration-response study of L-glutamate was performed in the presence of 10 μM glycine and that of glycine was performed in the presence of 10 μM glutamate. The response from each oocytes was individually normalized with the response obtained from the highest concentration of the agonist-alone application from the same oocyte (n = 6-10 oocytes per curve). Data represent mean ± S.E.M.

4.4.3   *UBP753 concentration-response*

UBP753 also exhibited a pan-PAM property with similar activity across all four subtypes of

NMDARs (Figure 4.4A). However, UBP753 showed a higher percentage of maximal potentiation

compared to UBP684. Its maximum potentiation at GluN2A, GluN2B, GluN2C and GluN2D

receptors was 277 %, 192.3 %, 262.6 % and 240.3 % respectively. But, its affinity as given by

EC_{50} was similar to that of UBP684 (Table 4.1). We also calculated the apparent affinity by

association and dissociation kinetic analysis (Figure 4.4). This gave the K_D value of 73.3 μM,

which was little higher than the EC_{50} value we obtained from the concentration-response study.

We also studied if UBP753 increases the affinity or efficacy of agonists at NMDARs. UBP753,

similar to that of UBP684, enhanced the L-glutamate and glycine efficacy at GluN2D-containing

NMDARs (Figure 4.4 C, D). However, UBP753 slightly reduced the L-glutamate affinity and did

not alter the glycine affinity for GluN2D receptors.

Table 4.2 EC$_{50}$ (µM) and % E$_{Max}$ values of agonists in absence and presence of UBP684

		Glutamate			
		EC$_{50}$ (µM)	*% E$_{Max}$*	*Hill slope*	*N*
GluN2B	Without UBP684	2.01 ± 0.19	104.6 ± 1.8	1.58	9
	With UBP684	2.08 ± 0.12	152.3 ± 6.3	1.48	7
GluN2D	Without UBP684	0.88 ± 0.05	99.6 ± 1.2	1.6	10
	With UBP684	1.4 ± 0.1***	141.1 ± 5.5	1.7	7
GluN2D	Without UBP753	0.93 ± 0.06	100.7 ± 1.6	1.8	15
	With UB753	1.3 ± 0.1**	128.3 ± 3.8	1.9	6
		Glycine			
		EC$_{50}$ (µM)	*% E$_{Max}$*	*Hill slope*	*N*
GluN2B	Without UBP684	0.87 ± 0.07	101.9 ± 2.7	1.4	19
	With UBP684	0.61 ± 0.05**	119.4 ± 3.0	1.38	19
GluN2D	Without UBP684	0.32 ± 0.04	97.0 ± 2.6	1.17	9
	With UBP684	0.25 ± 0.01	131.0 ± 2.9	1.99	6
GluN2D	Without UBP753	0.2 ± 0.04	96.5 ± 2.9	1.3	14
	With UBP753	0.22 ± 0.03	135.4 ± 3.8	0.9	7

$^{**}p < 0.01$ and $^{***}p < 0.001$ vs EC$_{50}$ value for L-glutamate or glycine without UBP684 or UBP753 at the same NMDAR subtypes
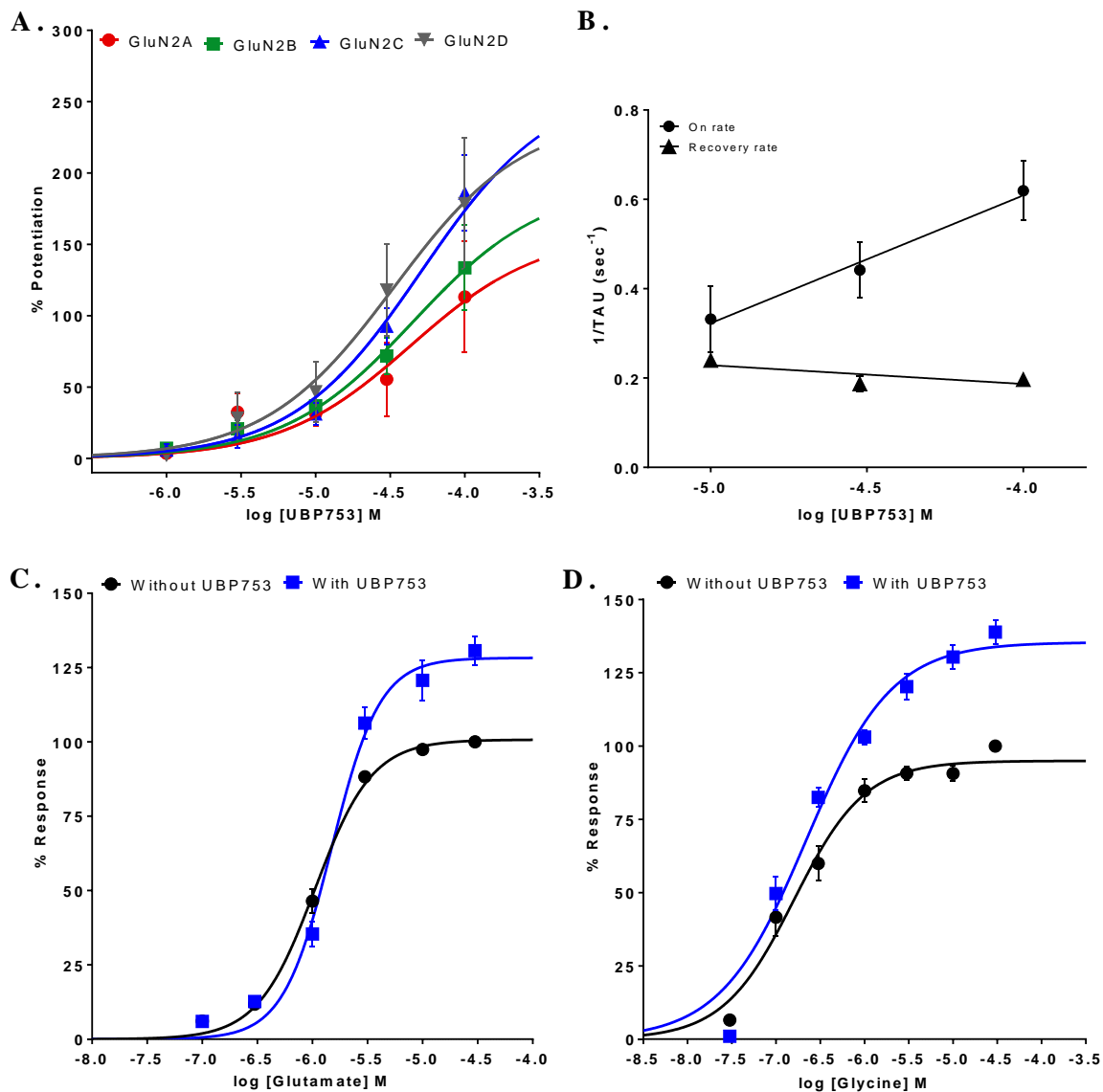
Figure 4.4 Concentration-response study of UBP753 and its effect on agonist affinity

(**A**) UBP753 was tested at increasing concentrations to determine its potency and efficacy at different NMDAR subunits expressed in *Xenopus laevis* oocytes. NMDAR-mediated current was induced by co-application of different concentrations of UBP753 with 10 μM of L-glutamate and 10 μM glycine and expressed as % potentiation of agonist-alone induced responses (n = 5-12 oocytes per subunit). (**B**) Affinity of UBP753 at GluN2D-containing NMDARs was also determined by exponential fit of the on-rates and off-rates of different concentrations of UBP753. Using the linear fit of 1/Tau$_{ONSET}$ and UBP753 concentration, K_D was calculated. The equation for the regression line is given by y = mx + b where m is the slope of the line and b is the y-intercept of the line. (**C**) A concentration-response study of L-glutamate in the presence of 10 μM glycine ± 30 μM UBP753 at GluN2D-containing NMDARs (n = 5-6 oocytes per curve). (**D**) A concentration-response study of glycine in presence of 10 μM L-glutamate ± 30 μM UBP753 at GluN2D containing NMDARs (n = 5-7 oocytes per curve). Data represent mean ± S.E.M.

4.4.4   Effect of membrane potential on UBP753 potentiation

UBP753 potentiating activity was voltage independent. At 100 µM, UBP753 potentiated

GluN2C-containing NMDARs by 88.0 ± 12.9 % (n = 5 oocytes) at + 40 mV and by 93.8 ± 8.5 %

(n = 5 oocytes) at – 60 mV which were not statistically different (Figure 4.5A,B). Also, 50 µM

UBP753 did not change the reversal potential of GluN2B receptors (Figure 4.5C). This suggests

that UBP753 does not bind within the receptor's ion channel. Additionally, UBP753 did not alter

the EC_{50} of ketamine channel blockade of the NMDAR response (Figure 4.5D). The IC_{50} value

for ketamine inhibition at GluN2C-containing receptors was 0.69 ± 0.12 µM (n = 5 oocytes) in

absence of UBP753 and was $0.73 \pm 0.0.03$ µM (n = 5 oocytes) in presence of 30 µM UBP753.

Hence, UBP753 and ketamine binding sites do not overlap and UBP753 does not allosterically

alter the ketamine binding site.
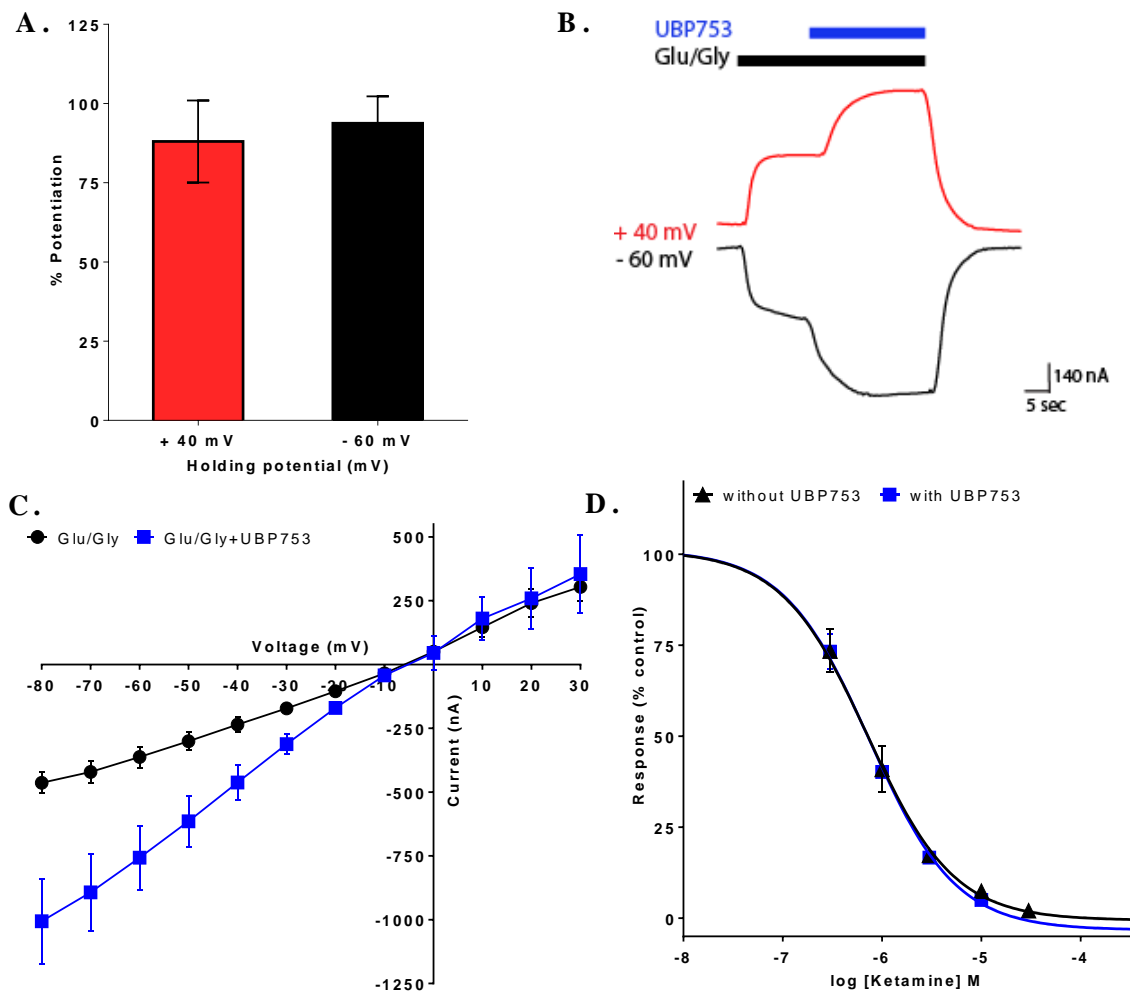
Figure 4.5 Effect of change in membrane potential on the potentiation by UBP753

(**A**) The potentiating activity of 100 μM of UBP753 was measured at -60 mV and +40 mV on the GluN2C subtype of NMDARs expressed in *Xenopus laevis* oocytes. A bar graph shows the percent potentiation of the agonist-induced (10 μM L-glutamate and 10 μM glycine) response at - 60 mV and + 40 mV (n = 5 oocytes). (**B**) A representative trace showing the potentiating activity of UB753 (100 μM) at - 60 mV and + 40 mV on GluN2C subtype of NMDARs. Scale bar: horizontal = time in sec, vertical = current in nA. (**C**) A current-voltage relationship curve in the absence (control) or the presence of 50 μM of UBP753 at GluN2B-containing NMDARs (n = 6 oocytes). (**D**) Ketamine inhibition of NMDAR response in the absence (n = 5 oocytes) or presence (n = 5 oocytes) of 30 μM of UBP753 at GluN2C-containing receptors. The concentration-response curve in the presence of UBP753 was normalized to the maximal response observed in the presence or absence of UBP753 (100 % Value). Data represent mean ± S.E.M.

4.4.5   Effect of redox modulation and GluN1 splice variants on UBP potentiation

Reduction of cysteine residues on the NMDAR complex is known to potentiate the NMDAR response. To determine if UBP753/UBP684 potentiation shares a common mechanism with NMDAR redox modulation, we compared the potentiating activity of UBP753 and UBP684 before and after the treatment of GluN2A-containing NMDARs with 3 mM DTT for 3 min. DTT treatment significantly ($p = 0.01$, paired t-test) lowered the potentiation by UBP753. The potentiation by 50 µM UBP753 at GluN2A-containing receptors before the DTT pretreatment was 82.1 ± 9.6 % (n = 8 oocytes). The potentiation by UBP753 was partially reduced to 62.8 ± 8.7 % (n = 8 oocytes) after the treatment with DTT (Figure 4.6A) and the difference was significant. However, the DTT did not significantly alter ($p = 0.3$) the potentiation by 50 µM of UBP684 (Figure 4.6B). UBP684 potentiated GluN2A receptors by 61.3 ± 7.3 % (n = 6 oocytes) before and by 53.1 ± 6.8 % (n = 6 oocytes) after the DTT treatment. These results suggest that changing the redox state of the receptor has a minimal effect on potentiation activity of UBP compounds.

We then sought to determine if the mechanism of potentiation by UBP684 is by relieving proton inhibition, this is the mechanism by which spermine by binding to the N-terminal domain enhances NMDAR responses. We co-expressed the GluN2D subtype of NMDARs with the GluN1 subunit with exon-5 (GluN1-1b) or without exon-5 (GluN1-1a), a N-terminal segment with 21 amino acids, which reduces proton sensitivity. We did not observe any significant difference in the potentiating activity (both EC_{50} and % E_{Max}) of UBP684 at GluN2D-containing receptors expressed with either of the two GluN1 splice variant forms (Figure 4.6C). This result implies that the potentiating mechanism of UBP684 is not by changing proton sensitivity in the manner by which spermine potentiates GluN2B-containing NMDARs.
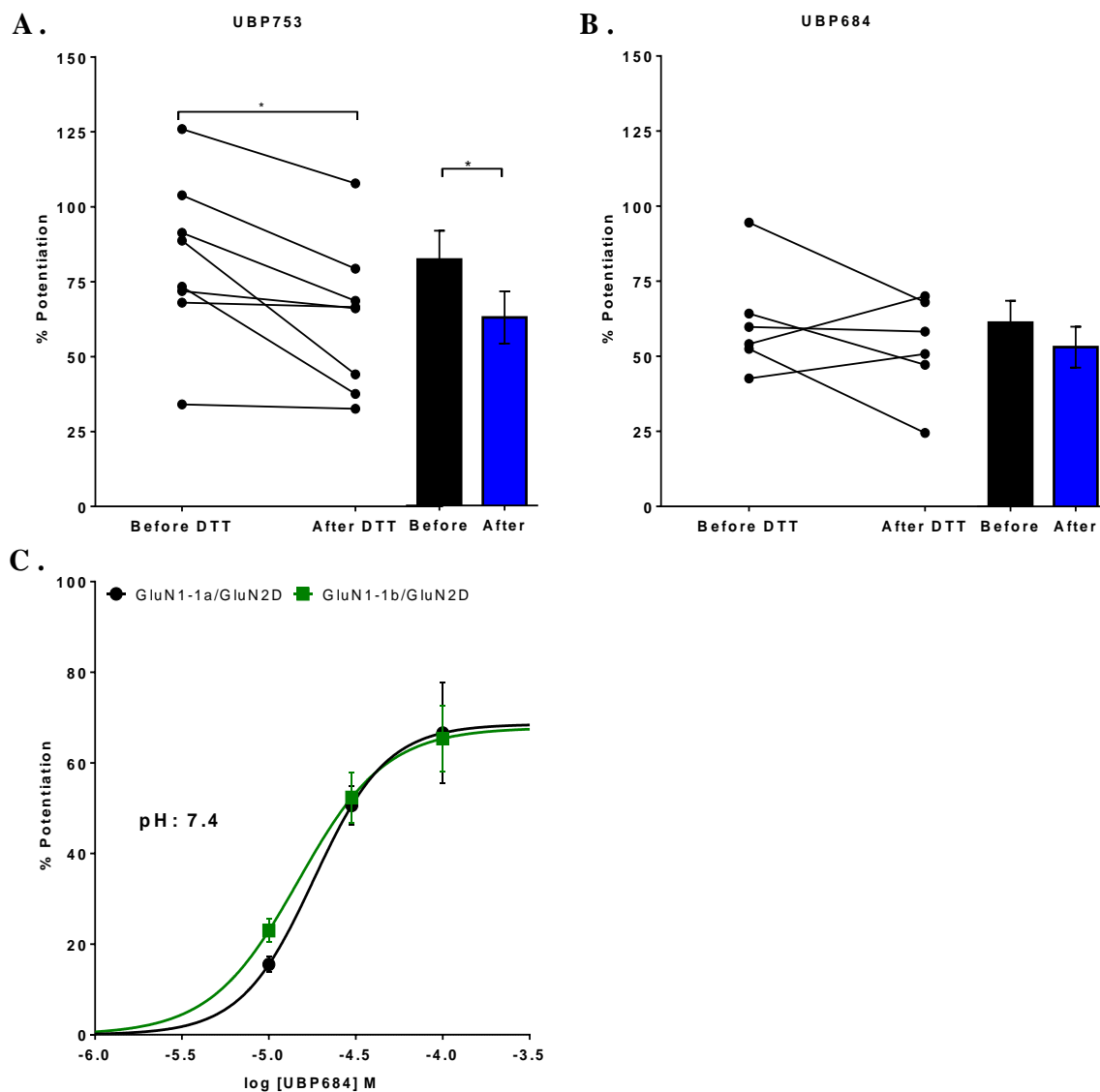
Figure 4.6 Effect of redox modulation and GluN1 splice variants on potentiation by UBPs

(**A**) UBP753 (50 µM) potentiation was measured before and after DTT (3 mM) treatment of GluN2A-containing NMDARs for 3 min (n = 8 oocytes). Data represent mean ± S.E.M. [*]p<0.05 (paired t-test). (**B**) A plot of UBP684 (50 µM) potentiation of GluN2A-containing NMDARs before and after the treatment with 3 mM DTT (n = 6 oocytes). (**C**) UBP684 concentration-response for the potentiation of GluN2D receptors co-expressed with GluN1-1a (absence of exon-5 segment; black curve) (n = 6 oocytes) or GluN1-1b (presence of exon-5 segment; green curve) subunits (n = 5 oocytes). Data represent mean ± S.E.M.

4.4.6 *Non-competitive nature of PAM and NAM binding*

We hypothesize that the negative allosteric activity of UBP-NAMs and positive allosteric activity

of UBP-PAMs comes from their binding to different sites. To determine if PAMs and NAMs

have different or overlapping binding sites, we studied their mode of interaction by performing a

concentration-response study of UBP684 at GluN2C-containing NMDARs in absence or presence

of UBP552, which is a general NMDAR NAM with an IC_{50} value of 5.1 µM at GluN2C-

containing NMDARs. UBP552 did not change the EC_{50} of UBP684 but it changed the %

maximal potentiation by UBP684 (Figure 4.7A). Similarly, UBP 512, another NAM at GluN2C-

containing receptors with an IC_{50} of 51 µM, did not change the UBP684 EC_{50} but it did change

the % maximal potentiation by UBP684 (Figure 4.7B). Both of these studies indicate a non-

competitive interaction between the binding of UBP-NAMs and UBP-PAMs. We also studied if

two PAMs are competing to each other for binding at the same site. Concentration-response study

of UBP684 in presence of 100 µM of UBP512, a GluN2A-selective PAM, also shows that both of

the PAMs do not compete for binding (Figure 4.7C). The result was interesting in that, the

presence of UBP512 significantly reduced the potentiating activity of UBP684 although both

have potentiating activity at GluN2A-containing NMDARs. Thus, UBP684 and UBP512 may

have distinct binding sites and the binding of UBP512 may non-competitively block UBP684's

ability to allosterically modulate NMDAR activity.
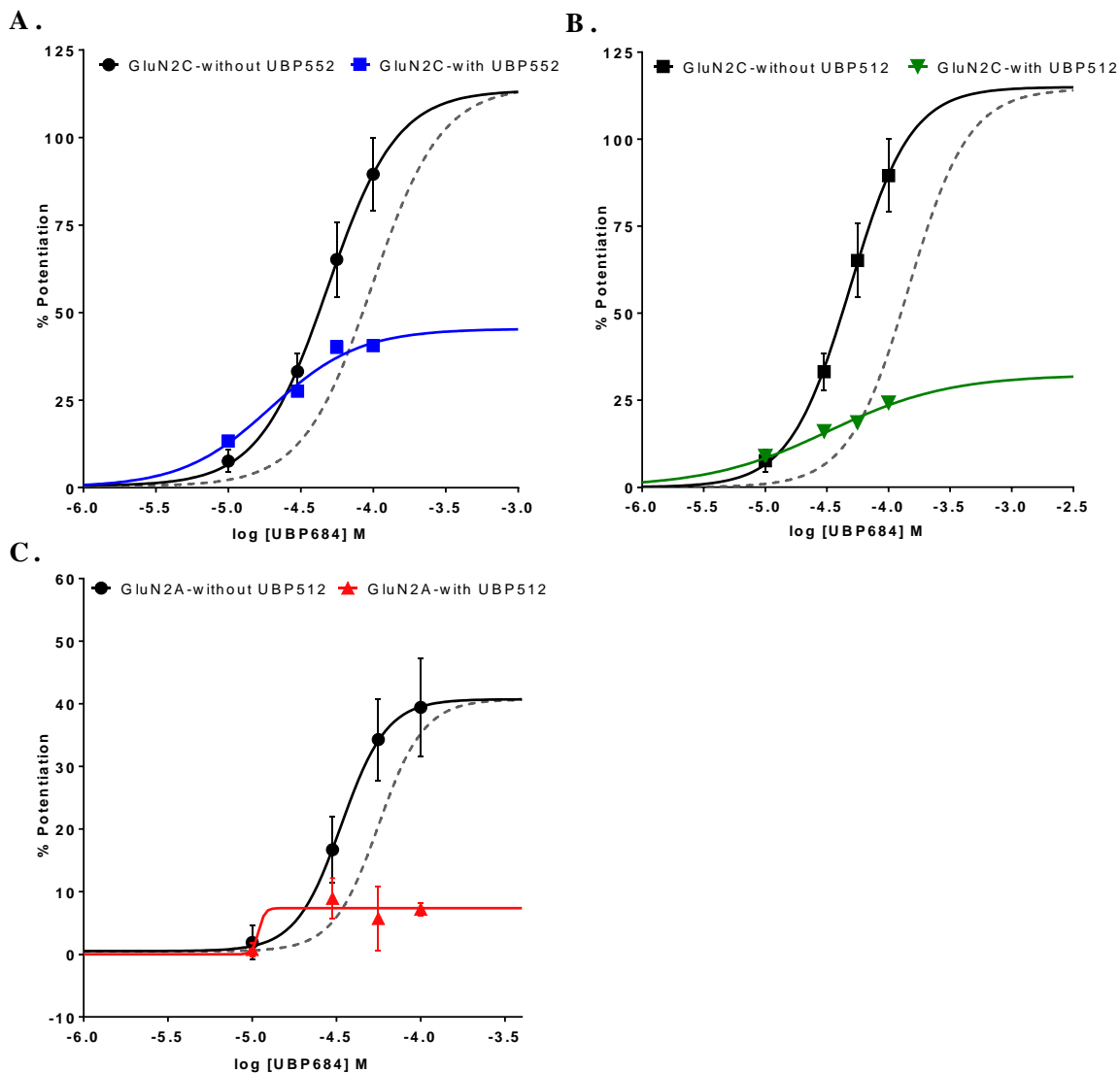
Figure 4.7 Allosteric potentiators do not compete for binding with allosteric inhibitors

(**A**) Concentration-response of UBP684 with (blue curve, n = 6 oocytes) or without (black curve, n = 7 oocytes) 5 μM UBP552, a general negative allosteric modulator at GluN2C-containing NMDARs. UBP684 response curve in presence of UBP552 was normalized to the UBP552-alone response. The dotted curve shows the expected shift in UBP684 concentration-response curve if the interaction between UBP684 and UBP552 was competitive. Data represent mean ± S.E.M. (**B**) Concentration-response of UBP684 with (green curve, n = 4 oocytes) or without (black curve, n = 7 oocytes) 100 μM of the negative allosteric modulator UBP512 at GluN2C- containing NMDARs. UBP684 response curve in presence of UBP512 was normalized to the UBP512-alone response. The dotted curve shows the expected shift in the UBP684 concentration-response curve if the interaction between UBP684 and UBP512 was competitive. Data represent mean ± S.E.M. (**C**) Concentration-response of UBP684 with (red curve, n = 5 oocytes) or without (black curve, n = 5 oocytes) 100 μM of the positive allosteric modulator UBP512 at GluN2A-containing NMDARs. The dotted curve shows the expected shift in UBP684 concentration-response curve if the interaction between UBP684 and UBP512 was competitive. Data represent mean ± S.E.M.

4.4.7 UBPs bind to both agonist-bound and agonist-unbound conformations of NMDARs

To evaluate receptor configurations to which the PAMs can bind, we performed different modes of application of these compounds to NMDARs. When UBP753 and UBP684 were pre-applied followed by agonist alone (sequential application), the response to the agonist was increased and the activation kinetics of the receptor was faster. When UBP753 was pre-applied for 30 seconds, it increased the NMDAR response to subsequent agonist application (Figure 4.8A). The time for activation, as calculated by a single exponential fit, was significantly reduced, when UBP753 was pre-applied, compared to the time for activation without pre-application (0.47 ± 0.06 s for pre-application versus 0.91 ± 0.09 s without pre-application; $p = 0.03$; n = 7-12 oocytes per group; one-way ANOVA followed by Tukey's multiple comparison test) (Figure 4.8B). However, co-application of UBP753 with agonists (without-preapplication) did not change the activation time of the receptor. Similarly, we pre-applied UBP684 (50 µM) for 30 seconds and measured NMDAR activation time (Figure 4.8A, lower panel). The sequential application of UBP684 also accelerated receptor activation kinetics (Figure 4.8C) and enhanced the amplitude of the NMDAR-mediated response (Figure 4.8D). The receptor activation time for GluN2B was 1.08 ± 0.13 s (n = 8 oocytes) in the absence of the pre-application. The pre-application of UBP684 (50 µM) significantly ($p = 0.007$, paired t-test) shortened the activation time to 0.69 ± 0.12 s (n = 8 oocytes). These results show that both UBP684 and UBP753 can bind to the closed state of the NMDAR. When UBP753 (100 µM) and the agonists were applied together, the activation time was significantly slower compared to sequential application as shown in Figure 4.8A-C. Importantly, activation was much faster than the rate of potentiation seen by UBP684/UBP753 when they were applied after obtaining a steady-state agonist response. Since UBP potentiation rate is significantly slower than the agonist activation rate, if UBP684/UBP753 only bound to the open state, then pre-and co-application and sequential application would have slower on-rate or no potentiation, respectively, compared to agonist alone.
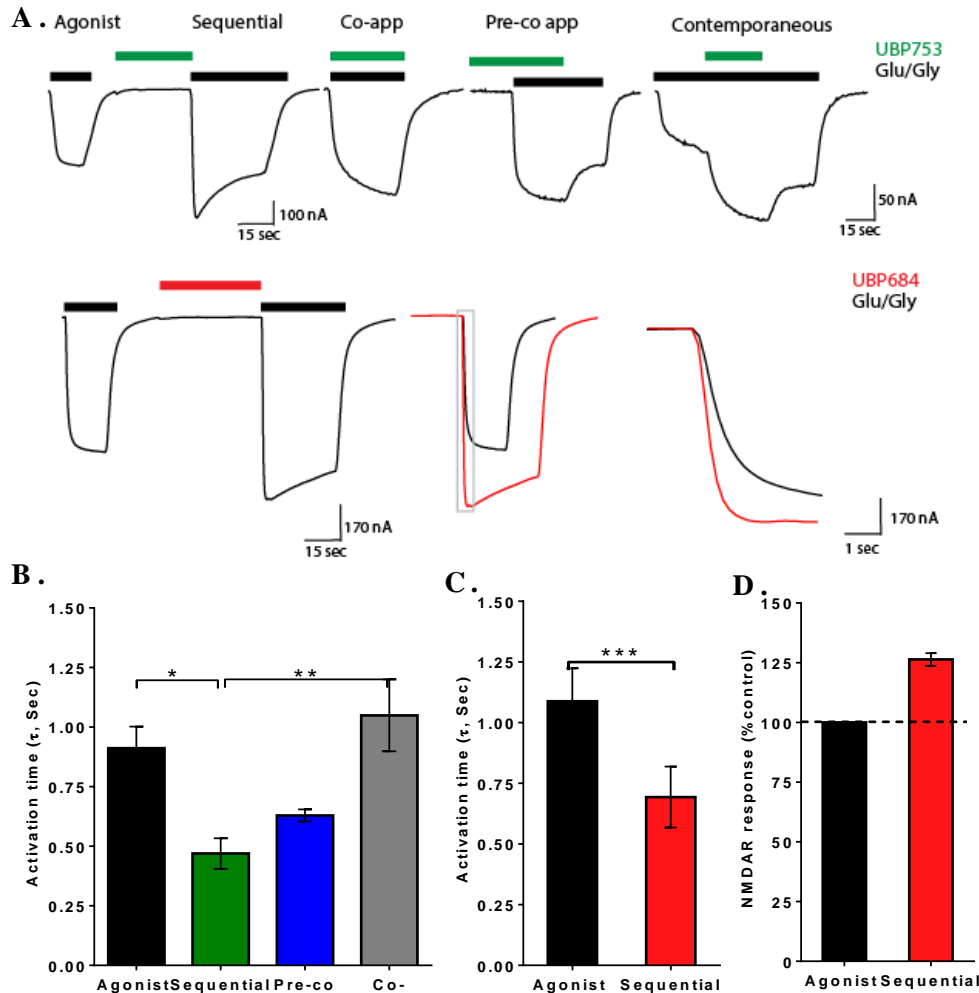
Figure 4.8 UBPs bind to both open and closed conformation of NMDARs

(**A**) Representative recordings from *Xenopus laevis* oocytes expressing GluN1/GluN2B NMDARs (top panel). Different protocols for the application of UBP753 (100 µM) were performed to evaluate its binding preference to different states of the receptors. In the sequential application, UBP753 was pre-applied for 30 sec and subsequent agonist- response (10 µM L-glutamate and 10 µM glycine) was measured. In the co-application, both of the agonists and UBP753 were applied together at the same time. In the pre-co application, UBP753 alone was pre-applied first and then UBP753 with agonists were co-applied. For the contemporaneous application, agonists were applied first to activate the receptor. After achieving the steady-state response, UBP753 along with the agonists were applied followed by agonists-alone application. Representative trace recording showing the effect of the pre-application of 50 µM of UBP684 on NMDAR activation by agonist (10 µM L-glutamate and 10 µM glycine) (lower panel). Super-imposed trace is shown in the middle and normalized trace with expanded time scale is shown on the right side of the lower panel. Scale bar: horizontal = time in sec, vertical = current in nA. (**B**, **C**) Estimation of the activation time constant (τ) by a single exponential fit for different application protocols of UBP 753 (**B**) and UBP684 (**C**). Data represent mean ± S.E.M. $^{*}p<0.05$, $^{**}p<0.01$ (one-way ANOVA followed by Tukey's multiple comparison test); $^{***}p<0.001$ (unpaired t-test). (**D**) Bar graph showing an increase in the NMDAR response after pre-application of UBP684 (50 µM) (n = 8 oocytes). Data represent mean ± S.E.M.

4.4.8   *Effect of UBP684 on NMDAR channel open probability*

To determine the mechanism of potentiation by UBP684, we sought to measure the channel open

probability (P_{open}). A conventional way of estimation of NMDAR channel open probability is the

measurement of the rate of block by the open channel blocker MK-801. Since open channel

blockers require an open channel for their binding, the rate of open channel blocking is

proportional to the open probability of the channel. Inhibition by 1 µM MK-801 was significantly

faster in the presence of 100 µM of UBP684 compared to block in the absence of UBP684

(Figure 4.9A-D). The rate of block of GluN2C receptors by MK801 in the absence of UBP684

was 3.69 ± 0.9 s (n = 3 oocytes). When 100 µM of UBP684 was pre- and co-applied with MK-

801, the rate of MK-801 block was significantly faster (1.1 ± 0.15 s; p = 0.02; unpaired t-test; n =

4 oocytes). As a control experiment, we also measured the rate of inhibition by an allosteric

inhibitor UBP792. We did not observe any significant difference on inhibition by this compound

in the presence or absence of UBP684 (Figure 4.9E). These results show that one of the

mechanisms of potentiation of NMDAR by UBP684 is by increasing the P_{open} of NMDARs.
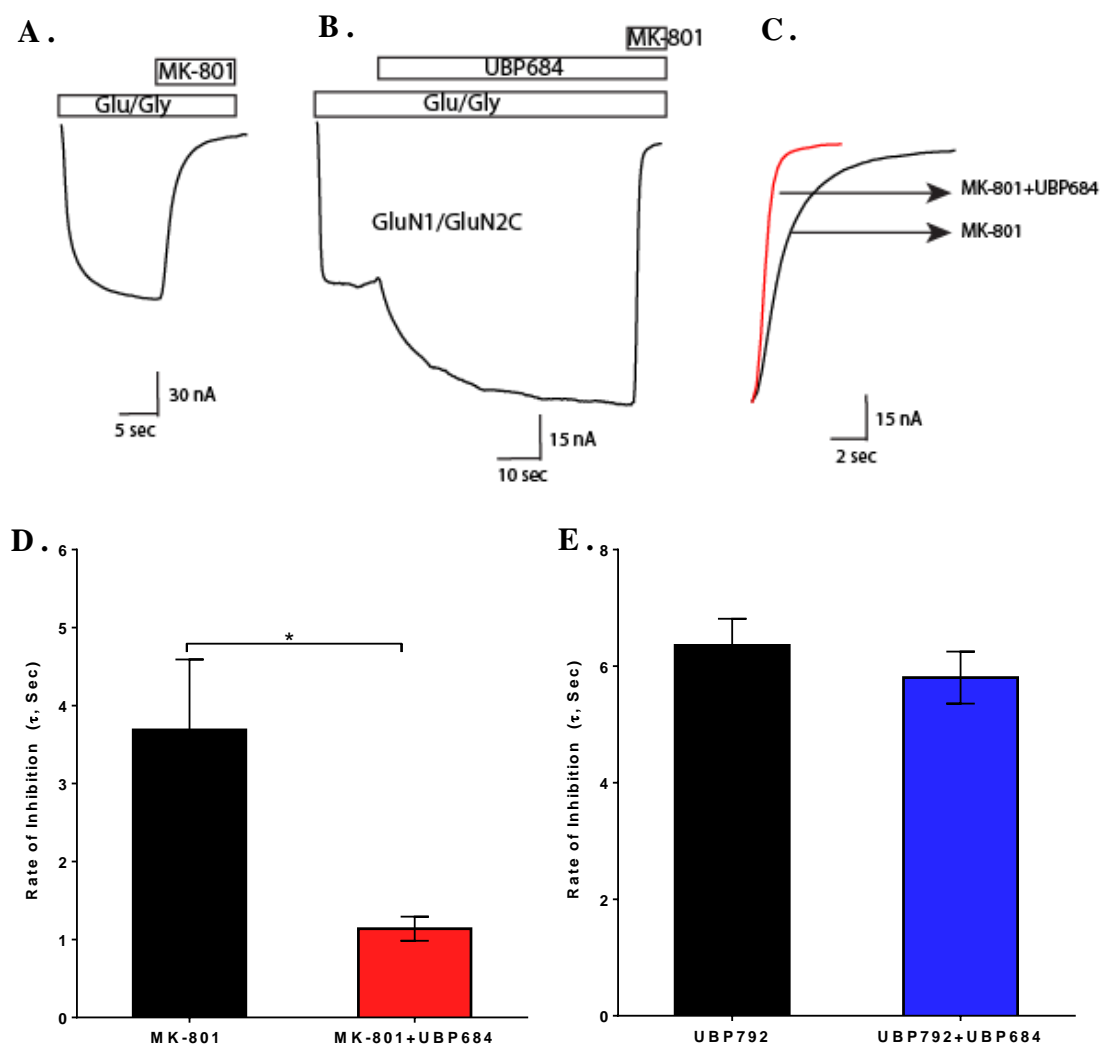
Figure 4.9 Effect of UBP684 on the channel open probability of GluN2C-containing NMDARs

(**A**) A trace from a two-electrode voltage-clamp recording showing the inhibition of an agonist-evoked (10 μM L-glutamate and 10 μM glycine) response by co-application of MK-801 (1 μM) and agonists at the GluN2C subtype of NMDARs. (**B**) Trace showing first the potentiation of the agonists-induced (10 μM L-glutamate and 10 μM glycine) response by co-application of UBP684 (100 μM) at GluN2C and then inhibition by MK-801 (1 μM) in presence of the agonists and UBP684. (**C**) Normalized trace showing the differential rate of MK-801 block in the absence (black) and the presence (red) of 100 μM of UBP684. Scale bar: horizontal = time in sec, vertical = current in nA. (**D**). Bar graph showing the rate of MK-801 block at GluN2C receptors by 1 μM of MK-801 in the presence (red bar; n = 4 oocytes) and in the absence (black bar; n = 3 oocytes) of 100 μM UBP684. Rate of inhibition by MK-801 was obtained from a single exponential function. Data represent mean ± S.E.M. $^{*}p<0.05$ (unpaired t-test). (**E**) Rate of inhibition by 10 μM of UBP792, a novel NMDAR NAM, in presence (blue bar, n = 6 oocytes) or absence (black bar, n = 6 oocytes) of UBP684. Data represent mean ± S.E.M.

4.4.9   UBP684 slows receptor deactivation following the removal of agonist

One possible mechanism of enhanced activity by UBP684 / UBP753 could be by prolonging the deactivation of the receptors. We investigated the effect of UBP684 and UBP753 on deactivation of GluN2D-containing receptors expressed in *Xenopus laevis* oocytes since GluN2D receptors have a remarkably slow deactivation time. The deactivation of the receptors in the constant presence of 50 µM of UBP684 was significantly slower as shown in Figure 4.10A. Deactivation time was 9.6 ± 1.6 s (n = 11 oocytes) in the presence of UBP684 which was significantly slower than the control (4.1 ± 0.6 s; n = 23 oocytes). Although there was a trend for prolonged deactivation by UBP753, it was not significant. The reason behind prolong deactivation by UBP684 might be due to slowing down the unbinding of one or both of the agonists from the receptors. We then investigated the effect of UBP684 on the deactivation time of individual agonists. We studied the dissociation/deactivation of glycine by washing out glycine in the continued presence of the PAM and L-glutamate. We did not observe any significant effect of either UBP684 or UBP753 on glycine dissociation/deactivation time (Figure 4.10B). However, using the same approach, we find that UBP684 significantly slowed the dissociation/deactivation time for L-glutamate (Figure 4.10C). Time for deactivation after L-glutamate removal from GluN2D-containing NMDARs in absence of UBP684 was 9.6 ± 1.7 s (n = 6 oocytes) and in presence of UBP684 was 20.2 ± 4.1 s (n = 7 oocytes) and the difference was significant ($p = 0.04$; one-way ANOVA, followed by Bonferroni's multiple comparison test). Interestingly, UBP753 did not have any significant effect on dissociation time of either agonists.
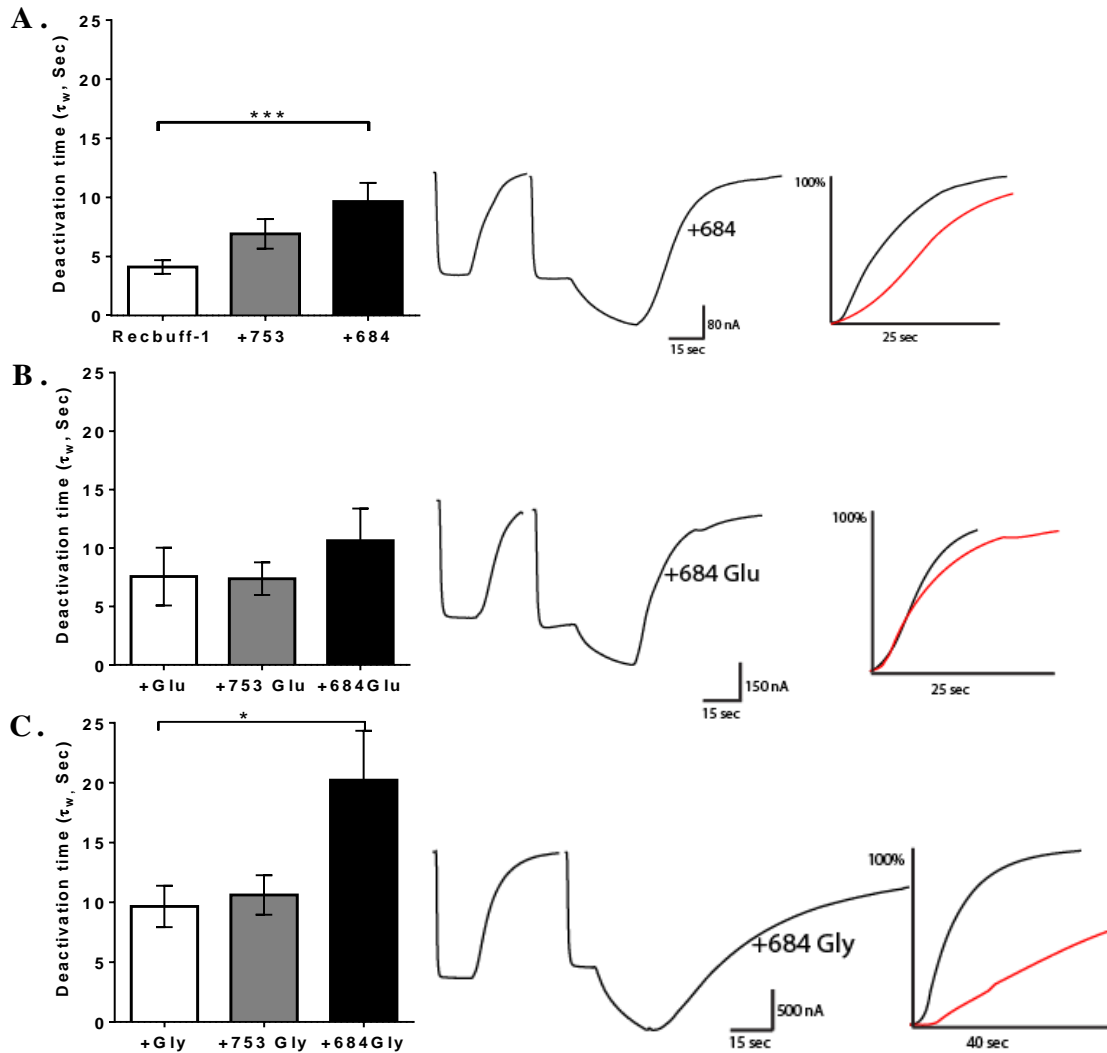
Figure 4.10 UBP684 slows the deactivation time of NMDARs

(**A**) Receptor deactivation time was studied by removing agonists (10 µM L-glutamate or10 µM glycine) after obtaining GluN1-1a/GluN2D steady-state response with /without UBP753 (50 µM) or UBP684 (50 µM). The deactivation time constant was obtained by a two-component exponential function. A representative trace of agonist dissociation in presence of UBP684 is shown in the middle and the super-imposed, normalized trace with (red) and without (black) UBP684 deactivation component is shown on the right (n = 7-15 oocytes per group). Data represent mean ± S.E.M. ***p<0.001 (one-way ANOVA followed by Bonferroni's multiple comparison test). (**B**) Deactivation time for glycine removal was studied in presence of the corresponding PAM and L-glutamate. Traces in the middle show the dissociation/deactivation kinetics of glycine and the trace on the right is the normalized trace of the dissociation component (with UBP684, red; without UBP684, black; n = 5 oocytes per group). Data represent mean ± S.E.M. (**C**) The deactivation time for L-glutamate removal in the presence of glycine and in presence/absence of UBP 684 or UBP753. The trace in the middle shows the dissociation/deactivation kinetics following L-glutamate removal and the trace on the right is the normalized trace of the deactivation kinetics (n = 6-7 oocytes per group). Scale bar: horizontal = time in sec, vertical = current in nA. Data represent mean ± S.E.M. *p<0.05 (one-way ANOVA followed by Bonferroni's multiple comparison test).

4.4.10   UBP684 potentiation is affected by the conformation of ligand binding domain of the GluN2 subunit

By introducing the two cysteine mutations in each ligand binding domain of GluN1 or GluN2A subunits, two NMDAR constructs with disulfide bridges were created which constrain the respective LBDs in the closed-cleft conformation and mimic the glycine-bound conformation of the LBD of GluN1 or the L-glutamate-bound conformation of the LBD of GluN2A-containing NMDARs. By co-expression of the disulfide crosslinked GluN1^c with the wildtype GluN2A or wildtype GluN1 with crosslinked GluN2A^c in *Xenopus laevis* oocytes, we evaluated the effect of constrained LBDs on UBP753 potentiation. Similar to the finding by Kussius and Popescu (Kussius, Popescu 2010), we confirmed that the receptors containing GluN1^c, which mimic the glycine bound conformation, were activated by L-glutamate alone and not by glycine alone. Also, the receptors containing GluN2A^c, which mimic the L-glutamate bound conformation, were activated by glycine and not by glutamate. Interestingly, the potentiation by UBP753 of GluN1^c containing GluN2A receptors was almost similar to that of wild type GluN2A receptors. However, the potentiation by UBP753 at GluN2A^c containing receptor was significantly reduced ([****]$p < 0.0001$, one-way ANOVA followed by Tukey's multiple comparison test) compared to the WT GluN2A receptors or GluN1^c containing GluN2A receptors as shown in Figure 4.11A. The potentiation by 100 µM of UBP753 at WT GluN2A, GluN1^c containing receptor and GluN2A^c containing was 51.3 ± 3.7 % (n = 17 oocytes), 39.4 ± 6.5 % (n = 9 oocytes), and 6.3 ± 1.4 % (n = 17 oocytes) respectively (Figure 4.11B). These results suggest that the mechanism of potentiation by UBP753 is by stabilizing the glutamate bound confirmation of GluN2 receptors.
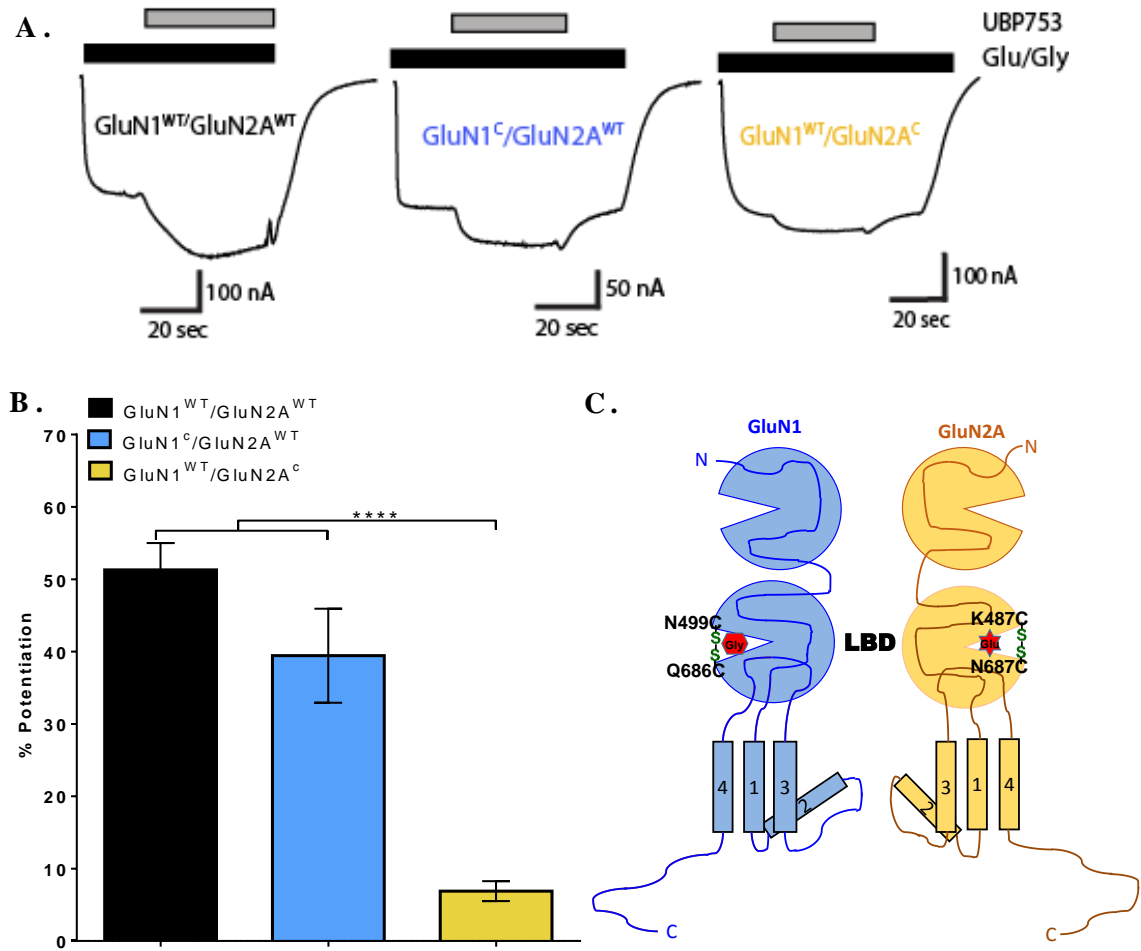
Figure 4.11 Effect of the LBD cleft conformation on potentiation by UBP753

(**A**) Representative recordings showing the effect of UBP753 (100 μM) on wildtype (GluN1/GluN2A), GluN1 LBD-locked (GluN1^c/GluN2A) and GluN2A LBD-locked (GluN1/GluN2A^c) NMDARs expressed in *Xenopus laevis* oocytes. Scale bar: horizontal = time in sec, vertical = current in nA. (**B**) A bar graph showing UBP753 potentiation of agonist-induced (10 μM L-glutamate and 10 μM glycine) response from oocytes expressing WT (n = 17 oocytes), GluN1 LBD-locked (n = 9 oocytes) and GluN2A LBD-locked (n = 16 oocytes) receptors. (**C**) Schematic showing the two cysteine point mutations in the LBD region of GluN1 (N499C and Q686C) leading to the glycine binding site-locked conformation and in the LBD of GluN2A (K487C and N687C) leading to the L-glutamate binding site-locked conformation. Data represent mean ± S.E.M. ****p<0.0001 (one-way ANOVA followed by Tukey's multiple comparison test).

4.4.11   *Effect of extracellular pH on NMDAR activity of UBP684 at GluN2A-D subtypes of NMDARs*

In pathological conditions, there is a change in extracellular pH in the brain's extracellular space, which can affect the function of allosteric modulators either making them more or less effective (Mott, Doherty et al. 1998, Pahk, Williams 1997). To predict how such conditions would affect PAM activity, we measured the effect of pH on the potentiating activity of UBP684 on GluN2A-, GluN2B-, GluN2C-, and GluN2D-containing NMDARs. Interestingly, the potentiating activity of UBP684 was eliminated at pH 8.4 and instead, it displayed NMDAR inhibitory activity in a subunit-dependent manner (Figure 4.12). At pH 7.4, UBP684 (100 μM) potentiated GluN2A-, GluN2B-, GluN2C-, and GluN2D-containing NMDARs by 64.6 ± 4.1 % (n = 16 oocytes), 83.3 ± 7.4 % (n = 14 oocytes), 96.9 ± 5.2 % (n = 23 oocytes), and 67.4 ± 6.6 % (n = 10 oocytes) respectively. In contrast, at pH 8.4, UBP684 inhibited the GluN2A-, GluN2B-, GluN2C- and GluN2D-containing NMDARs by 6.2 ± 1.0 % (n = 9 oocytes), 13.5 ± 1.8 % (n = 7 oocytes), 32.9 ± 2.8 % (n = 6 oocytes), and 55.7 ± 6.5 % (n = 6 oocytes) respectively. Thus, at alkaline pH, UBP684 becomes most inhibitory at GluN2D-containing receptors and least inhibitory at GluN2A-containing NMDARs. This result implies that proton inhibition might be necessary for the potentiating activity of UBP684.
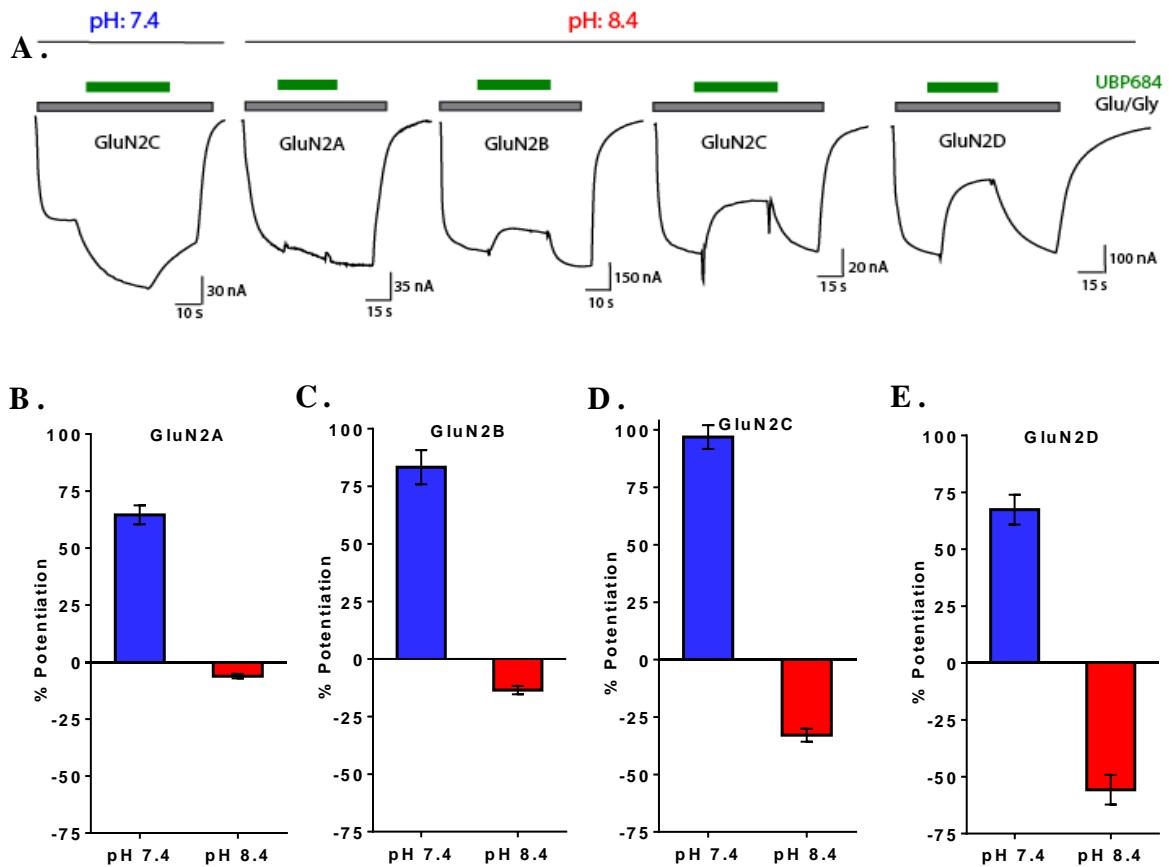
Figure 4.12 Effect of extracellular pH on NMDAR activity of UBP684 at GluN2A-D subtypes of NMDARs expressed in *Xenopus laevis* oocytes

(**A**) Representative current traces showing the effect of extracellular pH (7.4 and 8.4) on UBP684 activity, as measured by TEVC, at recombinant GluN1/GluN2A-D receptors expressed in *Xenopus laevis* oocytes. Currents were first evoked by 10 μM L-glutamate and 10 μM glycine and after achieving a steady-state, UBP684 (100 μM) was co-applied with the agonists. Scale bars: horizontal = time in sec and vertical = current in nA. (**B**, **C**, **D**, **E**) The NMDAR-mediated activity modulated by UBP684 at GluN2A (**B**; n => 9 oocytes), GluN2B (**C**; n => 7 oocytes), GluN2C (**D**; n => 6 oocytes) and GluN2D (**E**; n => 6 oocytes) was measured at extracellular pH of 7.4 and 8.4 from the same oocytes and the response was expressed as % potentiation above the agonist-alone induced response. Bar graphs above zero represent the % potentiation at pH 7.4 (blue bars) and below zero represent the % inhibition compared to agonist-alone when tested at pH 7.4 (blue) or pH 8.4 (red). Data represent mean ± S.E.M.

4.4.12   Effect of extracellular pH on NMDAR-mediated activity of UBP753 at the GluN2C subtype of NMDARs

We also tested if pH affects the potentiating activity of UBP753. We determined the effect of different pH conditions (acidic, physiological and alkaline) on potentiation by UBP753 (50 µM) at GluN2C-containing receptors. UBP753 potentiated the NMDAR response at the pH of 6.4 and 7.4 (163.3 ± 10.2 %, n = 14 oocytes; pH 6.4 and 102.4 ± 6.7 %, n =15 oocytes; pH 7.4) (Figure 4.13). Like UBP684, this compound also displayed NMDAR inhibitory activity in the alkaline pH condition (% inhibition was 30.5 ± 3.2, n = 16 oocytes; pH: 8.4). A sigmoidal fit of the data from these three pH conditions estimates that the compound switches between potentiation and inhibition at pH ~ 8.0 (Figure 4.13).
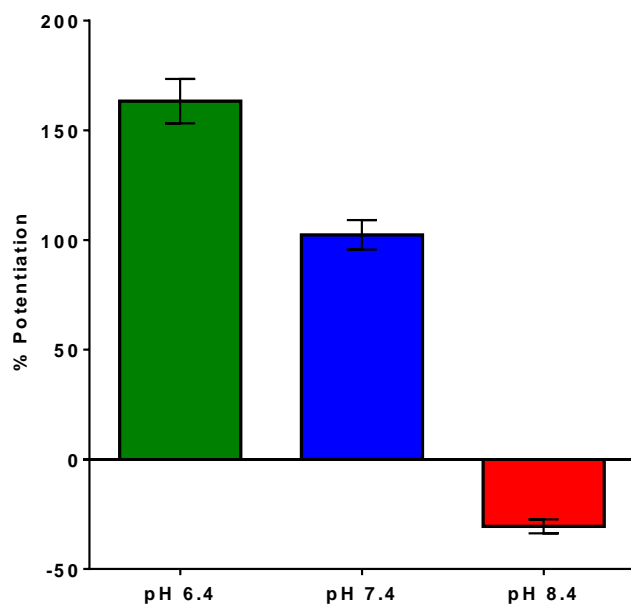
Figure 4.13 Effect of extracellular pH on UBP753 activity at the GluN2C subtype of NMDARs

UBP753 (50 µM) was tested at different pH conditions to study the effect of protons on its activity. Values above zero are % potentiation and below zero is % inhibition of the agonist-evoked response. n = > 14 oocytes; data represent mean ± S.E.M.

4.4.13 *Effect of UBP684 on the concentration-response of H⁺ inhibition at NMDARs*

We next wanted to determine if compounds are affecting the sensitivity of the NMDARs for

proton inhibition. We performed the concentration-response study with increasing concentrations

of protons on GluN2B- and GluN2D-containing NMDARs in presence and absence of 50 μM

UBP684. We found that UBP684 reduced H⁺ sensitivity at both GluN2B- and GluN2D-

containing NMDARs. There was a right shift on both of the curves in the presence of UBP684

(Figure 4.14). Proton inhibition at the GluN2D receptor was more affected than that at GluN2B-

containing receptors in the presence of UBP684.
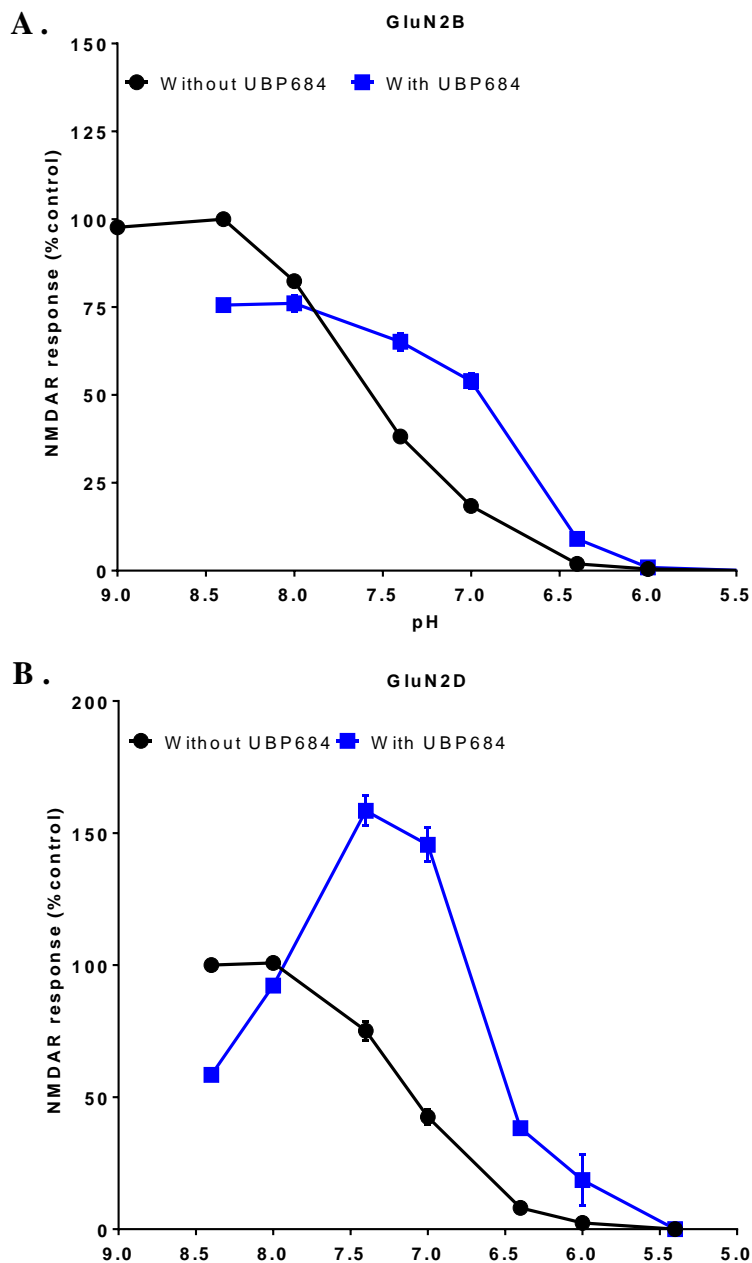
Figure 4.14 Effect of UBP684 on H$^+$ inhibition at GluN2B and GluN2D subtypes of NMDARs

(**A**, **B**) Effect of UBP684 (50 μM) on proton inhibition was studied on GluN2B- (**A**) and GluN2D- (**B**) containing NMDARs. NMDAR responses were measured with increasing concentrations of protons in absence (black curve; n = 8 oocytes, GluN2B; n = 12 oocytes, GluN2D) or presence (blue curve; n = 10 oocytes for GluN2B; n = 11 oocytes for GluN2D) of UBP684. Data from each oocyte was normalized to the NMDAR response obtained at pH 8.5 in absence of UBP684 from same oocyte. Data are mean ± S.E.M.

4.4.14   Effect of different GluN1 splice forms on UBP684-mediated changes in proton sensitivity at GluN2D receptors

These findings suggest that the mechanism of potentiation by UBP684 may be due to relief of proton inhibition. To evaluate this possibility, we compared the activity of UBP684 at GluN2D receptors co-expressed with GluN1 having exon-5 (GluN1-1b) to the activity at GluN2D receptors co-expressed with GluN1 lacking exon-5 (GluN1-1a). The exon-5 segment codes for an extra 21-amino acid sequence, which reduces the proton-sensitivity to the N-terminal domain (NTD) proton sensor site. Although, UBP684 significantly reduced proton sensitivity, we did not observe any change in the potentiating activity of UBP684 at GluN2D receptors containing GluN1-1a or GluN1-1b variants at all pH conditions tested (Figure 4.15 A) and UBP684 potentiated both variants with almost equal affinity and maximal effect (Figure 4.15 B). The EC_{50} values for UBP684 potentiation at GluN1-1a- or GluN1-1b-containing GluN2D receptors were 29.9 ± 6.5 μM (% E_{Max} = 68.6 ± 9.2, n = 6 oocytes) and 28.3 ± 6.1 μM (% E_{Max} = 67.8 ± 7.8, n = 5 oocytes) respectively, under physiologic pH conditions. However, in an alkaline pH condition, UBP684 inhibited GluN2D receptors with either GluN1-1a or GluN1-1b splice forms. The affinity for UBP684 inhibition at GluN1-1b-containing GluN2D receptors was slightly higher than the GluN1-1a-containing GluN2D receptors as shown by slight leftward shift in the concentration-response curve (Figure 4.15C). The IC_{50}s of UBP684 at GluN1-1a- and GluN1-1b-containing GluN2D receptors were 23.0 ± 3.2 μM (n = 4 oocytes, % I_{Max} = 69.8 ± 6.4) and 17.0 ± 2.7 μM (n = 5 oocytes, % I_{Max} = 73.8 ± 3.1) respectively, under the alkaline pH condition. These findings show that both the affinity and the % E_{Max} (or % I_{Max}) were not significantly changed by the presence of the GluN1 splice forms. Spermine is a GluN2B potentiator at physiological pH and becomes an inhibitor at alkaline pH. However, its responses to GluN1-1a and GluN1-1b are different. Thus, the requirement of protons for the potentiating activity of UBP684 is different from the requirement of protons for the potentiating activity of spermine.
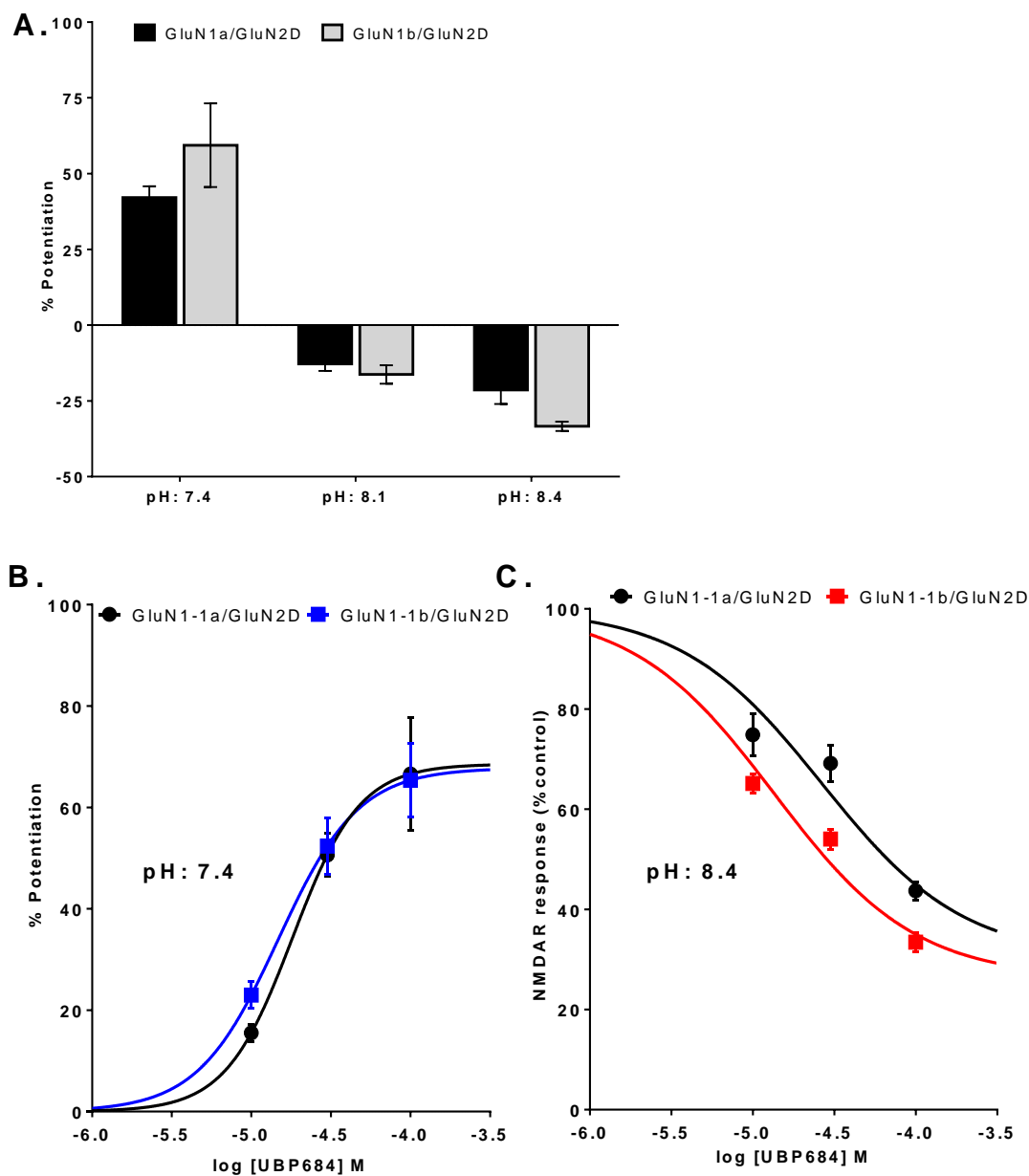
Figure 4.15 Effect of GluN1 splice variants on UBP684-mediated change in proton sensitivity at GluN2D receptors

(**A**) NMDAR activity was measured at GluN2D-containing receptors co-expressed with either GluN1 subunit without exon-5 (GluN1-1a; black bar) or with exon-5 (GluN1-1b; grey bar) in *Xenopus laevis* oocytes. Potentiation by 50 μM UBP684 was determined at different pH (7.4, 8.1, 8.4). Values above zero represent the % potentiation and below zero are % inhibition, n = 5-7 oocytes. (**B**) At pH 7.4, the effect of increasing concentrations of UBP684 on its potentiating activity at GluN2D- containing NMDARs co-expressed with either GluN1-1a (black; n = 6 oocytes) or with GluN1-1b (blue; n = 5 oocytes) was studied. (**C**) At pH 8.4, the effect of increasing concentrations of UBP684 on inhibitory activity at GluN2D-containing NMDARs co-expressed with either GluN1-1a (black; n = 5 oocytes) or with GluN1-1b (red; n = 5 oocytes) was measured. Data represent mean ± S.E.M.

4.4.15   *Effect of pH on potentiating activity of other known NMDAR PAMs*

The effect of protons we observed on the potentiating activity of UBP684/UBP753 led us to test for similar effects on the activity of other NMDAR PAMs. Pregnenolone sulfate (PS)-induced potentiation at both GluN2A- and GluN2B-containing NMDARs was reduced at alkaline pH. At a physiological pH of 7.4, PS (100 μM) potentiated GluN2A and GluN2B receptor activity by 95.6 ± 10.2 % (n = 12 oocytes) and 140.6 ± 20.0 % (n = 9 oocytes) respectively. At pH 8.4, the potentiation was significantly reduced to 49.7 % $\pm$ 6.7 (n = 9 oocytes) at GluN2A and 81.3 ± 10.1 (n = 8 oocytes) at GluN2B-containing NMDARs (Figure 4.16A). Similarly, we measured the activity of CIQ, a GluN2C/GluN2D-selective potentiator, at physiologic and alkaline pH. The alkaline pH condition significantly reduced the potentiating activity by 30 μM CIQ at GluN2C-containing NMDARs (54.7 ± 4.8 %; n = 13 oocytes at pH 7.4 *vs* 20.3 ± 1.7 %; n = 11 oocytes at pH 8.4) (Figure 4.16B). Although there was some reduction in the potentiating activity of both PS and CIQ at NMDARs, they were able to maintain the potentiating activity in the alkaline pH condition. However, GNE-8324, a GluN2A-specific potentiator, became an inhibitor at alkaline pH, which was similar to the activity that we observed for UBP684 and UBP753. GNE-6834 potentiated at GluN2A-containing receptors by 32.3 ± 2.6 % (n = 17) at pH 7.4 and inhibited the receptors by 5.6 ± 1.6 % (n = 16) at pH 8.4 (Figure 4.16 C). This finding suggests that GNE-8324 and UBP684 or UBP753 may share similar mechanisms of potentiation of NMDAR response.
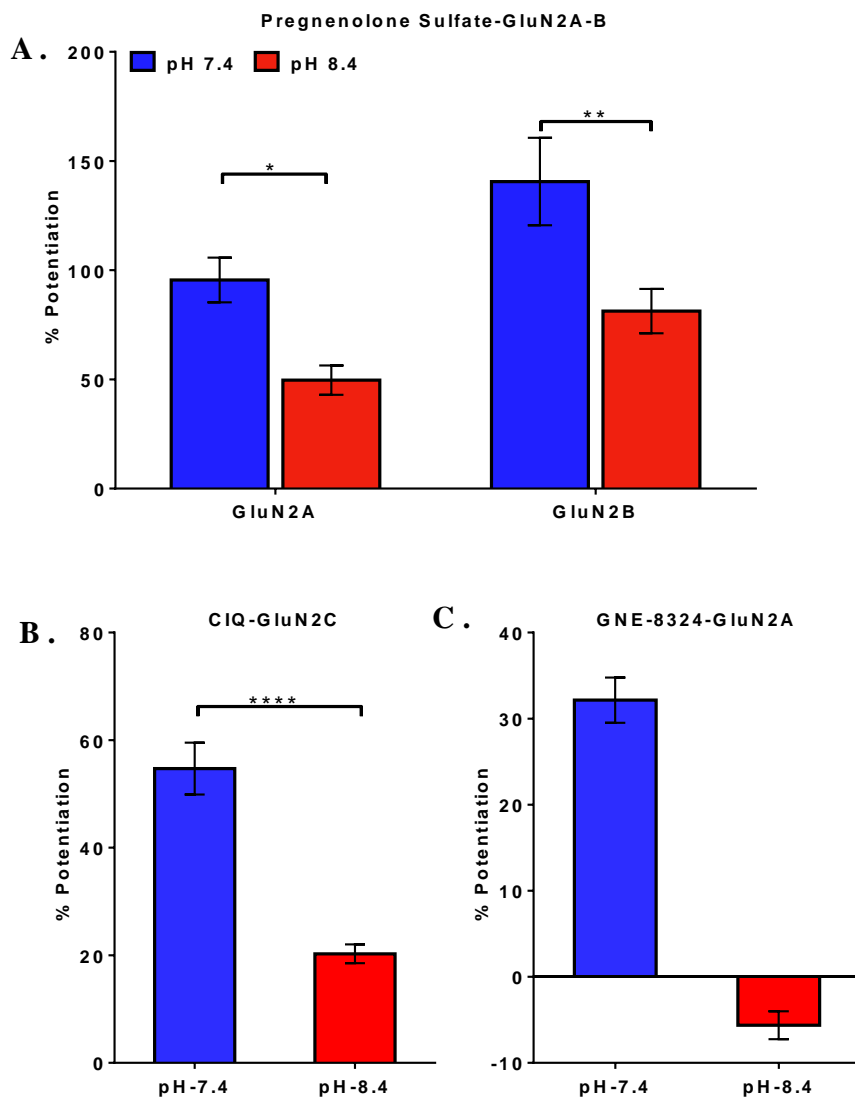
Figure 4.16 Effect of extracellular pH on the potentiating activity of other NMDAR PAMs

(**A**) The effect of pH on the enhancement of agonist-evoked (10 μM L-glutamate and 10 μM glycine) responses by pregnenolone sulfate (100 μM) at GluN2A and GluN2B subtypes of NMDARs expressed in *Xenopus laevis* oocytes. Pregnenolone sulfate-induced NMDAR current potentiation was studied at pH 7.4 (blue bars) and pH 8.4 (red bars) (n = > 8 oocytes for each bar). Data represent mean ± S.E.M. *p<0.05, **p<0.01. (**B**) Effect of pH on potentiation by 30 μM CIQ (a GluN2C/GluN2D-selective positive allosteric modulator of NMDARs) at GluN2C NMDARs (n = 11 oocytes). Data represent mean ± S.E.M. ****p<0.0001. (**C**) Effect of pH on potentiation by 30 μM GNE-8324 (a GluN2A-selective positive allosteric modulator of NMDARs) of NMDAR-mediated activity at GluN2A NMDARs. Values below zero represent % inhibition of agonist-induced responses (n = 15 oocytes). Data represent mean ± S.E.M.

4.4.16   Effect of GluN1 or GluN2A C-terminal truncation on the potentiating activity of UBP684 and pregnenolone sulfate

We then sought to determine role of the C-terminal on the potentiating activity of UBP684 since the C-terminal can control the gating of the NMDAR channel. Also, it has been reported that the phosphorylation state of the C-terminal is necessary for PS potentiation. We measured the potentiating activity of UBP684 (100 µM) at GluN2A-containing NMDARs with or without the C-terminal of either GluN1 or GluN2 subunits. The C-terminal deletion was achieved by introducing the stop codons at K838 of GluN1-1a (GluN1$^{\Delta ct}$) and K844 of GluN2A subunits (GluN2A$^{\Delta ct}$). We observed a significant reduction ($p = 0.0002$, one-way ANOVA followed by Bonferroni's multiple comparison test) on the potentiating activity of UBP684 at GluN2A receptors co-expressed with GluN1 having truncated C-terminal. However, there was no significant change in the potentiating activity of UBP684 at GluN2A subunits with the C-terminal truncation. The potentiation by UBP684 at GluN2A-WT, GluN1$^{\Delta ct}$/GluN2A, and GluN2A $^{\Delta ct}$ were 36.0 ± 4.7 % (n = 13 oocytes), 8.4 ± 2.1 % (n = 13 oocytes), and 25.2 ± 5.4 % (n = 12 oocytes) respectively (Figure 4.17A). In contrast to the activity of UBP684, the potentiating activity of pregnenolone sulfate at these receptors was opposite. GluN1 C-terminal truncation did not change the potentiating activity of 100 µM of PS at GluN2A-containing receptors. However, the C-terminal truncation from GluN2A subunit eliminated the potentiating activity of PS and converted it into an inhibitor. The potentiation by PS at WT GluN2A and GluN1$^{\Delta ct}$/GluN2A was 35.4 ± 6.8 % (n = 16 oocytes), and 32.0 ± 6.2 % (n = 14 oocytes) respectively and the difference was not statistically significant. However, PS was an inhibitor at NMDARs containing GluN2A $^{\Delta ct}$, and GluN1$^{\Delta ct}$/ GluN2A $^{\Delta ct}$ subunits. PS inhibited the GluN2A $^{\Delta ct}$, and GluN1$^{\Delta ct}$/ GluN2A $^{\Delta ct}$ subunit-containing NMDARs by 45.0 ± 3.0 % (n = 11 oocytes) and 55.0 ± 2.0 % (n = 4 oocytes) respectively (Figure 4.17 B). These results indicate that the C-terminal of GluN2A receptors is required for the potentiating activity of PS.
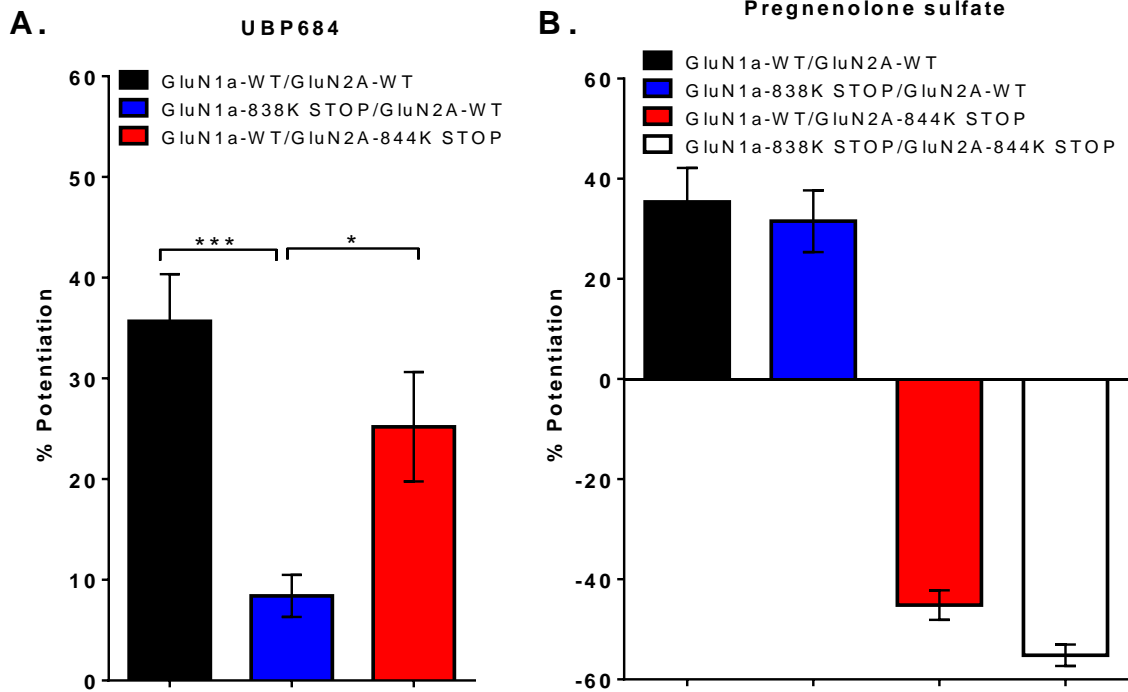
Figure 4.17 Effect of GluN1 or GluN2A C-terminal truncation on the potentiating activity of UBP684 and pregnenolone sulfate

(**A**) NMDARs truncated at K838 on GluN1-1a or K844 on GluN2A were expressed in *Xenopus laevis* oocytes and tested for potentiation by 100 μM UBP684 as indicated (n = 12 -13 oocytes). Data represent mean ± S.E.M. *p<0.05, ***p<0.001 (one-way ANOVA followed by Tukey's multiple comparison test). (**B**) Effect of C-terminal deletion from GluN1-1a and/or GluN2A was also tested for potentiating activity by 100 μM pregnenolone sulfate (n = 11-16 oocytes for WT and single truncation, n = 4 for double truncation). Data represent mean ± S.E.M.

4.4.17   *Effect of intracellular calcium on the potentiating activity of UBP684 at GluN2A- and GluN2B-containing NMDARs*

In the previous section, we found that the intracellular portion of the C-terminal can have a profound effect on PAM activity. Thus, intracellular factors may potentially alter PAM sensitivity. One of the intracellular factors to control the PAM activity may be Ca^{2+}. Intracellular calcium plays an important role in regulating NMDAR function. Similarly, receptor phosphorylation could also be changing PAM sensitivity as reported for PS. To study the effect of Ca^{2+} on the potentiating activity of UBP684, we removed intracellular Ca^{2+} from oocytes expressing GluN2A and GluN2B receptors by injecting a Ca^{2+} chelator (EGTA) and examined the UBP684 activity with reduced intracellular Ca^{2+} levels. We used two agonist-application paradigms: Sequential and contemporaneous. In the sequential application, UBP684 was applied first for 30 sec and the subsequent agonist-evoked response was measured and compared to the agonist-alone response before UBP684 application. In the contemporaneous application, we first activated receptors with agonists and then UBP684 was co-applied with agonists and the response obtained with co-application was compared with the agonist-alone induced response before the co-application. The sequential application of UBP684 (50 μM) enhanced the agonist-induced response by 15.3 ± 2.5 % (n = 9 oocytes) in water injected and by 1.7 ± 1.5 % (n = 13 oocytes) in the EGTA injected GluN2A oocytes (Figure 4.18A). The sequential application of UBP684 (50 μM) potentiated the agonist-induced response by 40.3 ± 5.5 % (n = 8 oocytes) in water-injected oocytes and by 30.0 ± 3.5 % (n = 10 oocytes) in the EGTA-injected GluN2B-expressing oocytes (Figure 4.18B). Similarly, the contemporaneous application of UBP684 (50 μM) in GluN2A receptors expressing oocytes potentiated the agonist response by 34.0 ± 13.0 % (n = 8 oocytes) in water-injected control oocytes and by 9.2 ± 2.7 % (n = 19 oocytes) in the EGTA-injected oocytes (Figure 4.18A). In GluN2B expressing oocytes, the contemporaneous application of UBP684 (50 μM) potentiated the agonist-induced response by 49.2 ± 7.5 % (n = 11 oocytes) in water-injected control oocytes and by 32.1 ± 2.2 % (n = 10 oocytes) in the EGTA-injected oocytes (Figure 4.18B)
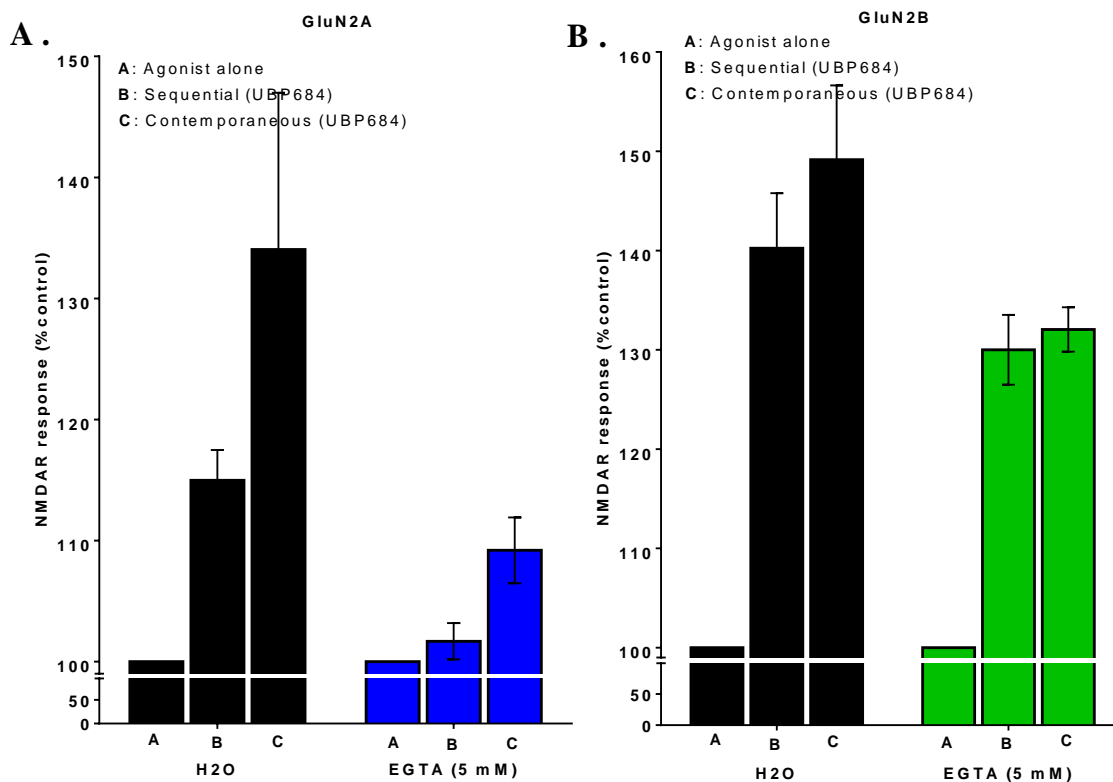
Figure 4.18 Effect of intracellular calcium on the potentiating activity of UBP684 at GluN2A-and GluN2B-containing NMDARs

(**A**) *Xenopus laevis* oocytes expressing GluN2A NMDARs were pre-injected with 100 nL of water as a control (black bar) or 100 nL of 5 mM of the EGTA (Ca^{2+} chelator; blue bar) and incubated in ND-96 for 2-3 h at 17 °C. Responses are shown for agonist-alone (10 μM L-glutamate and 10 μM glycine; bar A), agonist response following a 30-second pre-application of 50 μM of UBP684 (bar B; sequential application) or the agonist response when co-applied with UBP684 (Bar C) after obtaining an agonist-alone steady-state response (n = 8-19 oocytes). (**B**) Using similar methods as that for GluN2A, the effect of chelating intracellular Ca^{2+} with 5 mM of EGTA on the potentiating activity of UBP684 was studied on GluN2B-containing receptors. n = 8-16 oocytes in each group, data represent mean ± S.E.M.

4.4.18   *Effect of PKC activation on the potentiating activity of UBP753 and PS at GluN2B-containing NMDARs*

Since the removal of intracellular calcium by injecting EGTA reduced the potentiating activity of UBP684, we studied the effect of PKC on PAM activity of UBP753 to determine if reduced potentiation could potentially be due to blocking PKC dependent phosphorylation. We measured the potentiation by UBP753 (100 µM) and PS (100 µM) before and after the treatment of oocytes with PMA (2 µM), a PKC activator, for 10 minutes. PKC treatment significantly increased the UBP753-induced potentiation at GluN2B-containing NMDARs. UBP753 potentiated the GluN2B receptors mediated response by 141.0 ± 15.0 % (n = 6 oocytes) before and by 234.0 ± 45.0 % (n = 6 oocytes) after the PMA treatment (Figure 4.19A). However, the PMA treatment did not cause any change on potentiation by PS at GluN2B-containing NMDARs. The PS potentiated the NMDAR response by 79.0 ± 7.0 % (n = 5 oocytes) before and by 75.3 ± 8.4 % (n = 5 oocytes) after the treatment with PMA (Figure 4.19B). These results show that UBP753 activity is enhanced by PKC phosphorylation while PS activity is not dependent on PKC phosphorylation.
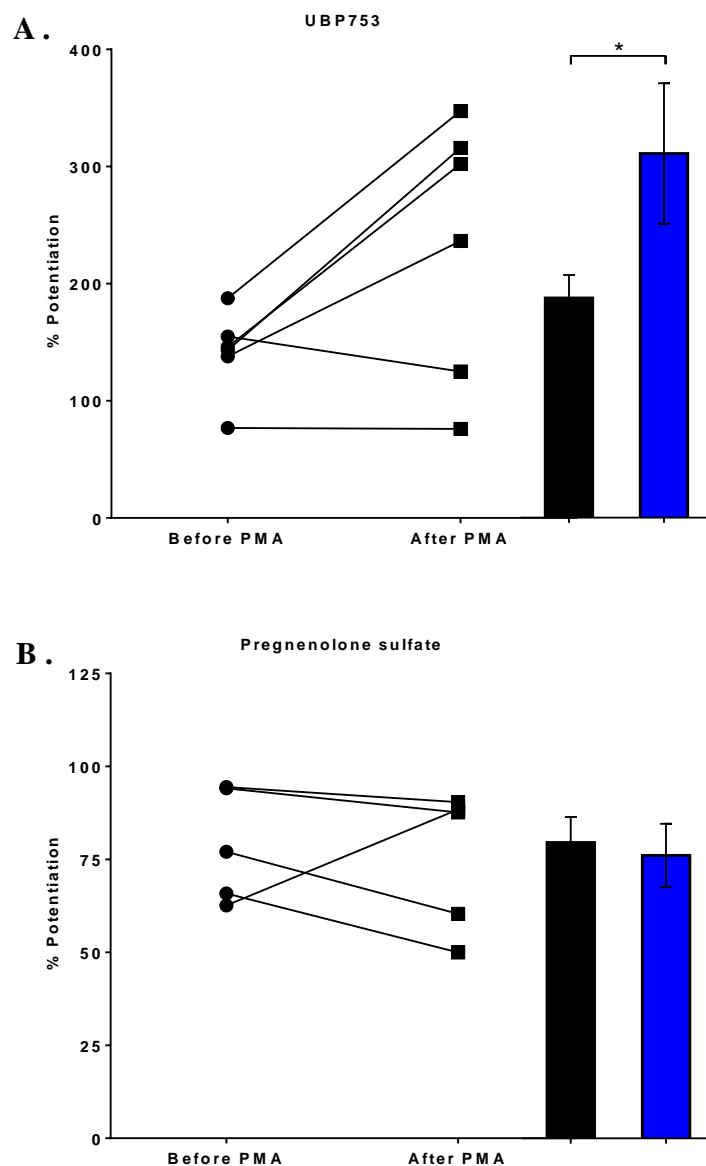
Figure 4.19 Effect of the PKC activation on the potentiating activity of UBP753 and PS at GluN2B-containing NMDARs

(**A**) After obtaining a stable agonist response with 10 μM L-glutamate and 10 μM glycine at GluN1-1a/GluN2B receptors, UBP753 (100 μM) was co-applied. Then, the same oocytes were treated with 2 μM of the PMA (PKC activator) for 10 minutes by bath perfusion and UBP753-induced potentiation was measured again. This UBP753-induced enhancement of the responses was compared to the potentiation produced before the PMA treatment (n = 6 oocytes). Data represent mean ± S.E.M, *p<0.005 (paired t-test). (**B**) The effect of PKC activation on the activity of pregnenolone sulfate was determined as in A by measuring agonist-induced responses before and after PMA treatment (n = 5 oocytes). Data represent mean ± S.E.M.

4.5   Discussion

Our laboratory previously has reported various NMDARs PAMs with different patterns of subunit selectivity. UBP512, a phenanthrene derivative, selectively potentiated GluN2A, did not have any effect on GluN2B, and inhibited GluN2C and GluN2D subtypes of NMDARs (Costa, Irvine et al. 2010). UBP710 selectively potentiated GluN2A and GluN2B and UBP551 selectively potentiated GluN2D and inhibited the other NMDAR subtypes (Costa, Irvine et al. 2010). Although these PAMs were selective, they did not exhibit a high magnitude of potentiation and were not highly potent. In attempt to identify general NMDAR PAMs, we recently have identified two compounds with NMDAR PAM activity, UBP684 and UBP753, which show greater efficacy and potency at NMDARs than our previously reported PAMs. Both of these compounds showed potentiating activity across all subtypes of NMDARs. These are the most-effective general NMDAR PAMs reported to date.

Since, during synaptic neurotransmission, there is a high level of glutamate release, it is important to know if UBP684 and UBP753 retain their PAM activity in the presence of saturating agonist concentration. We found that these compounds were able to potentiate all NMDAR subtypes in the presence of high agonist concentration (Figure 4.2). Consistent with this finding, these compounds increased glutamate and glycine efficacy with minimal effects on agonist affinity. There was a small reduction in potentiation by UBP684 at GluN2A and GluN2B receptors at high agonist concentration (Figure 4.3) which is consistent with the previous report that potentiation by PS at GluN2B receptors is reduced in presence of 1 mM glutamate (Horak, Vlcek et al. 2004). This might imply that UBP684 would increase agonist affinity at GluN2A or GluN2B receptors. UBP684 increased the apparent affinity of the glycine but not of the L-glutamate at GluN2B receptors. Similarly, UBP753 enhanced the efficacy of both L-glutamate and glycine but did not increase the apparent affinity of either of the agonists at GluN2D receptors. These results, in part, are consistent with the effect of PS on glutamate and glycine

efficacy and affinity where PS slightly increases agonist potency at GluN2B containing receptors and has a reduced effect on efficacy with high agonist concentrations (Malayev, Gibbs et al. 2002).

UBP684 enhances the NMDAR current by increasing the channel open probability of the receptor as evident by increase in rate of inhibition by an open channel blocker MK-801. Although it increased the channel P_{open}, it did not change the potency of blockade by ketamine, an open channel blocker of NMDARs. This implies that UBP684 binding does not alter the ketamine binding site in the pore or have a binding site that partially overlaps with ketamine. Previous studies with other PAMs like PS and SGE-201 also have shown that they do not have any effect on the potency of channel blockers such as memantine and ketamine at GluN2A receptors (Emnett, Eisenman et al. 2015) consistent with a binding site outside of the channel pore. These drugs are voltage-independent and they potentiate receptor responses with almost similar efficacy at both positive and negative membrane potentials. They also do not change the reversal potential of the NMDAR current (Figure 4.5).

From our previous studies, it is known that the activity of this class of drugs is not affected by deletion of the N-terminal domain of the NMDARs. Also, to determine if they bind to the C-terminal, we injected UBP684 directly inside the oocytes and measured UBP684 potentiation by bath application. UBP684 was still able to potentiate the current to the same magnitude (unpublished observation). This implies that UBP684 does not bind to C-terminal of the NMDARs. These findings suggest that UBP684/UBP753 must be binding either to the LBD domain similar to binding of recently reported GluN2A-selective potentiator GNE-6901(Hackos, Lupardus et al. 2016) or close to the transmembrane region similar to binding of GluN2C/ GluN2D potentiator CIQ (Mullasseril, Hansen et al. 2010).

Our study shows that these potentiators are still able to potentiate in a reducing environment. Although there was some reduction in % potentiation by UBP753 (Figure 4.6), absolute magnitude of potentiation could be similar because DTT treatment enhances the agonist response (Sullivan, Traynelis et al. 1994) and the enhanced agonist response after DTT treatment was used for the normalization of UBP753 potentiation after DTT treatment, which could have resulted in lower % potentiation by UBP753 after DTT. We also found that UBP684 potentiation is not reduced in the GluN1 splice form with exon-5. NMDARs with exon-5 show a reduction in proton inhibition (Traynelis, Hartley et al. 1995) and a corresponding reduction in spermine potentiation (which also reduces proton inhibition). Hence, the equal potentiation of NMDARs with GluN1-1a and GluN1-1b splice variant (Figure 4.6) suggests that the potentiation by UBP684 is not by relieving the proton inhibition of the receptors, at least not by the same mechanism as seen by spermine (Traynelis, Hartley et al. 1995). It also implies that spermine and UBP753 bind to different sites for their potentiating activity, which is supported by our previous report that the N-terminal deletion does not eliminate the PAM activity (Costa, Irvine et al. 2010).

From PAM/NAM competition studies, we know that the binding site for the potentiating and inhibiting activities of PAMs and NAMs are different. Although the NAMs and PAMs have similar structural features, they do not compete for binding and appear to exert their effect via different binding sites (Figure 4.7). Interestingly, the presence of one PAM (UBP512) eliminated the potentiating activity of another PAM (UBP684). This suggests that these two PAMs may have different binding sites. Given the multiplicity of homologous, but non-identical interfaces in a heteromeric complex, UBP684 and UBP512 may be binding in distinct, but structurally similar, binding sites.

Molecular docking studies of UBP684 binding shows that this compound can dock in the LBD region of GluN1-1a/GluN2A dimer interface (Figure 4.20) . The end of the alkyl side-chain of UBP684 terminates near the hinge region of GluN1 near Y535 residue and the carboxylic acid

group at 2-position of naphthalene in UBP684 interacts with the positively charged amino acid residues on the top of the LBD and near from NTD. The binding region revealed by this docking was similar to the binding site for GluN2A-selective PAM GNE-6901 as demonstrated by its crystal structure (Hackos, Lupardus et al. 2016).

Figure 4.20 UBP684 docking at the LBD dimer-interface

Molecular modeling of UBP684 binding to the GluN1/GluN2A receptor LBD dimer. (Top) UBP684 (space filled) is shown docked into the GluN1/GluN2A LBD intersubunit interface. Modelling suggests that the carboxylic acid group of UBP684 interacts with positively charged residues on the top of the LBD away from the transmembrane domains and near the N-terminal domains. The alkyl side-chain terminates near the LBD hinge region near the GluN1 Y535 shown in green. (Bottom) The same docking of UBP684 is shown rotated in the horizontal plane with the GluN1 LBD removed and GluN1's Y535 (green) shown for reference.

Our results also indicate that these PAMs bind in both presence and absence of agonists. Sequential application of both PAMs increased the onset time and NMDAR response of the agonist (Figure 4.8). Also, pre- and co-application of these compounds showed a rapid onset and sustained response. Both of these application paradigms suggest that UBP753 can bind to the agonist-unbound confirmation. In contrast, when agonist was co-applied with UBP753, with no prior exposure, the response displayed a slow onset rate. Contemporaneous application also displayed a slow onset of drug potentiation. These results imply that UBP753 can also bind in the presence of the agonists. The NMDAR response observed after pre-co-application was sustained for UBP753, whereas pre-co-application led to reduction in response for PS (Horak, Vlcek et al. 2004). This suggests that UBP753's affinity is not reduced by agonist as it is for PS.

Consistent with an increase in P_{open}, we found that UBP684 prolongs the deactivation time for GluN2D receptors (Figure 4.10). It especially slows the dissociation of L-glutamate from its binding site or the associated deactivation. Similar findings have been previously reported with PS where PS prolongs the GluN2A and GluN2B receptors deactivation rate (Ceccon, Rumbaugh et al. 2001).

The effect of UBP684 on deactivation time following L-glutamate removal (but not that following glycine removal) and the inability of UBP753 (or UBP684, data not shown) to potentiate GluN2A receptors with disulfide cross-linked LBD (Figure 4.11) implies that these drugs stabilize the glutamate-bound close-cleft conformation of the GluN2 LBD. In turn, this conformation stabilizes the open channel, thus increasing open channel probability.

Proton concentration in the tissue varies during different pathological conditions. During ischemic conditions, acidification occurs in brain tissue (Katsura, Asplund et al. 1992, Matsumoto, Obrenovitch et al. 1990). Hence, our aim was to determine the effect of different proton concentrations on the activity of these PAMs. Our study shows that the extracellular

proton concentration is crucial for the potentiating activity of these PAMs (UBP753 and

UBP684). The loss of potentiating activity of UBP684 at GluN2A, and reversal of activity from

potentiating to inhibitory at GluN2B-, GluN2C- and GluN2D-containing NMDARs when tested

at alkaline pH condition (Figure 4.12), shows that protons were important for PAM activity. This

is also supported by the enhanced UBP753 PAM activity at acidic pH (pH 6.4) (Figure 4.13).

These findings suggest that protons enhance the potentiating activity of PAMs and that reducing

the proton concentration adversely affects the PAM activity at NMDARs. Also, proton-dependent

activity of PAMs was dependent upon the type of the NMDAR subunit. These results suggest that

the PAMs cannot potentiate a highly efficacious NMDAR at alkaline pH, but if the receptor is

inhibited by protons, the PAMs can restore the channel function.

The inhibition by NAMs such as ifenprodil comes from increased apparent affinity of

protons for NMDAR inhibition (Pahk, Williams 1997, Mott, Doherty et al. 1998). Thus, it may be

possible that the potentiating activity of our PAMs was coming from a reduction in the affinity

for proton inhibition. The rightward shift in the proton concentration-response curve by the

presence of UBP684 at both GluN2B- and GluN2D-containing receptors (Figure 4.14) implies

that our PAM reduces the affinity/sensitivity of proton for NMDAR inhibition.

Since the potentiating activity of these tested PAM was highest at acidic pH, it is also

possible that UBP684 potentiating activity was coming from the relief of the proton block and it

should not have any effect at the NMDARs co-expressed with the GluN1-1b splice form which

has an extra 21 amino acid segment which is believed to block the proton sensor region.

However, similar activity observed at GluN2D with either GluN1-1a or GluN1-1b in all tested pH

conditions suggests that these drugs potentiate by different mechanisms (Figure 4.15A,B). The

slight increase in affinity for UBP684 inhibition at GluN1-1b compared to GluN1-1a containing

GluN2D receptors (Figure 4.15C) might be due to increase in the affinity of protons for NMDAR

inhibition. This finding is distinct from that found for the potentiating activity of spermine at

GluN2B receptors. Spermine does not potentiate at alkaline pH and has the highest level of potentiation at acidic pH, which is consistent with our finding about PAMs activity. However, spermine does not potentiate NMDARs with the GluN1-1b splice form, which was not consistent with the activity of our PAMs. UBP684/ UBP753 potentiate equally both the GluN1-1a and the GluN1-1b forms containing NMDARs at both acidic and physiologic pH conditions and there was even an enhanced inhibitory activity at GluN1-1b containing receptors in the alkaline pH condition. Also, spermine binds to the N-terminal domain and may reduce the sensitivity of the ATD proton sensor region by blocking the access to protons as. It is unlikely that UBP684/UBP753 bind to the N-terminal domain because the potentiating activity of structurally similar PAMs from our laboratory were not affected by deletion of N-terminal domain. Hence, these results show that the potentiating mechanism of our PAMs is different from that of spermine potentiation, but may involve other proton-sensitive regions such as the channel gating region (Low, Lyuboslavsky et al. 2003).

Although reduced proton concentration decreased the potentiating activity of the neurosteroid PS at GluN2A- and GluN2B- and that of CIQ at GluN2C-containing NMDARs, these PAMs were still able to retain their potentiating activity unlike the UBP PAMs (Figure 4.16A,B) and the GluN2A-selective PAM (GNE-8324) was not able to potentiate at alkaline pH (Figure 4.16C). Crystal structure shows that GNE-6901 binds at the heterodimer interface of the LBD. From molecular docking studies, we find that UBP PAMs may also be binding to the same binding site in the LBD dimer interface. It is possible that although they are not binding to the N-terminal domain close to the proton sensor region, their binding in LBD may change the conformation of the proton sensor region in the pore region thereby altering the proton sensitivity and NMDAR response.

During the course of study of these NMDAR modulators, we observed that there was more variability in the response of PAMs as compared to NAMs and competitive antagonists.

Thus, some cells displayed much greater PAM responses than other cells. This may be related to phosphorylation state or intracellular Ca^{2+} levels. The activity of other PAMs such as neurosteroids are affected by the phosphorylation state of the NMDARs. The C-terminal has many sites for phosphorylation. S897 in GluN1 and S900 and S929 in GluN2A are phosphorylation sites for PKA. Similarly, S890 and S897 in GluN1 and S1291, S1312 and S1416 in GluN2A are phosphorylation sites for PKC (see review by (Wang, Guo et al. 2014). Using the C-terminal truncated GluN1 or GluN2A subunits, we were able to measure and compare the potentiating activity of UBP PAMs and pregnenolone sulfate. There was a significant effect of GluN1 C-terminal truncation on the potentiating activity of UBP684 and GluN2A C-terminal truncation on the potentiating activity of pregnenolone sulfate. This finding with pregnenolone sulfate is consistent with the previous findings that activity of pregnenolone sulfate is phosphorylation dependent (Petrovic, Sedlacek et al. 2009). Our result, for the first time, shows that the GluN2A but not the GluN1 C-terminal is more important for the potentiating activity of PS (Figure 4.17B). Our results with UBP684 also implies that its potentiating activity is highly dependent on the GluN1 C-terminal, possibly due to phosphorylation state (Figure 4.17A). However, it is also possible that by deleting the C-terminal, it not only eliminates the phosphorylation sites for protein kinases, but also eliminates the binding site of intracellular anchor proteins, which may adversely affect the channel function. However, it is less likely that the elimination of C-terminal reduces the potentiating activity by deleting the PAM binding sites because the intracellular injection of UBP684 does not affect the potentiation by bath perfusion of UBP684.

Calcium is an important second messenger and regulates the function of many kinases, and thus affects phosphorylation. We observed that intracellular calcium is important for potentiating activity especially at GluN2A receptors (Figure 4.18). UBP684 displayed significantly-reduced potentiation in oocytes with chelated intracellular calcium. Thus, calcium is

necessary for PAM potentiating activity at GluN2A receptors. It is possible that reduced calcium might reduce the phosphorylation on GluN1 receptors as discussed previously which may affect potentiation. Interestingly, there was little effect of intracellular calcium reduction on the activity of UBP684 at GluN2B receptors.

We also found that the potentiating activity of UBP753 was enhanced by PKC activation (Figure 4.19A). However, PKC activation did not change the activity of pregnenolone sulfate (Figure 4.19B). Which is consistent with the previous finding that the potentiating activity of PS is dependent on PKA but not on PKC phosphorylation (Petrovic, Sedlacek et al. 2009). It will be interesting to test further the effect of PKC activation on the activity of UBP753 on GluN1-1b expressing NMDARs. Because, PMA treatment increases NMDAR response by 20-fold at NMDARs complexed with GluN1-1b splice form whereas just by 4-fold at NMDARs complexed GluN1-1a form (Durand, Gregor et al. 1992).

Chapter 5 Pharmacological and mechanistic characterization of novel NMDAR NAM

5 Mechanism of allosteric inhibition of NMDARs by the 2-napthoic acid derivative UBP792

5.1 Abstract

NMDARs are a subtype of ionotropic glutamate receptor that plays an important role in learning and memory. While optimal NMDAR function is necessary for CNS function, excessive NMDAR activity leads to neuro-pathological damage as seen in neurodegenerative diseases and epilepsy. Thus, agents that inhibit NMDAR function have therapeutic applications. In this chapter, we have characterized the inhibition mechanism of the prototype 2-naphthoic acid compound, UBP792, which shows a strong inhibitory activity at GluN2D receptors and least inhibitory activity at GluN2A-containing NMDARs. Inhibition by this compound is non-competitive and voltage-independent. This compound inhibits NMDARs responses by reducing the maximal efficacy and affinity of the agonists. The effect of protons on its activity was different from the effect seen on previously reported NAMs. This compound shows greater inhibition when the proton concentration is low and inhibition is not affected by exon-5 thus suggesting that the N-terminal proton sensor is not involved. The binding site of this compound is different from that of the general PAM (e.g. UBP684). Inhibition by this compound appears to involve stabilizing the open conformation of the GluN2 ligand-binding domain (LBD). These findings helps to define the mechanisms of allosteric inhibition of NMDARs by this compound, which can be utilized in the development of future NMDAR modulators with greater subunit selectivity and potency that can be used for therapeutic benefit as well as for experimental purposes.

5.2   Introduction

As discussed before, optimum activity of NMDARs is important for generation of LTD and LTP which are thought to play key roles in learning, memory, and cognition [see review by (Traynelis, Wollmuth et al. 2010)]. However, excessive NMDAR activation is believed to be the cause of neuronal cell death in stroke, traumatic brain injury and various neurodegenerative diseases. These findings have led to the development of a large number of NMDAR inhibitors over the past 30 years to provide neuroprotection in stroke, seizures, and neurodegenerative disorders. Since, maintaining normal NMDAR function is crucial, optimal inhibition of these receptors may possibly be achieved by the use of allosteric inhibitors. Since NAMs do not bind to the highly conserved orthosteric ligand-binding site, it provides an opportunity for subtype selectivity by binding to more varied, non-conserved regions of the receptor.

The GluN2 subunit determines many of the biological and pharmacological properties of the NMDARs (Vicini, Wang et al. 1998, Gielen, Retchless et al. 2009, Buller, Larson et al. 1994). These properties, combined with the varied developmental profiles and anatomical distributions of GluN2 subunits (Monyer, Burnashev et al. 1994, Ishii, Moriyoshi et al. 1993), imply that GluN2 subtype-selective agents would have distinct physiological and therapeutic properties. The ability to differentially inhibit specific NMDAR subtypes by the use of negative allosteric modulators (NAMs), while not affecting other populations, may provide therapeutic benefit.

Recently, research has focused on developing subtype-selective inhibitors to specifically target the subtypes responsible for the disease (Figure 5.1). Our group previously has published a series of novel NAMs such as UBP710, UBP552, UBP608 (Costa, Irvine et al. 2010, Irvine, Costa et al. 2012) with distinct patterns of selectivity at NMDARs GluN2 subunits. These agents do not act at the agonist binding site, the NTD or the channel pore. Hence the advantage of using these NAMs are (i) they may offer greater receptor subtype selectivity, and hence reduce adverse effects and (ii) they can have partial maximal inhibitory effects thus providing protection from excessive

NMDAR blockade. The compounds TCN-201 (Edman, McKay et al. 2012) and MPX-007 (Volkmann, Fanger et al. 2016) are NAMs, which selectively inhibit only GluN2A-containing NMDARs. Similarly, ifenprodil (Williams 1993), RO 25-6981 and 93-31(Yuan, Myers et al. 2015) are NAMs that selectively inhibit GluN2B-containing NMDARs. UBP512 (Costa, Irvine et al. 2010), QNZ46 (Mosley, Acker et al. 2010), DQP-1105(Acker, Yuan et al. 2011) and UBP710 (Costa, Irvine et al. 2010) selectively inhibit GluN2C- and GluN2D-containing NMDARs. Other compounds such as UBP552 and UBP618, inhibit all NMDAR subtypes with almost equal selectivity (Costa, Irvine et al. 2012).

In this chapter, we have studied the pharmacology and the mechanism of inhibitory action of UBP792, a prototype from this series of compounds.
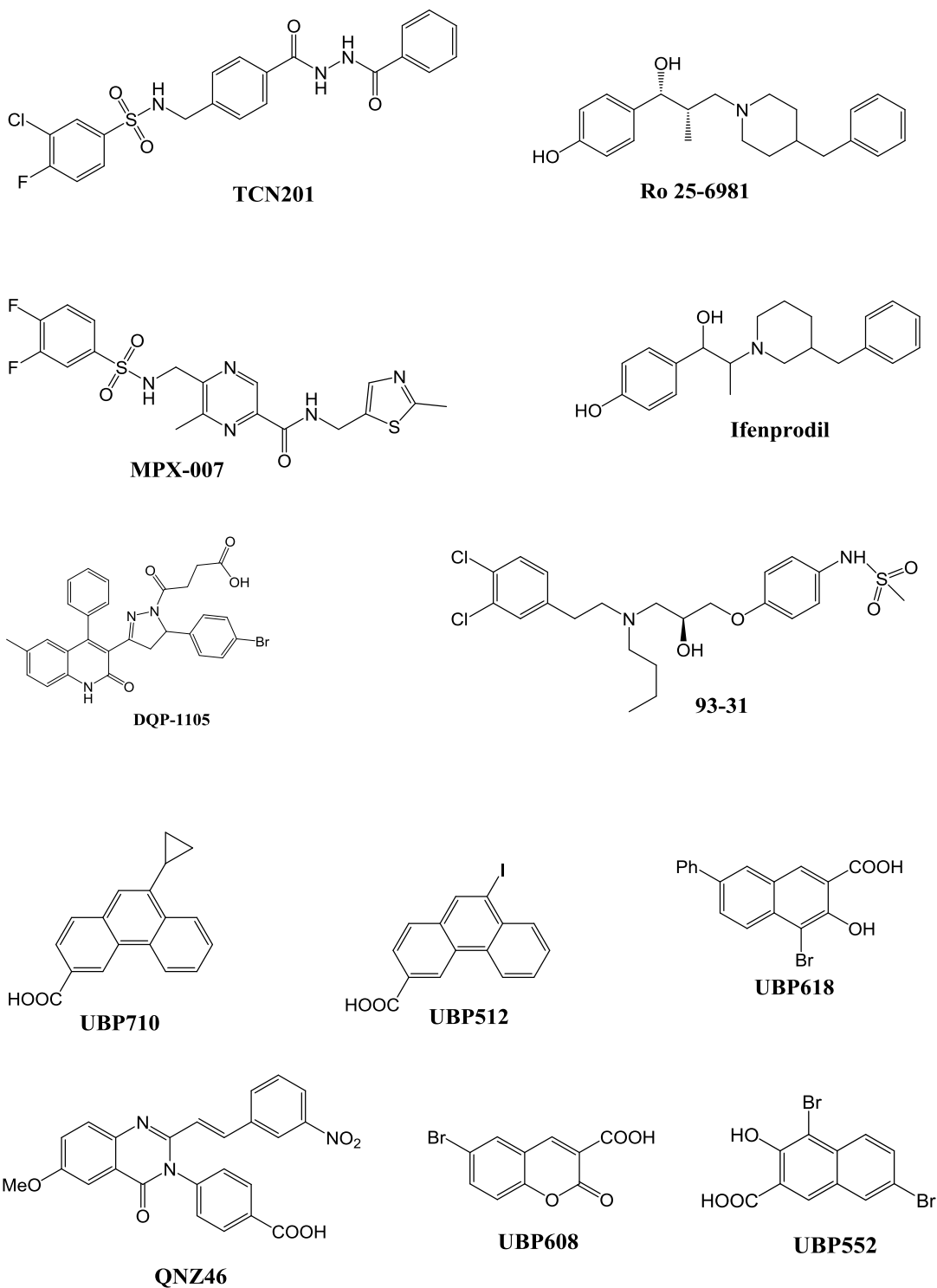
Figure 5.1 Chemical structures of known NMDAR allosteric inhibitors

5.3   Materials and methods

5.3.1   *Chemicals and compounds*

See the details in Chapter 3 (section 3.3.1).

5.3.2   *cDNA and cRNA preparation*

See the details described in Chapter 3 (sections 3.3.2 and 3.3.3).

5.3.3   *Two-electrode voltage clamp electrophysiology*

See the details described previously in Chapter 3 (section 3.3.4).

5.3.4   *Statistical analysis*

See the details described previously in Chapter 3 (section 3.3.5).

5.4   Results

5.4.1   Concentration-response study of UBP792 at recombinant GluN1/GluN2A-D receptors

UBP792 inhibited all four subtypes of NMDARs. It inhibited GluN2C and GluN2D receptors the most and GluN2A receptors the least (Figure 5.2). It showed a moderate inhibitory activity at GluN2B subtypes of NMDARs. The maximal inhibition by UBP792 at GluN2A-, GluN2B-, GluN2C-, and GluN2D-containing NMDARs was 30.0 ± 6.3 % (n = 12 oocytes), 61.3 ± 18.0 % (n = 5 oocytes), 80.1 ± 4.1 % (n = 16 oocytes), and 79.2 ± 3.0 % (n = 12 oocytes) respectively. The IC_{50} values for UBP792 inhibition were 30.0 ± 6.0 µM at GluN2A-, 32.0 ± 16.0 µM at GluN2B-, 8.0 ± 1.0 µM at GluN2C-, and 3.0 ± 0.5 µM at GluN2D-containing receptors (Table 3.3). It displayed a preference for inhibition at GluN2D- and GluN2C-containing receptors compared to GluN2B- and GluN2A-containing receptors. However, UBP792 inhibited only partially at the tested concentration (100 µM) and we did not try higher concentration to see if it causes full inhibition due to limited solubility.
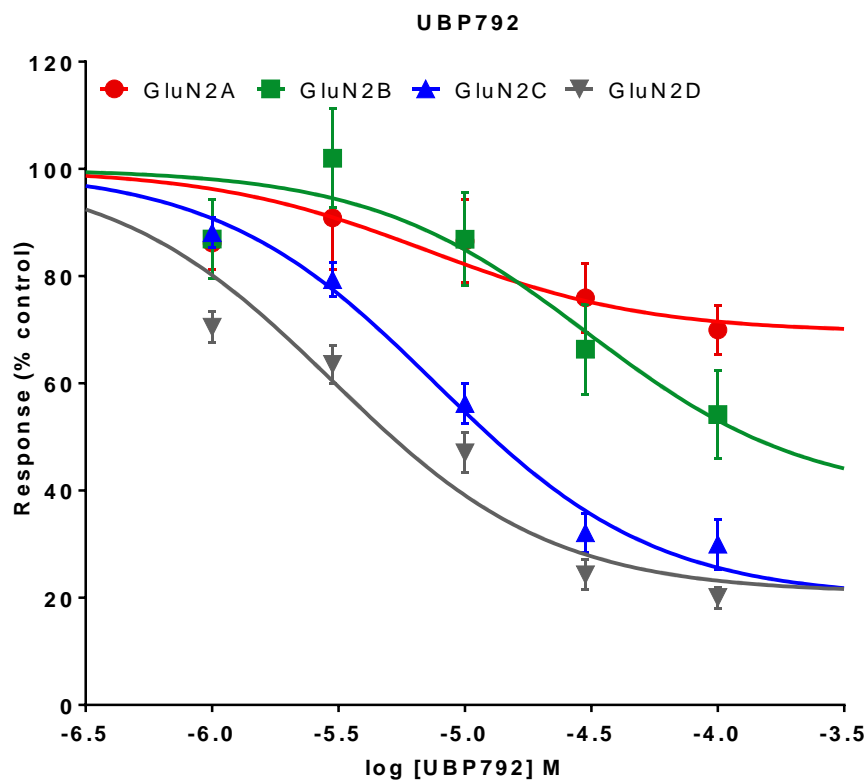
Figure 5.2 Concentration-response study of UBP792 at rat recombinant GluN1/GluN2A-D receptors expressed in *Xenopus laevis* oocytes.

NMDAR-mediated current was first evoked by agonists (10 μM of L-glutamate and 10 μM glycine) and after achieving a steady state response, UBP792 was tested for inhibitory activity at increasing concentrations to determine the potency and efficacy at GluN2A-D subtypes of NMDAs. The NMDAR response was measured and expressed as % inhibition of agonist-alone (control) response (n = 5-16 oocytes per subunit). Data represent mean ± S.E.M.

5.4.2   Effect of UBP792 on affinity and efficacy of NMDR agonists at GluN2D-
*   containing NMDARs.*

In order to determine the mechanism of UBP792 inhibition, we wanted to know if it is competing

with agonists at the ligand binding sites. We performed a concentration-response study of L-

glutamate and glycine at GluN2D-containing NMDARs in presence or absence of 5 μM of

UBP792. The compound reduced the % E_{Max} for both L-glutamate and glycine at GluN2D-

containing receptors. UBP792 inhibited the L-glutamate-induced NMDAR response by 40 %.

The L-glutamate-mediated maximal NMDAR response in absence of UBP792 was 99.7 ± 1.2 %

(n =10 oocytes) while it was 60.0 ± 2.5 % (n = 7 oocytes) in presence of 5 μM UBP792 (Figure

5.3). Similarly, UBP792 also inhibited the glycine-induced NMDAR response by 35 %. The

glycine-mediated maximal NMDAR response in absence of UBP792 was 101.0 ± 2.1 % (n =12

oocytes) while it was 64.3 ± 2.4 % (n = 7 oocytes) in presence of 5 μM UBP792 (Figure 5.3).

Although, UBP792 caused a slight increase in the EC_{50} for L-glutamate, there was a 6-fold

increase in EC_{50} for glycine (Table 5.1). We also evaluated the effect of high agonist

concentration on the inhibitory activity of UBP792. UBP792 (10 μM) inhibited the glycine

(mM)-mediated response with the same % of maximal inhibition (% $I_{max,}$) similar to the inhibition

of the 10 μM glycine-induced response. Hence, these results suggest that UBP792 is an allosteric

modulator, not competitive, and is binding to a different site than the ligand binding site unlike a

competitive antagonist.

Table 5.1 EC_{50} (μM) and % E_{Max} values of agonists in absence and presence of UBP792

	Glutamate			
	EC_{50} (μM)	*% E_{Max}*	*Hill slope*	*N*
Without UBP792	0.88 ± 0.05	99.7 ± 1.2	1.6	10
With UBP792	1.61 ± 0.3[*]	59.8 ± 2.5	1.2	7
	Glycine			
	EC_{50} (μM)	*% E_{Max}*	*Hill slope*	*N*
Without UBP792	0.4 ± 0.12[****]	101.0 ± 2.4	1.3	12
With UBP792	2.55 ± 0.4	64.3 ± 1.9	1.55	7

[*]p < 0.05 and [****] p < 0.0001 (unpaired t-test) vs EC_{50} value for L-glutamate or glycine without UBP792 at the same NMDAR subtypes
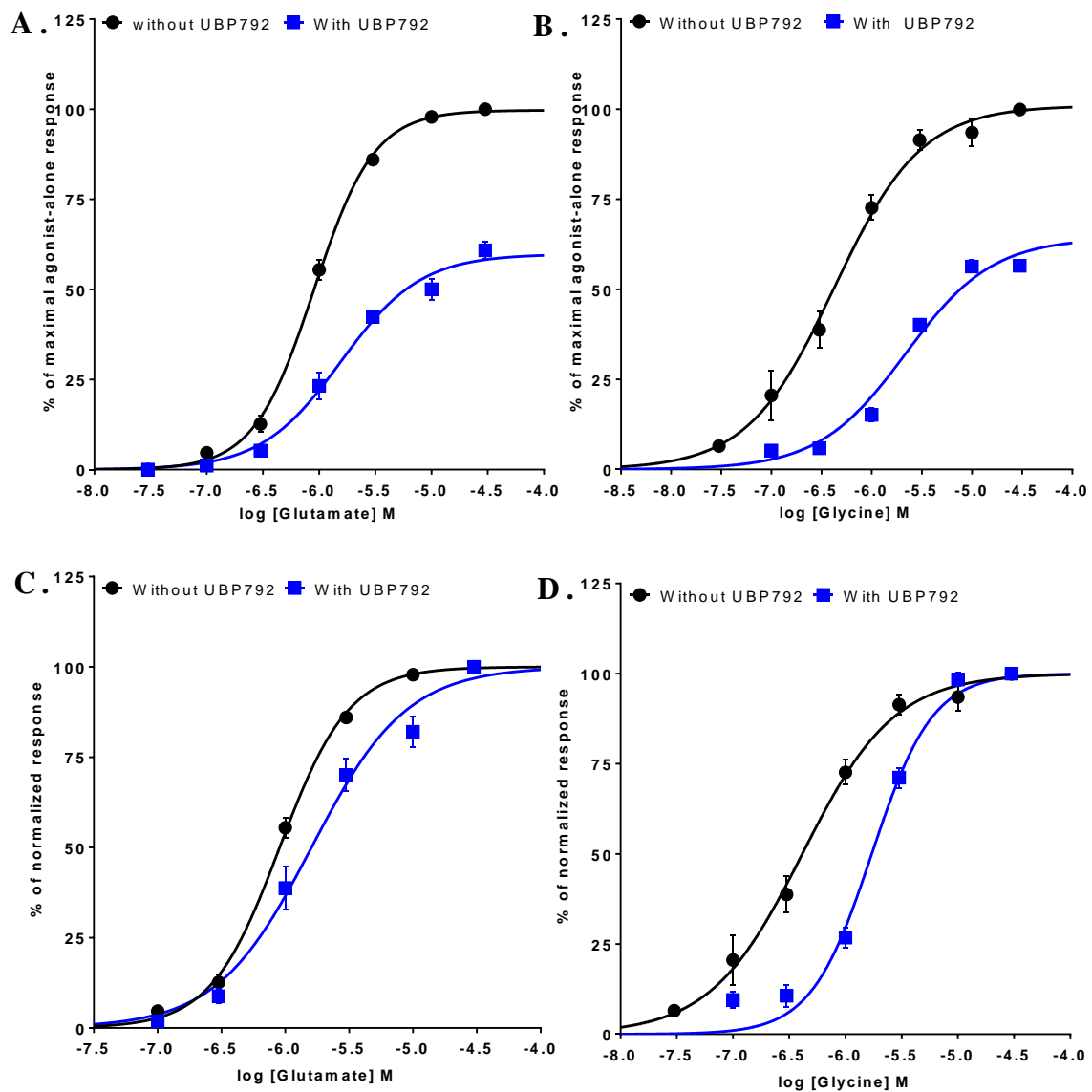
Figure 5.3 Effect of UBP792 on affinity and efficacy of NMDAR agonists

(**A**) Concentration-response study of L-glutamate at GluN2D-containing NMDARs was carried out with increasing concentrations of L-glutamate and a fixed concentration of glycine (10 μM) in the absence (black, n = 10 oocytes) and the presence (blue curve, n = 7 oocytes) of 5 μM of UBP792 to study the effect of UBP792 on affinity and efficacy of NMDAR agonists for recombinant NMDARs expressed in *Xenopus laevis* oocytes. Data from each oocyte were normalized to the response from the highest concentration of agonist-alone. Data represent mean ± S.E.M. (**B**) Concentration-response study of glycine at GluN2D-containing NMDARs was carried out with increasing concentrations of glycine and a fixed concentration of L-glutamate (10 μM) in absence (black, n = 12) and presence (blue curve, n = 7) of 5 μM UBP792. Data represent mean ± S.E.M. (**C,D**) The concentration-response curves for L-glutamate (**C**) or glycine (**D**) in absence and presence of UBP792 were normalized to the responses of 30 μM glutamate or 30 μM glycine and superimposed for better illustration of the shift in glutamate EC$_{50}$. Data represent mean ± S.E.M.

5.4.3 *Effect of high agonist concentration on NMDAR inhibitory activity of UBP792*

We also studied the effect of high agonist concentrations on the inhibitory activity of UBP792 to mimic the synaptic environment. Interestingly, UBP792 inhibition was stronger at GluN2C-containing NMDARs in high agonist condition (300 µM of L-glutamate and 300 µM of glycine, IC_{50} of 7.5 ± 0.9 µM, n = 5) compared to low agonist condition (10 µM of L-glutamate and 10 µM of glycine, IC_{50} of 10.5 ± 0.7 µM, n = 6) (Figure 5.4), and the difference in affinities was statistically significant (p = 0.035, unpaired t-test). This is also evident by the leftward shift in the concentration-response curves at GluN2C receptors (Figure 5.4). There was no difference in affinity at GluN2D receptors when tested at low or high agonist concentrations. The IC_{50} for UBP792 inhibition at GluN2D receptors was 3.7 ± 0.8 (n = 5) at low and 4.0 ± 0.5 µM (n = 5) at high agonists condition. Also, the % of maximal inhibition was increased in high agonist condition at both GluN2C- and GluN2D-containing receptors compared to the low agonist condition. This result also demonstrates that UBP792 is not a competitive antagonist at ligand binding site.
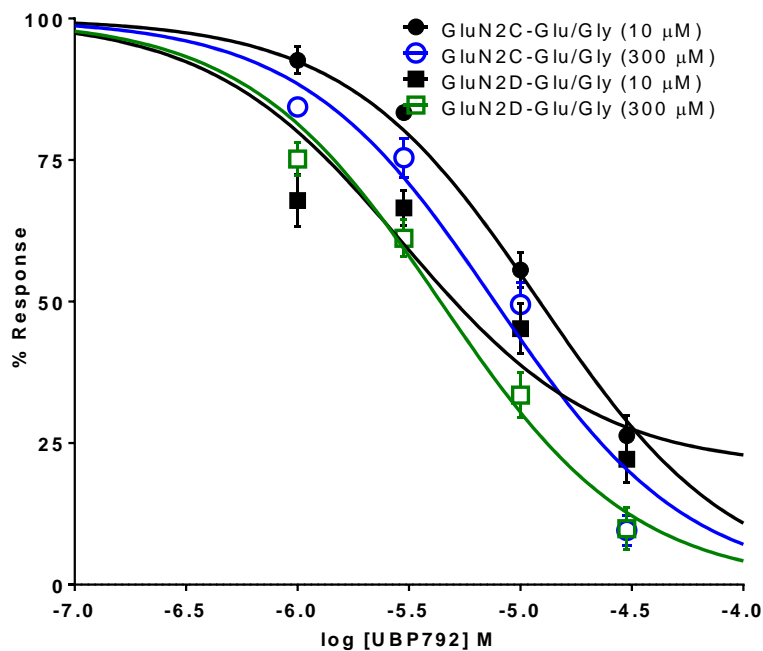
Figure 5.4 Effect of high agonist concentration on NMDAR inhibitory activity of UBP792

The inhibitory activity of UBP792 in different agonist concentrations was studied at recombinant GluN2C- and GluN2D-containing NMDARs in the presence of 300 µM L-glutamate and 300 µM glycine (open circles or squares) or in presence of 10 µM L-glutamate and 10 µM glycine (filled circles or squares) (n > 6 for each condition). Data are mean ± S.E.M.

5.4.4 *Effect of membrane potential on UBP792 NMDAR inhibitory activity*

At 30 µM, UBP792 inhibited GluN2C-containing NMDARs by 58.0 ± 11.6 % (n = 6) at + 40 mV

and by 55.6 ± 9.3 % (n = 7) at − 60 mV; the difference was not statistically significant (Figure

5.5). Hence, UBP792 inhibition is voltage-independent.
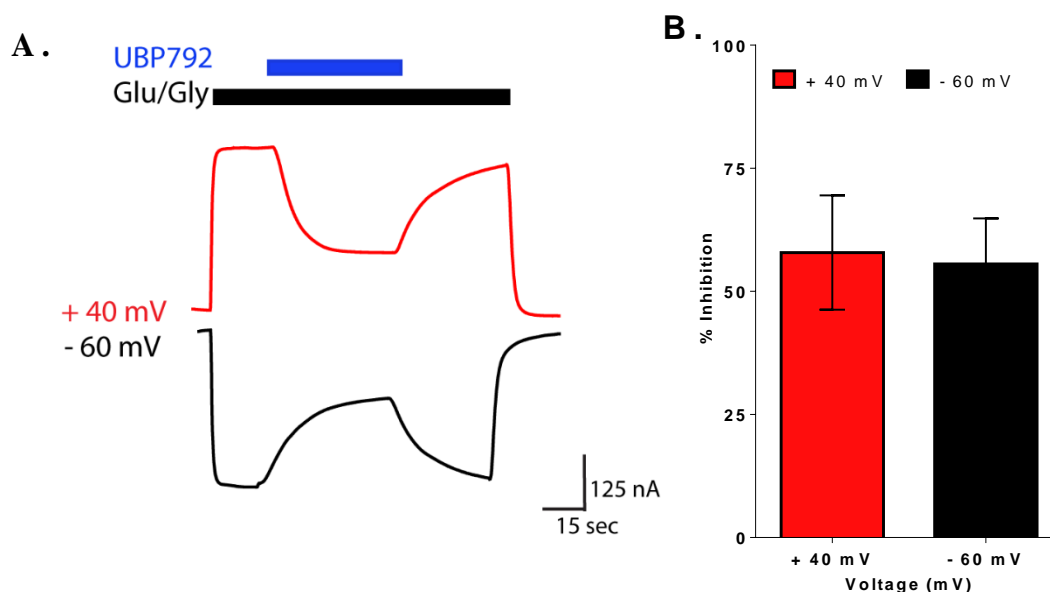
Figure 5.5 Effect of membrane potential on the NMDAR inhibitory activity of UBP792

(**A**) A trace showing the inhibitory activity of UBP792 (30 µM) was measured at - 60 mV (black) and + 40 mV (red) on the GluN2C subtype of NMDARs expressed in *Xenopus laevis* oocytes. Scale bar: horizontal = time in sec, vertical = current in nA. (**B**) Bar graph showing the percent inhibition of agonist-evoked (10 µM L-glutamate and 10 µM glycine) current at -60 mV (n = 6 oocytes, black bar) and +40 mV (n = 7 oocytes, red bar). Data represent mean ± S.E.M.

5.4.5   Effect of pH and GluN1 splice variant on the inhibitory activity of UBP792 at GluN2D-containing NMDARs

During different pathological conditions, there is a change in the concentration of protons in the extracellular space inside the brain. Thus, we were interested to determine if UBP792 maintains its inhibitory activity under different pH conditions. Although the % inhibition in the acidic condition was significantly lower compared to physiological and alkaline pH condition, UBP792 still inhibited across the pH range that we tested. UBP792 (30 μM) inhibited the GluN2D-mediated current by 45.1 ± 2.9 % (n = 11 oocytes), 76.5 ± 2.1 % (n = 8 oocytes) and 78.1 ± 2.2 (n = 10 oocytes) at pH 6.4, 7.4 and 8.4 respectively (Figure 5.6). We also measured UBP792 inhibitory activity GluN2D-containing receptors co-expressed with different GluN1 splice variants. GluN1 splice variants with an exon-5 segment (GluN1-1b) shows a reduction in proton inhibition compared to the splice variant without exon-5 (GluN1-1a). To find out if the mechanism of inhibition by UBP792 is similar to that of proton inhibition, we measured the inhibitory activity of UBP792 at GluN1-1b/GluN2D receptors and there was no apparent change in UBP792 inhibitory activity. We also performed a concentration-response study of UBP792 at pH 7.4 and pH 8.4 at GluN2D receptors co-expressed either with GluN1-1a or with GluN1-1b. The inhibitory activity of UBP792 was enhanced in the alkaline pH condition. This is similar to our finding with the PAMs in both case there is increased inhibitory activity in the alkaline condition. UBP792 showed similar inhibitory activity at GluN2D receptors with both of the GluN1 splice forms under both pH conditions (Figure 5.6,Table 5.2)

Table 5.2 IC$_{50}$ (μM) and % I$_{Max}$ values of UBP792 at GluN2D-containing NMDARs with different GluN1 splice variant forms at different pH conditions

	GluN1-1a/GluN2D			
	IC$_{50}$ (μM)	*% I$_{Max}$*	*Hill slope*	*N*
pH: 7.4	4.1 ± 0.3	94.9 ± 7.1	1.0	6
pH: 8.4	2.0 ± 0.08***	95.9 ± 2.3	1.0	4
	GluN1-1b/GluN2D			
	IC$_{50}$ (μM)	*% I$_{Max}$*	*Hill slope*	*N*
pH: 7.4	4.3 ± 0.15	97.3 ± 3.3	1.1	5
pH: 8.4	2.4 ± 0.1****	98.0 ± 2.0	1.1	5

***p <0.001 (t-test) vs IC$_{50}$ value for the same receptor at pH 7.4.

****p< 0.0001 (t-test) vs IC$_{50}$ value for the same receptor at pH 7.4.
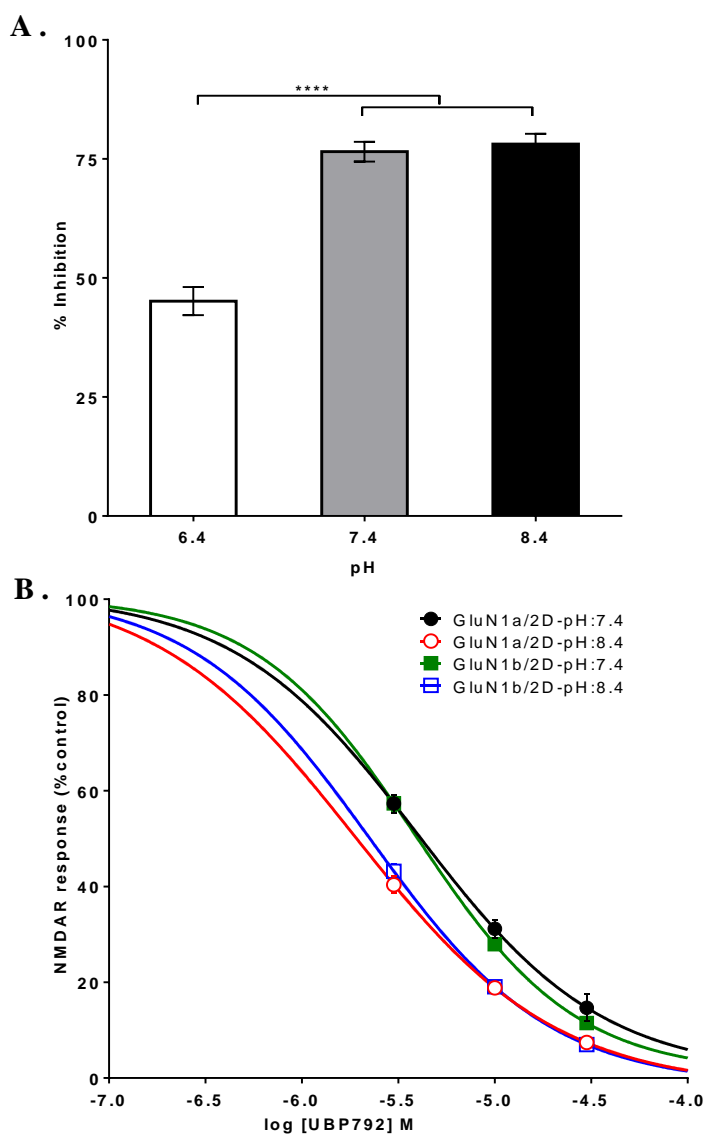
Figure 5.6 Effect of pH and GluN1 splice variants on the inhibitory activity of UBP792 at GluN2D-containing NMDARs

(**A**) The inhibition of NMDAR activity by 30 µM UBP792 was measured at GluN1-1a/GluN2D receptors under different pH conditions. UBP792 inhibited GluN2D-mediated NMDAR current evoked by 10 µM L-glutamate and 10 µM glycine at every pH tested (pH 6.4, n = 11 oocytes; pH 7.4, n = 8 oocytes; pH 8.4, n = 10 oocytes). Data represent mean ± S.E.M. ****p<0.0001 (one-way ANOVA followed by Tukey's multiple comparison test. (**B**) Concentration-response of UBP792 inhibition of GluN2D receptors co-expressed with GluN1-1a (absence of exon-5 segment) or GluN1-1b (presence or exon-5 segment) splice variants at pH 7.4 (GluN1-1a, black curve, n = 6 oocytes; GluN1-1b, green curve, n = 5 oocytes) and pH 8.4 (n = 4 oocytes at GluN1-1a, red curve and 5 oocytes at GluN1-1b containing receptors, blue curve). Data represent mean ± SEM.

5.4.6   Binding interactions of the NAM UBP792 and the PAM UBP684

We hypothesized that the binding site for the PAMs and NAMs are different. To determine if the

PAMs and the NAMs are interacting with each other during binding, we performed a

concentration-response study of the NAM UBP792 in the presence of 50 μM of the PAM

UBP684. The potency of UBP792 in the presence of UBP684 was enhanced (Figure 5.7). The

IC_{50} values for UBP792 at GluN2C receptors without UBP684 was 10.8 ± 1.8 μM and with

UBP684 it was 3.0 ± 0.4 μM and the difference was statistically significant ($p = 0.007$, unpaired

t-test). This shows that PAM and NAM bind to different sites. The binding interactions are non-

competitive. This is consistent with the converse experiment where a fixed concentration of a

NAM reduced the maximal response of a PAM but not its potency (Figure 4.7). The shift in

UBP684 affinity suggests that these binding sites are allosterically coupled.
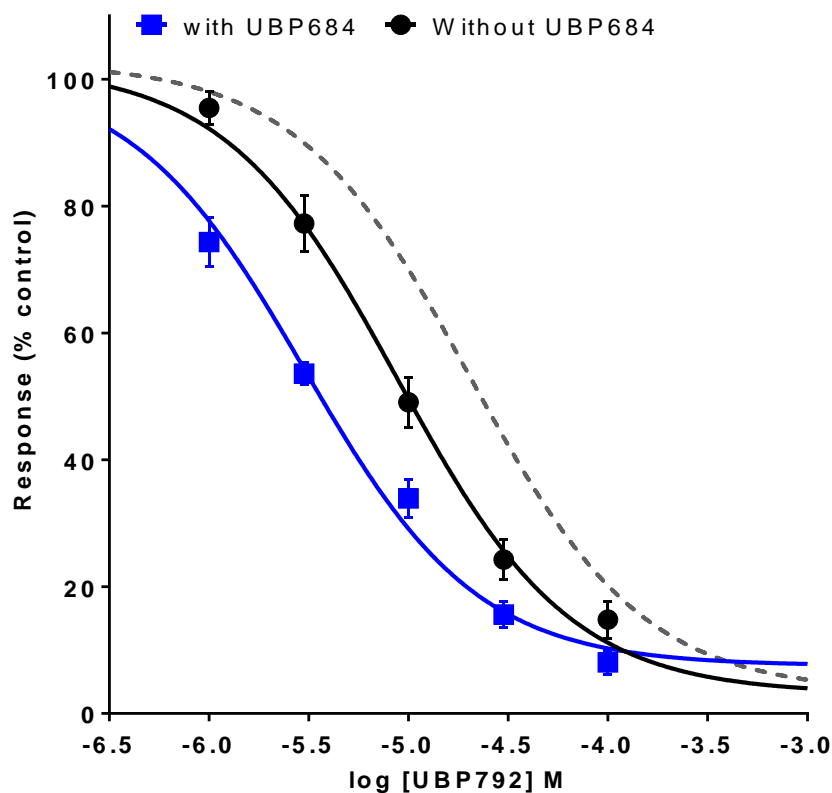
Figure 5.7 Effect of the PAM UBP684 on NMDAR response inhibition by the NAM UBP792

A concentration-response study of UBP792 with (blue curve, n = 5 oocytes) or without (black curve, n = 13 oocytes) 50 μM UB684, a positive allosteric modulator of GluN2C-containing NMDARs. The UBP792 response curve in presence of UBP684 was normalized with the UBP684-alone response as being 100 %. The dotted curve shows the expected shift in the UBP792 concentration-response curve if the interaction between UBP792 and UBP684 was competitive. Data represent mean ± S.E.M.

5.4.7   The inhibition by UBP792 is affected by the LBD-conformation of the GluN2 subunit

By introducing two cysteine residues in each ligand binding domain of GluN1 or GluN2A subunits, two mutant subunits are created with disulfide crosslinked LBDs which constrain the LBDs in the closed-cleft conformation and mimic the glycine-bound conformation of the LBD of GluN1 or the L- glutamate-bound conformation of the LBD of GluN2A receptors. By co-expression of disulfide-crosslinked GluN1^c (N499C and Q686C) with wildtype GluN2A or of wildtype GluN1 with crosslinked GluN2A^c (K487C and N687C) in *Xenopus laevis* oocytes, we evaluated the effect of constrained LBDs on the inhibitory activity of UBP792. Interestingly, the inhibition by 100 μM of UBP792 at GluN1^c-containing GluN2A receptors was similar to that of inhibition at wild type GluN2A receptors. However, UBP792 maximal inhibition at GluN2A^c-containing receptor was significantly reduced ([**]$p < 0.01$, one-way ANOVA followed by Tukey's multiple comparison test) compared to WT GluN2A receptors and GluN1^c-containing GluN2A receptors as shown in Figure 5.8. The inhibition by UBP792 at WT GluN2A, GluN1^c-containing receptors and GluN2A^c-containing receptors was 45.5 ± 8.6 % (n = 8 oocytes), 47.7 ± 5.5 % (n = 11 oocytes), and 14.7 ± 4.3 % (n = 10 oocytes) respectively. This suggests that the inhibition by UBP792 may require the opening of the GluN2 LBD or related down-stream conformational states. This finding also implies that UBP792 stabilizes the open conformation of the GluN2 LBD.
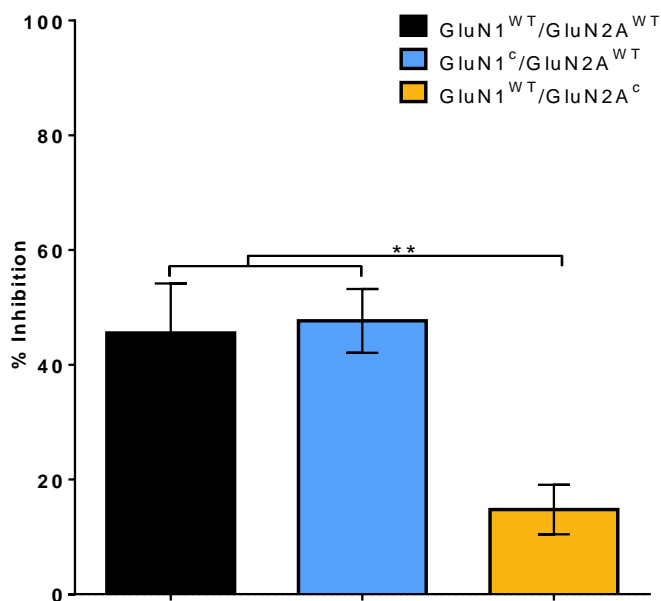
Figure 5.8 Effect of LBD cleft conformation on the inhibitory activity of UBP792

Cross-linking the cleft of the GluN1 LBD by introducing two cysteine point mutations (N499C and Q686C) locks the receptor in a conformation that mimics the glycine-bound conformation and cross-linking the cleft of the GluN2A LBD by introducing two cysteine point mutations (K487C and N687C) mimics the L-glutamate-bound conformation. Both of these constructs were separately expressed with complimentary WT subunit in *Xenopus laevis* oocytes and inhibitory activity of UBP792 (100 μM) was measured. A bar graph showing UBP792-mediated inhibition of agonists (10 μM L-glutamate and 10 μM glycine) evoked response from oocytes expressing WT (GluN1/GluN2A, n = 8 oocytes), GluN1 LBD-locked (GluN1^c/GluN2A, n = 11 oocytes) and GluN2A LBD-locked (GluN1/GluN2A^c, n = 10 oocytes) receptors. Data represent mean ± S.E.M. [**]p<0.01 (one-way ANOVA followed by Tukey's multiple comparison test).

5.5   Discussion

In this chapter, we studied the mechanism of the inhibitory action of UBP792, a prototype compound from a new series of 2-naphthoic acid derivatives. UBP792 was found to be a potent NAM which shows partial maximal inhibition at NMDARs. It is more potent and efficacious, although partial, at GluN2D- and GluN2C- than at GluN2B-containing receptors Figure 5.2, Table 3.3). Our findings indicate that this NAM maintains its inhibitory activity even at high agonist concentrations, which is important because of the high concentrations of glutamate released during synaptic neurotransmission (Figure 5.4). The non-competitive nature of UBP792's interaction with glutamate and glycine (Figure 5.3, Table 5.1) also implies that UBP792 binds allosterically to a site(s) other than the agonist binding sites. UBP792 inhibition was voltage-independent and use-independent (Figure 5.6). UBP792 can bind to the closed state of the receptor as indicated by a reduction in agonist-induced response after pre-application of UBP792 (unpublished observation).

In some pathological conditions, acidification occurs in the brain (Katsura, Asplund et al. 1992, Matsumoto, Obrenovitch et al. 1990). Some NAMs such as ifenprodil enhance the proton sensitivity thereby enhancing the proton inhibitory activity (Mott, Doherty et al. 1998, Pahk, Williams 1997). Similarly, another GluN2B NAM (93-31) also shows enhanced potency under acidic conditions (Yuan, Myers et al. 2015). However, in contrast to the enhanced inhibitory activity of ifenprodil and compound 93-31 at GluN2B-containing receptors at acidic pH, UBP792 displayed a reduced inhibitory activity at acidic pH and enhanced activity at alkaline pH condition suggesting that protons adversely affect the inhibitory activity of UBP792 (Figure 5.6). Also, there was no change in inhibitory activity of UBP792 at GluN2D receptors co-expressed with GluN1-1a or GluN1-1b splice forms. Both of these findings indicate that the mechanism of inhibition by UBP792 is different from the mechanism of inhibition by ifenprodil (Mott, Doherty

et al. 1998, Pahk, Williams 1997) and other GluN2B-selective NAMs such as 93-31 (Yuan, Myers et al. 2015).

We also found from this study that PAMs (e.g. UBP684) and NAMs have distinct binding sites (Figure 5.7). Interestingly, the PAM UBP684 even enhances the inhibitory potency of the NAM UBP792. It is possible that the binding of PAM may change the conformation of the NAM binding pocket and may increase the access of NAM to its binding site, thereby enhancing the activity.

This study also shows that UBP792 activity requires a conformational change in the GluN2, but not in GluN1, LBD. Thus, we suggest that UBP792 stabilizes the open conformation of the GluN2 LBD (Figure 5.8). It is possible that by stabilizing the GluN2 LBD, it may facilitate glutamate dissociation and receptor deactivation by a mechanism similar to that by which MPX-007 facilitates the glycine dissociation from GluN1 LBD causing receptor deactivation (Yi, Mou et al. 2016).

The possible binding sites and mechanisms of action of other subtype-selective NAMs have also been reported. QNZ46 is a quinazolin derivative with GluN2C/2D-specific NAM activity (Mosley, Acker et al. 2010). It requires the binding of L-glutamate for activity and is thought to bind at the LBD near the TMD (Hansen, Traynelis 2011) close to the possible binding site of CIQ, a GluN2C-PAM. Also, DQP-1105 is another GluN2C/2D-selective NAM which is also thought to bind, from mutagenesis study of GluN2D receptor, at the S2 domain (Acker, Yuan et al. 2011). TCN-201 and TCN-213 are GluN2A-selective NAMs (Bettini, Sava et al. 2010) and are thought to bind at the heterodimer interface of ligand binding domains (LBDs) of GluN1/GluN2A receptors (Bettini, Sava et al. 2010). TCN201 acts through the glycine binding site in a non-competitive manner (Edman, McKay et al. 2012).

We have also identified NAMs displaying greater subunit-selectivity. Compound UBP608, a coumarin carboxylic acid derivative, inhibits GluN2A receptors with 23-fold selectivity compared to GluN2D-containing receptors (Costa, Irvine et al. 2010) and 4-methyl substitution of this compound makes it a PAM from NAM (UBP 714) (Irvine, Costa et al. 2012). Other general NAMs developed from our group are UBP618 and UBP552, naphthalene derivatives, which are relatively potent NAMs (Costa, Irvine et al. 2012). UBP552 has an IC_{50} in the range of 3-7 μM and UBP618, has an IC_{50} of ~ 2 μM at each of the four NMDAR subtypes (Costa, Irvine et al. 2012). We expect that these previously described compounds share similar binding sites and mechanism of action with those described here for UBP684, UBP753 and UBP792. However, we found that the GluN2A PAM UBP512 could non-competitively inhibit the PAM activity of UBP684. This may indicate that there are two distinct PAM binding sites or that UBP512 also has NAM activity at NAM binding site that is completely inhibiting UBP684's PAM activity.

This study provides mechanistic insight into UBP792 inhibition at NMDARs. Although it is not highly selective for a particular subtype of NMDARs, its limited selectivity for GluN2C- and GluN2D-containing receptors should make it useful for studying the function of these receptors and provide opportunities for the discovery of future allosteric modulators with better potency and selectivity.

Chapter 6 Discussion and conclusions

In this dissertation research, we first evaluated the role of the GluN2D subunit in an acute animal model of schizophrenia. We studied the effect of acute administration of ketamine on different aspects of behavior and neurological functions, which are thought to be correlated to neuropathological changes seen in schizophrenia. We found that GluN2D plays an important role in most, but not in all, of the behavioral and neuropathological assays we tested. Ketamine-induced hyperactivation of prefrontal cortex required GluN2D subunits. This was supported by a c-FOS experiment as well as by the $[^{14}C]$-2-DG-uptake assay. This might be due to the result of ketamine blockade of NMDARs in inhibitory interneurons, especially PV-containing neurons in the cortex thereby causing disinhibition of pyramidal cell firing which is reflected by an increase in $[^{14}C]$-2-DG-uptake. It is also possible that ketamine may block NMDARs in inhibitory neurons in the thalamus which disinhibit the thalamic excitatory cells projecting to cortex. In both of these scenarios, there is increased prefrontal cortical activity. It is well known that ketamine and other non-competitive NMDAR blockers like MK-801 and PCP cause schizophrenia-like symptoms in animals. However, ketamine and PCP are not able to increase the locomotory activity in GluN2D-KO mice. Since, ketamine-induced locomotor activity is thought to correspond to the positive symptoms of schizophrenia, the absence of ketamine-induced activity in the GluN2D-KO mice suggests an important role for GluN2D subunits in the positive symptoms of schizophrenia. This might be either due to blockade of NMDARs in substantia nigra, which leads to disinhibition of dopaminergic cells projecting to striatum or by controlling other dopaminergic pathways. Consistent with this possibilities, others have shown that the GluN2D-KO mouse has a reduction in PCP-induced dopamine release (Hagino, Kasai et al. 2010).

The observation that mice lacking GluN2D subunits have defective memory retrieval suggests their importance in cognition and memory, which is also impaired in schizophrenics. Also, PV cells, which are found to be reduced in schizophrenics in the DLPFC and other brain areas were also reduced in mice lacking GluN2D. However, we did not see any role of GluN2D

in sensorimotor gating function (prepulse inhibition). Taken together, the findings in Chapter 1 imply that GluN2D subunit-containing NMDARs play an important role in regulating neurological, behavioral as well as memory functions impaired in schizophrenia. Enhancing NMDAR function, especially GluN2D subunit-mediated NMDAR function, by use of allosteric modulators may thus be therapeutically beneficial. Hence, research in subsequent chapters was focused on identifying novel NMDAR modulators with enhanced potency and selectivity.

The SAR studies (Chapter 3), revealed that the 2-position carboxyl group is critical for PAM activity of naphthalene derivatives. A 5-6 carbon chain length of the alkyl side-chain at the 6-position of naphthoic acid is optimal for PAM activity. Heteroatoms cannot be accommodated in the naphthalene ring and still retain PAM activity. If we substitute the naphthalene ring at 7-position of a PAM compound with a styryl group, it changes the property of the compound to a NAM. UBP684 and UBP753 were compounds with robust PAM activity and UBP792 with subtype-selective NAM activity in this series of 2-naphthoic acid derivatives. For both PAMs and NAMs we identified regions which tolerate substitutions. Future discoveries will target these allowed spaces. Also, we identified improved GluN2C- and GluN2D-selective derivatives of PPDA and UBP141 that are competitive antagonists. UBP791 is now the most GluN2C/GluN2D-selective competitive antagonist known. From this chapter, we obtained SAR properties of compounds for NAM, PAM and competitive antagonism.

From the PAM mechanism study (Chapter 4), we found that the PAMs enhance the NMDAR response by increasing agonist efficacy and slightly increasing the affinity of glutamate and glycine for NMDARs in a subunit-dependent manner. The activity of these PAMs is not affected by membrane voltage. Their binding does not change the conformation of channel pore as revealed by the ketamine concentration-response study. PAMs are able to potentiate even when the redox state of the receptor is changed. Thus, their mechanism of potentiation is different from that seen by redox agents. UBP684/UBP753 enhance the NMDAR current by increasing the open

probability of NMDARs and also by slowing down the dissociation of glutamate from its binding site (or the subsequent conformational change). Mainly, these PAMs stabilize the GluN2 conformation of the receptors in an active conformation (LBD-closed conformation). Consistent with this idea, molecular docking studies with UBP684 show that it can be docked in the inter-dimer space in the GluN1/GluN2A LBD with its alkyl chain terminating close to the hinge region. This site is similar to the site for the GluN2A-selective potentiator (GNE-6901) as revealed by crystallography (Hackos, Lupardus et al. 2016). This docking is consistent with our finding of slow glutamate dissociation/deactivation in the presence of UBP684 as well as reduced potentiation by UBP684 in GluN2A^c (LBD-locked) receptors.

The findings from this chapter also reveal that these compounds decrease the sensitivity to proton inhibition. However, their mechanism of action is not by relieving proton inhibition in the manner shown in spermine potentiation. We found that the extracellular proton concentration controls PAM activity in a subunit-dependent manner. We also observed that the GluN1 but not the GluN2A C-terminal was important for UBP684-induced PAM activity. We also observed that intracellular calcium is necessary for the PAM activity in GluN2A but not in GluN2B receptors. Also, the activation of PKC increases PAM activity indicating that PAM activity is at least partially PKC phosphorylation-dependent. Taken together, these studies suggest that the intracellular environment can alter the conformation of the transmembrane domains and in turn alter PAM activity and/or PAM binding. This is not surprising given that PKC, PKA and Ca^{2+} can alter the response of NMDARs to agonists.

From the NAM mechanism study (Chapter 5), we found that NAMs decrease the NMDAR response by reducing the efficacy and affinity of agonists. These NAMs are more potent at high agonist concentration and at high pH. The activity of these NAMs were adversely affected by proton concentration. Unfortunately, this property means that these NAMs loose inhibitory activity in acidic pathological conditions such as stroke. UBP792 may be binding near

a cluster of pH-sensitive residues near the channel gating mechanism as proposed for neurosteroids. Like PAMs, NAM activity was also not affected by a change in membrane potential and they do not compete with PAMs for binding to the NMDAR complex. Indeed, in a related family of ligand-gated ion channels known as AMPA receptors, negative allosteric modulators are thought to bind at a site at the top of transmembrane regions 1 and 4 (Balannik, Menniti et al. 2005, Sobolevsky, Rosconi et al. 2009) and an equivalent binding site may exist in NMDARs. However, it is also possible that they may bind to the PAM binding site. It has been reported that a GluN2A inhibitor binds at a similar site to potentiators at the dimer interface of the LBDs of GluN1/GluN2A, with the major difference being that the conformation of Y535 on GluN1 is different in the two sites (Hackos, Lupardus et al. 2016).

PAMs and NAMs discovered in this research have various potential therapeutic applications. PAMs may be useful in enhancing NMDAR function in a disease like schizophrenia and, perhaps, depression. Similarly, NAMs may help in protecting against neurological damage caused by excessive activation of NMDARs such as in stroke and traumatic brain injury. Studies have shown that GluN2D plays a role in tissue plasminogen activator (tPA)-induced stroke damage (Jullienne, Montagne et al. 2011). Hence GluN2D-preferring NAMs such as UBP792 should be useful in protecting from such damage. These GluN2C/GluN2D NAMs should also be useful in neuropathic pain since GluN2D receptors are also involved in pain pathways (Shiokawa, Kaftan et al. 2010, Tong, Kaftan et al. 2008).

Since these allosteric modulators bind to sites different from the highly conserved ligand binding sites and the receptor's channel pore, it may be possible to develop a modulator with yet greater subtype-selectivity. Also, different modulators offer different unique properties. For example, some modulators show high activity at reduced agonist concentration, which would be useful in regulating tonically-activated NMDARs only. Some modulators display high activity at the reduced pH, such modulators would therefore be more effective in the treatment of

pathological conditions which are associated with acidification of the brain tissue. Also, these modulators can have different maximal effects. For example, UBP792 and other NAMs show partial maximal inhibition of NMDAR response which therefore will help in reducing the side effects caused by maximum blockade of NMDARs by full antagonists. Since modulators offer better selectivity, we can control the activity of only certain subtypes and not affect the function of others. Modulators which enhance the NMDAR activity can also be used for cognitive enhancement as well (Collingridge, Volianskis et al. 2013). Overexpression of GluN2B receptors in mouse forebrain causes enhancement of memory and cognition (Tang, Shimizu et al. 1999). Another study also shows that increasing the GluN2B receptors expression in frontal lobe and hippocampus improves the memory in aged mice (Brim, Haskell et al. 2013). Enhancing GluN2C and GluN2D receptors function by use of a PAM improves MK-801-induced impairment in working memory (Suryavanshi, Ugale et al. 2014). Thus, GluN2B PAMs should be beneficial for improving memory and GluN2C/GluN2D PAMs may be beneficial for treating cognitive deficits seen in schizophrenia.

From this study, we identified prototype PAMs (UBP684/UBP753), NAMs (UBP792) and competitive antagonists (UBP791) and studied their mechanisms of action and different intra- and extra-cellular factors affecting their activity *in vitro*. Future studies should be focused on identifying the binding sites of these modulators. Although, our preliminary data indicate that they are possibly binding at the interface of GluN1/GluN2 LBD dimers, it is still possible that they may be binding to the regions near the membrane where CIQ (Ogden, Traynelis 2013) or neurosteroids are also thought to be bound (Kostakis, Jang et al. 2011). By carrying out a chimera/mutagenesis study, we should be able to find the location of the binding site and the amino acid residues important for their activity. If the binding site of these modulators is on GluN1 receptors, it may be difficult to develop compounds with subunit selectivity. However, if the binding site is on the GluN2 subunit, it may be possible to develop compounds with greater

selectivity. Our finding also suggests that there may be multiple binding sites for these modulators and they may display both PAM and NAM activity by binding to these different sites. Thus, the SAR information we have obtained is confounded by these factors. For example, if we observe an enhanced PAM activity of a compound by modification of certain structural features, it does not necessarily mean that the modification increased the PAM activity. It is possible that the modification could have resulted in a compound with less inhibitory activity.

The existence of native NMDARs in triheteromeric arrangements makes it important to test these modulators at triheteromeric NMDARs. The activity of these modulators at diheteromeric NMDARs might not be the same in triheteromeric receptors. For example, the inhibition by NAM UBP792 at GluN1/GluN2B/GluN2D containing heteromeric receptors could be different from inhibition at GluN1/GluN2B or GluN1/GluN2D-containing receptors. In addition, these compounds should be tested for their activity in neurons.

It will be interesting to test the PAM compounds with GluN2D receptors selectivity (e.g. UBP551) *in vivo* to determine if they are able to rescue the schizophrenia-like behavioral, cognitive and neuropathological deficits in a mouse model of schizophrenia. We anticipate from the findings in Chapter 2 that pretreatment of mice with UBP551 would reverse the behavioral deficits observed in mice with schizophrenia phenotype. However, it should be noted that UBP551 not only has GluN2D-PAM activity, but also has GluN2A-C NAM activity, which may affect the outcome of results. We are still developing other new compounds for PAM activity, especially at GluN2D receptors, utilizing the information obtained from Chapter 3. Our ultimate goal is to test a GluN2D specific PAM in a mouse model of schizophrenia.

This study reveals the importance of GluN2D subunit in schizophrenia-like behavior and neuropathology. Experimental findings from the SAR studies will help in designing selective PAMs and NAMs in future. We were able to develop efficacious general NMDAR PAMs,

GluN2C/GluN2D-preferring NAMs and potent GluN2C/GluN2D-preferring glutamate-site acting competitive antagonists. These agents can be used as experimental tools to further define the function of NMDAR subtypes. Unique mechanisms of NMDARs modulation by these PAMs and NAMs have been identified. These findings too will aid in future studies involved in drug design and development for the treatment of neurological diseases.

References

ABDUL-MONIM, Z., NEILL, J. and REYNOLDS, G., 2007. Sub-chronic psychotomimetic phencyclidine induces deficits in reversal learning and alterations in parvalbumin-immunoreactive expression in the rat. *Journal of Psychopharmacology,* **21**(2), pp. 198-205.

ABEKAWA, T., ITO, K., NAKAGAWA, S. and KOYAMA, T., 2007. Prenatal exposure to an NMDA receptor antagonist, MK-801 reduces density of parvalbumin-immunoreactive GABAergic neurons in the medial prefrontal cortex and enhances phencyclidine-induced hyperlocomotion but not behavioral sensitization to methamphetamine in postpubertal rats. *Psychopharmacology,* **192**(3), pp. 303-316.

ABEL, K.M., ALLIN, M.P., HEMSLEY, D.R. and GEYER, M.A., 2003. Low dose ketamine increases prepulse inhibition in healthy men. *Neuropharmacology,* **44**(6), pp. 729-737.

ACKER, T.M., YUAN, H., HANSEN, K.B., VANCE, K.M., OGDEN, K.K., JENSEN, H.S., BURGER, P.B., MULLASSERIL, P., SNYDER, J.P., LIOTTA, D.C. and TRAYNELIS, S.F., 2011. Mechanism for noncompetitive inhibition by novel GluN2C/D N-methyl-D-aspartate receptor subunit-selective modulators. *Molecular Pharmacology,* **80**(5), pp. 782-795.

ADAGE, T., TRILLAT, A., QUATTROPANI, A., PERRIN, D., CAVAREC, L., SHAW, J., GUERASSIMENKO, O., GIACHETTI, C., GRÉCO, B. and CHUMAKOV, I., 2008. *In vitro* and *in vivo* pharmacological profile of AS057278, a selective d-amino acid oxidase inhibitor with potential anti-psychotic properties. *European Neuropsychopharmacology,* **18**(3), pp. 200-214.

ALLEN, N.C., BAGADE, S., MCQUEEN, M.B., IOANNIDIS, J.P., KAVVOURA, F.K., KHOURY, M.J., TANZI, R.E. and BERTRAM, L., 2008. Systematic meta-analyses and field synopsis of genetic association studies in schizophrenia: the SzGene database. *Nature Genetics,* **40**(7), pp. 827-834.

ANIS, N., BERRY, S., BURTON, N. and LODGE, D., 1983. The dissociative anaesthetics, ketamine and phencyclidine, selectively reduce excitation of central mammalian neurones by N-methyl-aspartate. *British Journal of Pharmacology,* **79**(2), pp. 565-575.

ARANDA, P.S., LAJOIE, D.M. and JORCYK, C.L., 2012. Bleach gel: a simple agarose gel for analyzing RNA quality. *Electrophoresis,* **33**(2), pp. 366-369.

ARUNLAKSHANA, O. and SCHILD, H., 1959. Some quantitative uses of drug antagonists. *British Journal of Pharmacology and Chemotherapy,* **14**(1), pp. 48-58.

ASCHER, P. and NOWAK, L., 1988. The role of divalent cations in the N-methyl-D-aspartate responses of mouse central neurones in culture. *The Journal of Physiology,* **399**, pp. 247-266.

AUBERSON, Y.P., ALLGEIER, H., BISCHOFF, S., LINGENHOEHL, K., MORETTI, R. and SCHMUTZ, M., 2002. 5-Phosphonomethylquinoxalinediones as competitive NMDA receptor antagonists with a preference for the human 1A/2A, rather than 1A/2B receptor composition. *Bioorganic & Medicinal Chemistry Letters,* **12**(7), pp. 1099-1102.

AWOBULUYI, M., YANG, J., YE, Y., CHATTERTON, J.E., GODZIK, A., LIPTON, S.A. and ZHANG, D., 2007. Subunit-specific roles of glycine-binding domains in activation of NR1/NR3 N-methyl-D-aspartate receptors. *Molecular Pharmacology,* **71**(1), pp. 112-122.

BALANNIK, V., MENNITI, F.S., PATERNAIN, A.V., LERMA, J. and STERN-BACH, Y., 2005. Molecular mechanism of AMPA receptor noncompetitive antagonism. *Neuron,* **48**(2), pp. 279-288.

BALU, D.T. and COYLE, J.T., 2011. Neuroplasticity signaling pathways linked to the pathophysiology of schizophrenia. *Neuroscience & Biobehavioral Reviews,* **35**(3), pp. 848-870.

BARTOS, M., VIDA, I. and JONAS, P., 2007. Synaptic mechanisms of synchronized gamma oscillations in inhibitory interneuron networks. *Nature Reviews Neuroscience,* **8**(1), pp. 45-56.

BEASLEY, C.L. and REYNOLDS, G.P., 1997. Parvalbumin-immunoreactive neurons are reduced in the prefrontal cortex of schizophrenics. *Schizophrenia Research,* **24**(3), pp. 349-355.

BEATON, J., STEMSRUD, K. and MONAGHAN, D.T., 1992. Identification of a Novel N-Methyl-D-Aspartate Receptor Population in the Rat Medial Thalamus. *Journal of Neurochemistry,* **59**(2), pp. 754-757.

BEHRENS, M.M., ALI, S.S., DAO, D.N., LUCERO, J., SHEKHTMAN, G., QUICK, K.L. and DUGAN, L.L., 2007. Ketamine-induced loss of phenotype of fast-spiking interneurons is mediated by NADPH-oxidase. *Science,* **318**(5856), pp. 1645-1647.

BELFORTE, J.E., ZSIROS, V., SKLAR, E.R., JIANG, Z., YU, G., LI, Y., QUINLAN, E.M. and NAKAZAWA, K., 2009. Postnatal NMDA receptor ablation in corticolimbic interneurons confers schizophrenia-like phenotypes. *Nature Neuroscience,* **13**(1), pp. 76-83.

BENES, F.M. and BERRETTA, S., 2001. GABAergic interneurons: implications for understanding schizophrenia and bipolar disorder. *Neuropsychopharmacology,* **25**(1), pp. 1-27.

BENKE, D., HONER, M., HECKENDORN, R., POZZA, M.F., ALLGEIER, H., ANGST, C. and MOHLER, H., 1999. [3 H] CGP 61594, the first photoaffinity ligand for the glycine site of NMDA receptors. *Neuropharmacology,* **38**(2), pp. 233-242.

BENNEYWORTH, M.A., ROSEMAN, A.S., BASU, A.C. and COYLE, J.T., 2011. Failure of NMDA receptor hypofunction to induce a pathological reduction in PV-positive GABAergic cell markers. *Neuroscience Letters,* **488**(3), pp. 267-271.

BENVENISTE, H., DREJER, J., SCHOUSBOE, A. and DIEMER, N.H., 1984. Elevation of the extracellular concentrations of glutamate and aspartate in rat hippocampus during transient cerebral ischemia monitored by intracerebral microdialysis. *Journal of Neurochemistry,* **43**(5), pp. 1369-1374.

BENVENISTE, M. and MAYER, M., 1993. Multiple effects of spermine on N-methyl-D-aspartic acid receptor responses of rat cultured hippocampal neurones. *The Journal of Physiology,* **464**(1), pp. 131-163.

BERNSTEIN, H., KRAUSE, S., KRELL, D., DOBROWOLNY, H., WOLTER, M., STAUCH, R., RANFT, K., DANOS, P., JIRIKOWSKI, G.F. and BOGERTS, B., 2007. Strongly Reduced Number of Parvalbumin-Immunoreactive Projection Neurons in the Mammillary Bodies in Schizophrenia. *Annals of the New York Academy of Sciences,* **1096**(1), pp. 120-127.

BETTINI, E., SAVA, A., GRIFFANTE, C., CARIGNANI, C., BUSON, A., CAPELLI, A.M., NEGRI, M., ANDREETTA, F., SENAR-SANCHO, S.A., GUIRAL, L. and CARDULLO, F., 2010. Identification and characterization of novel NMDA receptor antagonists selective for NR2A- over NR2B-containing receptors. *The Journal of Pharmacology and Experimental Therapeutics,* **335**(3), pp. 636-644.

BICKEL, S., LIPP, H. and UMBRICHT, D., 2007. Impaired attentional modulation of auditory evoked potentials in N-methyl-d-aspartate NR1 hypomorphic mice. *Genes, Brain and Behavior,* **6**(6), pp. 558-568.

BILLINGSLEA, E.N., TATARD-LEITMAN, V.M., ANGUIANO, J., JUTZELER, C.R., SUH, J., SAUNDERS, J.A., MORITA, S., FEATHERSTONE, R.E., ORTINSKI, P.I. and GANDAL, M.J., 2014. Parvalbumin cell ablation of NMDA-R1 causes increased resting network excitability with associated social and self-care deficits. *Neuropsychopharmacology,* **39**(7), pp. 1603-1613.

BISCOE, T., EVANS, R., FRANCIS, A., MARTIN, M. and WATKINS, J., 1977. D-alpha-Aminoadipate as a selective antagonist of amino acid-induced and synaptic excitation of mammalian spinal neurones. *Nature,* **270**, pp. 743-745.

BLISS, T.V. and COLLINGRIDGE, G.L., 1993. A synaptic model of memory: long-term potentiation in the hippocampus. *Nature,* **361**(6407), pp. 31-39.

BRICKLEY, S.G., MISRA, C., MOK, M.H., MISHINA, M. and CULL-CANDY, S.G., 2003. NR2B and NR2D subunits coassemble in cerebellar Golgi cells to form a distinct NMDA receptor subtype restricted to extrasynaptic sites. *The Journal of Neuroscience,* **23**(12), pp. 4958-4966.

BRIM, B., HASKELL, R., AWEDIKIAN, R., ELLINWOOD, N., JIN, L., KUMAR, A., FOSTER, T. and MAGNUSSON, K., 2013. Memory in aged mice is rescued by enhanced expression of the GluN2B subunit of the NMDA receptor. *Behavioural Brain Research,* **238**, pp. 211-226.

BROTHWELL, S., BARBER, J., MONAGHAN, D.T., JANE, D., GIBB, A. and JONES, S., 2008. NR2B-and NR2D-containing synaptic NMDA receptors in developing rat substantia nigra pars compacta dopaminergic neurones. *The Journal of Physiology,* **586**(3), pp. 739-750.

BULLER, A.L. and MONAGHAN, D.T., 1997. Pharmacological heterogeneity of NMDA receptors: characterization of NR1a/NR2D heteromers expressed in Xenopus oocytes. *European Journal of Pharmacology,* **320**(1), pp. 87-94.

BULLER, A.L., LARSON, H.C., SCHNEIDER, B.E., BEATON, J.A., MORRISETT, R.A. and MONAGHAN, D.T., 1994. The molecular basis of NMDA receptor subtypes: native receptor diversity is predicted by subunit composition. *The Journal of Neuroscience,* **14**(9), pp. 5471-5484.

BULLOCK, W.M., BOLOGNANI, F., BOTTA, P., VALENZUELA, C.F. and PERRONE-BIZZOZERO, N.I., 2009. Schizophrenia-like GABAergic gene expression deficits in cerebellar Golgi cells from rats chronically exposed to low-dose phencyclidine. *Neurochemistry International,* **55**(8), pp. 775-782.

CAO, X., CUI, Z., FENG, R., TANG, Y., QIN, Z., MEI, B. and TSIEN, J.Z., 2007. Maintenance of superior learning and memory function in NR2B transgenic mice during ageing. *European Journal of Neuroscience,* **25**(6), pp. 1815-1822.

CARDIN, J.A., CARLÉN, M., MELETIS, K., KNOBLICH, U., ZHANG, F., DEISSEROTH, K., TSAI, L. and MOORE, C.I., 2009. Driving fast-spiking cells induces gamma rhythm and controls sensory responses. *Nature,* **459**(7247), pp. 663-667.

CARLEN, M., MELETIS, K., SIEGLE, J., CARDIN, J., FUTAI, K., VIERLING-CLAASSEN, D., RUEHLMANN, C., JONES, S.R., DEISSEROTH, K. and SHENG, M., 2011. A critical role for NMDA receptors in parvalbumin interneurons for gamma rhythm induction and behavior. *Molecular Psychiatry,* **17**(5), pp. 537-548.

CAVARA, N.A., ORTH, A. and HOLLMANN, M., 2009. Effects of NR1 splicing on NR1/NR3B-type excitatory glycine receptors. *BMC Neuroscience,* **10**(1), pp. 1.

CECCON, M., RUMBAUGH, G. and VICINI, S., 2001. Distinct effect of pregnenolone sulfate on NMDA receptor subtypes. *Neuropharmacology,* **40**(4), pp. 491-500.

CHANG, H. and KUO, C., 2008. Molecular determinants of the anticonvulsant felbamate binding site in the N-methyl-D-aspartate receptor. *Journal of Medicinal Chemistry,* **51**(6), pp. 1534-1545.

CHATTERTON, J.E., AWOBULUYI, M., PREMKUMAR, L.S., TAKAHASHI, H., TALANTOVA, M., SHIN, Y., CUI, J., TU, S., SEVARINO, K.A. and NAKANISHI, N., 2002. Excitatory glycine receptors containing the NR3 family of NMDA receptor subunits. *Nature,* **415**(6873), pp. 793-798.

CHAZOT, P.L. and STEPHENSON, F.A., 1997. Molecular dissection of native mammalian forebrain NMDA receptors containing the NR1 C2 exon: direct demonstration of NMDA receptors comprising NR1, NR2A, and NR2B subunits within the same complex. *Journal of Neurochemistry,* **69**(5), pp. 2138-2144.

CHEN, H.S. and LIPTON, S.A., 2005. Pharmacological implications of two distinct mechanisms of interaction of memantine with N-methyl-D-aspartate-gated channels. *The Journal of Pharmacology and Experimental Therapeutics,* **314**(3), pp. 961-971.

CHEN, N., MOSHAVER, A. and RAYMOND, L.A., 1997. Differential sensitivity of recombinant N-methyl-D-aspartate receptor subtypes to zinc inhibition. *Molecular Pharmacology,* **51**(6), pp. 1015-1023.

CHERIYAN, J., BALSARA, R.D., HANSEN, K.B. and CASTELLINO, F.J., 2016. Pharmacology of triheteromeric N-Methyl-d-Aspartate Receptors. *Neuroscience Letters,* **617**, pp. 240-246.

CHOI, D.W., 1992. Excitotoxic cell death. *Journal of Neurobiology,* **23**(9), pp. 1261-1276.

CHOI, D.W., 1988. Glutamate neurotoxicity and diseases of the nervous system. *Neuron,* **1**(8), pp. 623-634.

CHOI, D.W., MAULUCCI-GEDDE, M. and KRIEGSTEIN, A.R., 1987. Glutamate neurotoxicity in cortical cell culture. *The Journal of Neuroscience,* **7**(2), pp. 357-368.

CHOPRA, D.A., MONAGHAN, D.T. and DRAVID, S.M., 2015. Bidirectional Effect of Pregnenolone Sulfate on GluN1/GluN2A N-Methyl-D-Aspartate Receptor Gating Depending on Extracellular Calcium and Intracellular Milieu. *Molecular Pharmacology,* **88**(4), pp. 650-659.

CIABARRA, A.M., SULLIVAN, J.M., GAHN, L.G., PECHT, G., HEINEMANN, S. and SEVARINO, K.A., 1995. Cloning and characterization of chi-1: a developmentally regulated member of a novel class of the ionotropic glutamate receptor family. *The Journal of Neuroscience,* **15**(10), pp. 6498-6508.

CLINTON, S.M., HAROUTUNIAN, V., DAVIS, K.L. and MEADOR-WOODRUFF, J.H., 2003. Altered transcript expression of NMDA receptor-associated postsynaptic proteins in the thalamus of subjects with schizophrenia. *American Journal of Psychiatry,* **160**(6), pp. 1100-1109.

CLINTON, S.M. and MEADOR-WOODRUFF, J.H., 2004. Abnormalities of the NMDA Receptor and Associated Intracellular Molecules in the Thalamus in Schizophrenia and Bipolar Disorder. *Neuropsychopharmacology,* **29**(7), pp. 1353-1362.

COLGIN, L.L., DENNINGER, T., FYHN, M., HAFTING, T., BONNEVIE, T., JENSEN, O., MOSER, M. and MOSER, E.I., 2009. Frequency of gamma oscillations routes flow of information in the hippocampus. *Nature,* **462**(7271), pp. 353-357.

COLLINGRIDGE, G.L., ISAAC, J.T. and WANG, Y.T., 2004. Receptor trafficking and synaptic plasticity. *Nature Reviews Neuroscience,* **5**(12), pp. 952-962.

COLLINGRIDGE, G.L., OLSEN, R.W., PETERS, J. and SPEDDING, M., 2009. A nomenclature for ligand-gated ion channels. *Neuropharmacology,* **56**(1), pp. 2-5.

COLLINGRIDGE, G.L., VOLIANSKIS, A., BANNISTER, N., FRANCE, G., HANNA, L., MERCIER, M., TIDBALL, P., FANG, G., IRVINE, M.W. and COSTA, B.M., 2013. The NMDA receptor as a target for cognitive enhancement. *Neuropharmacology,* **64**, pp. 13-26.

COLQUHOUN, D., 2007. Why the Schild method is better than Schild realised. *Trends in Pharmacological Sciences,* **28**(12), pp. 608-614.

COMPAGNONE, N.A. and MELLON, S.H., 2000. Neurosteroids: biosynthesis and function of these novel neuromodulators. *Frontiers in Neuroendocrinology,* **21**(1), pp. 1-56.

CONN, P.J. and PIN, J., 1997. Pharmacology and functions of metabotropic glutamate receptors. *Annual Review of Pharmacology and Toxicology,* **37**(1), pp. 205-237.

COSTA, B.M., IRVINE, M.W., FANG, G., EAVES, R.J., MAYO-MARTIN, M.B., LAUBE, B., JANE, D.E. and MONAGHAN, D.T., 2012. Structure-activity relationships for allosteric NMDA receptor inhibitors based on 2-naphthoic acid. *Neuropharmacology,* **62**(4), pp. 1730-1736.

COSTA, B.M., FENG, B., TSINTSADZE, T.S., MORLEY, R.M., IRVINE, M.W., TSINTSADZE, V., LOZOVAYA, N.A., JANE, D.E. and MONAGHAN, D.T., 2009. N-methyl-D-aspartate (NMDA) receptor NR2 subunit selectivity of a series of novel piperazine-2,3-dicarboxylate derivatives: preferential blockade of extrasynaptic NMDA receptors in the rat hippocampal CA3-CA1 synapse. *The Journal of Pharmacology and Experimental Therapeutics,* **331**(2), pp. 618-626.

COSTA, B.M., IRVINE, M.W., FANG, G., EAVES, R.J., MAYO-MARTIN, M.B., SKIFTER, D.A., JANE, D.E. and MONAGHAN, D.T., 2010. A novel family of negative and positive allosteric modulators of NMDA receptors. *The Journal of Pharmacology and Experimental Therapeutics,* **335**(3), pp. 614-621.

COYLE, J.T., 2006. Glutamate and schizophrenia: beyond the dopamine hypothesis. *Cellular and Molecular Neurobiology,* **26**(4-6), pp. 363-382.

COYLE, J.T. and TSAI, G., 2004. NMDA receptor function, neuroplasticity, and the pathophysiology of schizophrenia. *International Review of Neurobiology,* **59**, pp. 491-515.

COYLE, J.T., TSAI, G. and GOFF, D., 2003. Converging evidence of NMDA receptor hypofunction in the pathophysiology of schizophrenia. *Annals of the New York Academy of Sciences,* **1003**(1), pp. 318-327.

CURTIS, D.R. and WATKINS, J.C., 1963. Acidic amino acids with strong excitatory actions on mammalian neurones. *The Journal of Physiology,* **166**, pp. 1-14.

DAI, J. and ZHOU, H., 2013. An NMDA receptor gating mechanism developed from MD simulations reveals molecular details underlying subunit-specific contributions. *Biophysical Journal,* **104**(10), pp. 2170-2181.

DAVIES, J., EVANS, R., HERRLING, P., JONES, A., OLVERMAN, H., POOK, P. and WATKINS, J., 1986. CPP, a new potent and selective NMDA antagonist. Depression of central neuron responses, affinity for [3 H] D-AP5 binding sites on brain membranes and anticonvulsant activity. *Brain Research,* **382**(1), pp. 169-173.

DAVIES, J. and WATKINS, J.C., 1979. Selective antagonism of amino acid-induced and synaptic excitation in the cat spinal cord. *The Journal of Physiology,* **297**(0), pp. 621-635.

DAVIS, J.M., CHEN, N. and GLICK, I.D., 2003. A meta-analysis of the efficacy of second-generation antipsychotics. *Archives of General Psychiatry,* **60**(6), pp. 553-564.

DAVIS, K.L., KAHN, R.S., KO, G. and DAVIDSON, M., 1991. Dopamine in schizophrenia: a review and reconceptualization. *The American Journal of Psychiatry,* **148**(11), pp. 1474-1486.

DINGLEDINE, R., BORGES, K., BOWIE, D. and TRAYNELIS, S.F., 1999. The glutamate receptor ion channels. *Pharmacological Reviews,* **51**(1), pp. 7-62.

DOISCHER, D., HOSP, J.A., YANAGAWA, Y., OBATA, K., JONAS, P., VIDA, I. and BARTOS, M., 2008. Postnatal differentiation of basket cells from slow to fast signaling devices. *The Journal of Neuroscience,* **28**(48), pp. 12956-12968.

DRACHEVA, S., MARRAS, S.A., ELHAKEM, S.L., KRAMER, F.R., DAVIS, K.L. and HAROUTUNIAN, V., 2001. N-methyl-D-aspartic acid receptor expression in the dorsolateral prefrontal cortex of elderly patients with schizophrenia. *American Journal of Psychiatry,* **158**(9), pp. 1400-1410.

DRAVID, S.M., ERREGER, K., YUAN, H., NICHOLSON, K., LE, P., LYUBOSLAVSKY, P., ALMONTE, A., MURRAY, E., MOSLEY, C. and BARBER, J., 2007. Subunit-specific mechanisms and proton sensitivity of NMDA receptor channel block. *The Journal of Physiology,* **581**(1), pp. 107-128.

DUAN, A.R., VARELA, C., ZHANG, Y., SHEN, Y., XIONG, L., WILSON, M.A. and LISMAN, J., 2015. Delta frequency optogenetic stimulation of the thalamic nucleus reuniens is sufficient to produce working memory deficits: relevance to schizophrenia. *Biological Psychiatry,* **77**(12), pp. 1098-1107.

DUNCAN, G.E., MIYAMOTO, S., GU, H., LIEBERMAN, J.A., KOLLER, B.H. and SNOUWAERT, J.N., 2002. Alterations in regional brain metabolism in genetic and pharmacological models of reduced NMDA receptor function. *Brain Research,* **951**(2), pp. 166-176.

DUNCAN, G.E., MIYAMOTO, S., LEIPZIG, J.N. and LIEBERMAN, J.A., 1999. Comparison of brain metabolic activity patterns induced by ketamine, MK-801 and amphetamine in rats: support for NMDA receptor involvement in responses to subanesthetic dose of ketamine. *Brain Research,* **843**(1), pp. 171-183.

DUNCAN, G.E., MIYAMOTO, S., LEIPZIG, J.N. and LIEBERMAN, J.A., 2000. Comparison of the effects of clozapine, risperidone, and olanzapine on ketamine-induced alterations in regional brain metabolism. *Journal of Pharmacology and Experimental Therapeutics,* **293**(1), pp. 8-14.

DUNCAN, G.E., MOY, S.S., LIEBERMAN, J.A. and KOLLER, B.H., 2006. Effects of haloperidol, clozapine, and quetiapine on sensorimotor gating in a genetic model of reduced NMDA receptor function. *Psychopharmacology,* **184**(2), pp. 190-200.

DUNCAN, G.E., MOY, S.S., PEREZ, A., EDDY, D.M., ZINZOW, W.M., LIEBERMAN, J.A., SNOUWAERT, J.N. and KOLLER, B.H., 2004. Deficits in sensorimotor gating and tests of social behavior in a genetic model of reduced NMDA receptor function. *Behavioural Brain Research,* **153**(2), pp. 507-519.

DUNCAN, G.E., ZORN, S. and LIEBERMAN, J.A., 1999. Mechanisms of typical and atypical antipsychotic drug action in relation to dopamine and NMDA receptor hypofunction hypotheses of schizophrenia. *Molecular Psychiatry,* **4**(5), pp. 418-428.

DURAND, G.M., GREGOR, P., ZHENG, X., BENNETT, M.V., UHL, G.R. and ZUKIN, R.S., 1992. Cloning of an apparent splice variant of the rat N-methyl-D-aspartate receptor NMDAR1 with altered sensitivity to polyamines and activators of protein kinase C. *Proceedings of the National Academy of Sciences of the United States of America,* **89**(19), pp. 9359-9363.

EDMAN, S., MCKAY, S., MACDONALD, L., SAMADI, M., LIVESEY, M., HARDINGHAM, G. and WYLLIE, D., 2012. TCN 201 selectively blocks GluN2A-containing NMDARs in a GluN1 co-agonist dependent but non-competitive manner. *Neuropharmacology,* **63**(3), pp. 441-449.

EHLERS, M.D., ZHANG, S., BERNHARDT, J.P. and HUGANIR, R.L., 1996. Inactivation of NMDA receptors by direct interaction of calmodulin with the NR1 subunit. *Cell,* **84**(5), pp. 745-755.

EMNETT, C.M., EISENMAN, L.N., MOHAN, J., TAYLOR, A.A., DOHERTY, J.J., PAUL, S.M., ZORUMSKI, C.F. and MENNERICK, S., 2015. Interaction between positive allosteric modulators and trapping blockers of the NMDA receptor channel. *British Journal of Pharmacology,* **172**(5), pp. 1333-1347.

ENGELHARDT, J.V., BOCKLISCH, C., TÖNGES, L., HERB, A., MISHINA, M. and MONYER, H., 2015. GluN2D-containing NMDA receptors-mediate synaptic currents in hippocampal interneurons and pyramidal cells in juvenile mice. *Frontiers in Cellular Neuroscience,* **9**, pp. 95.

EVANS, R., FRANCIS, A., HUNT, K., OAKES, D. and WATKINS, J., 1979. Antagonism of excitatory amino acid-induced responses and of synaptic excitation in the isolated spinal cord of the frog. *British Journal of Pharmacology,* **67**(4), pp. 591-603.

EVANS, R., FRANCIS, A., JONES, A., SMITH, D. and WATKINS, J., 1982. The effects of a series of ω-phosphonic α-carboxylic amino acids on electrically evoked and excitant amino acid-induced responses in isolated spinal cord preparations. *British Journal of Pharmacology,* **75**(1), pp. 65-75.

EVANS, R., FRANCIS, A. and WATKINS, J., 1978. Mg2 -like selective antagonism of excitatory amino acid-induced responses by α, ε-diaminopimelic acid, D-α-maminoadipate and HA-966 in isolated spinal cord of frog and immature rat. *Brain Research,* **148**(2), pp. 536-542.

FADEN, A.I., DEMEDIUK, P., PANTER, S.S. and VINK, R., 1989. The role of excitatory amino acids and NMDA receptors in traumatic brain injury. *Science,* **244**(4906), pp. 798-800.

FARINA, A.N., BLAIN, K.Y., MARUO, T., KWIATKOWSKI, W., CHOE, S. and NAKAGAWA, T., 2011. Separation of domain contacts is required for heterotetrameric assembly of functional NMDA receptors. *The Journal of Neuroscience,* **31**(10), pp. 3565-3579.

FENG, B., MORLEY, R.M., JANE, D.E. and MONAGHAN, D.T., 2005. The effect of competitive antagonist chain length on NMDA receptor subunit selectivity. *Neuropharmacology,* **48**(3), pp. 354-359.

FENG, B., TSE, H.W., SKIFTER, D.A., MORLEY, R., JANE, D.E. and MONAGHAN, D.T., 2004. Structure–activity analysis of a novel NR2C/NR2D-preferring NMDA receptor antagonist: 1-(phenanthrene-2-carbonyl) piperazine-2, 3-dicarboxylic acid. *British Journal of Pharmacology,* **141**(3), pp. 508-516.

FIELDS, R.D., 2008. White matter in learning, cognition and psychiatric disorders. *Trends in Neurosciences,* **31**(7), pp. 361-370.

FORSYTHE, I.D., WESTBROOK, G.L. and MAYER, M.L., 1988. Modulation of excitatory synaptic transmission by glycine and zinc in cultures of mouse hippocampal neurons. *The Journal of Neuroscience,* **8**(10), pp. 3733-3741.

FRADLEY, R.L., O'MEARA, G.F., NEWMAN, R.J., ANDRIEUX, A., JOB, D. and REYNOLDS, D.S., 2005. STOP knockout and NMDA NR1 hypomorphic mice exhibit deficits in sensorimotor gating. *Behavioural Brain Research,* **163**(2), pp. 257-264.

FRASSONI, C., BENTIVOGLIO, M., SPREAFICO, R., SÁNCHEZ, M.P., PUELLES, L. and FAIREN, A., 1991. Postnatal development of calbindin and parvalbumin immunoreactivity in the thalamus of the rat. *Developmental Brain Research,* **58**(2), pp. 243-249.

FRIES, P., 2009. Neuronal gamma-band synchronization as a fundamental process in cortical computation. *Annual Review of Neuroscience,* **32**, pp. 209-224.

FURUKAWA, H., 2012. Structure and function of glutamate receptor amino terminal domains. *The Journal of physiology,* **590**(1), pp. 63-72.

FURUKAWA, H., SINGH, S.K., MANCUSSO, R. and GOUAUX, E., 2005. Subunit arrangement and function in NMDA receptors. *Nature,* **438**(7065), pp. 185-192.

FURUKAWA, H. and GOUAUX, E., 2003. Mechanisms of activation, inhibition and specificity: crystal structures of the NMDA receptor NR1 ligand-binding core. *The EMBO Journal,* **22**(12), pp. 2873-2885.

GAO, X., SAKAI, K., ROBERTS, R.C., CONLEY, R.R., DEAN, B. and TAMMINGA, C.A., 2000. Ionotropic glutamate receptors and expression of N-methyl-D-aspartate receptor subunits in subregions of human hippocampus: effects of schizophrenia. *American Journal of Psychiatry,* **157**(7), pp. 1141-1149.

GARDONI, F., BELLONE, C., CATTABENI, F. and DI LUCA, M., 2001. Protein kinase C activation modulates alpha-calmodulin kinase II binding to NR2A subunit of N-methyl-D-aspartate receptor complex. *The Journal of Biological Chemistry,* **276**(10), pp. 7609-7613.

GHAFARI, M., HÖGER, H., KEIHAN FALSAFI, S., RUSSO-SCHLAFF, N., POLLAK, A. and LUBEC, G., 2012. Mass spectrometrical identification of hippocampal NMDA receptor subunits NR1, NR2A–D and five novel phosphorylation sites on NR2A and NR2B. *Journal of Proteome Research,* **11**(3), pp. 1891-1896.

GIBBS, T.T., RUSSEK, S.J. and FARB, D.H., 2006. Sulfated steroids as endogenous neuromodulators. *Pharmacology Biochemistry and Behavior,* **84**(4), pp. 555-567.

GIELEN, M., RETCHLESS, B.S., MONY, L., JOHNSON, J.W. and PAOLETTI, P., 2009. Mechanism of differential control of NMDA receptor activity by NR2 subunits. *Nature,* **459**(7247), pp. 703-707.

GIESE, K.P., FEDOROV, N.B., FILIPKOWSKI, R.K. and SILVA, A.J., 1998. Autophosphorylation at Thr286 of the alpha calcium-calmodulin kinase II in LTP and learning. *Science,* **279**(5352), pp. 870-873.

GODA, S.A., OLSZEWSKI, M., PIASECKA, J., REJNIAK, K., WHITTINGTON, M.A., KASICKI, S. and HUNT, M.J., 2015. Aberrant high frequency oscillations recorded in the rat nucleus accumbens in the methylazoxymethanol acetate neurodevelopmental model of schizophrenia. *Progress in Neuro-Psychopharmacology and Biological Psychiatry,* **61**, pp. 44-51.

GOEBEL, D.J. and POOSCH, M.S., 1999. NMDA receptor subunit gene expression in the rat brain: a quantitative analysis of endogenous mRNA levels of NR1< sub> Com, NR2A, NR2B, NR2C, NR2D and NR3A. *Molecular Brain Research,* **69**(2), pp. 164-170.

GOFF, D.C. and COYLE, J.T., 2001. The emerging role of glutamate in the pathophysiology and treatment of schizophrenia. *American Journal of Psychiatry,* **158**(9), pp. 1367-1377.

GOFF, D.C., HENDERSON, D.C., EVINS, A.E. and AMICO, E., 1999. A placebo-controlled crossover trial of D-cycloserine added to clozapine in patients with schizophrenia. *Biological Psychiatry,* **45**(4), pp. 512-514.

GOFF, D.C., TSAI, G., LEVITT, J., AMICO, E., MANOACH, D., SCHOENFELD, D.A., HAYDEN, D.L., MCCARLEY, R. and COYLE, J.T., 1999. A placebo-controlled trial of D-cycloserine added to conventional neuroleptics in patients with schizophrenia. *Archives of General Psychiatry,* **56**(1), pp. 21.

GONZALEZ-BURGOS, G., HASHIMOTO, T. and LEWIS, D.A., 2010. Alterations of cortical GABA neurons and network oscillations in schizophrenia. *Current Psychiatry Reports,* **12**(4), pp. 335-344.

GONZALEZ-BURGOS, G. and LEWIS, D.A., 2008. GABA neurons and the mechanisms of network oscillations: implications for understanding cortical dysfunction in schizophrenia. *Schizophrenia Bulletin,* **34**(5), pp. 944-961.

GREENWOOD, T.A., LIGHT, G.A., SWERDLOW, N.R., RADANT, A.D. and BRAFF, D.L., 2012. Association analysis of 94 candidate genes and schizophrenia-related endophenotypes. *PLoS One,* **7**(1), pp. e29630.

GRIFFIN, A.L., 2015. Role of the thalamic nucleus reuniens in mediating interactions between the hippocampus and medial prefrontal cortex during spatial working memory. *Frontiers in Systems Neuroscience,* **9**, pp. 29.

GULYAS, A.I., MEGIAS, M., EMRI, Z. and FREUND, T.F., 1999. Total number and ratio of excitatory and inhibitory synapses converging onto single interneurons of different types in the CA1 area of the rat hippocampus. *The Journal of Neuroscience,* **19**(22), pp. 10082-10097.

HACKOS, D.H., LUPARDUS, P.J., GRAND, T., CHEN, Y., WANG, T., REYNEN, P., GUSTAFSON, A., WALLWEBER, H.J., VOLGRAF, M. and SELLERS, B.D., 2016. Positive allosteric modulators of GluN2A-containing NMDARs with distinct modes of action and impacts on circuit function. *Neuron,* **89**(5), pp. 983-999.

HAGINO, Y., KASAI, S., HAN, W., YAMAMOTO, H., NABESHIMA, T., MISHINA, M. and IKEDA, K., 2010. Essential role of NMDA receptor channel ε4 subunit (GluN2D) in the effects of phencyclidine, but not methamphetamine. *PloS One,* **5**(10), pp. e13722.

HALENE, T.B., EHRLICHMAN, R.S., LIANG, Y., CHRISTIAN, E.P., JONAK, G.J., GUR, T.L., BLENDY, J.A., DOW, H.C., BRODKIN, E.S. and SCHNEIDER, F., 2009. Assessment of NMDA receptor NR1 subunit hypofunction in mice as a model for schizophrenia. *Genes, Brain and Behavior,* **8**(7), pp. 661-675.

HALIM, N.D., LIPSKA, B.K., HYDE, T.M., DEEP-SOBOSLAY, A., SAYLOR, E.M., HERMAN, M.M., THAKAR, J., VERMA, A. and KLEINMAN, J.E., 2008. Increased lactate levels and reduced pH in postmortem brains of schizophrenics: medication confounds. *Journal of Neuroscience Methods,* **169**(1), pp. 208-213.

HALL, J.G., MCLENNAN, H. and WHEAL, H.V., 1977. The actions of certain amino acids as neuronal excitants [proceedings. *The Journal of Physiology,* **272**(1), pp. 52P-53P.

HANSEN, K.B., OGDEN, K.K., YUAN, H. and TRAYNELIS, S.F., 2014. Distinct functional and pharmacological properties of Triheteromeric GluN1/GluN2A/GluN2B NMDA receptors. *Neuron,* **81**(5), pp. 1084-1096.

HANSEN, K.B., FURUKAWA, H. and TRAYNELIS, S.F., 2010. Control of assembly and function of glutamate receptors by the amino-terminal domain. *Molecular Pharmacology,* **78**(4), pp. 535-549.

HANSEN, K.B. and TRAYNELIS, S.F., 2011. Structural and mechanistic determinants of a novel site for noncompetitive inhibition of GluN2D-containing NMDA receptors. *The Journal of Neuroscience,* **31**(10), pp. 3650-3661.

HARRIS, E.W., GANONG, A.H., MONAGHAN, D.T., WATKINS, J.C. and COTMAN, C.W., 1986. Action of 3-((±)-2-car□ ypiperazin-4-yl)-propyl-1-phosphonic aci (CPP): a new and highly potent antagonist of N-methyl-d-aspartate receptors in the hippocampus. *Brain Research,* **382**(1), pp. 174-177.

HARRISON, P.J. and OWEN, M.J., 2003. Genes for schizophrenia? Recent findings and their pathophysiological implications. *The Lancet,* **361**(9355), pp. 417-419.

HARRISON, P. and WEINBERGER, D., 2004. Schizophrenia genes, gene expression, and neuropathology: on the matter of their convergence. *Molecular Psychiatry,* **10**(1), pp. 40-68.

HARTE, M.K., POWELL, S., SWERDLOW, N., GEYER, M. and REYNOLDS, G., 2007. Deficits in parvalbumin and calbindin immunoreactive cells in the hippocampus of isolation reared rats. *Journal of Neural Transmission,* **114**(7), pp. 893-898.

HASHIMOTO, K., FUJITA, Y., HORIO, M., KUNITACHI, S., IYO, M., FERRARIS, D. and TSUKAMOTO, T., 2009. Co-administration of a D-amino acid oxidase inhibitor potentiates the efficacy of D-serine in attenuating prepulse inhibition deficits after administration of dizocilpine. *Biological Psychiatry,* **65**(12), pp. 1103-1106.

HASHIMOTO, K., FUKUSHIMA, T., SHIMIZU, E., KOMATSU, N., WATANABE, H., SHINODA, N., NAKAZATO, M., KUMAKIRI, C., OKADA, S. and HASEGAWA, H.,

2003. Decreased serum levels of D-serine in patients with schizophrenia: evidence in support of the N-methyl-D-aspartate receptor hypofunction hypothesis of schizophrenia. *Archives of General Psychiatry,* **60**(6), pp. 572-576.

HASHIMOTO, T., VOLK, D.W., EGGAN, S.M., MIRNICS, K., PIERRI, J.N., SUN, Z., SAMPSON, A.R. and LEWIS, D.A., 2003. Gene expression deficits in a subclass of GABA neurons in the prefrontal cortex of subjects with schizophrenia. *The Journal of Neuroscience,* **23**(15), pp. 6315-6326.

HATTON, C.J. and PAOLETTI, P., 2005. Modulation of triheteromeric NMDA receptors by N-terminal domain ligands. *Neuron,* **46**(2), pp. 261-274.

HAWKINS, L.M., PRYBYLOWSKI, K., CHANG, K., MOUSSAN, C., STEPHENSON, F.A. and WENTHOLD, R.J., 2004. Export from the endoplasmic reticulum of assembled N-methyl-d-aspartic acid receptors is controlled by a motif in the c terminus of the NR2 subunit. *The Journal of Biological Chemistry,* **279**(28), pp. 28903-28910.

HERESCO-LEVY, U., JAVITT, D.C., ERMILOV, M., MORDEL, C., SILIPO, G. and LICHTENSTEIN, M., 1999. Efficacy of high-dose glycine in the treatment of enduring negative symptoms of schizophrenia. *Archives of General Psychiatry,* **56**(1), pp. 29-36.

HILLMAN, B.G., GUPTA, S.C., STAIRS, D.J., BUONANNO, A. and DRAVID, S.M., 2011. Behavioral analysis of NR2C knockout mouse reveals deficit in acquisition of conditioned fear and working memory. *Neurobiology of Learning and Memory,* **95**(4), pp. 404-414.

HIRAI, H., KIRSCH, J., LAUBE, B., BETZ, H. and KUHSE, J., 1996. The glycine binding site of the N-methyl-D-aspartate receptor subunit NR1: identification of novel determinants of co-agonist potentiation in the extracellular M3-M4 loop region. *Proceedings of the National Academy of Sciences of the United States of America,* **93**(12), pp. 6031-6036.

HIZUE, M., PANG, C. and YOKOYAMA, M., 2005. Involvement of N-methyl-D-aspartate-type glutamate receptor ϵ 1 and ϵ 4 subunits in tonic inflammatory pain and neuropathic pain. *Neuroreport,* **16**(15), pp. 1667-1670.

HOLLMANN, M., 1999. Structure of ionotropic glutamate receptors. *Ionotropic Glutamate Receptors in the CNS.* Springer, pp. 3-98.

HOLLMANN, M., BOULTER, J., MARON, C., BEASLEY, L., SULLIVAN, J., PECHT, G. and HEINEMANN, S., 1993. Zinc potentiates agonist-lnduced currents at certain splice variants of the NMDA receptor. *Neuron,* **10**(5), pp. 943-954.

HOMAYOUN, H. and MOGHADDAM, B., 2007. NMDA receptor hypofunction produces opposite effects on prefrontal cortex interneurons and pyramidal neurons. *The Journal of Neuroscience,* **27**(43), pp. 11496-11500.

HONER, M., BENKE, D., LAUBE, B., KUHSE, J., HECKENDORN, R., ALLGEIER, H., ANGST, C., MONYER, H., SEEBURG, P.H., BETZ, H. and MOHLER, H., 1998. Differentiation of glycine antagonist sites of N-methyl-D-aspartate receptor subtypes. Preferential interaction of CGP 61594 with NR1/2B receptors. *The Journal of Biological Chemistry,* **273**(18), pp. 11158-11163.

HORAK, M., VLCEK, K., CHODOUNSKA, H. and VYKLICKY, L., 2006. Subtype-dependence of N-methyl-D-aspartate receptor modulation by pregnenolone sulfate. *Neuroscience,* **137**(1), pp. 93-102.

HORAK, M., VLCEK, K., PETROVIC, M., CHODOUNSKA, H. and VYKLICKY, L.,Jr, 2004. Molecular mechanism of pregnenolone sulfate action at NR1/NR2B receptors. *The Journal of Neuroscience,* **24**(46), pp. 10318-10325.

HUANG, Z.J., 2009. Activity-dependent development of inhibitory synapses and innervation pattern: role of GABA signalling and beyond. *The Journal of physiology,* **587**(Pt 9), pp. 1881-1888.

HUNT, M.J., OLSZEWSKI, M., PIASECKA, J., WHITTINGTON, M.A. and KASICKI, S., 2015. Effects of NMDA receptor antagonists and antipsychotics on high frequency oscillations recorded in the nucleus accumbens of freely moving mice. *Psychopharmacology,* **232**(24), pp. 4525-4535.

HUNT, M.J. and KASICKI, S., 2013. A systematic review of the effects of NMDA receptor antagonists on oscillatory activity recorded in vivo. *Journal of Psychopharmacology,* **27**(11), pp. 972-986.

IKEDA, K., ARAKI, K., TAKAYAMA, C., INOUE, Y., YAGI, T., AIZAWA, S. and MISHINA, M., 1995. Reduced spontaneous activity of mice defective in the ε4 subunit of the NMDA receptor channel. *Molecular Brain Research,* **33**(1), pp. 61-71.

IKEDA, K., NAGASAWA, M., MORI, H., ARAKI, K., SAKIMURA, K., WATANABE, M., INOUE, Y. and MISHINA, M., 1992. Cloning and expression of the ε4 subunit of the NMDA receptor channel. *FEBS letters,* **313**(1), pp. 34-38.

IRVINE, M.W., COSTA, B.M., VOLIANSKIS, A., FANG, G., CEOLIN, L., COLLINGRIDGE, G.L., MONAGHAN, D.T. and JANE, D.E., 2012. Coumarin-3-carboxylic acid derivatives as potentiators and inhibitors of recombinant and native N-methyl-D-aspartate receptors. *Neurochemistry International,* **61**(4), pp. 593-600.

IRVINE, M.W., FANG, G., EAVES, R., MAYO-MARTIN, M.B., BURNELL, E.S., COSTA, B.M., CULLEY, G.R., VOLIANSKIS, A., COLLINGRIDGE, G.L. and MONAGHAN, D.T., 2015. Synthesis of a Series of Novel 3, 9-Disubstituted Phenanthrenes as Analogues of Known N-Methyl-d-aspartate Receptor Allosteric Modulators. *Synthesis,* **47**(11), pp. 1593-1610.

IRWIN, R.P., MARAGAKIS, N.J., ROGAWSKI, M.A., PURDY, R.H., FARB, D.H. and PAUL, S.M., 1992. Pregnenolone sulfate augments NMDA receptor mediated increases in intracellular Ca 2 in cultured rat hippocampal neurons. *Neuroscience letters,* **141**(1), pp. 30-34.

ISHII, T., MORIYOSHI, K., SUGIHARA, H., SAKURADA, K., KADOTANI, H., YOKOI, M., AKAZAWA, C., SHIGEMOTO, R., MIZUNO, N. and MASU, M., 1993. Molecular characterization of the family of the N-methyl-D-aspartate receptor subunits. *The Journal of Biological Chemistry,* **268**(4), pp. 2836-2843.

ITO, H.T., ZHANG, S., WITTER, M.P., MOSER, E.I. and MOSER, M., 2015. A prefrontal-thalamo-hippocampal circuit for goal-directed spatial navigation. *Nature,* **522**(7554), pp. 50-55.

JANG, M.K., MIERKE, D.F., RUSSEK, S.J. and FARB, D.H., 2004. A steroid modulatory domain on NR2B controls N-methyl-D-aspartate receptor proton sensitivity. *Proceedings of the National Academy of Sciences of the United States of America,* **101**(21), pp. 8198-8203.

JAVITT, D.C., 2007. Glutamate and schizophrenia: phencyclidine, N-methyl-d-aspartate receptors, and dopamine–glutamate interactions. *International Review of Neurobiology,* **78**, pp. 69-108.

JAVITT, D.C., SERSHEN, H., HASHIM, A. and LAJTHA, A., 1997. Reversal of phencyclidine-induced hyperactivity by glycine and the glycine uptake inhibitor glycyldodecylamide. *Neuropsychopharmacology,* **17**(3), pp. 202-204.

JAVITT, D.C. and ZUKIN, S.R., 1991. Recent advances in the phencyclidine model of schizophrenia. *Am J Psychiatry,* **148**(10), pp. 1301-1308.

JAVITT, D.C., ZYLBERMAN, I., ZUKIN, S.R. and HERESCO-LEVY, U., 1994. Amelioration of negative symptoms in schizophrenia by glycine. *The American Journal of Psychiatry,* **151**(8), pp. 1234-1236.

JEFFREY, M., LANG, M., GANE, J., WU, C., BURNHAM, W.M. and ZHANG, L., 2013. A reliable method for intracranial electrode implantation and chronic electrical stimulation in the mouse brain. *BMC Neuroscience,* **14**, pp. 82-2202-14-82.

JOHANSEN, T.H., CHAUDHARY, A. and VERDOORN, T.A., 1995. Interactions among GYKI-52466, cyclothiazide, and aniracetam at recombinant AMPA and kainate receptors. *Molecular Pharmacology,* **48**(5), pp. 946-955.

JOHNSON, J. and ASCHER, P., 1987. Glycine potentiates the NMDA response in cultured mouse brain neurons. *Nature,* **325**, pp. 529-531.

JOHNSTON, G., KENNEDY, S.M. and TWITCHIN, B., 1979. Action of the Neurotoxin kainic Acid on High Affinity Uptake of I-Glutamaic acid in rat Brain Slices. *Journal of Neurochemistry,* **32**(1), pp. 121-127.

JONES, M.L. and LEONARD, J.P., 2005. PKC site mutations reveal differential modulation by insulin of NMDA receptors containing NR2A or NR2B subunits. *Journal of Neurochemistry,* **92**(6), pp. 1431-1438.

JONES, R. and BÜHL, E., 1993. Basket-like interneurones in layer II of the entorhinal cortex exhibit a powerful NMDA-mediated synaptic excitation. *Neuroscience Letters,* **149**(1), pp. 35-39.

JONES, S. and GIBB, A.J., 2005. Functional NR2B-and NR2D-containing NMDA receptor channels in rat substantia nigra dopaminergic neurones. *The Journal of Physiology,* **569**(1), pp. 209-221.

JULLIENNE, A., MONTAGNE, A., ORSET, C., LESEPT, F., JANE, D.E., MONAGHAN, D.T., MAUBERT, E., VIVIEN, D. and ALI, C., 2011. Selective inhibition of GluN2D-containing N-methyl-D-aspartate receptors prevents tissue plasminogen activator-promoted neurotoxicity both in vitro and in vivo. *Molecular Neurodegeneration,* **6**(1), pp. 1.

KAALUND, S.S., RIISE, J., BROBERG, B.V., FABRICIUS, K., KARLSEN, A.S., SECHER, T., PLATH, N. and PAKKENBERG, B., 2013. Differential expression of parvalbumin in neonatal phencyclidine-treated rats and socially isolated rats. *Journal of Neurochemistry,* **124**(4), pp. 548-557.

KANIAKOVA, M., LICHNEROVA, K., VYKLICKY, L. and HORAK, M., 2012. Single amino acid residue in the M4 domain of GluN1 subunit regulates the surface delivery of NMDA receptors. *Journal of Neurochemistry,* **123**(3), pp. 385-395.

KANTHAN, R., SHUAIB, A., GRIEBEL, R. and MIYASHITA, H., 1995. Intracerebral human microdialysis. In vivo study of an acute focal ischemic model of the human brain. *Stroke; A Journal of Cerebral Circulation,* **26**(5), pp. 870-873.

KANTROWITZ, J.T. and JAVITT, D.C., 2010. N-methyl-d-aspartate (NMDA) receptor dysfunction or dysregulation: the final common pathway on the road to schizophrenia? *Brain Research Bulletin,* **83**(3), pp. 108-121.

KARAKAS, E., SIMOROWSKI, N. and FURUKAWA, H., 2011. Subunit arrangement and phenylethanolamine binding in GluN1/GluN2B NMDA receptors. *Nature,* **475**(7355), pp. 249-253.

KARAKAS, E. and FURUKAWA, H., 2014. Crystal structure of a heterotetrameric NMDA receptor ion channel. *Science,* **344**(6187), pp. 992-997.

KARAKAS, E., SIMOROWSKI, N. and FURUKAWA, H., 2009. Structure of the zinc-bound amino-terminal domain of the NMDA receptor NR2B subunit. *The EMBO Journal,* **28**(24), pp. 3910-3920.

KASHIWAGI, K., FUKUCHI, J., CHAO, J., IGARASHI, K. and WILLIAMS, K., 1996. An aspartate residue in the extracellular loop of the N-methyl-D-aspartate receptor controls sensitivity to spermine and protons. *Molecular Pharmacology,* **49**(6), pp. 1131-1141.

KASHIWAGI, K., MASUKO, T., NGUYEN, C.D., KUNO, T., TANAKA, I., IGARASHI, K. and WILLIAMS, K., 2002. Channel blockers acting at N-methyl-D-aspartate receptors: differential effects of mutations in the vestibule and ion channel pore. *Molecular Pharmacology,* **61**(3), pp. 533-545.

KATSURA, K., ASPLUND, B., EKHOLM, A. and SIESJÖ, B.K., 1992. Extra-and Intracellular pH in the Brain During Ischaemia, Related to Tissue Lactate Content in Normo-and Hypercapnic rats. *European Journal of Neuroscience,* **4**(2), pp. 166-176.

KAZI, R., GAN, Q., TALUKDER, I., MARKOWITZ, M., SALUSSOLIA, C.L. and WOLLMUTH, L.P., 2013. Asynchronous movements prior to pore opening in NMDA receptors. *The Journal of Neuroscience,* **33**(29), pp. 12052-12066.

KEILHOFF, G., BECKER, A., GRECKSCH, G., WOLF, G. and BERNSTEIN, H., 2004. Repeated application of ketamine to rats induces changes in the hippocampal expression of parvalbumin, neuronal nitric oxide synthase and cFOS similar to those found in human schizophrenia. *Neuroscience,* **126**(3), pp. 591-598.

KENNEDY, C., DES ROSIERS, M.H., JEHLE, J.W., REIVICH, M., SHARPE, F. and SOKOLOFF, L., 1975. Mapping of functional neural pathways by autoradiographic survey of local metabolic rate with (14C)deoxyglucose. *Science,* **187**(4179), pp. 850-853.

KHATRI, A., BURGER, P.B., SWANGER, S.A., HANSEN, K.B., ZIMMERMAN, S., KARAKAS, E., LIOTTA, D.C., FURUKAWA, H., SNYDER, J.P. and TRAYNELIS, S.F., 2014. Structural determinants and mechanism of action of a GluN2C-selective NMDA receptor positive allosteric modulator. *Molecular Pharmacology,* **86**(5), pp. 548-560.

KIM, J., LEE, H., SIM, S., BAEK, J., YU, N., CHOI, J., KO, H., LEE, Y., PARK, S. and KWAK, C., 2011. PI3K [gamma] is required for NMDA receptor-dependent long-term depression and behavioral flexibility. *Nature Neuroscience,* **14**(11), pp. 1447-1454.

KINARSKY, L., FENG, B., SKIFTER, D.A., MORLEY, R.M., SHERMAN, S., JANE, D.E. and MONAGHAN, D.T., 2005. Identification of subunit- and antagonist-specific amino acid

residues in the N-Methyl-D-aspartate receptor glutamate-binding pocket. *The Journal of Pharmacology and Experimental Therapeutics,* **313**(3), pp. 1066-1074.

KINNEY, J.W., DAVIS, C.N., TABAREAN, I., CONTI, B., BARTFAI, T. and BEHRENS, M.M., 2006. A specific role for NR2A-containing NMDA receptors in the maintenance of parvalbumin and GAD67 immunoreactivity in cultured interneurons. *The Journal of Neuroscience,* **26**(5), pp. 1604-1615.

KITTELBERGER, K., HUR, E.E., SAZEGAR, S., KESHAVAN, V. and KOCSIS, B., 2012. Comparison of the effects of acute and chronic administration of ketamine on hippocampal oscillations: relevance for the NMDA receptor hypofunction model of schizophrenia. *Brain Structure and Function,* **217**(2), pp. 395-409.

KLECKNER, N.W. and DINGLEDINE, R., 1988. Requirement for glycine in activation of NMDA-receptors expressed in Xenopus oocytes. *Science,* **241**(4867), pp. 835.

KOCSIS, B., 2012. Differential role of NR2A and NR2B subunits in N-methyl-D-aspartate receptor antagonist-induced aberrant cortical gamma oscillations. *Biological Psychiatry,* **71**(11), pp. 987-995.

KOCSIS, B., BROWN, R.E., MCCARLEY, R.W. and HAJOS, M., 2013. Impact of Ketamine on Neuronal Network Dynamics: Translational Modeling of Schizophrenia-Relevant Deficits. *CNS Neuroscience & Therapeutics,* **19**(6), pp. 437-447.

KORINEK, M., KAPRAS, V., VYKLICKY, V., ADAMUSOVA, E., BOROVSKA, J., VALES, K., STUCHLIK, A., HORAK, M., CHODOUNSKA, H. and VYKLICKY, L., 2011. Neurosteroid modulation of N-methyl-d-aspartate receptors: molecular mechanism and behavioral effects. *Steroids,* **76**(13), pp. 1409-1418.

KOROTKOVA, T., FUCHS, E.C., PONOMARENKO, A., VON ENGELHARDT, J. and MONYER, H., 2010. NMDA receptor ablation on parvalbumin-positive interneurons impairs hippocampal synchrony, spatial representations, and working memory. *Neuron,* **68**(3), pp. 557-569.

KOSTAKIS, E., JANG, M., RUSSEK, S.J., GIBBS, T.T. and FARB, D.H., 2011. A steroid modulatory domain in NR2A collaborates with NR1 exon-5 to control NMDAR modulation by pregnenolone sulfate and protons. *Journal of Neurochemistry,* **119**(3), pp. 486-496.

KOSTAKIS, E., SMITH, C., JANG, M.K., MARTIN, S.C., RICHARDS, K.G., RUSSEK, S.J., GIBBS, T.T. and FARB, D.H., 2013. The neuroactive steroid pregnenolone sulfate stimulates trafficking of functional N-methyl D-aspartate receptors to the cell surface via a noncanonical, G protein, and Ca2+-dependent mechanism. *Molecular Pharmacology,* **84**(2), pp. 261-274.

KOTERMANSKI, S.E. and JOHNSON, J.W., 2009. Mg2+ imparts NMDA receptor subtype selectivity to the Alzheimer's drug memantine. *The Journal of Neuroscience,* **29**(9), pp. 2774-2779.

KROGSGAARD-LARSEN, P., HONORE, T., HANSEN, J., CURTIS, D. and LODGE, D., 1980. New class of glutamate agonist structurally related to ibotenic acid. *Nature,* **284**(5751), pp. 64-66.

KRUPP, J.J., VISSEL, B., THOMAS, C.G., HEINEMANN, S.F. and WESTBROOK, G.L., 2002. Calcineurin acts via the C-terminus of NR2A to modulate desensitization of NMDA receptors. *Neuropharmacology,* **42**(5), pp. 593-602.

KRYSTAL, J.H., KARPER, L.P., SEIBYL, J.P., FREEMAN, G.K., DELANEY, R., BREMNER, J.D., HENINGER, G.R., BOWERS JR, M.B. and CHARNEY, D.S., 1994. Subanesthetic effects of the noncompetitive NMDA antagonist, ketamine, in humans: psychotomimetic, perceptual, cognitive, and neuroendocrine responses. *Archives of General Psychiatry,* **51**(3), pp. 199-214.

KUDOVA, E., CHODOUNSKA, H., SLAVIKOVA, B., BUDESINSKY, M., NEKARDOVA, M., VYKLICKY, V., KRAUSOVA, B., SVEHLA, P. and VYKLICKY, L., 2015. A New Class of Potent N-Methyl-d-Aspartate Receptor Inhibitors: Sulfated Neuroactive Steroids with Lipophilic D-Ring Modifications. *Journal of Medicinal Chemistry,* **58**(15), pp. 5950-5966.

KUNER, T., SEEBURG, P.H. and GUY, H.R., 2003. A common architecture for K channels and ionotropic glutamate receptors? *Trends in Neurosciences,* **26**(1), pp. 27-32.

KUNER, T., WOLLMUTH, L.P., KARLIN, A., SEEBURG, P.H. and SAKMANN, B., 1996. Structure of the NMDA receptor channel M2 segment inferred from the accessibility of substituted cysteines. *Neuron,* **17**(2), pp. 343-352.

KURYATOV, A., LAUBE, B., BETZ, H. and KUHSE, J., 1994. Mutational analysis of the glycine-binding site of the NMDA receptor: structural similarity with bacterial amino acid-binding proteins. *Neuron,* **12**(6), pp. 1291-1300.

KUSSIUS, C.L., KAUR, N. and POPESCU, G.K., 2009. Pregnanolone sulfate promotes desensitization of activated NMDA receptors. *The Journal of Neuroscience,* **29**(21), pp. 6819-6827.

KUSSIUS, C.L. and POPESCU, G.K., 2010. NMDA receptors with locked glutamate-binding clefts open with high efficacy. *The Journal of Neuroscience,* **30**(37), pp. 12474-12479.

KUTSUWADA, T., KASHIWABUCHI, N., MORI, H., SAKIMURA, K., KUSHIYA, E., ARAKI, K., MEGURO, H., MASAKI, H., KUMANISHI, T. and ARAKAWA, M., 1992. Molecular diversity of the NMDA receptor channel. *Nature,* **358**, pp. 36-41.

KVIST, T., STEFFENSEN, T.B., GREENWOOD, J.R., MEHRZAD TABRIZI, F., HANSEN, K.B., GAJHEDE, M., PICKERING, D.S., TRAYNELIS, S.F., KASTRUP, J.S. and BRAUNER-OSBORNE, H., 2013. Crystal structure and pharmacological characterization of a novel N-methyl-D-aspartate (NMDA) receptor antagonist at the GluN1 glycine binding site. *The Journal of Biological Chemistry,* **288**(46), pp. 33124-33135.

LAHTI, A.C., KOFFEL, B., LAPORTE, D. and TAMMINGA, C.A., 1995. Subanesthetic doses of ketamine stimulate psychosis in schizophrenia. *Neuropsychopharmacology,* **13**(1), pp. 9-19.

LAHTI, A.C., WEILER, M.A., TAMARA, M., PARWANI, A. and TAMMINGA, C.A., 2001. Effects of ketamine in normal and schizophrenic volunteers. *Neuropsychopharmacology,* **25**(4), pp. 455-467.

LAU, C.G. and ZUKIN, R.S., 2007. NMDA receptor trafficking in synaptic plasticity and neuropsychiatric disorders. *Nature Reviews Neuroscience,* **8**(6), pp. 413-426.

LAUBE, B., HIRAI, H., STURGESS, M., BETZ, H. and KUHSE, J., 1997. Molecular determinants of agonist discrimination by NMDA receptor subunits: analysis of the glutamate binding site on the NR2B subunit. *Neuron,* **18**(3), pp. 493-503.

LAUBE, B., KUHSE, J. and BETZ, H., 1998. Evidence for a tetrameric structure of recombinant NMDA receptors. *The Journal of Neuroscience,* **18**(8), pp. 2954-2961.

LAURIE, D.J., BARTKE, I., SCHOEPFER, R., NAUJOKS, K. and SEEBURG, P.H., 1997. Regional, developmental and interspecies expression of the four NMDAR2 subunits, examined using monoclonal antibodies. *Molecular Brain Research,* **51**(1), pp. 23-32.

LECEA, L.D., 1995. Developmental expression of parvalbumin mRNA in the cerebral cortex and hippocampus of the rat. *Molecular Brain Research,* **32**(1), pp. 1-13.

LEE, C., LÜ, W., MICHEL, J.C., GOEHRING, A., DU, J., SONG, X. and GOUAUX, E., 2014. NMDA receptor structures reveal subunit arrangement and pore architecture. *Nature,* **511**, pp. 191-197.

LEESON, P.D., BAKER, R., CARLING, R.W., CURTIS, N.R., MOORE, K.W., WILLIAMS, B.J., FOSTER, A.C., DONALD, A.E., KEMP, J.A. and MARSHALL, G.R., 1991. Kynurenic acid derivatives. Structure-activity relationships for excitatory amino acid antagonism and identification of potent and selective antagonists at the glycine site on the N-methyl-D-aspartate receptor. *Journal of Medicinal Chemistry,* **34**(4), pp. 1243-1252.

LEMA TOMÉ, C.M., MILLER, R., BAUER, C., SMITH, C., BLACKSTONE, K., LEIGH, A., BUSCH, J. and TURNER, C.P., 2008. Decline in age-dependent, MK801-induced injury coincides with developmental switch in parvalbumin expression: Somatosensory and motor cortex. *Developmental Psychobiology,* **50**(7), pp. 665-679.

LEONARD, A.S. and HELL, J.W., 1997. Cyclic AMP-dependent protein kinase and protein kinase C phosphorylate N-methyl-D-aspartate receptors at different sites. *The Journal of Biological Chemistry,* **272**(18), pp. 12107-12115.

LEWIS, D.A., HASHIMOTO, T. and VOLK, D.W., 2005. Cortical inhibitory neurons and schizophrenia. *Nature Reviews Neuroscience,* **6**(4), pp. 312-324.

LI, Q., CLARK, S., LEWIS, D.V. and WILSON, W.A., 2002. NMDA receptor antagonists disinhibit rat posterior cingulate and retrosplenial cortices: a potential mechanism of neurotoxicity. *The Journal of Neuroscience,* **22**(8), pp. 3070-3080.

LIAO, G.Y., WAGNER, D.A., HSU, M.H. and LEONARD, J.P., 2001. Evidence for direct protein kinase-C mediated modulation of N-methyl-D-aspartate receptor current. *Molecular Pharmacology,* **59**(5), pp. 960-964.

LIMAPICHAT, W., YU, W.Y., BRANIGAN, E., LESTER, H.A. and DOUGHERTY, D.A., 2012. Key binding interactions for memantine in the NMDA receptor. *ACS chemical Neuroscience,* **4**(2), pp. 255-260.

LINSENBARDT, A.J., CHISARI, M., YU, A., SHU, H.J., ZORUMSKI, C.F. and MENNERICK, S., 2013. Noncompetitive, voltage-dependent NMDA receptor antagonism by hydrophobic anions. *Molecular Pharmacology,* **83**(2), pp. 354-366.

LIPSKA, B.K., DEEP-SOBOSLAY, A., WEICKERT, C.S., HYDE, T.M., MARTIN, C.E., HERMAN, M.M. and KLEINMAN, J.E., 2006. Critical factors in gene expression in postmortem human brain: Focus on studies in schizophrenia. *Biological Psychiatry,* **60**(6), pp. 650-658.

LISMAN, J.E., COYLE, J.T., GREEN, R.W., JAVITT, D.C., BENES, F.M., HECKERS, S. and GRACE, A.A., 2008. Circuit-based framework for understanding neurotransmitter and risk gene interactions in schizophrenia. *Trends in neurosciences,* **31**(5), pp. 234-242.

LISMAN, J.E., PI, H.J., ZHANG, Y. and OTMAKHOVA, N.A., 2010. A thalamo-hippocampal-ventral tegmental area loop may produce the positive feedback that underlies the psychotic break in schizophrenia. *Biological Psychiatry,* **68**(1), pp. 17-24.

LISMAN, J., YASUDA, R. and RAGHAVACHARI, S., 2012. Mechanisms of CaMKII action in long-term potentiation. *Nature Reviews Neuroscience,* **13**(3), pp. 169-182.

LIVAK, K.J. and SCHMITTGEN, T.D., 2001. Analysis of relative gene expression data using real-time quantitative PCR and the $2-\Delta\Delta CT$ method. *Methods,* **25**(4), pp. 402-408.

LLINÁS, R., URBANO, F.J., LEZNIK, E., RAMÍREZ, R.R. and VAN MARLE, H.J., 2005. Rhythmic and dysrhythmic thalamocortical dynamics: GABA systems and the edge effect. *Trends in Neurosciences,* **28**(6), pp. 325-333.

LODGE, D. and MERCIER, M., 2015. Ketamine and phencyclidine: the good, the bad and the unexpected. *British Journal of Pharmacology,* **172**(17), pp. 4254-4276.

LOVINGER, D.M., WONG, K.L., MURAKAMI, K. and ROUTTENBERG, A., 1987. Protein kinase C inhibitors eliminate hippocampal long-term potentiation. *Brain Research,* **436**(1), pp. 177-183.

LOW, C.M., LYUBOSLAVSKY, P., FRENCH, A., LE, P., WYATTE, K., THIEL, W.H., MARCHAN, E.M., IGARASHI, K., KASHIWAGI, K., GERNERT, K., WILLIAMS, K., TRAYNELIS, S.F. and ZHENG, F., 2003. Molecular determinants of proton-sensitive N-methyl-D-aspartate receptor gating. *Molecular Pharmacology,* **63**(6), pp. 1212-1222.

LOW, C.M., ZHENG, F., LYUBOSLAVSKY, P. and TRAYNELIS, S.F., 2000. Molecular determinants of coordinated proton and zinc inhibition of N-methyl-D-aspartate NR1/NR2A receptors. *Proceedings of the National Academy of Sciences of the United States of America,* **97**(20), pp. 11062-11067.

LUSCHER, C. and MALENKA, R.C., 2012. NMDA receptor-dependent long-term potentiation and long-term depression (LTP/LTD). *Cold Spring Harbor Perspectives in Biology,* **4**(6), pp. 10.1101/cshperspect.a005710.

MADEIRA, C., FREITAS, M.E., VARGAS-LOPES, C., WOLOSKER, H. and PANIZZUTTI, R., 2008. Increased brain D-amino acid oxidase (DAAO) activity in schizophrenia. *Schizophrenia Research,* **101**(1), pp. 76-83.

MADRY, C., MESIC, I., BARTHOLOMÄUS, I., NICKE, A., BETZ, H. and LAUBE, B., 2007. Principal role of NR3 subunits in NR1/NR3 excitatory glycine receptor function. *Biochemical and Biophysical Research Communications,* **354**(1), pp. 102-108.

MAKINO, C., SHIBATA, H., NINOMIYA, H., TASHIRO, N. and FUKUMAKI, Y., 2005. Identification of single-nucleotide polymorphisms in the human N-methyl-D-aspartate receptor subunit NR2D gene, GRIN2D, and association study with schizophrenia. *Psychiatric Genetics,* **15**(3), pp. 215-221.

MALAYEV, A., GIBBS, T.T. and FARB, D.H., 2002. Inhibition of the NMDA response by pregnenolone sulphate reveals subtype selective modulation of NMDA receptors by sulphated steroids. *British Journal of Pharmacology,* **135**(4), pp. 901-909.

MALENKA, R.C. and BEAR, M.F., 2004. LTP and LTD: an embarrassment of riches. *Neuron,* **44**(1), pp. 5-21.

MALHOTRA, A.K., PINALS, D.A., ADLER, C.M., ELMAN, I., CLIFTON, A., PICKAR, D. and BREIER, A., 1997. Ketamine-induced exacerbation of psychotic symptoms and cognitive impairment in neuroleptic-free schizophrenics. *Neuropsychopharmacology,* **17**(3), pp. 141-150.

MALINOW, R., MADISON, D.V. and TSIEN, R.W., 1988. Persistent protein kinase activity underlying long-term potentiation. *Nature,* **335**, pp. 820-824.

MALINOW, R., SCHULMAN, H. and TSIEN, R.W., 1989. Inhibition of postsynaptic PKC or CaMKII blocks induction but not expression of LTP. *Science,* **245**(4920), pp. 862-866.

MAN, H., WANG, Q., LU, W., JU, W., AHMADIAN, G., LIU, L., D'SOUZA, S., WONG, T., TAGHIBIGLOU, C. and LU, J., 2003. Activation of PI3-kinase is required for AMPA receptor insertion during LTP of mEPSCs in cultured hippocampal neurons. *Neuron,* **38**(4), pp. 611-624.

MARTINEAU, M., BAUX, G. and MOTHET, J., 2006. D-serine signalling in the brain: friend and foe. *Trends in Neurosciences,* **29**(8), pp. 481-491.

MATSUMOTO, T., OBRENOVITCH, T.P., PARKINSON, N.A. and SYMON, L., 1990. Cortical activity, ionic homeostasis, and acidosis during rat brain repetitive ischemia. *Stroke; A Journal of Cerebral Circulation,* **21**(8), pp. 1192-1198.

MATSUZAKI, M., HONKURA, N., ELLIS-DAVIES, G.C. and KASAI, H., 2004. Structural basis of long-term potentiation in single dendritic spines. *Nature,* **429**(6993), pp. 761-766.

MAYER, M.L., WESTBROOK, G.L. and GUTHRIE, P.B., 1984. Voltage-dependent block by Mg+2 of NMDA responses in spinal cord neurones. *Nature,* **309**, pp. 261-263.

MCHUGH, T.J., BLUM, K.I., TSIEN, J.Z., TONEGAWA, S. and WILSON, M.A., 1996. Impaired hippocampal representation of space in CA1-specific NMDAR1 knockout mice. *Cell,* **87**(7), pp. 1339-1349.

MCHUGH, T.J., JONES, M.W., QUINN, J.J., BALTHASAR, N., COPPARI, R., ELMQUIST, J.K., LOWELL, B.B., FANSELOW, M.S., WILSON, M.A. and TONEGAWA, S., 2007. Dentate gyrus NMDA receptors mediate rapid pattern separation in the hippocampal network. *Science,* **317**(5834), pp. 94-99.

MCINTOSH, T.K., VINK, R., SOARES, H., HAYES, R. and SIMON, R., 1989. Effects of the N-methyl-D-aspartate receptor blocker MK-801 on neurologic function after experimental brain injury. *Journal of Neurotrauma,* **6**(4), pp. 247-259.

MCLENNAN, H. and LODGE, A.D., 1979. The antagonism of amino acid-induced excitation of spinal neurones in the cat. *Brain Research,* **169**(1), pp. 83-90.

MCNALLY, J.M., MCCARLEY, R.W., MCKENNA, J.T., YANAGAWA, Y. and BROWN, R.E., 2011. Complex receptor mediation of acute ketamine application on in vitro gamma oscillations in mouse prefrontal cortex: modeling gamma band oscillation abnormalities in schizophrenia. *Neuroscience,* **199**, pp. 51-63.

MEGURO, H., MORI, H., ARAKI, K., KUSHIYA, E., KUTSUWADA, T., YAMAZAKI, M., KUMANISHI, T., ARAKAWA, M., SAKIMURA, K. and MISHINA, M., 1992. Functional characterization of a heteromeric NMDA receptor channel expressed from cloned cDNAs. *Nature,* **357**, pp. 70-74.

MICU, I., PLEMEL, J.R., LACHANCE, C., PROFT, J., JANSEN, A.J., CUMMINS, K., VAN MINNEN, J. and STYS, P.K., 2016. The molecular physiology of the axo-myelinic synapse. *Experimental Neurology,* **276**, pp. 41-50.

MILLER, S.G. and KENNEDY, M.B., 1986. Regulation of brain Type II Ca2 calmodulin-dependent protein kinase by autophosphorylation: A Ca 2 -triggered molecular switch. *Cell,* **44**(6), pp. 861-870.

MISHINA, M., MORI, H., ARAKI, K., KUSHIYA, E., MEGURO, H., KUTSUWADA, T., KASHIWABUCHI, N., IKEDA, K., NAGASAWA, M. and YAMAZAKI, M., 1993.

Molecular and Functional Diversity of the NMDA Receptor Channela. *Annals of the New York Academy of Sciences,* **707**(1), pp. 136-152.

MIYAMOTO, S., LEIPZIG, J.N., LIEBERMAN, J.A. and DUNCAN, G.E., 2000. Effects of ketamine, MK-801, and amphetamine on regional brain 2-deoxyglucose uptake in freely moving mice. *Neuropsychopharmacology,* **22**(4), pp. 400-412.

MOGHADDAM, B. and ADAMS, B.W., 1998. Reversal of phencyclidine effects by a group II metabotropic glutamate receptor agonist in rats. *Science,* **281**(5381), pp. 1349-1352.

MOGHADDAM, B., ADAMS, B., VERMA, A. and DALY, D., 1997. Activation of glutamatergic neurotransmission by ketamine: a novel step in the pathway from NMDA receptor blockade to dopaminergic and cognitive disruptions associated with the prefrontal cortex. *The Journal of Neuroscience,* **17**(8), pp. 2921-2927.

MOHN, A.R., GAINETDINOV, R.R., CARON, M.G. and KOLLER, B.H., 1999. Mice with reduced NMDA receptor expression display behaviors related to schizophrenia. *Cell,* **98**(4), pp. 427-436.

MOHRMANN, R., KÖHR, G., HATT, H., SPRENGEL, R. and GOTTMANN, K., 2002. Deletion of the C-terminal domain of the NR2B subunit alters channel properties and synaptic targeting of N-methyl-D-aspartate receptors in nascent neocortical synapses. *Journal of Neuroscience Research,* **68**(3), pp. 265-275.

MONAGHAN, D.T., BRIDGES, R.J. and COTMAN, C.W., 1989. The excitatory amino acid receptors: their classes, pharmacology, and distinct properties in the function of the central nervous system. *Annual Review of Pharmacology and Toxicology,* **29**(1), pp. 365-402.

MONAGHAN, D.T. and COTMAN, C.W., 1982. The distribution of [3 H] kainic acid binding sites in rat CNS as determined by autoradiography. *Brain Research,* **252**(1), pp. 91-100.

MONAGHAN, D.T., HOLETS, V.R., TOY, D.W. and COTMAN, C.W., 1983. Anatomical distributions of four pharmacologically distinct 3H-L-glutamate binding sites. *Nature,* **306**, pp. 176-179.

MONAGHAN, D.T., IRVINE, M.W., COSTA, B.M., FANG, G. and JANE, D.E., 2012. Pharmacological modulation of NMDA receptor activity and the advent of negative and positive allosteric modulators. *Neurochemistry International,* **61**(4), pp. 581-592.

MONAGHAN, D.T. and COTMAN, C.W., 1985. Distribution of N-methyl-D-aspartate-sensitive L-[3H]glutamate-binding sites in rat brain. *The Journal of Neuroscience,* **5**(11), pp. 2909-2919.

MONY, L., ZHU, S., CARVALHO, S. and PAOLETTI, P., 2011. Molecular basis of positive allosteric modulation of GluN2B NMDA receptors by polyamines. *The EMBO Journal,* **30**(15), pp. 3134-3146.

MONYER, H., BURNASHEV, N., LAURIE, D.J., SAKMANN, B. and SEEBURG, P.H., 1994. Developmental and regional expression in the rat brain and functional properties of four NMDA receptors. *Neuron,* **12**(3), pp. 529-540.

MONYER, H. and SPRENGEL, R., 1992. Heteromeric NMDA receptors: molecular and functional distinction of subtypes. *Science,* **256**(5060), pp. 1217.

MOON, I.S., APPERSON, M.L. and KENNEDY, M.B., 1994. The major tyrosine-phosphorylated protein in the postsynaptic density fraction is N-methyl-D-aspartate

receptor subunit 2B. *Proceedings of the National Academy of Sciences of the United States of America,* **91**(9), pp. 3954-3958.

MORGAN, C.J., MOFEEZ, A., BRANDNER, B., BROMLEY, L. and CURRAN, H.V., 2004. Acute effects of ketamine on memory systems and psychotic symptoms in healthy volunteers. *Neuropsychopharmacology,* **29**(1), pp. 208-218.

MORI, H., MASAKI, H., YAMAKURA, T. and MISHINA, M., 1992. Identification by mutagenesis of a Mg2 -block site of the NMDA receptor channel. *Nature,* **358**, pp. 673-675.

MORIYOSHI, K., MASU, M., ISHII, T., SHIGEMOTO, R., MIZUNO, N. and NAKANISHI, S., 1991. Molecular cloning and characterization of the rat NMDA receptor. *Nature,* **354**(6348), pp. 31-37.

MORLEY, R.M., TSE, H., FENG, B., MILLER, J.C., MONAGHAN, D.T. and JANE, D.E., 2005. Synthesis and pharmacology of N 1-substituted piperazine-2, 3-dicarboxylic acid derivatives acting as NMDA receptor antagonists. *Journal of Medicinal Chemistry,* **48**(7), pp. 2627-2637.

MOSLEY, C.A., ACKER, T.M., HANSEN, K.B., MULLASSERIL, P., ANDERSEN, K.T., LE, P., VELLANO, K.M., BRÄUNER-OSBORNE, H., LIOTTA, D.C. and TRAYNELIS, S.F., 2010. Quinazolin-4-one derivatives: A novel class of noncompetitive NR2C/D subunit-selective N-methyl-D-aspartate receptor antagonists. *Journal of Medicinal Chemistry,* **53**(15), pp. 5476-5490.

MOTHET, J.P., PARENT, A.T., WOLOSKER, H., BRADY, R.O.,Jr, LINDEN, D.J., FERRIS, C.D., ROGAWSKI, M.A. and SNYDER, S.H., 2000. D-serine is an endogenous ligand for the glycine site of the N-methyl-D-aspartate receptor. *Proceedings of the National Academy of Sciences of the United States of America,* **97**(9), pp. 4926-4931.

MOTT, D.D., DOHERTY, J.J., ZHANG, S., WASHBURN, M.S., FENDLEY, M.J., LYUBOSLAVSKY, P., TRAYNELIS, S.F. and DINGLEDINE, R., 1998. Phenylethanolamines inhibit NMDA receptors by enhancing proton inhibition. *Nature Neuroscience,* **1**(8), pp. 659-667.

MUELLER, H.T. and MEADOR-WOODRUFF, J.H., 2004. NR3A NMDA receptor subunit mRNA expression in schizophrenia, depression and bipolar disorder. *Schizophrenia Research,* **71**(2), pp. 361-370.

MULLASSERIL, P., HANSEN, K.B., VANCE, K.M., OGDEN, K.K., YUAN, H., KURTKAYA, N.L., SANTANGELO, R., ORR, A.G., LE, P. and VELLANO, K.M., 2010. A subunit-selective potentiator of NR2C-and NR2D-containing NMDA receptors. *Nature Communications,* **1**, pp. 90.

NAKANISHI, S., 1992. Molecular diversity of glutamate receptors and implications for brain function. *Science,* **258**(5082), pp. 597-603.

NAKAZAWA, K., ZSIROS, V., JIANG, Z., NAKAO, K., KOLATA, S., ZHANG, S. and BELFORTE, J.E., 2012. GABAergic interneuron origin of schizophrenia pathophysiology. *Neuropharmacology,* **62**(3), pp. 1574-1583.

NEMOTO, E.M. and FRINAK, S., 1981. Brain tissue pH after global brain ischemia and barbiturate loading in rats. *Stroke; A Journal of Cerebral Circulation,* **12**(1), pp. 77-82.

NIEWOEHNER, B., SINGLE, F., HVALBY, Ø, JENSEN, V., MEYER ZUM ALTEN BORGLOH, S, SEEBURG, P., RAWLINS, J., SPRENGEL, R. and BANNERMAN, D., 2007. Impaired spatial working memory but spared spatial reference memory following

functional loss of NMDA receptors in the dentate gyrus. *European Journal of Neuroscience,* **25**(3), pp. 837-846.

NILSSON, P., HILLERED, L., PONTEN, U. and UNGERSTEDT, U., 1990. Changes in cortical extracellular levels of energy-related metabolites and amino acids following concussive brain injury in rats. *Journal of Cerebral Blood Flow and Metabolism,* **10**(5), pp. 631-637.

NOH, J., GWAG, B. and CHUNG, J., 2006. Underlying mechanism for NMDA receptor antagonism by the anti-inflammatory drug, sulfasalazine, in mouse cortical neurons. *Neuropharmacology,* **50**(1), pp. 1-15.

NOWAK, L., BREGESTOVSKI, P., ASCHER, P., HERBET, A. and PROCHIANTZ, A., 1984. Magnesium gates glutamate-activated channels in mouse central neurones. *Nature,* **307**, pp. 462-465.

OGDEN, K.K. and TRAYNELIS, S.F., 2013. Contribution of the M1 transmembrane helix and pre-M1 region to positive allosteric modulation and gating of N-methyl-D-aspartate receptors. *Molecular Pharmacology,* **83**(5), pp. 1045-1056.

OKATY, B.W., MILLER, M.N., SUGINO, K., HEMPEL, C.M. and NELSON, S.B., 2009. Transcriptional and electrophysiological maturation of neocortical fast-spiking GABAergic interneurons. *The Journal of Neuroscience,* **29**(21), pp. 7040-7052.

OLNEY, J.W., NEWCOMER, J.W. and FARBER, N.B., 1999. NMDA receptor hypofunction model of schizophrenia. *Journal of Psychiatric Research,* **33**(6), pp. 523-533.

OLNEY, J.W., 1969. Brain lesions, obesity, and other disturbances in mice treated with monosodium glutamate. *Science,* **164**(3880), pp. 719-721.

OLSZEWSKI, M., PIASECKA, J., GODA, S.A., KASICKI, S. and HUNT, M.J., 2013. Antipsychotic compounds differentially modulate high-frequency oscillations in the rat nucleus accumbens: a comparison of first- and second-generation drugs. *The International Journal of Neuropsychopharmacology,* **16**(5), pp. 1009-1020.

OMKUMAR, R.V., KIELY, M.J., ROSENSTEIN, A.J., MIN, K. and KENNEDY, M.B., 1996. Identification of a phosphorylation site for calcium/calmodulindependent protein kinase II in the NR2B subunit of the N-methyl-D-aspartate receptor. *Journal of Biological Chemistry,* **271**(49), pp. 31670-31678.

ORANJE, B., GISPEN-DE WIED, C.C., VERBATEN, M.N. and KAHN, R.S., 2002. Modulating sensory gating in healthy volunteers: the effects of ketamine and haloperidol. *Biological Psychiatry,* **52**(9), pp. 887-895.

OZYURT, E., GRAHAM, D.I., WOODRUFF, G.N. and MCCULLOCH, J., 1988. Protective effect of the glutamate antagonist, MK-801 in focal cerebral ischemia in the cat. *Journal of Cerebral Blood Flow and Metabolism,* **8**(1), pp. 138-143.

PAHK, A.J. and WILLIAMS, K., 1997. Influence of extracellular pH on inhibition by ifenprodil at N-methyl-D-aspartate receptors in Xenopus oocytes. *Neuroscience Letters,* **225**(1), pp. 29-32.

PAOLETTI, P., 2011. Molecular basis of NMDA receptor functional diversity. *European Journal of Neuroscience,* **33**(8), pp. 1351-1365.

PAOLETTI, P., BELLONE, C. and ZHOU, Q., 2013. NMDA receptor subunit diversity: impact on receptor properties, synaptic plasticity and disease. *Nature Reviews Neuroscience,* **14**(6), pp. 383-400.

PAOLETTI, P., PERIN-DUREAU, F., FAYYAZUDDIN, A., LE GOFF, A., CALLEBAUT, I. and NEYTON, J., 2000. Molecular organization of a zinc binding N-terminal modulatory domain in a NMDA receptor subunit. *Neuron,* **28**(3), pp. 911-925.

PAPADAKIS, M., HAWKINS, L.M. and STEPHENSON, F.A., 2004. Appropriate NR1-NR1 disulfide-linked homodimer formation is requisite for efficient expression of functional, cell surface N-methyl-D-aspartate NR1/NR2 receptors. *The Journal of Biological Chemistry,* **279**(15), pp. 14703-14712.

PAPOUIN, T., LADÉPÊCHE, L., RUEL, J., SACCHI, S., LABASQUE, M., HANINI, M., GROC, L., POLLEGIONI, L., MOTHET, J. and OLIET, S.H., 2012. Synaptic and extrasynaptic NMDA receptors are gated by different endogenous coagonists. *Cell,* **150**(3), pp. 633-646.

PARK-CHUNG, M., MALAYEV, A., PURDY, R.H., GIBBS, T.T. and FARB, D.H., 1999. Sulfated and unsulfated steroids modulate γ-aminobutyric acid A receptor function through distinct sites. *Brain Research,* **830**(1), pp. 72-87.

PARK-CHUNG, M., WU, F.S., PURDY, R.H., MALAYEV, A.A., GIBBS, T.T. and FARB, D.H., 1997. Distinct sites for inverse modulation of N-methyl-D-aspartate receptors by sulfated steroids. *Molecular Pharmacology,* **52**(6), pp. 1113-1123.

PEREZ-OTANO, I., SCHULTEIS, C.T., CONTRACTOR, A., LIPTON, S.A., TRIMMER, J.S., SUCHER, N.J. and HEINEMANN, S.F., 2001. Assembly with the NR1 subunit is required for surface expression of NR3A-containing NMDA receptors. *The Journal of Neuroscience,* **21**(4), pp. 1228-1237.

PETERS, S., KOH, J. and CHOI, D.W., 1987. Zinc selectively blocks the action of N-methyl-D-aspartate on cortical neurons. *Science,* **236**(4801), pp. 589-593.

PETROVIC, M., SEDLACEK, M., CAIS, O., HORAK, M., CHODOUNSKA, H. and VYKLICKY, L., 2009. Pregnenolone sulfate modulation of N-methyl-D-aspartate receptors is phosphorylation dependent. *Neuroscience,* **160**(3), pp. 616-628.

PETROVIC, M., SEDLACEK, M., HORAK, M., CHODOUNSKA, H. and VYKLICKY, L.,Jr, 2005. 20-oxo-5beta-pregnan-3alpha-yl sulfate is a use-dependent NMDA receptor inhibitor. *The Journal of Neuroscience,* **25**(37), pp. 8439-8450.

PETTIT, D., PERLMAN, S. and MALINOW, R., 1994. Potentiated transmission and prevention of further LTP by increased CaMKII activity in postsynaptic hippocampal slice neurons. *Science,* **266**(5192), pp. 1881.

PHILLIPS, K., COTEL, M., MCCARTHY, A., EDGAR, D., TRICKLEBANK, M., O'NEILL, M., JONES, M. and WAFFORD, K., 2012. Differential effects of NMDA antagonists on high frequency and gamma EEG oscillations in a neurodevelopmental model of schizophrenia. *Neuropharmacology,* **62**(3), pp. 1359-1370.

PRABAKARAN, S., SWATTON, J., RYAN, M., HUFFAKER, S., HUANG, J., GRIFFIN, J., WAYLAND, M., FREEMAN, T., DUDBRIDGE, F. and LILLEY, K., 2004. Mitochondrial dysfunction in schizophrenia: evidence for compromised brain metabolism and oxidative stress. *Molecular Psychiatry,* **9**(7), pp. 684-697.

PUNNAKKAL, P., JENDRITZA, P. and KÖHR, G., 2012. Influence of the intracellular GluN2 C-terminal domain on NMDA receptor function. *Neuropharmacology,* **62**(5), pp. 1985-1992.

QIU, S., HUA, Y.L., YANG, F., CHEN, Y.Z. and LUO, J.H., 2005. Subunit assembly of N-methyl-d-aspartate receptors analyzed by fluorescence resonance energy transfer. *The Journal of Biological Chemistry,* **280**(26), pp. 24923-24930.

QURESHI, A.I., ALI, Z., SURI, M.F., SHUAIB, A., BAKER, G., TODD, K., GUTERMAN, L.R. and HOPKINS, L.N., 2003. Extracellular glutamate and other amino acids in experimental intracerebral hemorrhage: an in vivo microdialysis study. *Critical Care Medicine,* **31**(5), pp. 1482-1489.

RACHLINE, J., PERIN-DUREAU, F., LE GOFF, A., NEYTON, J. and PAOLETTI, P., 2005. The micromolar zinc-binding domain on the NMDA receptor subunit NR2B. *The Journal of Neuroscience,* **25**(2), pp. 308-317.

RAMBOUSEK, L., BUBENIKOVA-VALESOVA, V., KACER, P., SYSLOVA, K., KENNEY, J., HOLUBOVA, K., NAJMANOVA, V., ZACH, P., SVOBODA, J. and STUCHLIK, A., 2011. Cellular and behavioural effects of a new steroidal inhibitor of the N-methyl-d-aspartate receptor 3α5β-pregnanolone glutamate. *Neuropharmacology,* **61**(1), pp. 61-68.

RAUNER, C. and KOHR, G., 2011. Triheteromeric NR1/NR2A/NR2B receptors constitute the major N-methyl-D-aspartate receptor population in adult hippocampal synapses. *The Journal of Biological Chemistry,* **286**(9), pp. 7558-7566.

RETCHLESS, B.S., GAO, W. and JOHNSON, J.W., 2012. A single GluN2 subunit residue controls NMDA receptor channel properties via intersubunit interaction. *Nature Neuroscience,* **15**(3), pp. 406-413.

REYNOLDS, G.P., ZHANG, Z.J. and BEASLEY, C.L., 2001. Neurochemical correlates of cortical GABAergic deficits in schizophrenia: selective losses of calcium binding protein immunoreactivity. *Brain Research Bulletin,* **55**(5), pp. 579-584.

RIOU, M., STROEBEL, D., EDWARDSON, J.M. and PAOLETTI, P., 2012. An alternating GluN1-2-1-2 subunit arrangement in mature NMDA receptors. *PloS One,* **7**(4), pp. e35134.

ROBERSON, E.D. and SWEATT, J.D., 1996. Transient activation of cyclic AMP-dependent protein kinase during hippocampal long-term potentiation. *Journal of Biological Chemistry,* **271**(48), pp. 30436-30441.

ROBERT FREEDMAN, 2003. Schizophrenia. *New England Journal of Medicine,* **349**, pp. 1738-1749.

ROOPUN, A.K., CUNNINGHAM, M.O., RACCA, C., ALTER, K., TRAUB, R.D. and WHITTINGTON, M.A., 2008. Region-specific changes in gamma and beta2 rhythms in NMDA receptor dysfunction models of schizophrenia. *Schizophrenia Bulletin,* **34**(5), pp. 962-973.

ROSSI, P., SOLA, E., TAGLIETTI, V., BORCHARDT, T., STEIGERWALD, F., UTVIK, J.K., OTTERSEN, O.P., KOHR, G. and D'ANGELO, E., 2002. NMDA receptor 2 (NR2) C-terminal control of NR open probability regulates synaptic transmission and plasticity at a cerebellar synapse. *The Journal of Neuroscience,* **22**(22), pp. 9687-9697.

ROTHMAN, S.M. and OLNEY, J.W., 1987. Excitotoxity and the NMDA receptor. *Trends in Neurosciences,* **10**(7), pp. 299-302.

SAKIMURA, K., KUTSUWADA, T., ITOT, I., MANABEL, T., TAKAYAMA, C., SUGLYAMAT, H. and MISHINA, M., 1995. Reduced hippocampal LTP and spatial learning in mice lacking NMDA receptor Ɛ1 subunit
 . *Nature,* **373**, pp. 151-155.

SAKURADA, K., MASU, M. and NAKANISHI, S., 1993. Alteration of Ca2+ permeability and sensitivity to Mg2+ and channel blockers by a single amino acid substitution in the N-methyl-D-aspartate receptor. *The Journal of Biological Chemistry,* **268**(1), pp. 410-415.

SALUSSOLIA, C.L., PRODROMOU, M.L., BORKER, P. and WOLLMUTH, L.P., 2011. Arrangement of subunits in functional NMDA receptors. *The Journal of neuroscience : the official journal of the Society for Neuroscience,* **31**(31), pp. 11295-11304.

SÁNCHEZ-PÉREZ, A.M. and FELIPO, V., 2005. Serines 890 and 896 of the NMDA receptor subunit NR1 are differentially phosphorylated by protein kinase C isoforms. *Neurochemistry International,* **47**(1), pp. 84-91.

SANTANGELO FREEL, R.M., OGDEN, K.K., STRONG, K.L., KHATRI, A., CHEPIGA, K.M., JENSEN, H.S., TRAYNELIS, S.F. and LIOTTA, D.C., 2013. Synthesis and structure activity relationship of tetrahydroisoquinoline-based potentiators of GluN2C and GluN2D containing N-Methyl-D-Aspartate receptors. *Journal of Medicinal Chemistry,* **56**(13), pp. 5351-5381.

SAPKOTA, K., MAO, Z., SYNOWICKI, P., LIEBER, D., LIU, M., IKEZU, T., GAUTAM, V. and MONAGHAN, D.T., 2016. GluN2D N-Methyl-d-Aspartate Receptor Subunit Contribution to the Stimulation of Brain Activity and Gamma Oscillations by Ketamine: Implications for Schizophrenia. *The Journal of Pharmacology and Experimental Therapeutics,* **356**(3), pp. 702-711.

SAUER, J.F. and BARTOS, M., 2010. Recruitment of early postnatal parvalbumin-positive hippocampal interneurons by GABAergic excitation. *The Journal of Neuroscience,* **30**(1), pp. 110-115.

SCHELL, M.J., MOLLIVER, M.E. and SNYDER, S.H., 1995. D-serine, an endogenous synaptic modulator: localization to astrocytes and glutamate-stimulated release. *Proceedings of the National Academy of Sciences of the United States of America,* **92**(9), pp. 3948-3952.

SCHIAVONE, S., SORCE, S., DUBOIS-DAUPHIN, M., JAQUET, V., COLAIANNA, M., ZOTTI, M., CUOMO, V., TRABACE, L. and KRAUSE, K., 2009. Involvement of NOX2 in the development of behavioral and pathologic alterations in isolated rats. *Biological Psychiatry,* **66**(4), pp. 384-392.

SCHMIDT, C. and HOLLMANN, M., 2009. Molecular and functional characterization of Xenopus laevis N-methyl-d-aspartate receptors. *Molecular and Cellular Neuroscience,* **42**(2), pp. 116-127.

SCHMIDT, C. and HOLLMANN, M., 2008. Apparent homomeric NR1 currents observed in Xenopus oocytes are caused by an endogenous NR2 subunit. *Journal of Molecular Biology,* **376**(3), pp. 658-670.

SCHORGE, S. and COLQUHOUN, D., 2003. Studies of NMDA receptor function and stoichiometry with truncated and tandem subunits. *The Journal of Neuroscience,* **23 (4)**, pp. 1158-1158.

SEEBURG, P.H., 1993. The TINS/TiPS Lecture the molecular biology of mammalian glutamate receptor channels. *Trends in Neurosciences,* **16**(9), pp. 359-365.

SHIOKAWA, H., KAFTAN, E.J., MACDERMOTT, A.B. and TONG, C., 2010. NR2 subunits and NMDA receptors on lamina II inhibitory and excitatory interneurons of the mouse dorsal horn. *Molecular Pain,* **6**(1), pp. 1.

SIMON, R.P., SWAN, J.H., GRIFFITHS, T. and MELDRUM, B.S., 1984. Blockade of N-methyl-D-aspartate receptors may protect against ischemic damage in the brain. *Science,* **226**(4676), pp. 850-852.

SMOTHERS, C.T. and WOODWARD, J.J., 2009. Expression of glycine-activated diheteromeric NR1/NR3 receptors in human embryonic kidney 293 cells Is NR1 splice variant-dependent. *The Journal of Pharmacology and Experimental Therapeutics,* **331**(3), pp. 975-984.

SMOTHERS, C.T. and WOODWARD, J.J., 2007. Pharmacological characterization of glycine-activated currents in HEK 293 cells expressing N-methyl-D-aspartate NR1 and NR3 subunits. *The Journal of Pharmacology and Experimental Therapeutics,* **322**(2), pp. 739-748.

SNYDER, M.A. and GAO, W., 2013. NMDA hypofunction as a convergence point for progression and symptoms of schizophrenia. *Frontiers in Cellular Neuroscience,* **7**, pp. 31.

SOBOLEVSKY, A.I., ROSCONI, M.P. and GOUAUX, E., 2009. X-ray structure, symmetry and mechanism of an AMPA-subtype glutamate receptor. *Nature,* **462**(7274), pp. 745-756.

SODHI, M.S., SIMMONS, M., MCCULLUMSMITH, R., HAROUTUNIAN, V. and MEADOR-WOODRUFF, J.H., 2011. Glutamatergic gene expression is specifically reduced in thalamocortical projecting relay neurons in schizophrenia. *Biological Psychiatry,* **70**(7), pp. 646-654.

SOHAL, V.S., ZHANG, F., YIZHAR, O. and DEISSEROTH, K., 2009. Parvalbumin neurons and gamma rhythms enhance cortical circuit performance. *Nature,* **459**(7247), pp. 698-702.

SPOOREN, W., MOMBEREAU, C., MACO, M., GILL, R., KEMP, J.A., OZMEN, L., NAKANISHI, S. and HIGGINS, G.A., 2004. Pharmacological and genetic evidence indicates that combined inhibition of NR2A and NR2B subunit containing NMDA receptors is required to disrupt prepulse inhibition. *Psychopharmacology,* **175**(1), pp. 99-105.

STANDAERT, D.G., BERNHARD LANDWEHRMEYER, G., KERNER, J.A., PENNEY JR, J.B. and YOUNG, A.B., 1996. Expression of NMDAR2D glutamate receptor subunit mRNA in neurochemically identified interneurons in the rat neostriatum, neocortex and hippocampus. *Molecular Brain Research,* **42**(1), pp. 89-102.

STERN-BACH, Y., BETTLER, B., HARTLEY, M., SHEPPARD, P.O., O'HARA, P.J. and HEINEMANN, S.F., 1994. Agonist selectivity of glutamate receptors is specified by two domains structurally related to bacterial amino acid-binding proteins. *Neuron,* **13**(6), pp. 1345-1357.

SUCHER, N.J., AKBARIAN, S., CHI, C.L., LECLERC, C.L., AWOBULUYI, M., DEITCHER, D.L., WU, M.K., YUAN, J.P., JONES, E.G. and LIPTON, S.A., 1995. Developmental and regional expression pattern of a novel NMDA receptor-like subunit (NMDAR-L) in the rodent brain. *The Journal of Neuroscience,* **15**(10), pp. 6509-6520.

SUGIHARA, H., MORIYOSHI, K., ISHII, T., MASU, M. and NAKANISHI, S., 1992. Structures and properties of seven isoforms of the NMDA receptor generated by alternative splicing. *Biochemical and Biophysical Research Communications,* **185**(3), pp. 826-832.

SULLIVAN, J.M., TRAYNELIS, S.F., CHEN, H.V., ESCOBAR, W., HEINEMANN, S.F. and LIPTON, S.A., 1994. Identification of two cysteine residues that are required for redox modulation of the NMDA subtype of glutamate receptor. *Neuron,* **13**(4), pp. 929-936.

SULLIVAN, P.F., KENDLER, K.S. and NEALE, M.C., 2003. Schizophrenia as a complex trait: evidence from a meta-analysis of twin studies. *Archives of General Psychiatry,* **60**(12), pp. 1187.

SUN, J., JIA, P., FANOUS, A.H., VAN DEN OORD, E., CHEN, X., RILEY, B.P., AMDUR, R.L., KENDLER, K.S. and ZHAO, Z., 2010. Schizophrenia gene networks and pathways and their applications for novel candidate gene selection. *PloS One,* **5**(6), pp. e11351.

SUN, Y., OLSON, R., HORNING, M., ARMSTRONG, N., MAYER, M. and GOUAUX, E., 2002. Mechanism of glutamate receptor desensitization. *Nature,* **417**(6886), pp. 245-253.

SURYAVANSHI, P., UGALE, R., YILMAZER-HANKE, D., STAIRS, D. and DRAVID, S., 2014. GluN2C/GluN2D subunit-selective NMDA receptor potentiator CIQ reverses MK-801-induced impairment in prepulse inhibition and working memory in Y-maze test in mice. *British Journal of Pharmacology,* **171**(3), pp. 799-809.

SWAN, J.H. and MELDRUM, B.S., 1990. Protection by NMDA antagonists against selective cell loss following transient ischaemia. *Journal of Cerebral Blood Flow and Metabolism,* **10**(3), pp. 343-351.

TAKEUCHI, T., KIYAMA, Y., NAKAMURA, K., TSUJITA, M., MATSUDA, I., MORI, H., MUNEMOTO, Y., KURIYAMA, H., NATSUME, R. and SAKIMURA, K., 2001. Roles of the glutamate receptor ε2 and δ2 subunits in the potentiation and prepulse inhibition of the acoustic startle reflex. *European Journal of Neuroscience,* **14**(1), pp. 153-160.

TALUKDER, I. and WOLLMUTH, L.P., 2011. Local constraints in either the GluN1 or GluN2 subunit equally impair NMDA receptor pore opening. *The Journal of General Physiology,* **138**(2), pp. 179-194.

TAMMINGA, C., 1999. Glutamatergic aspects of schizophrenia. *The British Journal of Psychiatry,* **174**, pp. 12-15.

TANG, Y., SHIMIZU, E., DUBE, G.R., RAMPON, C., KERCHNER, G.A., ZHUO, M., LIU, G. and TSIEN, J.Z., 1999. Genetic enhancement of learning and memory in mice. *Nature,* **401**(6748), pp. 63-69.

TANG, C.M., DICHTER, M. and MORAD, M., 1990. Modulation of the N-methyl-D-aspartate channel by extracellular H+. *Proceedings of the National Academy of Sciences of the United States of America,* **87**(16), pp. 6445-6449.

TINGLEY, W.G., EHLERS, M.D., KAMEYAMA, K., DOHERTY, C., PTAK, J.B., RILEY, C.T. and HUGANIR, R.L., 1997. Characterization of protein kinase A and protein kinase C phosphorylation of the N-methyl-D-aspartate receptor NR1 subunit using phosphorylation site-specific antibodies. *Journal of Biological Chemistry,* **272**(8), pp. 5157-5166.

TONG, C., KAFTAN, E.J. and MACDERMOTT, A.B., 2008. Functional identification of NR2 subunits contributing to NMDA receptors on substance P receptor-expressing dorsal horn neurons. *Molecular Pain,* **4**(1), pp. 1.

TORREY, E.F., BARCI, B.M., WEBSTER, M.J., BARTKO, J.J., MEADOR-WOODRUFF, J.H. and KNABLE, M.B., 2005. Neurochemical markers for schizophrenia, bipolar disorder, and major depression in postmortem brains. *Biological Psychiatry,* **57**(3), pp. 252-260.

TOVAR, K.R., MCGINLEY, M.J. and WESTBROOK, G.L., 2013. Triheteromeric NMDA receptors at hippocampal synapses. *The Journal of Neuroscience,* **33**(21), pp. 9150-9160.

TRAYNELIS, S.F. and CULL-CANDY, S.G., 1990. Proton inhibition of N-methyl-D-aspartate receptors in cerebellar neurons. *Nature,* **345**(6273), pp. 347-350.

TRAYNELIS, S.F., HARTLEY, M. and HEINEMANN, S.F., 1995. Control of proton sensitivity of the NMDA receptor by RNA splicing and polyamines. *Science,* **268**(5212), pp. 873-876.

TRAYNELIS, S.F., WOLLMUTH, L.P., MCBAIN, C.J., MENNITI, F.S., VANCE, K.M., OGDEN, K.K., HANSEN, K.B., YUAN, H., MYERS, S.J. and DINGLEDINE, R., 2010. Glutamate receptor ion channels: structure, regulation, and function. *Pharmacological Reviews,* **62**(3), pp. 405-496.

TSAI, G.E. and LIN, P., 2010. Strategies to enhance N-methyl-D-aspartate receptor-mediated neurotransmission in schizophrenia, a critical review and meta-analysis. *Current Pharmaceutical Design,* **16**(5), pp. 522-537.

TURNER, C.P., DEBENEDETTO, D., WARE, E., STOWE, R., LEE, A., SWANSON, J., WALBURG, C., LAMBERT, A., LYLE, M. and DESAI, P., 2010. Postnatal exposure to MK801 induces selective changes in GAD67 or parvalbumin. *Experimental Brain Research,* **201**(3), pp. 479-488.

UHLHAAS, P.J., HAENSCHEL, C., NIKOLIĆ, D. and SINGER, W., 2008. The role of oscillations and synchrony in cortical networks and their putative relevance for the pathophysiology of schizophrenia. *Schizophrenia Bulletin,* **34**(5), pp. 927-943.

UHLHAAS, P.J. and SINGER, W., 2010. Abnormal neural oscillations and synchrony in schizophrenia. *Nature Reviews Neuroscience,* **11**(2), pp. 100-113.

UHLHAAS, P.J. and SINGER, W., 2013. High-frequency oscillations and the neurobiology of schizophrenia. *Dialogues in Clinical Neuroscience,* **15**(3), pp. 301-313.

ULBRICH, M.H. and ISACOFF, E.Y., 2008. Rules of engagement for NMDA receptor subunits. *Proceedings of the National Academy of Sciences of the United States of America,* **105**(37), pp. 14163-14168.

URAKAWA, S., TAKAMOTO, K., HORI, E., SAKAI, N., ONO, T. and NISHIJO, H., 2013. Rearing in enriched environment increases parvalbumin-positive small neurons in the amygdala and decreases anxiety-like behavior of male rats. *BMC Neuroscience,* **14**(1), pp. 1-11.

VALES, K., RAMBOUSEK, L., HOLUBOVA, K., SVOBODA, J., BUBENIKOVA-VALESOVA, V., CHODOUNSKA, H., VYKLICKY, L. and STUCHLIK, A., 2012. 3α5β-Pregnanolone glutamate, a use-dependent NMDA antagonist, reversed spatial learning deficit in an animal model of schizophrenia. *Behavioural Brain Research,* **235**(1), pp. 82-88.

VICINI, S., WANG, J.F., LI, J.H., ZHU, W.J., WANG, Y.H., LUO, J.H., WOLFE, B.B. and GRAYSON, D.R., 1998. Functional and pharmacological differences between recombinant N-methyl-D-aspartate receptors. *Journal of Neurophysiology,* **79**(2), pp. 555-566.

VOLGRAF, M., SELLERS, B.D., JIANG, Y., WU, G., LY, C.Q., VILLEMURE, E., PASTOR, R.M., YUEN, P., LU, A. and LUO, X., 2016. Discovery of GluN2A-Selective NMDA Receptor Positive Allosteric Modulators (PAMs): Tuning Deactivation Kinetics via Structure-Based Design. *Journal of Medicinal Chemistry,* **59**(6), pp. 2760-2779.

VOLKMANN, R.A., FANGER, C.M., ANDERSON, D.R., SIRIVOLU, V.R., PASCHETTO, K., GORDON, E., VIRGINIO, C., GLEYZES, M., BUISSON, B. and STEIDL, E., 2016. MPX-004 and MPX-007: New Pharmacological Tools to Study the Physiology of NMDA Receptors Containing the GluN2A Subunit. *PloS One,* **11**(2), pp. e0148129.

VOLLENWEIDER, F., LEENDERS, K., SCHARFETTER, C., ANTONINI, A., MAGUIRE, P., MISSIMER, J. and ANGST, J., 1997. Metabolic hyperfrontality and psychopathology in the ketamine model of psychosis using positron emission tomography (PET) and [18 F] fluorodeoxyglucose (FDG). *European Neuropsychopharmacology,* **7**(1), pp. 9-24.

VON ENGELHARDT, J., DOGANCI, B., JENSEN, V., HVALBY, Ø, GÖNGRICH, C., TAYLOR, A., BARKUS, C., SANDERSON, D.J., RAWLINS, J.N.P. and SEEBURG, P.H., 2008. Contribution of hippocampal and extra-hippocampal NR2B-containing NMDA receptors to performance on spatial learning tasks. *Neuron,* **60**(5), pp. 846-860.

VREUGDENHIL, M., JEFFERYS, J.G., CELIO, M.R. and SCHWALLER, B., 2003. Parvalbumin-deficiency facilitates repetitive IPSCs and gamma oscillations in the hippocampus. *Journal of Neurophysiology,* **89**(3), pp. 1414-1422.

VYKLICKY, V., KRAUSOVA, B., CERNY, J., BALIK, A., ZAPOTOCKY, M., NOVOTNY, M., LICHNEROVA, K., SMEJKALOVA, T., KANIAKOVA, M. and KORINEK, M., 2015. Block of NMDA receptor channels by endogenous neurosteroids: implications for the agonist induced conformational states of the channel vestibule. *Scientific Reports,* **5**.

WANG, C., MCINNIS, J., ROSS-SANCHEZ, M., SHINNICK-GALLAGHER, P., WILEY, J. and JOHNSON, K., 2001. Long-term behavioral and neurodegenerative effects of perinatal phencyclidine administration: implications for schizophrenia. *Neuroscience,* **107**(4), pp. 535-550.

WANG, H. and GAO, W., 2009. Cell type-specific development of NMDA receptors in the interneurons of rat prefrontal cortex. *Neuropsychopharmacology,* **34**(8), pp. 2028-2040.

WANG, J.Q., GUO, M., JIN, D., XUE, B., FIBUCH, E.E. and MAO, L., 2014. Roles of subunit phosphorylation in regulating glutamate receptor function. *European Journal of Pharmacology,* **728**, pp. 183-187.

WANG, Y.T. and SALTER, M.W., 1994. Regulation of NMDA receptors by tyrosine kinases and phosphatases. *Nature,* **369**(6477), pp. 233-235.

WATANABE, M., INOUE, Y., SAKIMURA, K. and MISHINA, M., 1993a. Distinct distributions of five N-methyl-D-aspartate receptor channel subunit mRNAs in the forebrain. *Journal of Comparative Neurology,* **338**(3), pp. 377-390.

WATANABE, M., INOUE, Y., SAKIMURA, K. and MISHINA, M., 1993b. Distinct Spatio-temporal Distributions of the NMDA Receptor Channel Subunit mRNAs in the Brain. *Annals of the New York Academy of Sciences,* **707**(1), pp. 463-466.

WATANABE, M., INOUE, Y., SAKIMURA, K. and MISHINA, M., 1992. Developmental changes in distribution of NMDA receptor channel subunit mRNAs. *Neuroreport,* **3**(12), pp. 1138-1140.

WATANABE, J., BECK, C., KUNER, T., PREMKUMAR, L.S. and WOLLMUTH, L.P., 2002. DRPEER: a motif in the extracellular vestibule conferring high Ca2+ flux rates in NMDA receptor channels. *The Journal of Neuroscience,* **22**(23), pp. 10209-10216.

WATKINS, J., 1962. The synthesis of some acidic amino acids possessing neuropharmacological activity. *Journal of Medicinal Chemistry,* **5**(6), pp. 1187-1199.

WATKINS, J. and EVANS, R., 1981. Excitatory amino acid transmitters. *Annual Review of Pharmacology and Toxicology,* **21**(1), pp. 165-204.

WATSON, G., HOOD, W., MONAHAN, J. and LANTHORN, T., 1988. Kynurenate antagonizes actions of N-methyl-D-aspartate through a glycine-sensitive receptor. *Neuroscience Research Communications,* **2**(3), pp. 169-174.

WEICKERT, C., FUNG, S., CATTS, V., SCHOFIELD, P., ALLEN, K., MOORE, L., NEWELL, K., PELLEN, D., HUANG, X. and CATTS, S., 2013. Molecular evidence of N-methyl-D-aspartate receptor hypofunction in schizophrenia. *Molecular Psychiatry,* **18**(11), pp. 1185-1192.

WENZEL, A., FRITSCHY, J.M., MOHLER, H. and BENKE, D., 1997. NMDA receptor heterogeneity during postnatal development of the rat brain: differential expression of the NR2A, NR2B, and NR2C subunit proteins. *Journal of Neurochemistry,* **68**(2), pp. 469-478.

WILLIAMS, K., 1993. Ifenprodil discriminates subtypes of the N-methyl-D-aspartate receptor: selectivity and mechanisms at recombinant heteromeric receptors. *Molecular Pharmacology,* **44**(4), pp. 851-859.

WÖHR, M., ORDUZ, D., GREGORY, P., MORENO, H., KHAN, U., VÖRCKEL, K., WOLFER, D., WELZL, H., GALL, D. and SCHIFFMANN, S.N., 2015. Lack of parvalbumin in mice leads to behavioral deficits relevant to all human autism core symptoms and related neural morphofunctional abnormalities. *Translational Psychiatry,* **5**(3), pp. e525.

WOLLMUTH, L.P., KUNER, T. and SAKMANN, B., 1998. Adjacent asparagines in the NR2-subunit of the NMDA receptor channel control the voltage-dependent block by extracellular Mg2. *The Journal of Physiology,* **506**(1), pp. 13-32.

WOOD, M.W., VANDONGEN, H.M. and VANDONGEN, A.M., 1995. Structural conservation of ion conduction pathways in K channels and glutamate receptors. *Proceedings of the National Academy of Sciences of the United States of America,* **92**(11), pp. 4882-4886.

WU, F.S., GIBBS, T.T. and FARB, D.H., 1991. Pregnenolone sulfate: a positive allosteric modulator at the N-methyl-D-aspartate receptor. *Molecular Pharmacology,* **40**(3), pp. 333-336.

YAGHOUBI, N., MALAYEV, A., RUSSEK, S.J., GIBBS, T.T. and FARB, D.H., 1998. Neurosteroid modulation of recombinant ionotropic glutamate receptors. *Brain Research,* **803**(1), pp. 153-160.

YAMAMOTO, T., NAKAYAMA, T., YAMAGUCHI, J., MATSUZAWA, M., MISHINA, M., IKEDA, K. and YAMAMOTO, H., 2016. Role of the NMDA receptor GluN2D subunit in the expression of ketamine-induced behavioral sensitization and region-specific activation of neuronal nitric oxide synthase. *Neuroscience Letters,* **610**, pp. 48-53.

YAMAMOTO, H., KAMEGAYA, E., SAWADA, W., HASEGAWA, R., YAMAMOTO, T., HAGINO, Y., TAKAMATSU, Y., IMAI, K., KOGA, H., MISHINA, M. and IKEDA, K., 2013. Involvement of the N-methyl-D-aspartate receptor GluN2D subunit in phencyclidine-induced motor impairment, gene expression, and increased Fos immunoreactivity. *Molecular Brain,* **6**, pp. 56-6606-6-56.

YAMASAKI, M., OKADA, R., TAKASAKI, C., TOKI, S., FUKAYA, M., NATSUME, R., SAKIMURA, K., MISHINA, M., SHIRAKAWA, T. and WATANABE, M., 2014.

Opposing role of NMDA receptor GluN2B and GluN2D in somatosensory development and maturation. *The Journal of Neuroscience,* **34**(35), pp. 11534-11548.

YANG, Y., GE, W., CHEN, Y., ZHANG, Z., SHEN, W., WU, C., POO, M. and DUAN, S., 2003. Contribution of astrocytes to hippocampal long-term potentiation through release of D-serine. *Proceedings of the National Academy of Sciences of the United States of America,* **100**(25), pp. 15194-15199.

YI, F., MOU, T., DORSETT, K.N., VOLKMANN, R.A., MENNITI, F.S., SPRANG, S.R. and HANSEN, K.B., 2016. Structural Basis for Negative Allosteric Modulation of GluN2A-Containing NMDA Receptors. *Neuron,* **91**(6), pp. 1316-1329.

YIZHAR, O., FENNO, L.E., PRIGGE, M., SCHNEIDER, F., DAVIDSON, T.J., O'SHEA, D.J., SOHAL, V.S., GOSHEN, I., FINKELSTEIN, J. and PAZ, J.T., 2011. Neocortical excitation/inhibition balance in information processing and social dysfunction. *Nature,* **477**(7363), pp. 171-178.

YOUNG, A.B. and FAGG, G.E., 1990. Excitatory amino acid receptors in the brain: membrane binding and receptor autoradiographic approaches. *Trends in Pharmacological Sciences,* **11**(3), pp. 126-133.

YUAN, H., MYERS, S.J., WELLS, G., NICHOLSON, K.L., SWANGER, S.A., LYUBOSLAVSKY, P., TAHIROVIC, Y.A., MENALDINO, D.S., GANESH, T. and WILSON, L.J., 2015. Context-dependent GluN2B-selective inhibitors of NMDA receptor function are neuroprotective with minimal side effects. *Neuron,* **85**(6), pp. 1305-1318.

YUAN, H., HANSEN, K.B., VANCE, K.M., OGDEN, K.K. and TRAYNELIS, S.F., 2009. Control of NMDA receptor function by the NR2 subunit amino-terminal domain. *The Journal of Neuroscience,* **29**(39), pp. 12045-12058.

YUNG-CHI, C. and PRUSOFF, W.H., 1973. Relationship between the inhibition constant (K i) and the concentration of inhibitor which causes 50 per cent inhibition (I 50) of an enzymatic reaction. *Biochemical Pharmacology,* **22**(23), pp. 3099-3108.

ZHANG, Y., BUONANNO, A., VERTES, R.P., HOOVER, W.B. and LISMAN, J.E., 2012. NR2C in the thalamic reticular nucleus; effects of the NR2C knockout. *PloS One,* **7**(7), pp. e41908.

ZHANG, Y., LLINAS, R.R. and LISMAN, J., 2009. Inhibition of NMDARs in the nucleus reticularis of the thalamus produces delta frequency bursting. *Frontiers in Neural Circuits,* **3**, pp. 1-9.

ZHANG, Z. and SUN, Q., 2011. Development of NMDA NR2 subunits and their roles in critical period maturation of neocortical GABAergic interneurons. *Developmental neurobiology,* **71**(3), pp. 221-245.

ZHANG, Y., BEHRENS, M.M. and LISMAN, J.E., 2008. Prolonged exposure to NMDAR antagonist suppresses inhibitory synaptic transmission in prefrontal cortex. *Journal of Neurophysiology,* **100**(2), pp. 959-965.

ZHOU, Q., HOMMA, K.J. and POO, M., 2004. Shrinkage of dendritic spines associated with long-term depression of hippocampal synapses. *Neuron,* **44**(5), pp. 749-757.

November 8, 2016

Kiran Sapkota
Pharmacology & Experimental Neuroscience Department
University of Nebraska Medical Center
601 S Saddle Creek Road
Omaha, NE 68106

Email: knsapkota11@gmail.com

Dear Kiran Sapkota:

This is to grant you permission to include the following article in your thesis entitled "Target Validation and Pharmacological Characterization of Novel NMDAR Modulators" for the University of Nebraska Medical Center:

Kiran Sapkota, Zhihao Mao, Paul Synowicki, Dillon Lieber, Meng Liu, Tsuneya Ikezu, Vivek Gautam, and Daniel T. Monaghan, GluN2D *N*-Methyl-D-Aspartate Receptor Subunit Contribution to the Stimulation of Brain Activity and Gamma Oscillations by Ketamine: Implications for Schizophrenia, *J Pharmacol Exp Ther* 2016, 356(3):702-711,
DOI: http://dx.doi.org/10.1124/jpet.115.230391

On the first page of each copy of this article, please add the following:

Reprinted with permission of the American Society for Pharmacology and Experimental Therapeutics. All rights reserved.

In addition, the original copyright line published with the paper must be shown on the copies included with your thesis.

Sincerely yours,

Richard Dodenhoff
Journals Director